

6-23-2008

# Effects of Compression Loading, Injury, and Age on Intervertebral Disc Mechanics, Biology and Metabolism Using Large Animal Organ and Cell Culture Systems

Casey Korecki  
*University of Vermont*

Follow this and additional works at: <http://scholarworks.uvm.edu/graddis>

---

## Recommended Citation

Korecki, Casey, "Effects of Compression Loading, Injury, and Age on Intervertebral Disc Mechanics, Biology and Metabolism Using Large Animal Organ and Cell Culture Systems" (2008). *Graduate College Dissertations and Theses*. Paper 126.

This Dissertation is brought to you for free and open access by the Dissertations and Theses at ScholarWorks @ UVM. It has been accepted for inclusion in Graduate College Dissertations and Theses by an authorized administrator of ScholarWorks @ UVM. For more information, please contact [donna.omalley@uvm.edu](mailto:donna.omalley@uvm.edu).

EFFECTS OF COMPRESSION LOADING, INJURY, AND AGE ON  
INTERVERTEBRAL DISC MECHANICS, BIOLOGY AND METABOLISM USING  
LARGE ANIMAL ORGAN AND CELL CULTURE SYSTEMS

A Dissertation Presented

by

Casey L. Korecki

to

The Faculty of the Graduate College

of

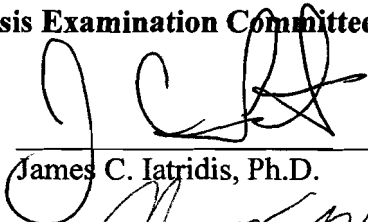
The University of Vermont

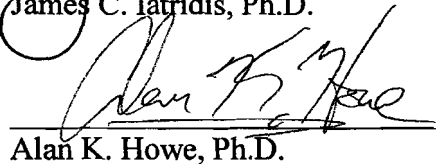
In Partial Fulfillment of the Requirements  
for the Degree of Doctor of Philosophy  
Specializing in Mechanical Engineering


May, 2008

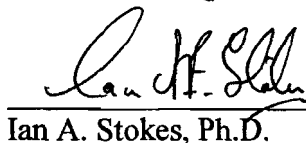
**Accepted by the Faculty of the Graduate College, The University of Vermont, in partial fulfillment of the requirements for the degree of Doctor of Philosophy specializing in Mechanical Engineering.**


**Thesis Examination Committee:**

  
\_\_\_\_\_  
James C. Iatridis, Ph.D. **Advisor**

  
\_\_\_\_\_  
Alan K. Howe, Ph.D.

  
\_\_\_\_\_  
Helene M. Langevin, M.D.

  
\_\_\_\_\_  
Ian A. Stokes, Ph.D.

  
\_\_\_\_\_  
Margaret J. Boppstein, Ph.D. **Chairperson**

  
\_\_\_\_\_  
Frances E. Carr, Ph.D. **Vice President for Research  
and Dean of Graduate Studies**

Date: March 26<sup>th</sup>, 2008

## ABSTRACT

The intervertebral disc (IVD) is a complex orthopaedic tissue that is located between the vertebrae in the spine. Degeneration of the IVD is thought to be a contributor to low back pain (LBP), which affects up to 80% of the population at enormous economic cost. The role of the intervertebral disc in supporting and resisting applied loading to the spine, along with the observation of disorders associated with abnormal spinal loading, provide support to the theory that applied mechanical loading is crucial in maintaining the health of the intervertebral disc. The encompassing goal of this work was to examine the biological response of the intervertebral disc to changes in the surrounding mechanical environment in a large animal model. Aim 1 utilized an organ culture model to explore the relationship between disc mechanics and biology in needle puncture injury, a commonly used model of experimentally induced disc degeneration, thus providing a possible mechanism for *in vivo* injury induced disc degeneration models. Aim 2 was to explore the interaction between the amplitude of applied mechanical loading and intervertebral disc cell signaling, also performed in an organ culture model to include cell-matrix signal transduction. Aim 3 addressed frequency and age effects on the IVD response to mechanical stimulation, performed *in vitro* to control for the effects of varying matrix compositions between old and young animals. Finally, Aim 4 utilized k-means and fuzzy c-means clustering techniques to reveal patterns in experimental phenotype (determined by gene expression data) and gene response to experimental conditions. The application of biclustering, where the gene responses within experimental phenotypes are clustered to elucidate possible mechanisms for different gene level-responses to experimental conditions, was also accomplished. Finally, the ability for the model to predict the behavior of other genes critical to IVD mechanobiology, or in determining the membership of an unexamined experimental phenotype was explored. Overall, applied dynamic compression was not found to significantly alter disc mechanics, while a disruption in the annulus through needle puncture rapidly decreased the compressive modulus. Changes in disc mechanics may precede biological remodeling, with little evidence of remodeling present without mechanical alteration. Aging, however, crucially impacts disc cell biology, particularly in the nucleus pulposus, and will interact with applied loading to further impact the ability for the intervertebral disc cells to maintain a healthy extracellular matrix.



## Citations

**Material from this thesis has been published in the following form:**

Korecki CL, MacLean JJ, Iatridis JC, Dynamic compression effects on intervertebral disc mechanics and biology. *Spine*: In Press, accepted January 29, 2008

**Material from this thesis has been published in the following form:**

Korecki CL, Costi JJ, Iatridis JC, Needle puncture injury affects intervertebral disc mechanics and biology in an organ culture model. *Spine*, 33: 235-41, 2008

**Material from this thesis has been submitted to the Journal of Orthopaedic Research on March 10<sup>th</sup>, 2008 in the following form:**

Korecki CL, Kuo CK, Tuan RS, Iatridis JC, Intervertebral disc cell response to dynamic compression is age and frequency dependent: *J Orthop Res*: Submitted March, 2008

## **Acknowledgements**

This research was possible due to the direct and indirect support of many people.

Although space constrains me to thank only a number of them, the help, thoughtful discussions and encouragement of many more individuals is reflected in this work.

I would like to thank my advisor, Dr. James Iatridis, for hiring me into the Mechanical Engineering program, and giving me a spot in the Spine Bioengineering Lab. I have been incredibly lucky to have an advisor as dedicated and hard-working as you, and I really appreciate all the time and effort you have put into helping me succeed. I'd also like to thank all the members of the Spine Bioengineering Lab I have had the privilege to work with over the years, and am happy to look back on many of you as friends in addition to co-workers.

I wish also to thank people I have considered mentors over the years. Mr Gates and Mr. Davenport at Springstead high school, whose lessons about science remain firmly in my mind although high school seems like a long time ago. Dr. Glen Niebur and Dr. Ryan Roeder, who allowed me my first opportunity to do bioengineering research at the University of Notre Dame thus firmly cementing my plans to go to graduate school.

Most importantly, I'd like to thank my friends and family. To my friends, particularly Maureen Cherwin and Amy Johnson, graduate school has consumed

much of my time leaving me as a very difficult person to stay in contact with (and often forgetful of birthdays and other special occasions), and I can't thank you both enough for putting up with it and still calling back repeatedly. My parents, Nicholas and Sheree, have been a source of constant support and inspiration throughout my life and I am grateful for the opportunity to thank them for all their sacrifices along the way to help me succeed. I'm very grateful for my brother John, who often helped put things in perspective, as well as providing technical help with the final chapter. My grandparents, Doris and John Comiskey, who provided such love and support throughout my life and especially during college (in addition to a much needed meal during Easter and Thanksgiving), and who are also a model of hard work and perseverance. You are both very missed. To Tom, my fiancée, for enduring a five-year separation that has been filled with many late night conversations about cells, mechanics, and frustration over experiments gone awry. I know a lesser man would not have handled it with as much compassion and humor as you, and I look forward to spending the rest of our lives together.

## Table of Contents

Citations .....	ii
Acknowledgements .....	iii
CHAPTER 1 Introduction.....	1
CHAPTER 2 Background.....	9
2.1 Intervertebral disc structure and biology .....	9
2.2 Intervertebral disc development .....	10
2.3 The healthy intervertebral disc .....	11
2.4 Pathological changes associated with IVD degeneration .....	17
2.5 Intervertebral disc research.....	18
2.5.1 In vivo models .....	22
2.5.1.1 Relevant research .....	22
2.5.2 Organ culture .....	25
2.5.2.1 Relevant research .....	27
2.5.3 Tissue culture.....	29
2.5.3.1 Relevant research .....	29

2.5.4 Cell culture.....	30
2.5.4.1 Relevant research.....	31
2.6 Summary.....	34
CHAPTER 3 Needle Puncture Injury Affects Intervertebral Disc Mechanics and Biology in an Organ Culture Model .....	36
3.1 Abstract.....	37
3.2 Precis.....	39
3.3 Key Points.....	39
3.4 Key Words .....	39
3.5 Introduction.....	40
3.6 Materials and Methods .....	41
3.7 Results .....	44
3.8 Discussion.....	46
3.9 References.....	51
3.10 Tables and Figures .....	55
3.11 Study Clarifications .....	63
CHAPTER 4 Dynamic Compression Effects on Intervertebral Disc Mechanics and Biology.....	64
4.1 Abstract.....	65

4.2	Precis.....	67
4.3	Key Points.....	67
4.4	Key Words .....	67
4.5	Introduction.....	68
4.6	Materials and Methods .....	70
4.7	Results .....	75
4.8	Discussion.....	76
4.9	References.....	80
4.10	Tables and Figures .....	82
4.11	Study Clarifications .....	88
CHAPTER 5	Intervertebral Disc Cell Response to Dynamic Compression is Age and Frequency Dependent .....	90
5.1	Abstract.....	91
5.2	Introduction.....	92
5.3	Materials and Methods .....	94
5.4	Results .....	97
5.5	Discussion.....	99
5.6	References.....	102
5.7	Tables and Figures.....	105

5.8 Study Clarifications .....	110
CHAPTER 6 Application of Clustering and Biclustering Analyses to Explore the Role of Mechanics, Aging, Time, and Culture Model on Gene Expression Patterns .....	111
6.1 Introduction.....	111
6.2 Methods .....	117
6.2.1 Experimental framework .....	117
6.2.2 Computational Framework .....	124
6.2.3 Visualization of the results through factorization.....	131
6.2.4 Implementation of the algorithms.....	134
6.3 Results .....	139
6.3.1 Experiment clustering .....	139
6.3.1.1 K-means .....	139
6.3.1.2 Perturbation of data.....	144
6.3.1.3 Manhattan city block metric .....	149
6.3.1.4 Fuzzy c-means .....	149
6.3.2 Gene Expression Clustering .....	156
6.3.2.1 Full data sets, Kmeans clustering .....	156
6.3.2.2 Full data sets, fuzzy c-means .....	160
6.3.2.3 Sub-matrix analysis – Kmeans .....	167
6.3.3 Gene patterns in experimental grouping.....	168
6.3.4 Predictive model .....	171
6.3.4.1 Predicting other genes.....	171
6.3.4.2 Predicting groups of experiments based on ‘ phenotype’ .....	175
6.4 Discussion.....	177

6.5 Conclusions .....	182
CHAPTER 7 Summary.....	183
Appendix 1: Immunohistochemistry methods.....	214
Appendix 2: Data for clustering analysis.....	217



## List of Tables

Table 3-1: Height lost between culture days. No significant differences were noted between groups. Values are expressed as Average $\pm$ SEM .....	55
Table 3-2: Average GAG loss to culture media (as a percentage of total initial disc weight) and percent water content of intervertebral disc tissue for outer annulus (OA), inner annulus (IA), nucleus pulposus (NP) regions. No significant differences were noted between groups. Values are expressed as Average $\pm$ SEM.....	55
Table 5-1: Average GAG ( $\mu$ g) and DNA (ng) content plus/minus SEM for constructs. Stars (*) indicate significantly lower amounts between age groups, (#) indicate significant differences between loading groups.....	105
Table 6-1: Experimental groups. 4 loading conditions (Control, 0.1, 1, and 3 Hz) will be explored at 4 time points (Days 0, 7, 14, 21) and in young and mature cells for a total of 32 experimental groups per tissue (AF or NP).....	118
Table 6-2: 31 genes were analyzed using real-time RT-PCR for all 32 experimental groups in each tissue (AF or NP).....	119
Table 6-3: Comparison between groups from study #2 (chapter 4) and clustered data experimental groups as well as analyzed genes.....	137
Table 6-4: Rand Indexes for clusters generated from data with the addition of gaussian noise. A Rand Index of 1 means complete agreement between matrices, and approaching zero means no association between matrices.....	145
Table 6-5: Cluster membership as a table for AF experimental 'phenotype'. Color of cells corresponds to their value of membership where $>0.75$ is red, $0.5 - 0.74$ is yellow, $0.25 - 0.49$ is green, $0.1 - 0.24$ is blue, and white is $<0.1$ . . For naming convention, M – mature, Y – young, the number is the experimental time point, then loading is indicated by a C – control, L – 0.1 Hz or Low, M – 1 Hz or Medium, and H – 3 Hz or High. ....	152
Table 6-6: Cluster membership as a table for NP experimental 'phenotype'. Color of cells corresponds to their value of membership where $>0.75$ is red, $0.5 - 0.74$ is yellow, $0.25 - 0.49$ is green, $0.1 - 0.24$ is blue, and white is $<0.1$ . For naming convention, M – mature, Y – young, the number is the experimental time point, then loading is indicated by a C – control, L – 0.1 Hz or Low, M – 1 Hz or Medium, and H – 3 Hz or High .....	156
Table 6-7: Membership of each cluster for the AF and NP with k-means clustering. ...	160

Table 6-8: Cluster membership as a table for AF genes. Color of cells corresponds to their value of membership where >0.75 is red, 0.5 - 0.74 is yellow, 0.25 - 0.49 is green, 0.1 - 0.24 is blue, and white is <0.1 .....	163
Table 6-9: Cluster membership as a table for NP genes. Color of cells corresponds to their value of membership where >0.75 is red, 0.5 - 0.74 is yellow, 0.25 - 0.49 is green, 0.1 - 0.24 is blue, and white is <0.1 .....	166
Table 6-10: Rand indices indicating similarities in memberships between sub-matrices (with each other and with the full data set). Indices were based on membership lists from an optimal run. ....	167
Table 6-11: Membership lists for Mature and Young AF and NP generated by clustering the sub-matrices .....	168
Table 6-12: Gene memberships for each experimental outcome cluster in the AF.....	170
Table 6-13: Gene memberships for each experimental outcome cluster in the NP.....	171
Table 6-14: Gene distance from centroids found for the full, mature and young full AF data set except the three genes 'held back'. The gene is expected to belong to the group it is closest in space to (smallest distance between the gene expression value and cluster centroid). The smallest value is in bold. Groups correspond to those shown in Table 6-7.....	173
Table 6-15: Gene distance from centroids found for the full, mature and young NP data except the three genes 'held back'. The gene is expected to belong to the group it is closest in space to (smallest distance between the gene expression value and cluster centroid). Groups correspond to those shown in Table 6-7 (NOTE: members are not the same between AF and NP).....	174
Table 6-16: Distances between test groups and cluster centroids found from experimental 'phenotypes' in the AF. The lowest value, and therefore cluster membership, is noted in bold. Groups correspond to those in Figure 6-6 .....	176
Table 6-17: Distances between test groups and cluster centroids found from experimental 'phenotypes' in the NP. The lowest value, and therefore cluster membership, is noted in bold. Groups correspond to those in Figure 6-7 .....	176

## List of Figures

Figure 1-1: Normal (L) and degenerated (R) human intervertebral disc. (Images courtesy of James Iatridis and Ian Stokes) .....	1
Figure 2-1: The intervertebral disc is composed of outer collagen layers (AF) and an inner gelatinous core (NP) .....	10
Figure 2-2: AF tissue. Green is collagen type VI, red is collagen type I. Blue is staining DNA of cells. Note the highly organized structure, and that the cells tend to line up along the fiber direction (indicated as along plane with arrow, and into the plane of the paper with a X. See appendix 1.....	12
Figure 2-3: IA tissue near the AF (A) and closer to the NP (B). Green is collagen type VI, red is collagen type I. Blue is DAPI staining (DNA of cells). Note the transition to less collagen type I, and more extensive pericellular matrices as compared to the AF. See appendix 1. ....	14
Figure 2-4: (Top) NP cells <i>in situ</i> stained with calcein-AM, which emits a green fluorescence in live cells. Note the cellular processes extending from the cells (white arrows). Scale Bar = 100 uM in horizontal direction, 5 um in vertical direction. (Bottom) NP cells stained <i>in situ</i> stained for Collagen type VI (green) with DAPI (blue, DNA stain). The cell processes seem to be composed at least partially of collagen type VI. Scale bar bottom left in red = 50 um.....	15
Figure 2-5: Representation of benefits and drawbacks of each intervertebral disc testing model. Each method of study has benefits and disadvantages. In general as the similarity to the <i>in vivo</i> case increases, the control one has over the boundary conditions and experimental inputs decreases .....	19
Figure 2-6: Obvious differences exist between porcine lumbar discs (L) and bovine caudal (R). Cross sectional geometries are different, along with different compositional profiles, with the porcine NP remaining highly gelatinous and the bovine more fibrous. Images are at different magnifications, making size not to scale. The porcine IVD shown (Lumbar) is approximately 3 inches in its greatest length whereas the bovine caudal disc is only 1 inch in diameter. ....	20
Figure 3-1: Timeline for mechanical intervention protocol. Daily loading consisted of Test 1, Dynamic Loading, and Test 2. A baseline static load (0.2 MPa) was applied for the remaining culture duration. The intervention protocol was repeated each day for 5 days of the 6 day culture period. Note: timeline is not to scale .....	56

Figure 3-2 : Sectioning orientations for histology and viability images. Tissue was oriented in two different planes to capture localized response to needle puncture injury (radial section) or a more global tissue response (sagittal section). Radial and sagittal sections were created for all groups tested..... 57

Figure 3-3 : Average  $\pm$  SEM nominal dynamic loading modulus for pre-load (top) and post-load (bottom) tests. A significant difference between groups or time points is indicated by sharing of a common symbol. .... 58

Figure 3-4: Average  $\pm$  SEM creep during the one hour dynamic loading protocol at each day. Significantly more creep was observed at all time points in the needle puncture groups than in the dynamic control group (star indicates a difference relative to all other groups at that time point). .... 59

Figure 3-5 : Viability images of OA (left) and NP (right) in the large needle group. Needle puncture regions are on top oriented radially (perpendicular to needle track, with needle track centered in field of view), control images are on bottom oriented sagittally ( the direction that would be perpendicular to the needle track if one existed). Dead cells are fluorescent and appear as red/white (white arrow), live cells are black (black arrow). Images are at 20X, scale bar = 100  $\mu$ m ..... 60

Figure 3-6: Representative histology images of needle puncture discs (top) and control discs (bottom) of the OA (L), IA (middle), and NP (R) revealing annulus fiber disruption in the needle group. Collagen stains red, proteoglycans blue, and cell nuclei black. Needle insertion sites were positioned in the center of the field of view. OA needle group image is of a large needle puncture group, IA and NP are of a small needle puncture. All images are at 2.5X, scale bar = 1mm. .... 61

Figure 3-7: Evidence of an increase in NP cell number and possible remodeling local to an insertion site in a large needle puncture disc. Image on left is a 2.5X, scale bar = 1mm. Boxed area on left is magnified on the right, image is at 20X, scale bar = 100  $\mu$ m. .... 62

Figure 4-1: Test protocol schematic detailing loading protocol (Top). Illustration showing tissue harvest protocol (Bottom). Note:schematic diagram not to scale..... 82

Figure 4-2: Average  $\pm$  SEM sulfate incorporation rates for all testing groups (OA – outer annulus, IA – inner annulus, NP – nucleus pulposus). A trend of increasing sulfate incorporation was seen in the annulus regions, but not in the nucleus. .... 83

Figure 4-3: Representative viability images at 20x magnification. black = live, white = dead. Scale bar in black = 400  $\mu$ m. Columns represent tissue regions (OA – outer annulus, IA – inner annulus, NP – nucleus pulposus) and rows represent test groups. No changes in cell viability were observed. .... 84

Figure 4-4: Average $\pm$ SEM nominal dynamic loading modulus for pre-load (top) and post-load (bottom) tests.....	85
Figure 4-5: Average $\pm$ SEM height loss for the one hour dynamic loading protocol. Significantly more height was lost at all time points in the high force dynamic loading groups than in the low force group. ....	86
Figure 4-6: Gene expression fold change results as average $\pm$ SEM for anabolic (aggrecan, collagen types I and II, versican), anti-catabolic (TIMP-1) (left column) and catabolic (MMP -2, -3, 13 and ADAMTS4) (right column) genes for tissue from annulus fibrosus (top row) and nucleus pulposus (bottom row) regions. Significant differences ( $p < 0.05$ ) between groups are marked with a * while significant differences from static controls (using a t-test with hypothesized mean of zero) are marked with a § symbol (found in low groups in the NP for collagen type I and MMP3). Note that low and high groups are normalized to tail matched static controls.....	87
Figure 4-7: Schematic of mechanical testing protocol. Discs were initially confined with 0.2 MPa. A one-minute test from 0.2 - 0.4 MPa was performed at 1 Hz. Then discs were loaded from 0.2 - 1 (LOW) or 2.5 MPa (HIGH) at 1 Hz for 1 hour. The 0.2 MPa static load was then returned to the disc to prevent swelling. NOTE NOT TO SCALE.....	88
Figure 5-1: GAG/DNA content (ug/ng) of the nucleus pulposus (top) and annulus fibrosus (bottom) after seven days. Values are shown as averages plus/minus SEM. Results for cells derived from young tissue are shown in black, mature cells in grey. Stars (*) indicate significantly lower amounts between age groups, bars – indicate significant differences between loading groups.....	106
Figure 5-2: Nitrite concentrations (uM) normalized to the number of constructs in each well of the nucleus pulposus (top) and annulus fibrosus (bottom) after seven days. Values are shown as averages plus/minus SEM. Results for cells derived from young tissue are shown in black, mature cells in grey. No significant differences were found between groups. ....	107
Figure 5-3: qRT-PCR data for nucleus pulposus cells. Results for cells derived from young tissue are shown in black, mature cells in grey. Values are shown as averages plus/minus SEM. Stars (*) indicate significantly lower amounts between age groups, bars – indicate significant differences between age groups, bars – indicate significant differences between loading groups.....	108

Figure 5-4: qRT-PCR data for annulus fibrosus cells. Results for cells derived from young tissue are shown in black, mature cells in grey. Values are shown as averages plus/minus SEM. Stars (\*) indicate significantly lower amounts between age groups, bars – indicate significantly lower amounts between age groups, bars – indicate significant differences between loading groups..... 109

Figure 6-1: Visual representation of clustering methods. The top two represent hierarchical methods, where data points are grouped into larger and larger clusters. Meaningful clusters can be isolated by cutting the clustering tree at a certain cluster number (4 for the top right image). The bottom two panels represent partitioning methods. In k-means, (bottom left) three optimal cluster centers are found (red circle with x) and each data point is chosen to belong exclusively to one or another group. In fuzzy c-means (bottom right) optimal cluster centers are found (red, blue, yellow circles with X) and each data point can belong to a combination of the cluster centers (green data belongs to red and yellow centroids)..... 113

Figure 6-2: Two clustering approaches were used; first experiments were clustered using their gene expression as a phenotype (L), and clustering genes that exhibit similar expression patterns between experimental conditions (R). In both simplified examples shown here, H and L indicate a ‘high’ or ‘low’ gene expression respectively. The data from the first two columns is represented as the x and y axis of the associated graph. In both cases, two groups were similar (row is highlighted with the same color) and the data points are shown graphically along with a circle representing they are ‘clustered’ ..... 116

Figure 6-3: Experimental flow chart..... 135

Figure 6-4: XB and DI validity measurements for AF k-means clustering of experimental 'phenotypes'. The optimal cluster number was found to be k=4 (shown with black line) ..... 141

Figure 6-5: XB and DI validity measurements for NP k-means clustering of experimental 'phenotypes'. The optimal cluster number was found to be k=6 (shown with black line) ..... 142

Figure 6-6: Cluster membership for AF experimental 'phenotype', where the optimal cluster number was determined to be k = 4. Each color corresponds to a different cluster (meaning each group with the same color belongs to the same cluster) Loading groups are the columns; age and time of sampling are the rows..... 143

Figure 6-7: Cluster membership for NP experimental 'phenotype', where the optimal cluster number was determined to be k = 6. : Each color corresponds to a different cluster (meaning each group with the same color belongs to the same cluster). Loading groups are the columns; age and time of sampling are the rows..... 143

- Figure 6-8: XB and DI validity measurements for AF k-means clustering of experimental 'phenotypes'. Three runs with perturbed data (blue, red and yellow) along with the original indices (blue) are shown. The optimal cluster number was found to be  $k=4$  in all cases (black line)..... 146
- Figure 6-9: XB and DI validity measurements for NP k-means clustering of experimental 'phenotypes'. Three runs with perturbed data (blue, red and yellow) along with the original indices (blue) are shown. The optimal cluster number was found to be  $k=6$  in all cases (black line)..... 147
- Figure 6-10: Cluster membership for AF experimental 'phenotype' (top) and NP 'phenotype' (bottom). The optimal cluster number was determined to be  $k = 4$  for the AF and  $k = 6$  for the NP. Each box corresponding to a group is divided into 4 slivers corresponding to perturbed data 1, 2, and 3, then the original data. Each color corresponds to a different cluster (meaning each group with the same color belongs to the same cluster). When repeated incidences of a particular cluster membership were found, the boxes were grouped (for instance, in the AF mature 7 control group had 4 slivers of green, which were grouped to be one big green Likewise, Young 7 day control in the AF had 3 slivers of red and one of blue, so the three reds were grouped and the blue was separate). Loading groups are the columns; age and time of sampling are the rows. Note the AF is represented with 4 colors, but for ease of interpretation between runs, the NP is in separate colors for separate clusters between runs unless the cluster membership was maintained for a full block for another group (for example mature 7 1 Hz and Mature 14 1 Hz share 'red' as mature 7 1 Hz membership was maintained throughout) ..... 148
- Figure 6-11: MPC, SC, S, XB indices for AF experimental 'phenotype' grouping. The optimal cluster number was found to be  $c = 4$ , indicated with a black line..... 150
- Figure 6-12: Cluster memberships for AF experimental 'phenotype'. Each color corresponds to a separate cluster. Fuzzy c-means allows for a membership in multiple clusters. O – mature (old), Y – young, the number is the experimental time point, then loading is indicated by a C – control, L – 0.1 Hz or Low, M – 1 Hz or Medium, and H – 3 Hz or High. .... 151
- Figure 6-13: MPC, SC, S, XB indices for NP experimental 'phenotype' grouping. The optimal cluster number was found to be  $c = 5$ , indicated with a black line..... 154
- Figure 6-14: Cluster memberships for NP experimental 'phenotype'. Each color corresponds to a separate cluster. Fuzzy c-means allows for a membership in multiple clusters. O – mature (old), Y – young, the number is the experimental time point, then loading is indicated by a C – control, L – 0.1 Hz or Low, M – 1 Hz or Medium, and H – 3 Hz or High. .... 155

Figure 6-15: XB and DI validity measurements for AF k-means clustering of genes. The optimal cluster number was found to be  $k=4$  (shown with black line)..... 158

Figure 6-16: XB and DI validity measurements for NP k-means clustering of genes. The optimal cluster number was found to be  $k=4$  (shown with black line)..... 159

Figure 6-17: MPC, SC, S, XB indices for AF gene grouping. The optimal cluster number was found to be  $c = 3$ , indicated with a black line. .... 161

Figure 6-18: Cluster memberships for AF genes. Each color corresponds to a separate cluster. Fuzzy c-means allows for a membership in multiple clusters ..... 162

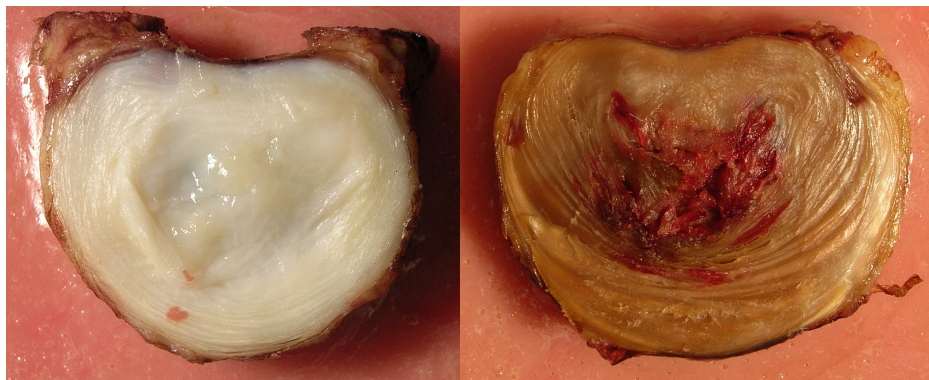
Figure 6-19: MPC, SC, S, XB indices for NP gene grouping. The optimal cluster number was found to be  $c = 5$ , indicated with a black line. .... 164

Figure 6-20: Cluster memberships for AF genes. Each color corresponds to a separate cluster. Fuzzy c-means allows for a membership in multiple clusters ..... 165



## **CHAPTER 1 Introduction**

The intervertebral disc (IVD) is a complex orthopaedic tissue that is located between the vertebrae in the spine. The IVD consists of four integrated biologically and structurally unique components; the annulus which is divided into an outer and inner component, the nucleus pulposus, and the cartilage endplates which serve as an interface between the IVD and the proximal and distal vertebrae. The complexity of the tissue structure, and its crucial role in providing spinal flexibility and load support, contributes to the risk for the IVD to be affected by a host of pathologies. One such pathology, degeneration of the IVD, is thought to be a contributor to low back pain (LBP).



**Figure 1-1: Normal (L) and degenerated (R) human intervertebral disc. (Images courtesy of James Iatridis and Ian Stokes)**

One study has shown LBP to affect approximately 80% of all Americans at some point during their lifetime (Andersson, 1998), with similar numbers for Canadians (Cote et al., 1998). A national health survey covering two years in France demonstrated that more than half of the population aged 30-64 years had experienced LBP in the previous year, with 17% of the survey population experiencing LBP for 30 days or more (Gourmelen et al., 2007). An increase in LBP incidence has been reported among those

performing heavy labor. A four-month study on underground miners in Ghana reported 67.2% of workers had experienced LBP in the past year, with 90% reporting the pain as being moderate to very severe (Bio et al., 2007). Likewise 72.8% of sewer workers in Vienna, Austria reported LBP during the previous 12 months, higher than the reported rate for neck pain (52.4%) and upper back (54.8%) indicating the lower back region as one particularly prone to injury (Friedrich et al., 2000). In a study of a rural Chinese population an increased risk of LBP was associated with farming, performing moderate to heavy labor, or exposure (current or former) to vibration (Barrero et al., 2006).

While LBP exists regardless of gender, some evidence points to increased prevalence in women. A French survey showed a statistically significant increase in reports of LBP, both as a one time occurrence (57.2% among women, 54% among men) and as recurring for 30 days or more over two years (18.9% among women, 15.4% among men) (Gourmelen et al., 2007). In a study of Iranian industrial workers, 27% of females and 20% of males reported an episode of LBP in a year (Ghaffari et al., 2006). In a rural Chinese population, an increased prevalence of LBP was found in women as compared to men across ages (25-64 years) (Barrero et al., 2006). In contrast, no association with gender was found in a survey of Canadian individuals (Cassidy, 1998).

The high rate of incidence is accompanied by large medical costs. In the United States in 1998 approximately \$90.7 billion in expenses were incurred by individuals with back pain, and 26.3 billion of total incremental expenditures were attributable to back pain (Luo et al., 2004). LBP is a common affliction, affecting people across ethnic, economic, and gender lines at enormous economic cost. Despite this clear impetus for

close examination, the mechanism of the spinal degenerative process is not known.

However, pathologies associated with the intervertebral disc have been implicated as a major contributor (Vernon-Roberts and Pirie, 1977, Battie and Videman, 2006).

One potential mechanism by which the intervertebral disc can contribute to LBP is through disc degenerative disease (DDD). A proposed mechanism for DDD induced back pain is that structural disruption of the IVD may result in stress concentrations developing in the outer annulus, where nerve innervation has been reported, thus triggering a painful stimulation of these nerves (Adams, 2004). Conflicting evidence on the influence of mechanical factors, such as occupations requiring heavy lifting, or long durations of truck driving, in contributing to LBP and DDD has been reported. Evidence pointing to a positive association between the level of lifestyle or occupational back loading and lower back pain (Videman et al., 1990, Evans et al., 1989, Frymoyer et al., 1983) or DDD (Dupuis, 1994). However, some studies suggest the correlation may be weak or non-existent between occupational mechanical loading and LBP (Videman and Battie, 1999) or DDD (Battie et al., 1995, Drerup et al., 1999). One complicating aspect to any study of the long-term effects of mechanical loading on the spine is the increased presentation of DDD with advanced age (Vernon-Roberts et al., 2007), which may mean a survey of occupational activities may reflect behavior at retirement rather than account of a lifetime of heavy mechanical exposures (Gibbons et al., 1995). Additional factors and pathologies that may contribute to back pain also include genetic (Battie et al., 1995) or lifestyle differences between people.

The development of a controlled model for the human intervertebral disc, providing the ability to address the role mechanical loading may have on the disc, and specifically what biological changes are associated with repeated mechanical loading, is considered a priority. The ideal model would be free of genetic, occupational or environmental factors (such as a non-smoker), motivating the use of an animal model. The animal model must be a close representation of the human disc with regards to biology and mechanics, and should allow for the simultaneous examination of many dependant variables. The ideal model for this would be an *ex vivo* animal model, which historically has not existed. The development of such a model, however, would allow for the application of realistic levels and modes of mechanical loading to a highly controlled sample population.

The role of the intervertebral disc in supporting and resisting applied loading to the spine, along with the observation of disorders associated with abnormal spinal loading, provide support to the theory that applied mechanical loading is crucial in maintaining the health of the intervertebral disc. As with other orthopaedic tissues, studies have sought to elucidate the connection between applied loading and the resulting biological changes that occur to the disc. However, it is still largely unknown how mechanical loads are transmitted to the cellular level, how cells sense mechanical loading, and what aspects of mechanical loading are important to the maintenance of a healthy intervertebral disc.

A variety of models have been used to study intervertebral disc mechanobiology. In addition to *in vivo* models, tissue level experiments, in which the intact intervertebral

disc is cultured, maintain normal cell-matrix interactions, which closely resemble the *in vivo* case. However, due to the non-linear and multiscale nature of mechanotransduction, equal magnitudes of applied stress at the tissue scale may result in different magnitudes of observed stress on the cellular scale. Cellular level experiments, in which cells are removed from the surrounding native tissue and encased in an artificial matrix, results in a highly reproducible and defined magnitude of stress applied to the cell at the expense of some possible mechanisms of cell mechanotransduction and the ability to directly extrapolate the results to the *in vivo* situation.

Another complication to the study of intervertebral disc degeneration is the long time scale typically required for degenerative signs to occur. Previous researchers have induced disc degeneration on a rapid time scale with methods such as chemical degradation or needle puncture injury, both of which have been found to induce degenerative changes in the affected intervertebral disc in an *in vivo* model. More recent studies have provided evidence for a rapid biological response to the needle injury, followed by a more prolonged accumulation of pathological changes. Structural changes induced by needle puncture may alter the ability for the intervertebral disc to resist an applied load, or simply cause a redistribution of disc stresses resulting in abnormal regional loading profiles.

**The overall goal of this work was to examine the biological response of the intervertebral disc to changes in the surrounding mechanical environment in a large animal model.** Two approaches were used to address this goal: first addressing the role of active mechanical loading in intervertebral disc extracellular maintenance and

turnover, and second addressing the ability for passively applied changes to the intervertebral disc mechanical environment to explain long-term biological changes observed in animal models of degeneration. The combined use of these two methods to alter the mechanical environment comprehensively addressed the ability for mechanical loading to influence biological homeostatic behavior as well as provide a model for mechanically induced pathological disc degeneration. The use of a large animal organ culture system is particularly relevant and of recent interest, as the bovine disc has been shown to more closely represent the behavior of human tissue than currently used animal models (Oshima et al., 1993) and few organ culture systems exist for the bovine IVD (Lee et al., 2006, Roberts et al., 2008). Finally, patterns in the gene expression profiles in response to mechanical loading and aging were identified and compared between organ culture and cell culture studies to identify potential new avenues of research.

**Hypothesis1: Needle puncture injury will lead to immediate and progressive alterations in disc mechanics and biology.**

**Aim 1:** This study utilized a bovine organ culture model to characterize the mechanical and biological response of the intervertebral disc to a needle puncture injury, a commonly used model of experimentally induced disc degeneration, thus providing a possible mechanism for *in vivo* injury induced disc degeneration models.

**Hypothesis 2: Dynamic loading applied to the intervertebral disc will stimulate cell biosynthetic response in a magnitude dependent manner.**

**Aim 2:** This study explored the interaction between mechanical loading and intervertebral disc cell signaling in situ. This study used an organ culture experiment that focused on the response of the intervertebral disc to load magnitude effects.

**Hypothesis 3: Dynamic loading applied to intervertebral disc cells will to stimulate cell biosynthesis in a frequency and age dependent manner.**

**Aim 3:** A cell culture study addressed frequency and age effects on the IVD response to mechanical stimulation. To control for the effects of varying matrix compositions between old and young animals, this study used a three-dimensional alginate cell culture system.

**Hypothesis 4: Clustering analysis can be used to find patterns in the intervertebral disc response to aging and mechanical loading over time. Further, the response of individual genes, and the response of the intervertebral disc to mechanical loading in an organ culture model, can be predicted by comparing with patterns found in a cell culture model.**

**Aim 4:** This study identified experimental groups that are linked by similar gene expression profiles and genes that are commonly linked by experimental protocols. Then, by applying an approach known as biclustering, the gene profiles of the linked experimental groups were clustered to identify the genes responsible for the differences

between groups. Finally, the predictive value of the developed clusters was examined by first finding the membership of genes not used in the clustering analysis, and second using the clusters to predict groupings from data from a mechanically loaded organ culture model.



## **CHAPTER 2 Background**

### **2.1 Intervertebral disc structure and biology**

Two of the primary functions of the spine are load support and flexibility (Adams, 2002), which are accomplished by a unique blend of structural components. The adult human spine is made up of 24 vertebral bodies, which serve as a non-flexible support system, separated by 23 intervertebral discs, which add flexibility and shock absorbing capacity to the overall spinal structure.

The intervertebral discs are composed of two structurally distinct regions, the annulus fibrosus (AF) and the nucleus pulposus (NP), which blend to create a third region, the transition zone or inner annulus (IA) (Figure 2-1). The disc is bounded superiorly and inferiorly by cartilaginous and bony endplates that integrate the disc structure to the vertebral bodies. The endplates, along with the annular periphery, provide the pathways for nutrient and water transport into and out of the disc. The disc is the largest avascular structure in the human body, making the endplate's role as a path for nutrient and water supply highly important (Urban et al., 1978). Overall the disc is largely acellular, with cells making up only approximately 1% of the total volume (Roberts et al., 2006).

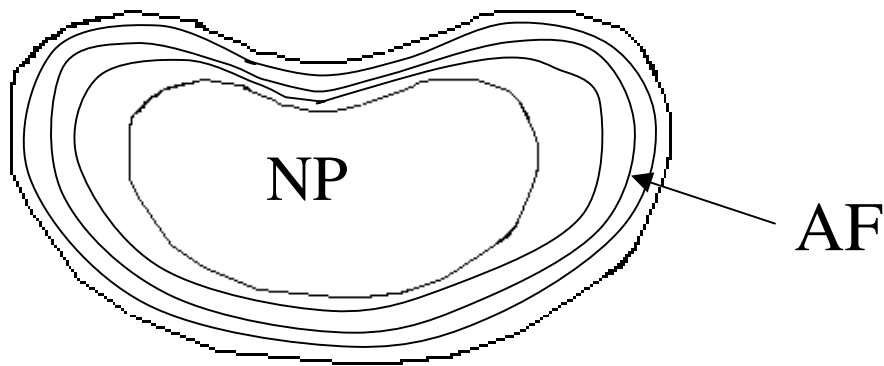


**Figure 2-1: The intervertebral disc is composed of outer collagen layers (AF) and an inner gelatinous core (NP)**

## **2.2 Intervertebral disc development**

In humans, the vertebral column begins to form at week 4, followed by the formation of somites from the mesenchyme (Roberts et al., 2006). In the rat at E15, the future IVD consists of bunched mesenchyme with little definition, however on E16 the notochord starts to bulge noticeably and some organ structure begins to form. At this stage, the IVD exists as three distinct regions, the AF, IA and NP. The AF consists of oriented fibroblastic cells predicated the deposition of the highly oriented AF structure, the IA exists as a contiguous part of the vertebral bodies possibly serving as an anchor the IVD to the developing vertebral bodies, and the NP is entirely composed of the notochord remnant. Although a source of debate, it is generally accepted that the nucleus pulposus is mostly the product of the notochord, which can be observed immediately postnatally, and disappears with age in a species dependent manner (Pazzaglia, 2006, Roberts et al., 2006, Pazzaglia et al., 1989). In contrast, cells in the annular regions are developed from the mesenchyme (Rufai et al., 1995). In species where the notochord remnant disappears, the

vacant notochordal space is replaced with more fibrous tissue reminiscent of the annulus fibrosus (Pazzaglia et al., 1989) however the mechanism and reason for the replacement is unclear.

Various molecular events are also essential for IVD development. For instance, Pax-1 was strongly expressed in the AF from 14.5 days post conception (dpc) into adulthood, patched (ptc) and Sonic Hedgehog were expressed strongly from 14.5 dpc into adulthood, and Noggin was localized to the endplate (DiPaola et al., 2005). Although the study of IVD development is more than 100 years old, questions as to how the complex structure develops and the importance of signaling between the notochord and mesenchyme remain unanswered.

### **2.3 The healthy intervertebral disc**

The AF is composed of highly structured fibers composed primarily of collagen type I, microfibrils (Yu et al., 2007) and elastin (Yu et al., 2002) that are further organized into concentric lamellar layers (Adams, 2002). The interlamellar space also contains linking elements of elastin and microtubules (Yu et al., 2007) and small amounts of proteoglycans. Fibers of the AF adopt orientations from plus-minus 62 degrees (from the vertical axis of the spine) at the outer edge of the annulus to plus-minus 45 degrees more centrally to support the developed loads (Cassidy et al., 1989). Cells of the AF have a sparse to nonexistent pericellular matrix (PCM), are primarily fibroblastic, elongated, and exist in oriented clusters with long aligned processes. Cells are often found running parallel to the fiber bundles of the AF, existing both between adjacent fiber bundles and embedded within them (Figure 2-2). The healthy AF exists primarily in

tension, resisting the internal swelling pressure developed by the NP under compression and the concentric laminar structure also provides excellent support for torsion and bending on the spine structure.

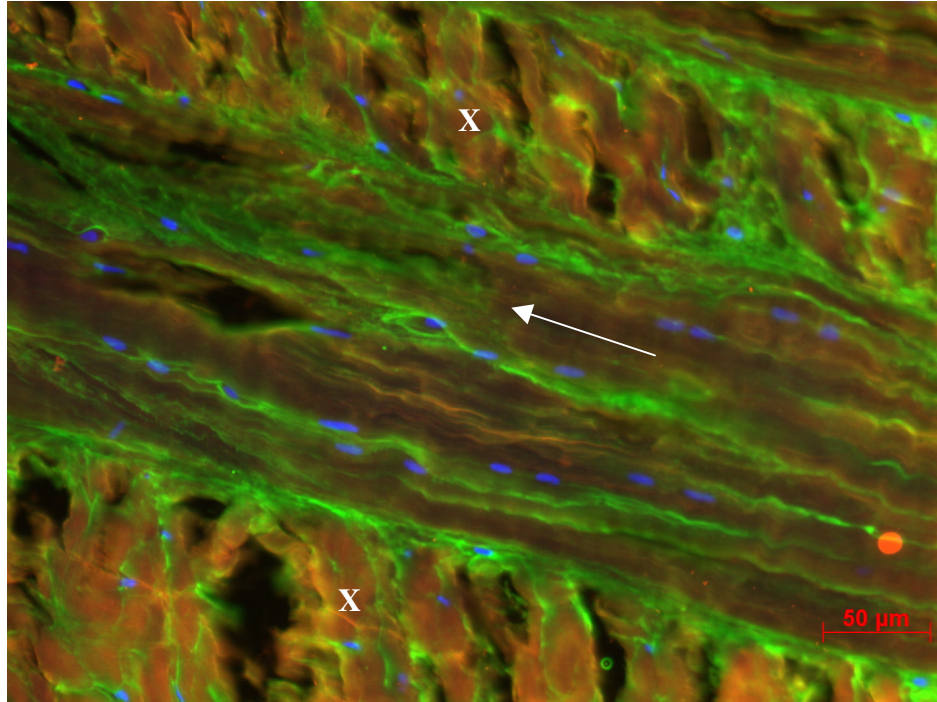


**Figure 2-2: AF tissue. Green is collagen type VI, red is collagen type I. Blue is staining DNA of cells. Note the highly organized structure, and that the cells tend to line up along the fiber direction (indicated as along plane with arrow, and into the plane of the paper with a X. See appendix 1.**

The IA mechanically behaves both to resist the swelling pressure of the NP and is in tension, as well as providing an element of resistance to axial compression. The dual role of this tissue is reflected in its extracellular composition of collagen type I and some collagen type II, along with microfibrils, elastin, and proteoglycans (Yu et al., 2007). Unlike the AF, where the ECM components are largely co-localized, elastin fibers and microfibrils are not co-localized. Whereas elastin fibers have been reported to primarily lie parallel to one another and form lamella reminiscent of the AF, microfibrils form a

network-like matrix, which is much less oriented. Elastin and microfibrils both exist in the PCM as well as in the ECM in this region (Yu et al., 2007). IA cells differ from those in the AF in that they are more rounded, form distinct lamellae rich in collagen and elastin, and produce more pericellular matrix (PCM) than AF cells (Roberts et al., 2006), (Figure 2-3).

The NP in healthy discs is proteoglycan rich, resulting in a high water content, and has a sparse network of randomly oriented fibers (Roughley et al., 2002). The fiber composition of the NP consists of collagen type II and elastin fibers existing primarily as a randomly oriented network in the extracellular matrix, while microfibrils exist in the pericellular matrix (Yu et al., 2007). The NP structure serves as the primary support structure for compressive loading in the disc. Unlike AF cells, NP cells are typically referred to as chondrocyte-like and are correspondingly rounded and contain an extensive PCM (Roberts et al., 2006). NP cells also have extensive cytoplasm filled cellular projections extending through the ECM (Figure 2-4), which may serve as mechanosensors.

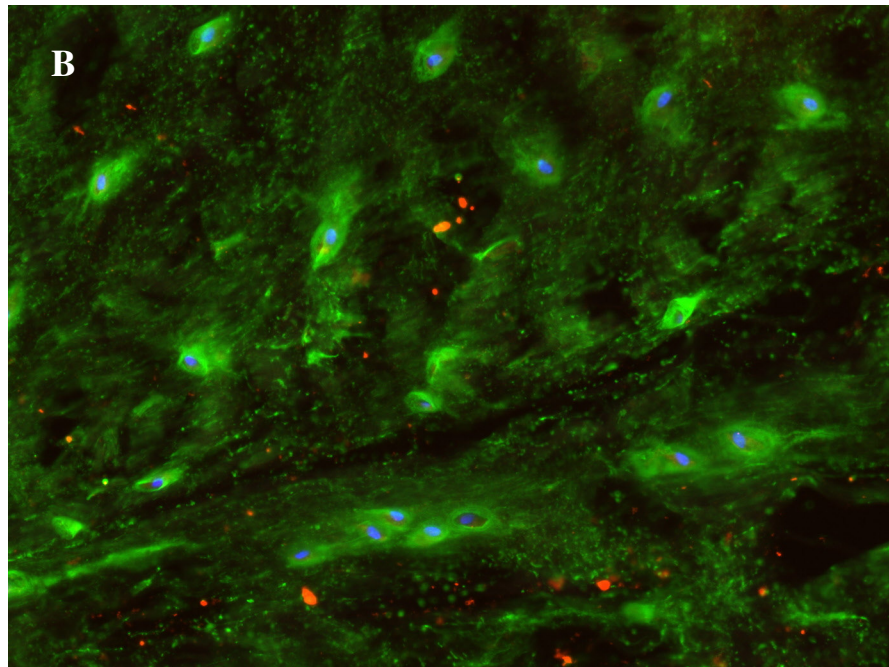
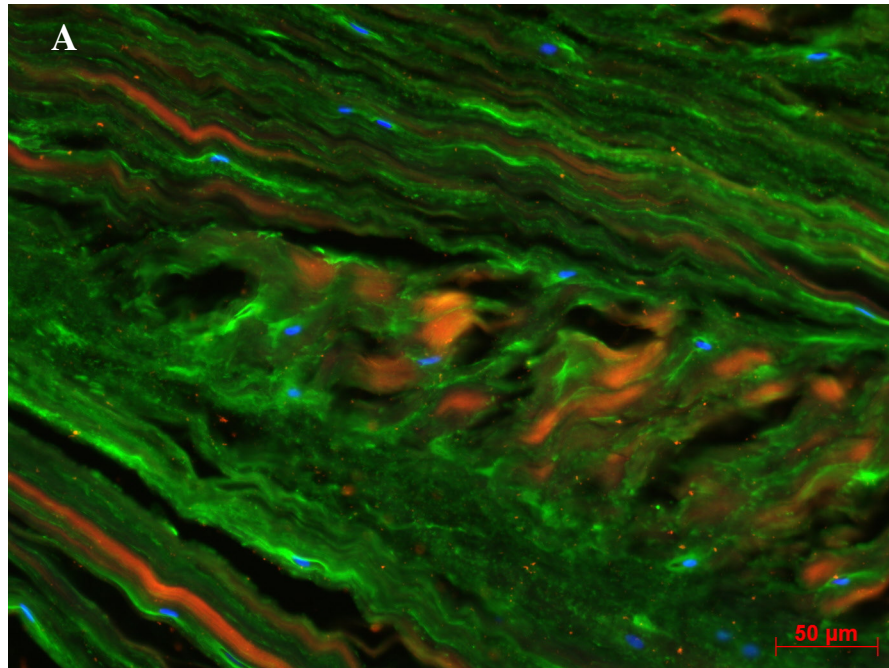


**Figure 2-3: IA tissue near the AF (A) and closer to the NP (B). Green is collagen type VI, red is collagen type I. Blue is DAPI staining (DNA of cells). Note the transition to less collagen type I, and more extensive pericellular matrices as compared to the AF. See appendix 1.**



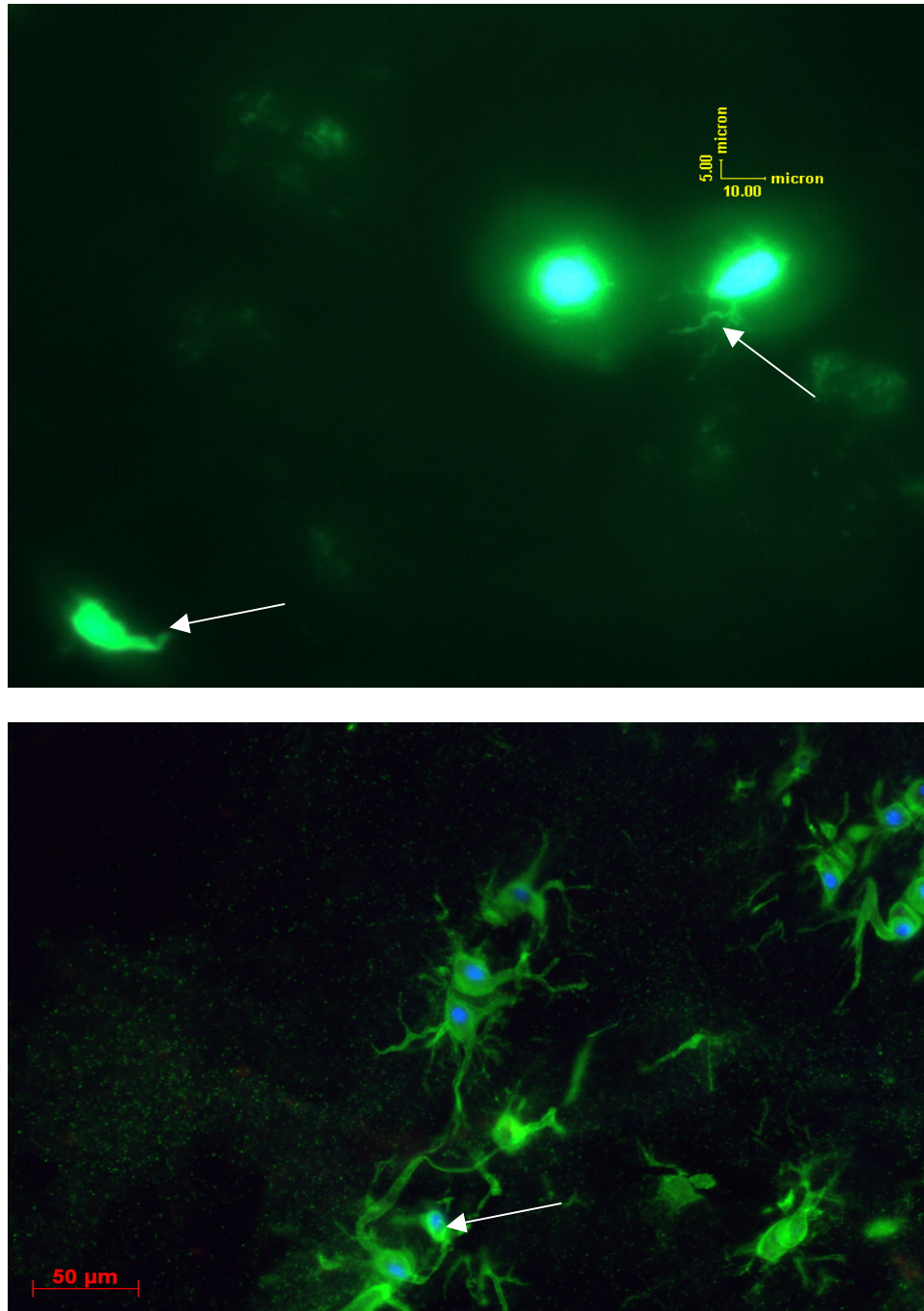


Figure 2-4: (Top) NP cells *in situ* stained with calcein-AM, which emits a green fluorescence in live cells. Note the cellular processes extending from the cells (white arrows). Scale Bar = 100  $\mu\text{m}$  in horizontal direction, 5  $\mu\text{m}$  in vertical direction. (Bottom) NP cells stained *in situ* stained for Collagen type VI (green) with DAPI (blue, DNA stain). The cell processes seem to be composed at least partially of collagen type VI. Scale bar bottom left in red = 50  $\mu\text{m}$ .

NC cells have been found to not proliferate in culture, and will produce only small amounts of collagen II in comparison with AF cells from the same animal (Poiraudéau et al., 1999). Despite the clear differences between NP, NC and AF cells, a unique cell-surface marker for NC cells has not yet been found. The age that NC cells disappear varies with animal species, and precedes intervertebral disc degeneration in humans. NC cells have been found to stimulate NP cell proteoglycan production, and evidence points to a secreted factor mediating this interaction (Erwin and Inman, 2006, Erwin et al., 2006). Further, 3-D alginate culture with cells from non-chondrodystrophoid (NC containing) animals was found to synthesize proteoglycan aggregates of lower molecular weight than for cultures from cells of chondrodystrophoid (non-NC containing) animals, resulting in higher proteoglycan content in alginate beads containing NC cells (Cappello et al., 2006).



## **2.4 Pathological changes associated with IVD degeneration**

Previous studies have shown that endplate fracture and subsequent calcification can precede changes in disc mechanics (Yoganandan et al., 1994). Endplate fracture and calcification theoretically disrupts disc homeostasis in two ways, one a cellular process and one a compositional process. Endplate calcification may disrupt normal nutrient transport (Urban et al., 2001) leading to a loss of cell viability and metabolism which could contribute to changed matrix turnover. Another possible disruption is theoretically a loss of NP material through the fracture site, which would be followed by a loss of proteoglycan content and subsequently a decrease in water content. The decrease in hydration would lead to an altered loading profile in which the NP is no longer able to support the same level of compressive loading, causing the less optimal case of AF tissue supporting these stresses (van Dieen et al., 1999).

While mechanical loading on the spine is needed to maintain spinal health, mechanical overload can cause permanent damage leading to disc degeneration (Stokes and Iatridis, 2004). Studying the spinal response to various levels of loading can illuminate the critical factors in differentiating a healthy load from a damaging one. Previous studies on spinal responses to loading conditions have largely used motion segments, or vertebrae-disc-vertebrae structures. In these cases, mechanics of the vertebral bodies and the endplate structure can obscure the response due to the intervertebral disc. Also, the viscoelastic properties of the disc (long time constants) dictate long mechanical testing times, which are performed in nutritionally deprived conditions, (usually after freezing and without glucose which is needed for cell viability

and metabolism (Bibby and Urban, 2004). Examining the biologic response of the disc to such loading is thus made impossible.

An important parameter that contributes to disc degeneration may be cell death. Loss of cell viability should lead to a decrease in matrix biosynthesis, which in turn could lead to disc degenerative changes. Two types of cell death have been identified in the IVD, necrosis and apoptosis (Bibby et al., 2002, Bibby and Urban, 2004, Lotz and Chin, 2000, Risbud et al., 2003). Necrosis is the means by which cells die due to a large insult, either mechanical or toxic, and is characterized by cell swelling and lysis, and can trigger an inflammatory response (Kroemer et al., 1998). Apoptosis is an active, energy requiring, means of programmed cell death, which will occur under normal physiologic conditions (Grogan et al., 2002). Past studies have focused on the *in vivo* apoptotic response to static loading (Lotz and Chin, 2000), *in vivo* viability response in scoliotic discs (Bibby et al 2002), viability in nutrient deprived conditions (Bibby et al., 2002, Bibby and Urban, 2004, Horner et al., 2002) and cell viability in organ culture systems with static loading (Risbud et al., 2003).

## **2.5 Intervertebral disc research**

Four model types currently exist in the study of the intervertebral disc. The first is to examine the intervertebral disc *in vivo*, typically using small animals such as mice, rats, or rabbits as a model. The second is *ex vivo* organ tissue culture, which has been performed with larger animals such as sheep and cows, but also with rabbits, mice and rats. The third is *ex vivo* tissue culture, which has largely been performed with bovine and

human tissue. Finally, in vitro cell culture which has been performed on many cell sources including rats, mice, pigs, cows and humans.

For example, while in vivo models most closely represent the in vivo state of the IVD, it is extremely difficult to introduce chemical growth factors in a reproducible and consistent manner to the entire IVD structure, and the inverse statement is true for cell culture (Figure 2-5).

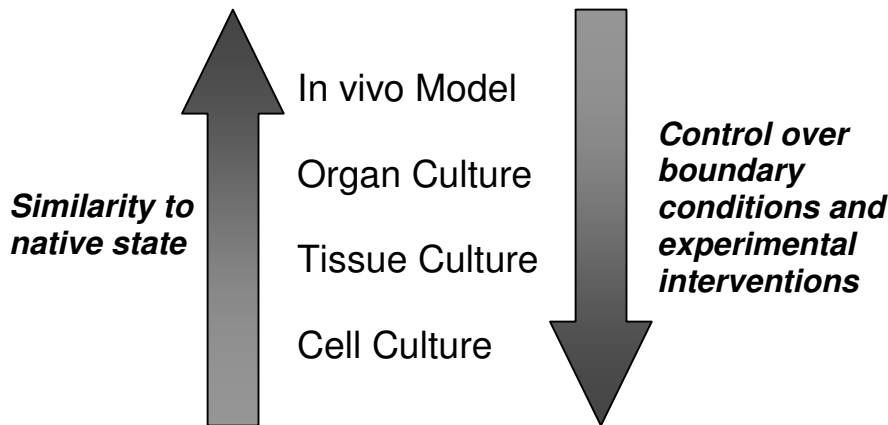


**Figure 2-5: Representation of benefits and drawbacks of each intervertebral disc testing model. Each method of study has benefits and disadvantages. In general as the similarity to the *in vivo* case increases, the control one has over the boundary conditions and experimental inputs decreases**

As with most biological systems, much of the research on the intervertebral disc has involved the use of animal tissue. As the study of the biology and mechanics of the intervertebral disc has progressed, closer scrutiny of the relevance to the human intervertebral disc has become necessary. Three main considerations are important when evaluating the ability of an animal model to represent the human case. First the geometric and biomechanical properties of the intervertebral disc, both of which are related to the disc structure. Second, the cellular phenotype and biosynthetic rates of the IVD must be considered, as they will affect the relevance of conclusions drawn from biological assays.

Finally, the transport properties and matrix composition profile are significant, as they impact (and are impacted by) the biology and biomechanics of the IVD.

From a biomechanical standpoint, the geometry of the disc influences the stress profile developed across the cross-section of the disc. The aspect ratio, or the ratio of the diameter to height, also will affect the ability of the disc to develop large hydrostatic forces in the NP in response to an applied load. Differences exist in both aspects between species, obviously scaling issues develop as an animal's size increases or decreases, but additionally caudal discs will generally be circular in cross section whereas lumbar discs will be more 'kidney-bean' shaped (O'Connell et al., 2007) (Figure 2-6).

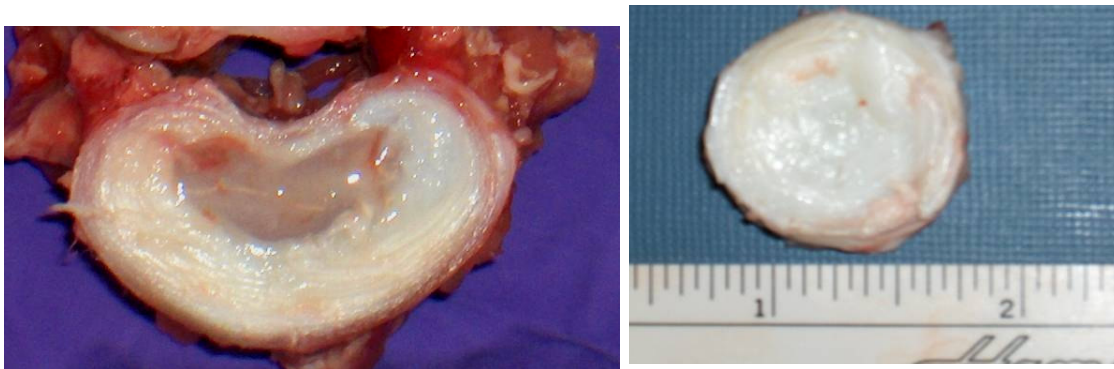


**Figure 2-6: Obvious differences exist between porcine lumbar discs (L) and bovine caudal (R). Cross sectional geometries are different, along with different compositional profiles, with the porcine NP remaining highly gelatinous and the bovine more fibrous. Images are at different magnifications, making size not to scale. The porcine IVD shown (Lumbar) is approximately 3 inches in its greatest length whereas the bovine caudal disc is only 1 inch in diameter.**

Another factor that could influence the way applied loads are transmitted is the shape of the disc at the endplate junction, which is known to vary between species (Alini et al., 2007). Inherent flexibility in the spine varies along the length of the spine

(generally greater in the thoracic than the lumbar region, for example) and also between species (Alini et al., 2007), which can affect the physiological relevance of an applied loading regime.

The biology of the IVD varies quite significantly both between levels (Wiseman et al., 2005, Melrose et al., 1994) and between species. The most obvious difference existing between animal models and a human disc is the existence of notochord cells in the nucleus pulposus. In humans, the notochord remnant slowly disappears, and is typically absent by 4-10 years of age (Alini et al., 2007). This is also the case in cows and sheep (Hunter et al., 2003). However, some species such as the mouse, rat, cat, pig, and rabbit, retain the notochord cells long into adulthood (Hunter et al., 2004). Dogs fall into both categories, where the notochord is absent in some species, and retained in others, at maturity. A highly gelatinous NP also characterizes species retaining the notochord, whereas the NP is more fibrous where the notochord has disappeared (Figure 2-6). The structural difference associated with this cellular phenotype transition has led some researchers to speculate that the notochord is responsible for the maintenance of the high proteoglycan and low collagen content of the intervertebral disc.

Many reviews have focused on the relevance of the bovine disc to the human lumbar disc. Oshima determined the biosynthetic rate, proteoglycan, collagen, and water content profiles were similar between human lumbar and bovine caudal across the cross section of the disc (Oshima et al., 1993). Another study found similar profiles of collagen type II and DNA content in addition to validating water content and proteoglycan content similarities between human lumbar and bovine caudal discs

(Demers et al., 2004). Demers also compared old and young human lumbar and bovine caudal IVDs and found the young bovine IVD to be a good representation of a less than 15 year old human disc, while older bovine discs are good representation of a 15 to 40 year old human lumbar disc (Demers et al., 2004).

### **2.5.1 In vivo models**

In vivo studies offer the benefit of modeling the physiologic case, leaving the IVD in its normal placement among the vertebrae and exposed to native biochemical and mechanical signals. Normal musculature, ligaments, and tendon attachments are maintained, along with all normal nutrient and biochemical signaling factors and pathways. Negatives associated with in vivo testing include ethics, cost, difficulty extrapolating the usually small animal results to the human condition, and the difficulty in isolating the response due to the mechanical loading from results due to other confounding factors (such as an inflammatory response or the response of the surrounding vertebral bone or musculature to the experimental factor). In addition the lack of direct control over the nutrient boundary conditions complicates studies of growth factors or other chemical inputs.

#### **2.5.1.1 Relevant research**

Basic science studies on the intervertebral disc environment and biology have led to important findings as to the delicate state of the normal and degenerated intervertebral disc. In vivo disc nutrition (Urban et al., 1977) and oxygen tension (Ejeskar and Holm, 1979) studies were both performed in a canine model. Biosynthesis and metabolism were also studied using  $^{35}\text{S-SO}_4$  in the mouse (Venn and Mason, 1983). The effect of

dehydration on disc hydration, and the effects on compressive stiffness was studied in a rat model (Han et al., 2001). In vivo studies on stimulatory and inflammatory mediators have also led to better understanding of IVD biology and pathology. For example, the effect of TNF-alpha as a possible mechanism of chemically mediated pathology following NP herniation was studied in vivo (Igarashi et al., 2000) as well as the effect on LMP-1 on BMP regulation in a rabbit model (Yoon et al., 2004). Rand et al., 2001 explored pathways of inflammation by investigating the recruitment of macrophages by nucleus pulposus cells in a murine model (Rand et al., 2001). Anderson et al., 2005 found a fibronectin fragment to be stimulatory for IVD degeneration in a rat model (Anderson et al., 2005). Other studies have explored complications from spinal surgery or development to affect the health of the intervertebral disc. The effect of infection on the development of the spine was examined in an ovine model (Walters et al., 2005) and later the penetration of antibiotics into the disc after IV injection was examined (Walters et al., 2006). Aebli et al., 2006 studied the thermal profile of an intervertebral disc when adjacent vertebrae were undergoing vertebroplasty (Aebli et al., 2006). Also, Forslund et al., 2006 examined ultrasound to promote herniated material resorption (Forslund et al., 2006).

In vivo studies on disc degeneration have also proved instrumental in understanding the development and course of IVD pathology. Two categories of disc degeneration exist, those occurring spontaneously in some animals, and those experimentally induced. Spontaneously occurring disc degeneration include sand rats (Moskowitz et al., 1990) normal aging in baboons (Lauerma et al., 1992) as well as a

host of mouse gene knockout models (Aszodi et al., 1998, Lettice et al., 1999, Madsen et al., 2002, Sahlman et al., 2001). Experimentally induced disc injury studies include chymopapain injected discs performed in canines (Wakano et al., 1983, Nitobe et al., 1988, Lu et al., 1997, Bradford et al., 1984) also extended to porcine discs (Keller et al., 1988), rats (Norcross et al., 2003) and sheep (Sasaki et al., 2001). Chemonucleolysis was also studied in humans (Leivseth et al., 1999). Studies have also introduced degeneration in vivo using stab (Kaigle et al., 1998, Kaigle et al., 1997, Kaigle et al., 1995, Osti et al., 1990) needle puncture (Aoki et al., 2006, Masuda et al., 2005), direct endplate rupture (Cinotti et al., 2005) and injection of material (BRD-U) (Zhou et al., 2007). Mechanically induced injury models have also been developed in a variety of animal models. Injury was induced using compression in a mouse-tail model (Hsieh and Lotz, 2003, Lotz et al., 1998) a rat model (Iatridis et al., 1999, MacLean et al., 2003) and a rabbit model (Kroeber et al., 2002, Guehring et al., 2005, Omlor et al., 2006). The study of disc compression induced degeneration followed by distraction was performed in the rabbit (Kroeber et al., 2005). Likewise proteoglycans and collagen were studied in a canine model of in vivo compression (Hutton et al., 1998, Hutton et al., 2000) and tail suspension (simulated weightlessness in rats (Hutton et al., 2002). Injury has also been induced using torsion to a rabbit model (Hadjipavlou et al., 1998, Hadjipavlou et al., 1998), by bending in a mouse model (Court et al., 2001) and by kyphotic deformity and fusion in a sheep model (Oda et al., 1999). Mechanical stress caused narrowing of disc space in lumbar section of rats (Neufeld, 1992). The response to dynamic mechanical loading has also been studied in vivo, including in pigs (Ekstrom et al., 2004, Ekstrom et



al., 1996), rat (MacLean et al., 2005, Maclean et al., 2004, MacLean et al., 2003) and mice (Walsh and Lotz, 2004, Ching et al., 2004, Ching et al., 2003), including a force cell design for an implant was examined in a baboon (Ledet et al., 2000).

Interventions to repair the disc have almost exclusively implemented in vivo animal models and have included repair by surgical instrumentation (Allen et al., 2004, Bass et al., 2006, Cunningham et al., 2002, Hu et al., 2006, Kadoya et al., 2001, Krijnen et al., 2006, Lowe et al., 2005, Nau et al., 2007, Takahata et al., 2003, Vuono-Hawkins et al., 1994) by chemical intervention (Karppinen et al., 1995) such as FGF (Minamide et al., 1999), OP-1 (An et al., 2005, Masuda and An, 2006, Miyamoto et al., 2006, Imai et al., 2007, Imai et al., 2007), GDF-5 (Chujo et al., 2006)(BMP2) (Huang et al., 2007) and PRP (Nagae et al., 2007), by gene therapy (Leo et al., 2004, Nishida et al., 2006, Nishida et al., 1999, Nishida et al., 1998, Riew et al., 2003, Sobajima et al., 2004, Wallach et al., 2003, Walsh et al., 2004, Yoon, 2004, Zhan et al., 2004) and autologous and allograph cell implantation (Luk et al., 2003, Okuma et al., 2000, Ledet et al., 2002, Gorenssek et al., 2004, Sakai et al., 2005, So et al., 2007). Revell et al., 2007 affected repair using injectable polymers in a pig model (Revell et al., 2007). Diagnostic techniques have used against keratin sulfate in the mouse (Kairemo et al., 2001). A study of pain relief from herniated NP was also performed in rabbit (Iwatsuki et al., 2005, Hashizume et al., 2007).

### **2.5.2 Organ culture**

The application of an intervertebral disc organ culture model allows the examination of the mechanical and biologic response of the disc to loading conditions. This approach has a few benefits over other cases. First, the ex vivo state aids in the

monitoring of environmental factors, such as the geometry of loading surfaces and the introduction of cytokines, lending a closer control over experimental conditions while retaining the in situ environment (cell-matrix interaction is maintained). Second, larger discs, which are potentially more closely representative of the human case, can be studied allowing for multiple measurements on adjacent tissue. Tissue swelling can be constrained by the application of an external load (Lee et al., 2006, Korecki et al., 2007), which will maintain the normal intervertebral disc structure and composition profile. Finally, the approach is more ethically feasible and a large number of specimens can be obtained.

While an organ culture model does not allow an exact in vivo stress/strain simulation, controlled investigation of loading or injury induced response of cells, tissue matrix, and interactions between these two can be achieved. The use of organ culture models in intervertebral discs is relatively new in practice, and few thus far have examined mechanical responses of the disc to loading, which define tissue functionality. Instead, these systems have mostly focused on the biological response to loading and culture conditions through metabolic and viability assays. In contrast, the technique has been used extensively in cartilage tissues, both with and without the underlying subchondral bone, to study the response of tissues to impact loading, dynamic loading, and static loading eg: (Duda et al., 2001, Jeffrey et al., 1995, Kurz et al., 2001, Milentijevic et al., 2003, Morel and Quinn, 2004, Quinn et al., 1998).

### 2.5.2.1 Relevant research

The main concern in IVD organ culture is the constraint of the excised IVD tissue. With no boundary in place, the nucleus pulposus often will swell to the point where it dislodges from the annulus, or normal disc architecture is lost. The main strategies to overcome this are to retain the endplates on the IVD, apply an osmotic pressure to limit swelling, or to apply an external load to the disc to maintain swelling pressure in the NP.

Perhaps the most challenging method is retaining the endplates, especially as the size of the animal model increases. This is due to a few factors. First, the thickness of the cartilage endplate varies between species, making it necessary to retain some of the bony endplate in many cases. Secondly, and most importantly, the endplate is a primary nutrition route for the IVD, with many capillary buds allowing for nutrient transport. Post-mortem, reports of impaired endplate route nutrition (Lee et al., 2006, Gantenbein et al., 2006) have been attributed to such clogging, leading researchers set on retaining endplates in a large animal model to resort to whole animal heparinization (Gantenbein et al., 2006) which is not always feasible. For this reason, many of the explant models retaining endplates have been developed in small animal models, where endplates can be more effectively cleaned and nutrition is not as easily compromised. Studies on the endplate have focused endplate transport in a sheep model (Ayotte et al., 2001) and on mechanical compression induced apoptosis in the endplates of mouse IVD organ cultures (Ariga et al., 2003, Risbud et al., 2003) established a rat whole organ culture model which maintained NP cell viability for 1 week, later (Risbud et al., 2006) applying this

model to the study of the effects of TGF beta 1 and 3 on the ERK signaling pathways in the nucleus pulposus. Kim et al., 2005 examined the resorption of the NP in a rat organ culture system after endplate injury, providing support for a theory that the notochordal cell disappearance is related to such injury and the resulting cell population is derived from the endplates (Kim et al., 2005). Lim et al., 2006 also developed a rat organ culture system able to retain cell viability for 14 days (Lim et al., 2006). Haschtmann et al., established a rabbit IVD culture model (Haschtmann et al., 2006) and examined the response of a rabbit organ culture model to diurnal osmotic loading for 28 days (Haschtmann et al., 2006).

The second most commonly used strategy in organ culture is to constrain swelling using an applied load. Lee et al., 2006 established a model for bovine intervertebral disc tissue to constrain swelling by the application of a static compression load (Lee et al., 2006). Later studies expanded on this concept by comparing the effects of a static and diurnal load on the maintenance of water, gag and cell viability of the IVD (Korecki et al., 2007). Takada et al., 2004 cultured IVD tissue without endplates with macrophages to examine IL-6 production (Takada et al., 2004).

Studies on the mechanobiology of the IVD in organ culture have been performed in a variety of ways. Researchers have examined the effect of hydrostatic loading (Chiba et al., 1998, Risbud et al., 2003), static compression (Ariga et al., 2003, Lee et al., 2006), and dynamic osmotic loading (Haschtmann et al., 2006) and compressive loading (Korecki et al., 2007) on the intervertebral disc. Thus far, no studies on dynamic compression loading have been performed in IVD organ culture.

### **2.5.3 Tissue culture**

Like organ culture, tissue culture involves studying the intervertebral disc *ex vivo* while maintaining cell-matrix interactions. However, unlike organ culture, the tissue is typically cut into pieces, and often the NP and AF are separated from each other. In this model system tissue swelling is often unconstrained and mechanical function of the entire structure is lost. This model system has proved to be quite useful for studying normal and degenerated human tissue, as small samples of tissue are easier to obtain from a surgical procedure than an entire intact IVD.

#### **2.5.3.1 Relevant research**

One main research thrust for tissue culture has been on metabolism and biosynthesis of the IVD, which has been examined in human tissue (Oegema et al., 1979, Bayliss et al., 1988, Liu et al., 1991, Maroudas et al., 1975) and experimentally modified by lactate and pH concentration in bovine and human tissue (Ohshima and Urban, 1992). Bovine disc tissue was also examined for biosynthetic rates and compared to human discs (Ohshima et al., 1995). Horner et al., 2001 studied the effect of nutrient supply on the viability of nucleus pulposus cells (Horner et al., 2002). Nemoto et al., 1997 examined MMP production in normal and degenerated human IVD tissue (Nemoto et al., 1997).

A second main avenue of tissue culture research is on herniation of NP material. The effect of MMP-3s on the resorption of herniated NP material (Kato et al., 2004) the ability for such treated tissue to attract macrophages (Haro et al., 2002) and the release of TNF-alpha by MMP-7 treated tissue (Haro et al., 2005). Kang et al., 1996 examined the

MMP, NO, IL-6, and PGE2 production of spontaneously herniated NP tissue (Kang et al., 1996).

Other studies have focused on mechanical loading on IVD tissue, the effects of growth factors, and interaction with other cells. Ishihara examined the effect of hydrostatic loading on biosynthesis using human and bovine disc explants (Ishihara et al., 1996). The effect of osmolarity was also examined in bovine NP tissue (Ishihara et al., 1997). Maynard et al., 1998 studied the effect of 2 weeks of hypergravity on the AF of rat IVDs (Maynard, 1998). Le Maitre et al., 2004 studied cell and tissue function up to 21 days in culture (tissue) where the tissue was either unconstrained or constrained to limit swelling, finding constrained culture was similar to control tissue but unconstrained culture had dramatic differences from freshly harvested tissue (Le Maitre et al., 2004). Thompson et al., 1991 examined the effect of growth factors on canine IVD tissue (Thompson et al., 1991). Li et al., 2000 examined the effect of IVD material on the behavior of osteoblast cells in a direct contact and co culture model (Li et al., 2000).

#### **2.5.4 Cell culture**

Cell culture requires removing the cells from the native IVD matrix. Typically this is accomplished through an ECM digestion using cocktails of enzymes such as collagenase, dispase, or pronase protease. The isolated cells can then be seeded onto tissue culture plastic for 2-D examination of cell behavior, or onto an artificial matrix for 3-D culture. A large host of different artificial matrices exist, many of which have been utilized for tissue engineering approaches in various tissues. The choice of culture system has implications for the behavior of the cells, both as far as maintenance of

normal cell phenotype as well as how efficiently experimental factors such as mechanical loading or introduced chemical factors are passed from the matrix to the cell.

#### 2.5.4.1 Relevant research

Normal biosynthesis has been studied in cell culture to further define the behavior of IVD cells and to compare and contrast differences between NP, AF, IA and even articular chondrocytes. For instance, the secretion of secretory leucine proteinase inhibitor by IVD cells and articular cartilage chondrocytes (Jacoby et al., 1993), the differences in proteoglycan epitopes secreted by encased ovine IVD cells into alginate AF, IA and NP (Melrose et al., 2000, Melrose et al., 2003, Melrose et al., 2001) and the secretion of factors from the mouse IVD NP cells in culture (Rand et al., 1997) have all been studied, with the latter study finding basal secretion of IL-6 and -10 but not -1 *in vitro*. Chiba et al., 1998 studied the ECM composition created by IVD cells in alginate (Chiba et al., 1998) with later studies also examining the ECM from cultured sheep NP (Sun et al., 2001), rabbit NP (Gan et al., 2003, Gan et al., 2003), and canine IVD cells (Masuda et al., 2002) and normal, degenerated, and scoliotic human IVD (Stern et al., 2004). Other cell culture studies have supported *in vivo* models. Chiba et al., 2006 compared the effect of chemonucleolysis by chondroitinase ABC and chymopapain, finding chymopapain treatment to more dramatically affect the ability for the cells to restore their ECM (Chiba et al., 2006). Ichimura et al., 1991 also examined factors affecting the proteoglycan, collagen and DNA content of rat IVD cells in culture (Ichimura et al., 1991).

Another research topic addressed by cell culture studies has been the effect of stimulatory or inhibitory factors to affect IVD cells. Shinmei et al., 1988 studied the effect of recombinant IL-1 on the proteoglycan content of AF and NP cells from the rabbit cultured in vitro (Shinmei et al., 1988), later built upon by other researchers (Osada et al., 1996, Jimbo et al., 2005). Other stimulatory factors examined have included ‘substance P’ (Ashton and Eisenstein, 1996) a synthetic peptide of link protein (Gruber and Hanley, 2003) and notably OP-1 (Zhang et al., 2004, Takegami et al., 2002) and GDF-5 (Wang et al., 2004), both of which later were applied to in vivo models to repair degenerated discs. Additionally, Yoo et al., 1992 examined suppression of proteoglycan synthesis in cultured canine IVD cells by anti-inflammatory cocktails (Yoo et al., 1992). Pattison 2002 examined the production of MMP2 in NP cells in alginate with TGF-beta and IL-1 (Pattison et al., 2001). Kim et al., 2003 showed nicotine to inhibit collagen II and proteoglycan synthesis in the IVD (Kim et al., 2003). Similarly, Akmal et al., 2004 studied the response of IVD cells to nicotine and found a general decrease in DNA, collagen and proteoglycan content in response to the application of nicotine (Akmal et al., 2004). Gruber et al., 2004 found AF cells in 3D culture from degenerated discs could be modified with cytokines to produce extracellular matrix (Gruber et al., 2004). Aota et al., 2006 studied the effect of lipopolysaccharide (LPS) on bovine NP and AF cells and articular chondrocytes, finding different responses between all three cells, reinforcing the important observation that NP cells are not the same as articular chondrocytes (Aota et al., 2006). Finally, introducing a possible mechanism for nerve ingrowth into the IVD, a



recent study found pro-inflammatory cytokines to stimulate the expression of nerve growth factor by IVD cells (Abe et al., 2007).

Investigation into artificial matrices and how they affect IVD cells has also been an important contribution to the future of intervertebral disc tissue engineering, as well as characterizing the varying matrices and their ability to house IVD cells in such a way that they retain normal in vivo characteristics. Lee et al., 2001 cultured cells as pellets and found the method to be feasible and applicable to future studies (Lee et al., 2001). The prevalence of alginate, agarose and collagen scaffolds in the literature has inspired some researchers to carefully characterize their ability to maintain IVD cell phenotype.

Maldonado et al., 1992 characterized the metabolism of canine IVD cells cultured in 3D microspheres of alginate (Maldonado and Oegema, 1992). Gruber et al., 1997

investigated the responsiveness of IVD cells in 3D culture in either alginate or agarose culture, and the cell response to TGF beta and later looked a variety of matrix substrates on the behavior of IVD cells (Gruber et al., 1997). The mechanical properties of the alginate as well as the encased cell constructs were also examined (Baer et al., 2003).

Kluba et al., 2005 studied the effect of culture system and the state of the donor cells on the resulting efficacy in culture (Kluba et al., 2005). New scaffolds have also been developed and characterized. For instance, IVD cells on bioactive glass (Gan et al., 2000), a gelatin/chondroitin-6-sulfate polymer scaffold (Yang et al., 2005), Atelocollagen (Sakai et al., 2006) and chitosan based scaffolds (Roughley et al., 2006) for induce NP cell repair have all been examined. Hamilton et al., 2006 created an improved nucleus pulposus to cartilage endplate interface through culture (Hamilton et al., 2006). Johnson

et al., 2006 studied the effect of substrate topography on creating aligned scaffolds for AF cell repair, finding culture of AF cells on grooved PCL scaffolds caused the AF cells to align (Johnson et al., 2006).

Mechanical stimulation applied to IVD cells has also led to observations on IVD cell responsiveness without the surrounding tissue matrix. Iwashina et al., 2006 and Miyamoto et al., 2005 studied the effect of low intensity pulsed ultrasound (LIPUS) on IVD cells cultured in alginate, finding the cells were stimulated to proliferate and metabolism (as measured by radioactive tracers) increased (Miyamoto et al., 2005, Iwashina et al., 2006). Static compression as studied in porcine cells encased in alginate (Chen et al., 2004). Other researchers have studied the effect of hydrostatic pressure on porcine and rabbit IVD cells cultured in alginate, finding a frequency of 5 Hz to disrupt protein metabolism (Kasra et al., 2006, Kasra et al., 2003). The effects of hydrostatic pressure have also been studied in bovine and human IVD cells in a collagen gel (Neidlinger-Wilke et al., 2006).

## **2.6 Summary**

Study of the intervertebral disc is complicated due to inhomogeneity in tissue structure and cell type across the cross-section of the disc. The bovine intervertebral disc was chosen, as it is a good model for the tissue structure and cell type and behavior of the human lumbar intervertebral disc. In general, careful consideration must be given to the appropriate culture system to address the hypotheses of a study. This body of work utilizes both organ and cell culture models to explore the role of mechanics, aging, and time on the biological and mechanical behaviors of the intervertebral disc. The use of

organ culture facilitates the simultaneous study of tissue mechanics and cellular response, as was necessary to answer the hypotheses in Chapters 3 and 4. Cell culture models control cellular boundary conditions more carefully than organ culture systems. In particular, the use of a cell culture system ensured the initial mechanical boundary conditions were homogeneous between mature and young cells to address the effect of loading conditions for chapters 5 and 6.

## **CHAPTER 3 Needle Puncture Injury Affects Intervertebral Disc**

### **Mechanics and Biology in an Organ Culture Model**

Casey L. Korecki, MS, John J. Costi, PhD, James C. Iatridis, PhD

School of Engineering, College of Engineering and Mathematical Sciences  
University of Vermont,  
Burlington, Vermont, 05405, USA

Acknowledgements: We gratefully acknowledge Arthur Michalek for assistance with the creation of computer code for mechanical parameter analysis. This study was supported by the Whitaker foundation and National Institutes of Health (R01AR051146)

## **3.1 Abstract**

### **Study Design**

A bovine intervertebral disc organ culture model was used to study the effect of needle puncture injury on short-term disc mechanics and biology.

### **Objective**

To test the hypothesis that significant changes in intervertebral disc structure, mechanics, and cellular response would be present within one week of needle puncture injury with a large gage needle but not with a small gage needle.

### **Summary of Background Data**

Defects in annulus fibrosus induced by needle puncture injury can compromise mechanical integrity of the disc and lead to degeneration in animal models. The immediate and short-term mechanical and biological response to annulus injury through needle puncture in a large animal model is not known.

### **Methods**

Bovine caudal intervertebral discs were harvested, punctured posterolaterally using 25G and 14G needles, and placed in organ culture for 6 days. Discs underwent a daily dynamic compression loading protocol for 5 days from 0.2 – 1 MPa at 1 Hz for 1 hour. Disc structure and function were assessed with measurements of dynamic modulus, creep, height loss, water content, proteoglycan loss to the culture medium, cell viability and histology.

## **Results**

Needle puncture injury caused a rapid decrease in dynamic modulus and increase in creep during 1 hour loading, although no changes were detected in water content, disc height, or proteoglycan lost to the media. Cell viability was maintained except for localized cell death at the needle insertion site. An increase in cell number and possible remodeling response was seen in the insertion site in the nucleus pulposus.

## **Conclusions**

Relatively minor disruption in the disc from needle puncture injury had immediate and progressive mechanical and biological consequences with important implications for the use of discography, and repair/regeneration techniques. Results also suggest diagnostic techniques sensitive to mechanical changes in the disc may be important for early detection of degenerative changes in response to annulus injury.

### **3.2 Precis**

The effect of needle puncture injury on intervertebral disc mechanics and biology was examined using a bovine organ culture model. Small and large gage needle insertion resulted in immediate and progressive effects on mechanical properties with localized evidence for structural changes and a cellular response localized to the needle track.

### **3.3 Key Points**

- The influence of insertion of 25 G and 14 G needles on the short-term mechanical and biological response of the disc was investigated using a bovine organ culture model
- Immediate and progressive changes in disc stiffness and viscoelastic behaviors were detected following needle puncture injury with both small and large gage needles.
- Needle puncture injury resulted in localized structural disruption, loss of cell viability, and matrix remodeling. Gross tissue water and proteoglycan contents, and cell viability were maintained.
- Results suggest needle puncture injury results in important mechanical changes that may lead to subsequent degenerative remodeling, in a manner that would be difficult to detect with traditional imaging techniques that do not assess biomechanical function.
- Anulus puncture injury via small and large gage needles results in localized and generalized biological and mechanical consequences with implications for discography and injection of biological treatment agents.

### **3.4 Key Words**

Spine, Intervertebral disc, organ culture, needle puncture, bovine, discography, mechanics, dynamic compression loading

### 3.5 Introduction

Low back pain is a common and costly affliction leading to around 19 million physician visits and approximately \$20 billion in costs in the United States per year.<sup>1</sup> The causes of low back pain are multifactorial and complex, yet disc degeneration is often a contributor, particularly in its early unstable stage.<sup>2,3</sup>

Current and future procedures for intervertebral disc diagnosis, repair and regeneration often require needle injection to the nucleus pulposus (NP) through the annulus fibrosus (AF). For example discography, which requires injection of a radio opaque dye into the NP, has a best-case positive predictive value of 50% to 60%, and results in potential AF damage through needle puncture.<sup>4</sup> Intradiscal electrothermal treatment also requires puncture of the AF and additional annular disruption using a catheter.<sup>5</sup> Future treatments including growth factor therapy,<sup>6</sup> tissue engineering,<sup>7</sup> and gene and cell therapy<sup>8,9</sup> may also require puncture of the AF using a needle.

There is evidence in animal models that defects in the AF structure, such as those induced by needle insertion, can compromise disc and motion segment mechanical integrity,<sup>10-13</sup> and lead to mild and moderate degeneration over time.<sup>13-17</sup> It is generally believed that needle puncture injury with small gage needles is not expected to cause damage while needle puncture injury with large gage needles leads to degenerative changes. AF needle puncture injury to the disc in rabbits using needles of different gages has been demonstrated to result in slow progressive degeneration as measured using MRI, X-ray, histology and PCR.<sup>6,15,16,18</sup> Differences in scaling and in biology between small and large animal models leaves unanswered questions regarding extrapolation of



needle puncture injury studies to the human condition. The creation of peripheral AF tears in sheep and pig models also demonstrated evidence of degeneration when evaluated longitudinally for morphological, biochemical and biomechanical changes.<sup>19-22</sup> These studies focused on the medium to long-term effects of disc injury on degeneration, and there is very limited information on the immediate and short-term mechanical and biological response to annulus injury through needle puncture in a large animal model.

The purpose of this study was to test the hypothesis that significant changes in disc structure, mechanics, and cellular response would be present within one week after needle puncture injury with a large gage needle but not with a small gage needle. To study the effect of the needle puncture injury under reproducible conditions in a large animal model, we utilized a bovine caudal intervertebral disc organ culture model. This *ex vivo* system allows precise control over the mechanical and chemical boundaries of the disc, the ability to obtain mechanical parameters over time for the same disc, and the ability to study these interactions in a large animal system where the effects of tissue disruption may be evaluated in the absence of substantial inflammatory response as found *in vivo*.

### **3.6 Materials and Methods**

Bovine tails were obtained from a local abattoir within 4 hours post-mortem and randomly assigned to an unpunctured control group (N=10), and one of two needle puncture groups (small = 25G syringe, N=11; large = 14G syringe, N=12). Musculature surrounding the intervertebral disc was removed. Caudal discs were punctured using a posterolateral approach through the AF taking care to only puncture as far as the NP.

Discs were removed from vertebral endplates and initial disc heights, diameters, and wet weights were measured prior to culturing. Specimens were then placed in an organ culture chamber and incubated in standard culture conditions at 37C and 5% CO<sub>2</sub> under a 0.2 MPa static load as previously described.<sup>23</sup> Media consisting of DMEM (4.5 g/L glucose, 110 mg/L sodium pyruvate, with L-glutamine), supplemented with 10% Fetal Bovine Serum, 100 units/mL of penicillin/streptomycin, 0.1 mg/mL gentamicin, 0.75 mg/L fungizone, 0.02 M HEPES buffer, and 50 µg/ml ascorbic acid, was continuously circulated through the chamber (1.1 mL/min) and changed every 2 days.

The loading protocol for all IVDs consisted of 4 conditions: Baseline, Test 1, Dynamic Loading, and Test 2 (Figure 3-1). IVDs were initially loaded under a baseline static load of 0.2 MPa for 12 hours.<sup>23</sup> Chambers were then individually attached to an incubator-housed loading device for 3 cyclic tests lasting slightly more than one hour: *Test 1* consisted of a one minute test (0.2-0.4 MPa, 1Hz) that was sinusoidally applied to obtain a pre-loading dynamic nominal modulus; *Dynamic Loading* consisted of one hour of sinusoidal loading from 0.2-1.0 MPa at 1 Hz; and *Test 2* consisted of a repeat of the one minute test to obtain a post-loading nominal dynamic modulus. Creep during one hour of dynamic loading was calculated from displacements that were recorded from the loading device at points corresponding to 0.2 MPa load for the first and last cycles of the one hour dynamic loading test, and the initial height at the first cycle was compared between days to compare height lost over the culture duration. Dynamic stiffnesses were calculated using custom written MATLAB code (The MathWorks, Natick, MA) and for ease of comparison across animals, all stiffness measurements were normalized by initial

IVD cross-sectional area and presented as a ‘nominal modulus.’ After the 3 test cycles, the baseline 0.2 MPa static load was again applied to each chamber and at least 12 hours of recovery was allowed between dynamic load cycles. Each chamber experienced loading once per day, adding to 5 total times during the 6 day culture period.

Glycosaminoglycan (GAG) content released to the media was assayed using the dimethylmethylene blue (DMMB) assay<sup>24</sup> using DMEM (4.5 g/L glucose, 110 mg/L sodium pyruvate, with L-glutamine) and chondroitin-4 sulfate to create a standard curve. Media aliquots were collected before every loading experiment and frozen at  $-20^{\circ}\text{C}$  prior to analysis. Regional water contents for the outer and inner annulus (OA, IA), and NP were determined for each group by comparing the wet weights and dry weights (after lyophilization) of tissue samples isolated from the disc.

Tissue samples were isolated both along the needle track and on the opposite side of the disc from the insertion site to assess cell viability both local to the needle track and in the overall tissue (Figure 3-2). Samples were immersed in TBSS (Tyrode’s Buffered Saline Solution) with 1 mg/ml 3-(4,5-dimethylthiazol-2-yl)-2,5-diphenyl-tetrazolium bromide (MTT thiazole blue, Sigma Aldrich, St. Louis, MO) for live cell staining and 1  $\mu\text{M}$  ethidium homodimer-1 (Molecular Probes, Eugene, OR) for dead cell staining and allowed to incubate for 2 hours. Excess dye was removed by placing the tissue samples in PBS on a shaker for 10 minutes and samples were frozen at  $-80^{\circ}\text{C}$ . Frozen tissue was sectioned using a cryotome into 10  $\mu\text{m}$  thick slices either perpendicular or parallel to the needle insertion track to obtain radial or sagittal sections (Figure 2) for evaluation of the disc and needle insertion path. Images of each section were obtained at 20x under

fluorescent (ethidium) and brightfield (MTT) lighting conditions. This technique was shown to be effective in assessing cell viability in all regions of the bovine IVD.<sup>23</sup>

Tissue samples encompassing the needle track were fixed in formalin for 7-10 days, embedded in paraffin, and stained with alcian blue (proteoglycans), picosirius red (collagen), and Weigert's hematoxylin (cell nucleus) for histologic appearance.<sup>25</sup> Tissue was again sectioned either perpendicular or parallel to the needle track for radial and sagittal evaluation of the disc and needle insertion path.

For all quantitative variables, ANOVA with Bonferroni-adjusted post-hoc comparisons were performed using  $p < 0.05$  significance level. All values are reported as averages  $\pm$  SEM.

### **3.7 Results**

The nominal dynamic modulus was significantly affected by needle puncture injury ( $P=0.009$ ), with average pre-load and post-load values for the large needle group being significantly lower than for control (Figure 3-3). No significant differences existed for pre or post load modulus between small and large needle groups, nor between small needle and control groups ( $P > 0.19$ ). Regardless of experimental group, the nominal dynamic modulus increased post-load as compared to pre-load, however no significant differences were noted between groups ( $P=0.076$ ). A small but significant increase in pre-load dynamic modulus was observed between day 2 and day 1 in the small needle puncture group ( $P=0.0028$ ) (Figure 3-3a), and in post-load dynamic modulus for the large needle puncture group between day 1 with days 2 and 5 ( $P=0.042$ ) (Figure 3-3b). No

significant increase in either the pre-load or post-load dynamic modulus was seen over time in the control group ( $P>0.062$ ).

Needle puncture injury also affected the creep during the one hour dynamic loading with significantly more creep observed in needle puncture than control groups (Figure 4-4,  $P<0.006$ ). No significant differences were seen between large and small needle groups. Disc height recorded at 0.2 MPa during the first cycle of dynamic loading decreased over time for all groups, and tended to decrease more for needle puncture groups, however no significant differences were detected (Table 3-1).

Regional tissue water contents were not significantly affected by needle puncture injury ( $P>0.125$ ). Combining all groups, average OA water content was  $57.21 \pm 0.75\%$ , IA water content was  $71.92 \pm 0.75\%$  and NP water content was  $80.24 \pm 0.56\%$ . The amount of GAG released to the media, reported as a percentage of initial disc wet weight, was small and not significantly affected by either large or small needle puncture ( $P>0.125$ ). Average GAG release to the media was  $0.060 \pm 0.005\%$  of the initial disc weight (Table 3-2).

Localized cell death was observed in the area adjacent to the needle tracks. Cell viability was maintained elsewhere in the disc, with no observable differences between groups (Figure 3-5). Histology revealed annulus fiber disruption (Figure 3-6), and a localized area of increased cell number and possible remodeling in the NP of both needle groups (Figure 3-7).

### 3.8 Discussion

The purpose of this study was to evaluate the immediate and short-term changes in disc structure, mechanics, and cellular response resulting from small and large gage needle puncture injury. A bovine organ culture model was used to ensure homogeneous mechanical and chemical boundary conditions, to allow for multiple dependant variables to be examined on the same tissue, and to separate the inherent intervertebral disc tissue response from a more systemic inflammatory response. Localized disruption in the disc tissue from both small and large needle puncture injury was demonstrated to rapidly compromise local disc structure, elastic and viscoelastic mechanical properties. Evidence of a cellular response was also present in the NP region of both needle puncture injury groups, with increased cell death around the needle track, and regions of increased cell number and matrix remodeling along the needle track. Needle puncture injury did not affect GAG released from the disc or water content after recovery. Significant biological and structural alterations in the disc in response to large gage needle puncture was anticipated and consistent with the hypothesis, but the significant alterations in response to small gage needle puncture was surprising and contrasted the hypothesis.

The results of this study indicate that needle puncture, with even a small needle, is sufficient to initiate immediate and progressive alterations in disc height, stiffness and viscoelastic properties (i.e., creep during one hour of loading) that do not recover. In all groups, the largest changes in disc mechanics were observed between days one and two, indicating the largest response to the mechanical loading occurred during the first day.

While some of the changes are probably due to a preconditioning type of response, disc mechanics in needle puncture groups were further altered, indicating that the majority of additional tissue damage probably occurred during the first day's loading. A previous *in vitro* study demonstrated that mechanical stiffness, viscoelastic relaxation, and water content all recovered within 18 hours following cyclic loading (although no measurements were taken at the 12 hour time point).<sup>26</sup> While discs were only allowed 12 hours of recovery between loading events in this study, the removal of vertebral endplates leads to significantly faster recovery times.<sup>27</sup> Therefore, it can be concluded that mechanical changes reported in this study are associated with needle puncture injury and not due to the loading protocol. It is also noteworthy that water content in all discs in this study did recover within 12 hours after loading, consistent with MRI measurements of Johannessen et al.<sup>26</sup> In this context, this study provides support to the concept that diagnostic techniques capable of evaluating biomechanical behaviors may be effective at evaluating early degenerative changes in the disc, whereas traditional MRI evaluations that focus on water content alone may miss important structural changes resulting from injury.

Degenerative changes of the disc may be induced as a result of pathological loading and mechanical damage, biological remodeling, response to injury and proinflammatory cytokines, or a combination of all of these. In this study no significant increase in GAG lost to the medium was detected for small and large needle puncture due to leaching of proteoglycans from the needle track, but we did find structural disruptions and altered mechanics. We infer that loss of GAG in annulus injury models of

degeneration may be associated with three interactive pathways: damage accumulation from pathological loading that might involve depressurization of the NP and larger, more ubiquitous structural defects than AF needle puncture injury alone, chronic biological remodeling that includes proteolytic cleavage of aggrecan into smaller fragments; and biological response to proinflammatory cytokines in response to injury in vivo.<sup>28</sup>

Several animal models of disc degeneration use needle puncture or other annulus injury to induce degenerative changes. Rabbit IVDs, when subjected to annular stab and needle puncture into the NP using 16-21G needles resulted in changes that were consistent with degeneration after eight weeks.<sup>15,16</sup> With a 23G needle, Kim et al. reported nuclear herniation after needle puncture.<sup>17</sup> In our study, no extrusion of NP material was observed but immediate and significant mechanical and cellular changes were found. With smaller gage needle (28G), and saline injection into the rabbit NP, non-significant trends of decreased disc height and proteoglycan and collagen content in the AF and NP were observed at two weeks that persisted after eight weeks.<sup>6</sup> Moderate degeneration occurred after 12 months and marked degeneration after 18 months in pig and sheep models that had peripheral AF tears induced surgically with clear loss of disc height and biochemical changes in the matrix.<sup>19-21</sup> In an 18 month sheep study, AF delamination was produced by injecting saline using a 27G needle into the outer third of, and parallel to, the anterolateral AF fibers, and compared to a 27G needle puncture without saline injection.<sup>13</sup> Of particular interest was the finding that both the saline injected and non-injected needle injuries showed morphologic evidence of mild to moderate degeneration, lamellar thickening in the region of the injury, and altered



biomechanical behaviors. This study supports annulus injury as a potential pathway towards progressive disc degeneration and demonstrated that even small needle puncture resulted in immediate and progressive changes to the IVD biomechanics and cellular response.

Overall disc cell viability remained high, consistent with previous studies using this organ culture system,<sup>23,29</sup> with the only exception in the area immediately adjacent to the needle track. The maintenance of cell viability in the disc away from the needle injury suggests that cell viability was not affected by altered disc mechanics associated with needle puncture injury. On the other hand, localized cell death was likely due to the severing of collagen fibers as the needle entered the disc, and it is possible that the observed changes in mechanical behavior could have induced more general apoptosis in response to altered stresses.<sup>30</sup> In a rabbit needle puncture injury model, Sobajima et al. reported an early upregulation of mRNA for IL-1 $\beta$ , MMP-3 and I-NOS in the nucleus that may have been associated with altered mechanics of the IVD because the needle puncture only penetrated the AF and not the NP.<sup>31</sup> Catabolic remodeling of mRNA expression in response to altered mechanical loading is well-documented<sup>32,33</sup> and also supported by results of this study that found early mechanical changes of the IVD in response to needle puncture injury.

Bovine discs were used in this study because they are a large animal model with IVDs that are reported to have composition and biosynthetic rates similar to human IVDs.<sup>34</sup> Sparse notochordal cell populations in both adult bovine and sheep populations also mimic the situation seen in humans, where notochordal cells disappear during the

second decade.<sup>35</sup> The NP in bovine and other large animals also tends to be more fibrous, preventing an immediate prolapse of NP material through the experimental AF defect when the needle is pulled out, similar to an adult human.

We conclude that a relatively minor disruption in the disc from small and large gage needle puncture had immediate and progressive mechanical and biological consequences with important implications for the use of needle puncture in discography, and repair/regeneration techniques of degenerated discs. Results suggest that altered mechanics and subsequent changes in metabolism resulting from small and large needle puncture injury may be a possible mechanism for degenerative remodeling. Results also suggest early matrix disruption results in mechanical changes that would be difficult to detect from traditional imaging techniques that do not assess mechanical function. This study provides a greater basic science understanding of needle puncture models of degeneration in large animals and suggests that altered mechanics resulting from needle puncture injury may be a possible mechanism for degenerative changes. As with any model system, further studies on human tissue are warranted before any direct recommendations can be made on needle size for clinical applications.

### 3.9 References

1. Katz JN. Lumbar disc disorders and low-back pain: socioeconomic factors and consequences. *J Bone Joint Surg Am* 2006;88 Suppl 2:21-4.
2. Anderson DG, Albert TJ, Fraser JK, Risbud M, Wuisman P, Meisel HJ, Tannoury C, Shapiro I, Vaccaro AR. Cellular therapy for disc degeneration. *Spine* 2005;30:S14-9.
3. Vernon-Roberts B, Pirie CJ. Degenerative changes in the intervertebral discs of the lumbar spine and their sequelae. *Rheumatol Rehabil* 1977;16:13-21.
4. Carragee EJ, Lincoln T, Parmar VS, Alamin T. A gold standard evaluation of the "discogenic pain" diagnosis as determined by provocative discography. *Spine* 2006;31:2115-23.
5. Singh K, Ledet E, Carl A. Intradiscal therapy: a review of current treatment modalities. *Spine* 2005;30:S20-6.
6. An HS, Takegami K, Kamada H, Nguyen CM, Thonar EJ, Singh K, Andersson GB, Masuda K. Intradiscal administration of osteogenic protein-1 increases intervertebral disc height and proteoglycan content in the nucleus pulposus in normal adolescent rabbits. *Spine* 2005;30:25-31; discussion -2.
7. Sato M, Kikuchi M, Ishihara M, Ishihara M, Asazuma T, Kikuchi T, Masuoka K, Hattori H, Fujikawa K. Tissue engineering of the intervertebral disc with cultured annulus fibrosus cells using atelocollagen honeycomb-shaped scaffold with a membrane seal (ACHMS scaffold). *Med Biol Eng Comput* 2003;41:365-71.
8. Gruber HE, Hoelscher GL, Leslie K, Ingram JA, Hanley EN, Jr. Three-dimensional culture of human disc cells within agarose or a collagen sponge: assessment of proteoglycan production. *Biomaterials* 2006;27:371-6.
9. Nishida K, Gilbertson LG, Robbins PD, Evans CH, Kang JD. Potential applications of gene therapy to the treatment of intervertebral disc disorders. *Clin Orthop Relat Res* 2000:S234-41.
10. Thompson RE, Percy MJ, Barker TM. The mechanical effects of intervertebral disc lesions. *Clin Biomech (Bristol, Avon)* 2004;19:448-55.
11. Thompson RE, Percy MJ, Downing KJ, Manthey BA, Parkinson IH, Fazzalari NL. Disc lesions and the mechanics of the intervertebral joint complex. *Spine* 2000;25:3026-35.

12. Keller TS, Holm SH, Hansson TH, Spengler DM. 1990 Volvo Award in experimental studies. The dependence of intervertebral disc mechanical properties on physiologic conditions. *Spine* 1990;15:751-61.
13. Fazzalari NL, Costi JJ, Hearn TC, Fraser RD, Vernon-Roberts B, Hutchinson J, Manthey BA, Parkinson IH, Sinclair C. Mechanical and pathologic consequences of induced concentric anular tears in an ovine model. *Spine* 2001;26:2575-81.
14. Adams MA, Freeman BJ, Morrison HP, Nelson IW, Dolan P. Mechanical initiation of intervertebral disc degeneration. *Spine* 2000;25:1625-36.
15. Sobajima S, Kompel JF, Kim JS, Wallach CJ, Robertson DD, Vogt MT, Kang JD, Gilbertson LG. A slowly progressive and reproducible animal model of intervertebral disc degeneration characterized by MRI, X-ray, and histology. *Spine* 2005;30:15-24.
16. Masuda K, Aota Y, Muehleman C, Imai Y, Okuma M, Thonar EJ, Andersson GB, An HS. A novel rabbit model of mild, reproducible disc degeneration by an annulus needle puncture: correlation between the degree of disc injury and radiological and histological appearances of disc degeneration. *Spine* 2005;30:5-14.
17. Kim KS, Yoon ST, Li J, Park JS, Hutton WC. Disc degeneration in the rabbit: a biochemical and radiological comparison between four disc injury models. *Spine* 2005;30:33-7.
18. Kim KW, Ha KY, Park JB, Woo YK, Chung HN, An HS. Expressions of membrane-type I matrix metalloproteinase, Ki-67 protein, and type II collagen by chondrocytes migrating from cartilage endplate into nucleus pulposus in rat intervertebral discs: a cartilage endplate-fracture model using an intervertebral disc organ culture. *Spine* 2005;30:1373-8.
19. Kaapa E, Han X, Holm S, Peltonen J, Takala T, Vanharanta H. Collagen synthesis and types I, III, IV, and VI collagens in an animal model of disc degeneration. *Spine* 1995;20:59-66; discussion -7.
20. Melrose J, Ghosh P, Taylor TK, Hall A, Osti OL, Vernon-Roberts B, Fraser RD. A longitudinal study of the matrix changes induced in the intervertebral disc by surgical damage to the annulus fibrosus. *J Orthop Res* 1992;10:665-76.
21. Osti OL, Vernon-Roberts B, Fraser RD. 1990 Volvo Award in experimental studies. Annulus tears and intervertebral disc degeneration. An experimental study using an animal model. *Spine* 1990;15:762-7.

22. Latham JM, Percy, M.J., Costi, J.J., Moore, R., Fraser, R.D. and Vernon-Roberts, B. . Mechanical consequences of anular tears and subsequent intervertebral disc degeneration. *Clinical Biomechanics* 1994;9:211-9.
23. Korecki CL, MacLean, J.J., Iatridis, J.C. Characterization of an in vitro intervertebral disc organ culture system. *Eur Spine J* (in press); DOI 10.1007/s00586-007-0327-9
24. Farndale RW, Buttle DJ, Barrett AJ. Improved quantitation and discrimination of sulphated glycosaminoglycans by use of dimethylmethylene blue. *Biochim Biophys Acta* 1986;883:173-7.
25. Gruber HE, Ingram J, Hanley EN, Jr. An improved staining method for intervertebral disc tissue. *Biotech Histochem* 2002;77:81-3.
26. Johannessen W, Vresilovic EJ, Wright AC, Elliott DM. Intervertebral disc mechanics are restored following cyclic loading and unloaded recovery. *Ann Biomed Eng* 2004;32:70-6.
27. Maclean JJ, Owen JP, Iatridis JC. Role of endplates in contributing to compression behaviors of motion segments and intervertebral discs. *J Biomech* 2006.
28. Adams MA, Roughley PJ. What is intervertebral disc degeneration, and what causes it? *Spine* 2006;31:2151-61.
29. Lee CR, Iatridis JC, Poveda L, Alini M. In vitro organ culture of the bovine intervertebral disc: effects of vertebral endplate and potential for mechanobiology studies. *Spine* 2006;31:515-22.
30. Lotz JC, Colliou OK, Chin JR, Duncan NA, Liebenberg E. Compression-induced degeneration of the intervertebral disc: an in vivo mouse model and finite-element study. *Spine* 1998;23:2493-506.
31. Sobajima S, Shimer AL, Chadderdon RC, Kompel JF, Kim JS, Gilbertson LG, Kang JD. Quantitative analysis of gene expression in a rabbit model of intervertebral disc degeneration by real-time polymerase chain reaction. *Spine J* 2005;5:14-23.
32. MacLean JJ, Lee CR, Alini M, Iatridis JC. The effects of short-term load duration on anabolic and catabolic gene expression in the rat tail intervertebral disc. *J Orthop Res* 2005;23:1120-7.
33. Lotz JC. Animal models of intervertebral disc degeneration: lessons learned. *Spine* 2004;29:2742-50.

34. Oshima H, Ishihara H, Urban JP, Tsuji H. The use of coccygeal discs to study intervertebral disc metabolism. *J Orthop Res* 1993;11:332-8.

35. Oda J, Tanaka H, Tsuzuki N. Intervertebral disc changes with aging of human cervical vertebra. From the neonate to the eighties. *Spine* 1988;13:1205-11.

### 3.10 Tables and Figures

**Table 3-1: Height lost between culture days. No significant differences were noted between groups. Values are expressed as Average  $\pm$  SEM**

<b>Group</b>	Day 1 - Day 2 mm $\pm$ SEM	Day 1 - Day 3 mm $\pm$ SEM	Day 1 - Day 4 mm $\pm$ SEM	Day 1 - Day 5 mm $\pm$ SEM
Control	0.200 $\pm$ 0.052	0.229 $\pm$ 0.036	0.192 $\pm$ 0.040	0.209 $\pm$ 0.036
Small	0.234 $\pm$ 0.039	0.192 $\pm$ 0.023	0.275 $\pm$ 0.043	0.272 $\pm$ 0.045
Large	0.234 $\pm$ 0.056	0.277 $\pm$ 0.031	0.288 $\pm$ 0.033	0.307 $\pm$ 0.043

**Table 3-2: Average GAG loss to culture media (as a percentage of total initial disc weight) and percent water content of intervertebral disc tissue for outer annulus (OA), inner annulus (IA), nucleus pulposus (NP) regions. No significant differences were noted between groups. Values are expressed as Average  $\pm$  SEM.**

<b>Group</b>	<b>GAG loss to media</b>	<b>% Water content</b>		
		OA	IA	NP
Control	0.067 $\pm$ 0.007	59.65 $\pm$ 1.72	73.32 $\pm$ 1.66	78.92 $\pm$ 1.24
Small	0.053 $\pm$ 0.006	57.1 $\pm$ 1.21	72.08 $\pm$ 1.10	80.73 $\pm$ 1.04
Large	0.065 $\pm$ 0.009	57.36 $\pm$ 1.12	71.82 $\pm$ 1.24	80.80 $\pm$ 0.45

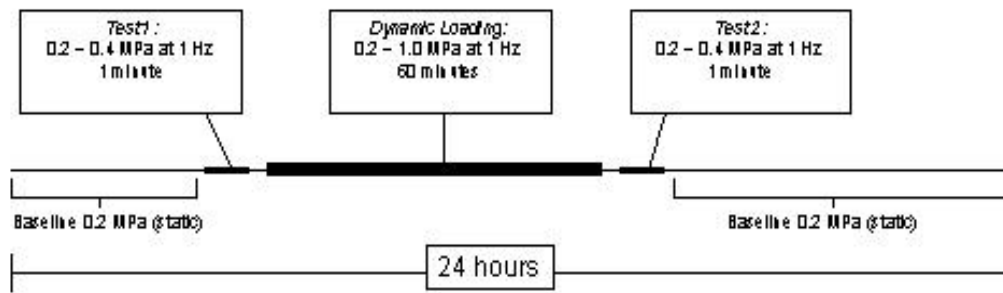


**Figure 3-1: Timeline for mechanical intervention protocol. Daily loading consisted of Test 1, Dynamic Loading, and Test 2. A baseline static load (0.2 MPa) was applied for the remaining culture duration. The intervention protocol was repeated each day for 5 days of the 6 day culture period. Note: timeline is not to scale**



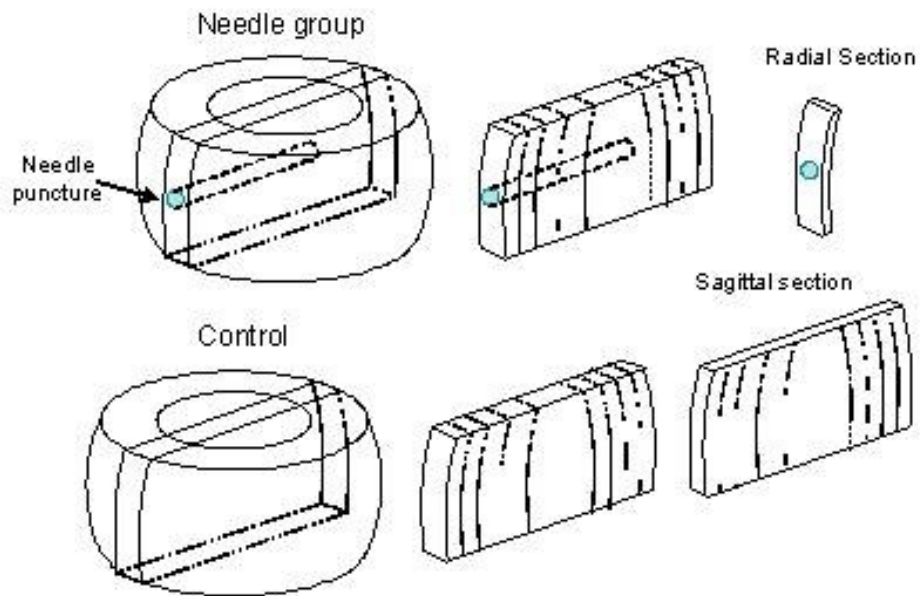


**Figure 3-2 : Sectioning orientations for histology and viability images. Tissue was oriented in two different planes to capture localized response to needle puncture injury (radial section) or a more global tissue response (sagittal section). Radial and sagittal sections were created for all groups tested**

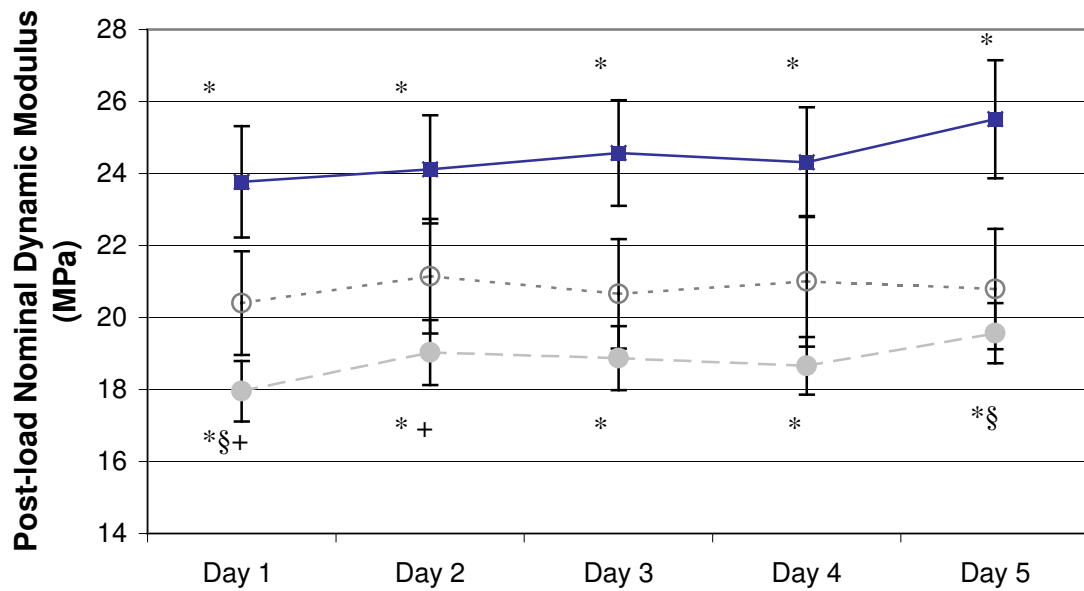
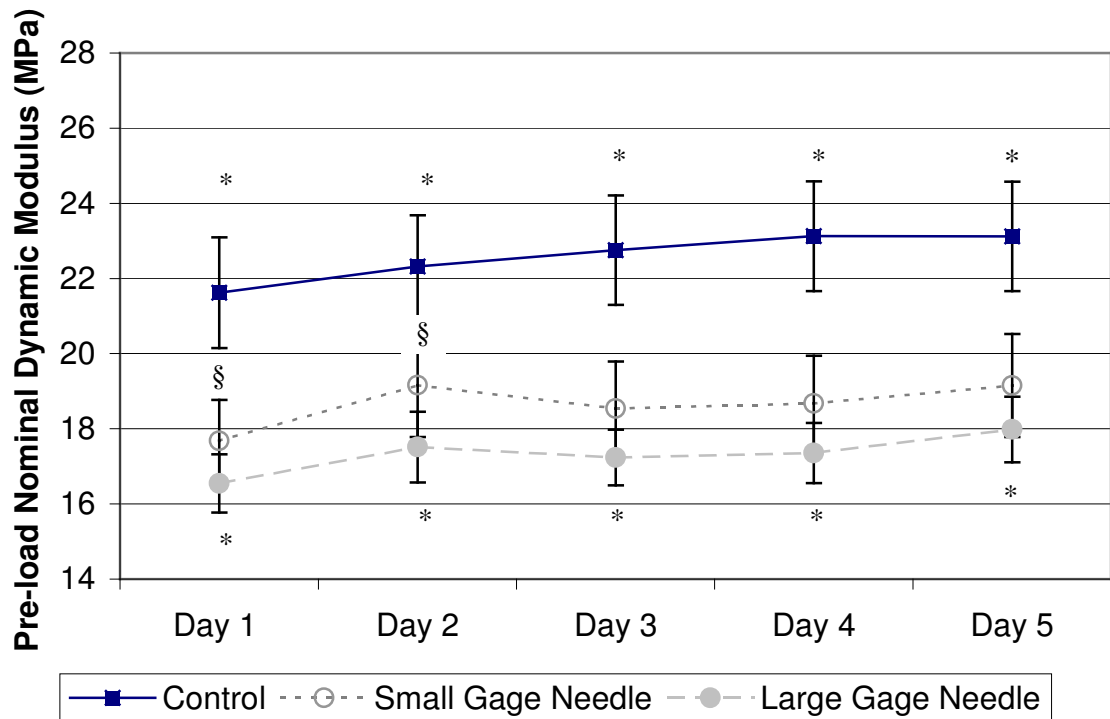
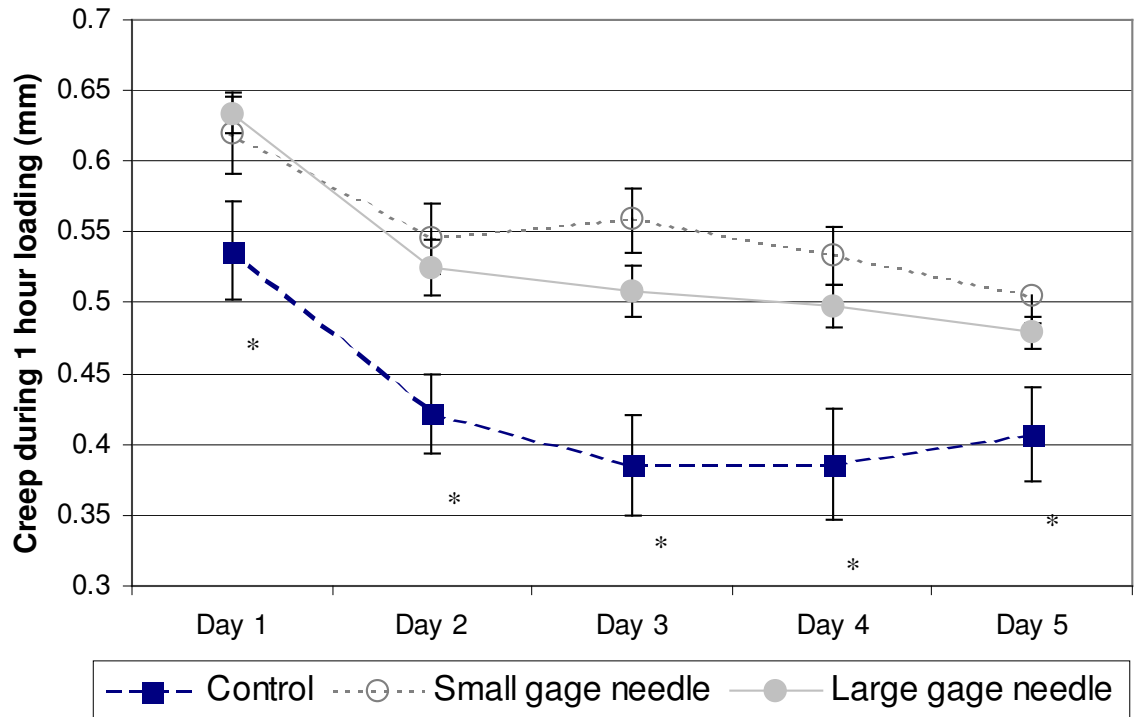


Figure 3-3 : Average  $\pm$  SEM nominal dynamic loading modulus for pre-load (top) and post-load (bottom) tests. A significant difference between groups or time points is indicated by sharing of a common symbol.



**Figure 3-4: Average  $\pm$  SEM creep during the one hour dynamic loading protocol at each day. Significantly more creep was observed at all time points in the needle puncture groups than in the dynamic control group (star indicates a difference relative to all other groups at that time point).**

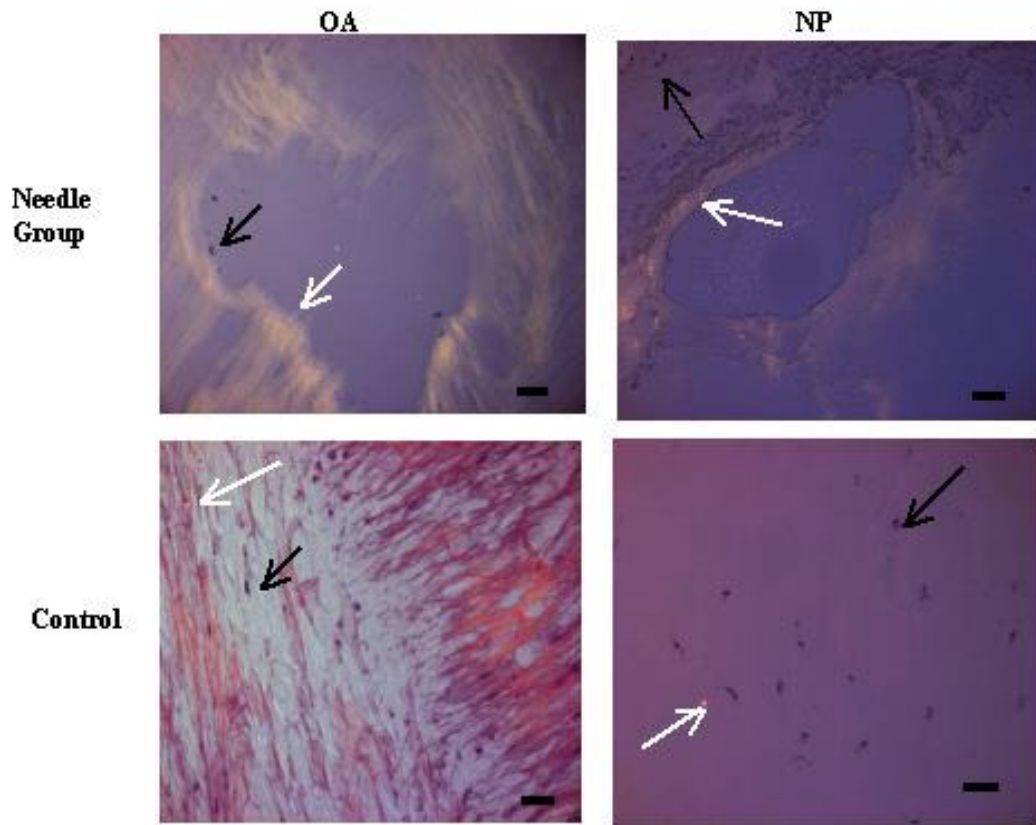
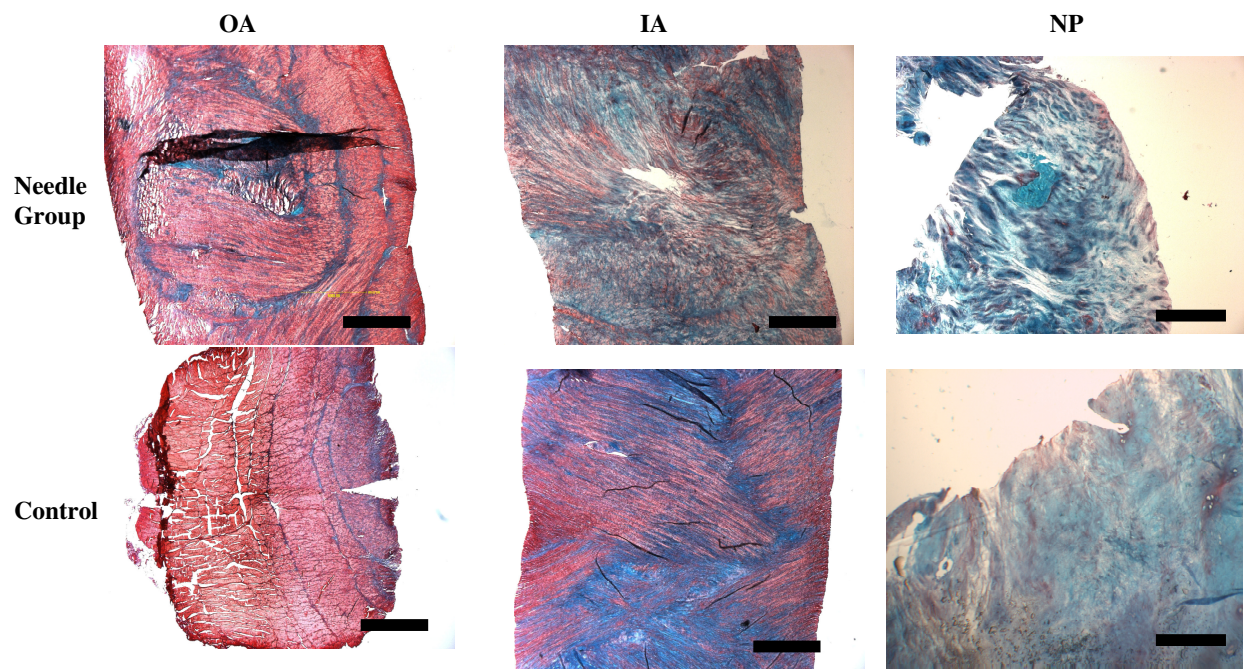
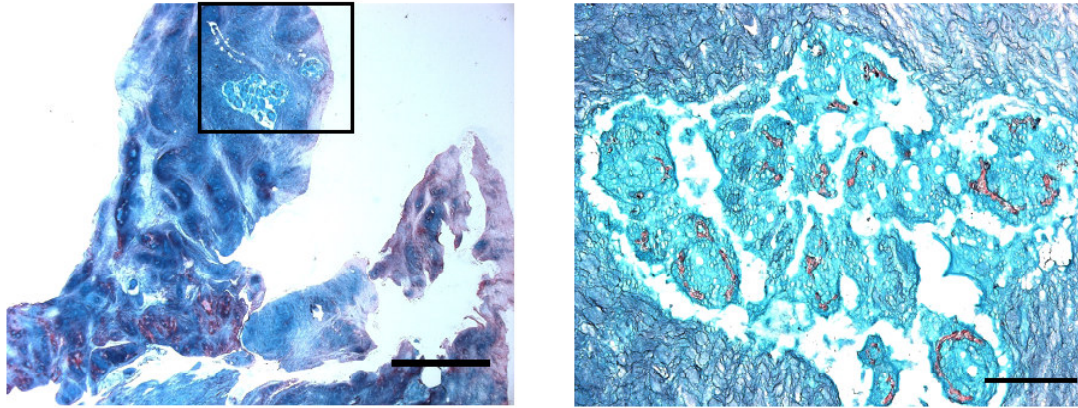


Figure 3-5 : Viability images of OA (left) and NP (right) in the large needle group. Needle puncture regions are on top oriented radially (perpendicular to needle track, with needle track centered in field of view), control images are on bottom oriented sagittally ( the direction that would be perpendicular to the needle track if one existed). Dead cells are fluorescent and appear as red/white (white arrow), live cells are black (black arrow). Images are at 20X, scale bar = 100  $\mu$ m



**Figure 3-6: Representative histology images of needle puncture discs (top) and control discs (bottom) of the OA (L), IA (middle), and NP (R) revealing annulus fiber disruption in the needle group. Collagen stains red, proteoglycans blue, and cell nuclei black. No Needle insertion sites were positioned in the center of the field of view. OA needle group image is of a large needle puncture group, IA and NP are of a small needle puncture. All images are at 2.5X, scale bar = 1mm.**



**Figure 3-7: Evidence of an increase in NP cell number and possible remodeling local to an insertion site in a large needle puncture disc. Image on left is a 2.5X, scale bar = 1mm. Boxed area on left is magnified on the right, image is at 20X, scale bar = 100  $\mu$ m.**

### **3.11 Study Clarifications**

This section is added as an addendum to the previous published chapter to address specific comments that arose during the dissertation defense.

Alterations in disc height were not significant (Table 3.1), however a trend of increased height loss was found in the needle puncture groups between culture days (as stated in the conclusion).

The immediate (day 1) decrease in nominal dynamic modulus in the needle puncture groups as compared to the control groups (n=10) can be further verified by comparing both the needle puncture and the control groups to the 'Low' load group in chapter 4. All of these groups were treated with similar mechanical loading protocols, and all (n =10 for control, n = 10 for low load group) were significantly different than that found in the needle puncture groups (n = 10 for large and n = 10 for small gage needle).

This study contributes a possible mechanism for the needle-puncture induced disc degeneration models, in which alterations in disc mechanics begins a progressive degenerative cascade.

## **CHAPTER 4 Dynamic Compression Effects on Intervertebral Disc**

### **Mechanics and Biology**

Casey L. Korecki, Jeffrey J. MacLean, James C. Iatridis\*

School of Engineering, College of Engineering and Mathematical Sciences  
University of Vermont, Burlington, Vermont, 05405, USA

#### Acknowledgments

We gratefully acknowledge Dr. Karin Wurtz for primer sequences and Arthur Michalek for assistance with the creation of computer code for mechanical parameter analysis.

Funded by NIH grant R01 AR051146.



## **4.1 Abstract**

### **Study Design**

A bovine intervertebral disc organ culture model was used to study the effect of dynamic compression magnitude on mechanical behavior and measurement of biosynthesis rate, cell viability, and mRNA expression.

### **Objective**

The objective of this study was to examine the effect of loading magnitude on intervertebral disc mechanics and biology in an organ culture model.

### **Summary of Background Data**

The *in vivo* and cell culture response of intervertebral disc cells to dynamic mechanical loading provides evidence the disc responds in a magnitude dependant manner. However, the ability to link mechanical behavior of the disc with biological phenomena has been limited. A large animal organ culture system facilitates measurements of tissue mechanics and other biological response parameters on the same sample allowing a broader understanding of disc mechanobiology.

### **Methods**

Bovine caudal intervertebral discs were placed in organ culture for 6 days and assigned to a static control group or one of two dynamic compression loading protocols (0.2 – 1 MPa or 0.2 – 2.5 MPa) at 1 Hz for 1 hour for 5 days. Disc structure was assessed with measurements of dynamic modulus, creep, height loss, water content, and proteoglycan loss to the culture medium. Cellular responses were assessed through changes in cell viability, metabolism, and qRT-PCR analyses.

## **Results**

Increasing magnitudes of compression increased disc modulus and creep, however all mechanical parameters recovered each day. In the annulus, significant increases in gene expression for collagen type I and a trend of increasing sulfate incorporation were observed. In the nucleus, increasing gene expression for collagen type I and MMP3 was observed between magnitudes and between static controls and the lowest magnitude of loading.

## **Conclusions**

Results support the hypothesis that biological remodeling precedes damage to the intervertebral disc structure, that compression is a healthy loading condition for the disc, and further support the link between applied loading and biological remodeling.

## **4.2 Precis**

A bovine organ culture system was used to evaluate effects of dynamic compression magnitude on disc structure, function, viability, biosynthesis rate and real time RT-PCR. Results support the concept that intervertebral disc tissue structure is tolerant to applied mechanical compression, with an increase in biosynthesis rate and no observed permanent damage to the tissue structure at physiological load magnitudes.

## **4.3 Key Points**

- The biological and mechanical responses of the cultured intervertebral disc to applied dynamic compression were examined
- No permanent compromise in disc mechanical properties was observed throughout the culture period
- Biosynthesis rates and gene expression responses were affected by disc region and dynamic compression magnitude, particularly for collagen type 1 and MMP3
- Dynamic compression magnitude increased biosynthesis rates and did not result in structural disruption, suggesting it is a healthy loading condition for the disc.
- Results suggest biological changes occur prior to structural damage to the intervertebral disc

## **4.4 Key Words**

Spine, Intervertebral disc, organ culture, bovine, mechanics, dynamic compression loading

## 4.5 Introduction

Experimental evidence points to a threshold of loading necessary for intervertebral disc (IVD) extra cellular matrix maintenance, where too little load (i.e., immobilization) will reduce biosynthesis rates and overloading can cause structural damage and altered biomechanical behaviors.<sup>1-3</sup> Dynamic loading is commonly experienced during daily activity, and is particularly important to include when attempting to identify loading patterns that introduce risks to IVD structure, biomechanics, and biosynthesis. Furthermore, a cyclic loading component is necessary to distinguish between immobilization and overloading. *In vivo* studies demonstrated there is a frequency, magnitude and duration effect of applied mechanical loading on IVD cells,<sup>2,4</sup> further supporting the importance of a better understanding of such loading patterns on the IVD.

The motion segment complex provides 6 degree of freedom mobility, but its structural components are sensitive to damage under distinct loading conditions. Complex loading regimes (e.g., bending and compression), on the spine can result in disc damage and herniation.<sup>3,5-8</sup> Compression loading on the spine is known to put the vertebral endplate at risk of fracture, which is then associated with a loss of nucleus pressurization due to damage at the discovertebral junction.<sup>6,9</sup> Evidence of biological remodeling in disc tissue occurs in response to compressive loading magnitudes insufficient to cause vertebral endplate failure,<sup>2</sup> raising the possibility that thresholds of structural failure overestimate the levels of loading which are detrimental to intervertebral disc health.

The biological response of the IVD to dynamic loading has been previously examined *in vivo*<sup>1,2,10-12</sup> and in cell culture studies,<sup>4,13,14</sup> while the effects of mechanical loading on IVD structure and mechanics have been studied extensively on non-viable tissue *in vitro*, leaving unanswered questions about the effects of such mechanical changes on living cell populations. Mechanical loading is known to influence the IVD, however unanswered questions remain regarding the dependence on other signaling pathways existing *in vivo* (e.g., proinflammatory molecules), and whether the loss of cell-tissue matrix contact *in vitro* is detrimental to normal mechanical signal transduction. The ability to examine biological remodeling pathways while also quantifying structural and mechanical changes induced in response to mechanical loading is a critical step towards understanding how the relationship between biomechanical loading and biological remodeling might contribute toward a progressive degenerative cascade in the IVD.

The use of an organ culture model facilitates investigation into cellular responses to mechanical loading while the disc is largely intact. Organ culture provides complete control over mechanical boundary conditions while allowing for measurement of mechanical properties throughout the culture duration. Chemical boundary conditions can also be controlled, eliminating the effect of other signaling pathways present *in vivo*, while maintaining viable cells and normal cell-matrix interactions. Currently, however, few studies have investigated the response of the IVD in organ culture to dynamic loading. Developing and testing a large animal organ culture system is important because of its ability to be more directly translated to human IVDs and also because of the ability to evaluate multiple mechanical and biological dependent variables on the same IVD.

The aim of this study was to examine the effects of varying physiological magnitudes of dynamic compression on intact intervertebral disc structure, biomechanics, cell metabolism, and water content in three disc regions. The hypotheses were that low magnitudes of dynamic compression would enhance anabolic remodeling while high magnitudes of dynamic compression would demonstrate early signs of disc damage and catabolic remodeling. Specifically, dynamic compression applied to the intervertebral disc structure at low magnitudes of active physiological loading in a human (0.2 – 1 MPa, e.g., standing up from a chair<sup>15</sup>) will promote anabolic remodeling, including increased biosynthesis rates, while loading at larger magnitudes of active physiological loading in a human (0.2 – 2.5 MPa, e.g., lifting 20 kg with round back<sup>15</sup> but less than failure of bovine caudal motion segment<sup>16,17</sup>) will result in early signs of remodeling including structural damage, loss of cell viability, and catabolic remodeling as measured through biomechanical properties, histology, biochemical measurements, sulfate incorporation, and qRT-PCR.

## **4.6 Materials and Methods**

Three intervertebral discs, corresponding to caudal levels c2-3, c3-4, and c4-5, were dissected from twelve beef cattle (ages 18-24 months) under sterile conditions within 4 hours of slaughter. Dissection included removal of vertebral endplates from the intervertebral disc using a straight edge razor blade to maintain transport through the endplate route.<sup>18</sup> Following dissection, discs were rinsed in Tyrode's Balanced Salt Solution (TBSS) containing 0.3 µl/ml penicillin/streptomycin and 0.1 µl/ml fungizone (Invitrogen, Carlsbad, CA).

Discs were assigned to one of three groups consisting of two dynamic loading conditions (**low**, **high**) and one static control (**static**). Each group consisted of N=12 discs, with equal numbers of each disc level assigned to each group as the anatomic level of the disc is known to affect cell metabolism and tissue composition. Discs were placed into a custom built organ culture chamber described previously<sup>18,19</sup> and housed in an incubator at 37°C and 5% CO<sub>2</sub>. Culture media consisting of DMEM (4.5 g/L glucose, 110 mg/L sodium pyruvate, with L-glutamine), supplemented with 100 units/mL of penicillin/streptomycin, 0.1 mg/mL gentamicin, 0.75 mg/L fungizone, 0.02 M HEPES buffer, 50 µg/mL ascorbic acid (Invitrogen, Carlsbad, CA), and 10mL/L FBS (Atlanta Biological, Atlanta, GA) was continuously circulated at 1.1 mL/min and replaced every two days.

All groups were initially confined with an applied stress of 0.2 MPa for 12 hours.<sup>19</sup> Chambers were then individually attached to an incubator-housed loading device for the start of the experimental protocol (Figure 4-1). First, a one minute test (0.2-0.4 MPa, 1Hz) was applied sinusoidally to obtain a pre-loading dynamic nominal modulus for all groups. Control discs (**static** group) were removed from the loading device and the 0.2 MPa static load was replaced, and a dynamic load was applied to the two test groups (**low** and **high**). Dynamic loading consisted of one hour of sinusoidal loading at 1 Hz, with amplitudes of 0.2 – 1 MPa for the **low** load group and 0.2 – 2.5 MPa for the **high** load group. After the dynamic loading cycle, a repeat of the one minute test was performed to obtain a post-loading nominal dynamic modulus. After the 3 test cycles, the baseline 0.2 MPa static load was again applied to each chamber and at least 12 hours of

recovery was allowed between dynamic load cycles. Each chamber experienced loading once per day, adding to 5 total times during the 6 day culture period.

Creep during one hour of dynamic loading was calculated from displacements that were recorded from the loading device at points corresponding to 0.2 MPa load for the first and last cycles of the one hour dynamic loading test, and the initial height at the first cycle was compared between days to compare height lost over the culture duration. Dynamic stiffnesses were calculated using custom written MATLAB code (The MathWorks, Natick, MA) and for ease of comparison across animals, all stiffness measurements were normalized by initial IVD cross-sectional area and presented as a 'nominal modulus'.

Structural parameters assessed included changes in intervertebral disc diameter and height. Initial height and diameter measurements were obtained using three caliper measurements in each dimension, recorded prior to the start of the culturing process, and immediately following culture termination. Proteoglycan content released to the culture media was assessed using the DMMB colorimetric assay. Aliquots of culture media were centrifuged at 10,000 rpm for 3 minutes prior to the application of the DMMB assay. A standard curve was generated using chondroitin-6-sulfate and DMEM, and sample absorbances were read on a microplate reader. Regional tissue water content was calculated following tissue dissection, weighing, and lyophilization to obtain a dry tissue weight.

Cell metabolism was assessed using the  $^{35}\text{S}$  incorporation assay. Immediately following culture termination, sections of intervertebral disc tissue from each of the tissue



regions (OA, IA, NP) were dissected (Figure 4-1), weighed, and placed in 2 mL of culture medium without FBS containing 2.5  $\mu\text{Ci}$  of  $^{35}\text{S}$  (Perkin-Elmer, Boston, MA) and brought to an approximate osmolarity of 400mOsm by the addition of 1.5% v/v 5M NaCl and 0.4M KCl to reduce tissue swelling. Samples were incubated for 6 hours at 37°C and 5%  $\text{CO}_2$ , after which they were removed from the radiolabel medium and digested with proteinase-K (0.5 mL of 1 mg/mL at 57°C). Radioactive media was stored for each tissue sample to allow for later normalization. After digestion, non-incorporated sulfate was removed by exhaustive dialysis against distilled water. Radioactivity of samples was measured using a scintillation counter, and was normalized to incubation media radioactivity and tissue sample dry weight. To minimize potential artifacts due to GAG leaching that may have occurred during the radiolabel incubation step, the sample dry weight was calculated based on measurements of specimen wet weight and water content of paired tissue samples that were taken prior to the incubation (Figure 4-1).

Cell viability was examined using 3-(4,5-dimethylthiazol-2-yl)-2,5-diphenyltetrazolium bromide (MTT, Sigma-Aldrich, St Louis, MO) to stain vital cells through the formation of precipitate by active mitochondria, and ethidium homodimer-1 (Invitrogen, Carlsbad, CA) to stain the DNA of non-vital cells with compromised nuclear envelopes. Tissue sections approximately 10 mm by 5 mm were dissected through the disc in the sagittal plane (Figure 1) and placed into a TBSS solution containing 1 mg/mL MTT and 1  $\mu\text{M}$  ethidium homodimer -1. After a 2 hour staining period, samples were removed from the stain solution and placed on a shaker in TBSS for 10 minutes to remove excess dye. The tissue was then frozen in isopentane floated in liquid nitrogen

and stored at  $-80^{\circ}\text{C}$  until sectioning on a cryotome. Five  $10\mu\text{m}$  thick sections were taken for each tissue region (OA, IA and NP) beginning at the tissue surface and every  $250\mu\text{m}$  thereafter. For each of the 15 resulting slides, representative images were captured at 20x magnification (Zeiss axiocam, Zeiss, Thornwood, NY) first under fluorescent light to capture cells stained with ethidium homodimer -1 (Rhodamine filter : ex/em of  $546\text{nm}/617\text{nm}$ ) and then under brightfield light to capture precipitate formed with MTT by vital mitochondria.

qRT-PCR was performed on tissue isolated from the annulus and nucleus regions. The OA and IA were pooled to ensure sufficient tissue quantity for RNA isolation. Expression levels were quantified using SYBR green for aggrecan, versican, collagen types I and II, TIMP -1, MMP -2, -3 and -13, and ADAMTS -4 were normalized to 18S expression levels (to generate  $\Delta\text{Ct}$  values). Expression levels for experimental groups (low and high) were normalized to tail-matched static controls (to generate  $\Delta\Delta\text{Ct}$  values).

A one-way ANOVA was used to evaluate the effect of loading group (static, low, high) on changes in disc mechanics, diameter, height, water content, GAG content in the media, and  $^{35}\text{S}$  incorporation. All statistical analyses on qRT-PCR data were performed on the  $\Delta\Delta\text{Ct}$  values. A one way ANOVA was used to compare loading groups (low and high).<sup>8</sup> Fishers PLSD post-hoc test was used to detect differences between loading groups with a significance level of  $p < 0.05$  for all ANOVA tests. For qRT-PCR data an additional student's t test with hypothesized mean of zero was used to evaluate statistical

differences between static controls (static) and loading groups (low and high) which were normalized to the static controls.

## 4.7 Results

All data are presented as average  $\pm$  SEM. No significant changes in disc height or diameter were found at the end of the culture period for any of the test groups. The average height loss was  $14.8 \pm 1.95\%$  and diameter gain was  $42.6 \pm 1.62\%$ . Proteoglycan loss to the culture media was also not significantly affected by mechanical loading with an average of  $0.065 \pm 0.004\%$  of the initial disc wet weight. Likewise, no significant differences in regional tissue water content were found between groups, with regional differences in tissue water content maintained. Average tissue water contents were  $59.25 \pm 0.700\%$  in the OA,  $73.59 \pm 0.617\%$  in the IA and  $79.8 \pm 0.562\%$  in the NP. A trend of increasing sulfate incorporation (Figure 4-2) with increasing load magnitude was observed in the OA and IA; however no corresponding trend was noted in the NP. Viability was not significantly different between loading groups (Figure 4-3).

The pre-loading dynamic modulus was not significantly different between loading groups at any time point (Figure 4-4). There was a significant increase in the pre-load modulus between day 1 and day 2 for all groups, but no further significant increases occurred throughout the culture duration for any group. The post-load dynamic modulus significantly increased with increasing load magnitude. Likewise, the magnitude of creep observed during the one hour of dynamic loading was greater with increasing load magnitudes (Figure 4-5). No significant difference was noted in the starting disc height between days, indicating a complete recovery of the lost disc height between days.

Gene expression in the annulus region was not found to be significantly different with respect to static controls ( $p>0.05$ ) (Figure 4-6). Significant changes in collagen type 1 regulation were found between loading magnitudes, with downregulation observed in the low group and upregulation in the high group ( $p=0.48$ ). In the nucleus pulposus, significant upregulation of collagen type 1 ( $p=0.002$ ) and MMP3 ( $p=0.01$ ) gene expression was observed in the low group relative to static controls. Significant differences in gene expression were also observed between low and high loading groups for collagen 1 ( $p=0.018$ ) and MMP3 ( $p=0.01$ ).

#### **4.8 Discussion**

The effect of dynamic compression on the mechanical and biological state of the intervertebral disc was examined at two loading magnitudes to test the hypotheses that low magnitudes of dynamic compression would increase anabolic remodeling while high magnitudes of dynamic compression would demonstrate early signs of disc damage and catabolic remodeling. The use of an organ culture system enabled measurement of mechanical properties throughout the culture duration while maintaining cell viability and metabolism, thus allowing for regional measurements of sulfate incorporation, qRT-PCR, histology, and water content. Overall, the results support the concept that the intervertebral disc tissue structure is rather tolerant to applied mechanical compression, with no observed permanent damage to the tissue structure. Load magnitude dependent increases in anabolic mRNA expression and sulfate incorporation suggest that dynamic compression increases disc metabolic rate and enhances anabolic remodeling. Significant differences in gene expression were also observed between loading magnitudes in both

the annulus fibrosus and nucleus pulposus regions for collagen type I, and in the nucleus pulposus region for MMP3.

The magnitude of applied loading in this study was chosen to reflect expected magnitudes observed in vivo.<sup>15</sup> The nominal dynamic modulus and creep magnitude of the disc increased with increasing load magnitude as would be expected due to nonlinear material behaviors associated with tissue compaction at higher loading magnitudes, however all changes were fully recovered within 12 hours. The recovery times observed in this study are consistent with literature on the topic, with previous studies observing complete recovery after 18 hours.<sup>20</sup> Additionally, the removal of the vertebral endplates necessary to maintain cell viability<sup>18</sup> has been shown to speed recovery time.<sup>21</sup> While the removal of endplates from the intervertebral disc is anticipated to affect absolute values of local strains in the intervertebral disc, it is not expected to affect relative comparisons between loading magnitudes. It is possible that the magnitude dependent increase in sulfate incorporation in the annulus fibrosus but not the nucleus pulposus is associated with a loss of pressurization in the nucleus due to removal of endplates. The loss of disc height and increase in disc diameter observed is consistent with previous studies on the bovine intervertebral disc in culture,<sup>19</sup> and is likely associated with post mortem muscle relaxation resulting in an increase in disc hydration.<sup>9</sup> The full recovery of disc properties, combined with no significant changes in disc height, diameter, water content and GAG loss to the culture media, provide evidence that applied compression loading results in no permanent damage to the intervertebral disc structure even up to magnitudes of 2.5 MPa.

Previous studies examining the biological response of the intervertebral disc to dynamic loading have been performed *in vivo*<sup>1,2,12</sup> and on cell cultures<sup>4,13,14</sup>. Tissue culture and organ culture studies primarily examined the effects of static loading<sup>16,18,22</sup> or diurnal loading (applied osmotically<sup>23</sup> or through compression<sup>19</sup>). The current study method links the response of isolated cells to that of the *in vivo* situation by retaining the *in situ* cell environment. While a direct comparison across studies and methodology is difficult due to the use of different species, as well as varying loading magnitudes, frequencies and modes of application (compression, hydrostatic, tension), it is fairly consistent that collagen type I and MMP3 are affected by applied mechanical stimulation in the intervertebral disc in a region specific manner.<sup>2,14</sup>

In conclusion, increased cell metabolism at loading magnitudes insufficient to cause observable disc damage in this study point to the ability of mechanical loading to stimulate disc remodeling as measured on gene and protein levels. Results also suggest that dynamic compression is a healthy loading condition due to the lack of observable signs of intervertebral disc damage at high stress levels in this study, combined with other studies on risky loading patterns on the disc that defined lateral bending and flexion as the loading patterns that place the disc at most risk of injury.<sup>8</sup> Furthermore, It is interesting that load magnitude had a progressive increase in expression of many genes in the anulus while collagen-I and MMP3 in the nucleus region were all down-regulated following a substantial increase in load magnitude. These observations demonstrate combined mechanical, biological, and chemical remodeling in response to dynamic compression. Consequently, results motivate the need for further studies on the effects of applied

loading on the biological response of the intervertebral disc under more damaging conditions that might include bending and endplate fracture under compression.

## 4.9 References

1. Walsh AJ, Lotz JC. Biological response of the intervertebral disc to dynamic loading. *J Biomech* 2004;37:329-37.
2. Maclean JJ, Lee CR, Alini M, et al. Anabolic and catabolic mRNA levels of the intervertebral disc vary with the magnitude and frequency of in vivo dynamic compression. *J Orthop Res* 2004;22:1193-200.
3. Stokes IA, Iatridis JC. Mechanical conditions that accelerate intervertebral disc degeneration: overload versus immobilization. *Spine* 2004;29:2724-32.
4. Kasra M, Merryman WD, Loveless KN, et al. Frequency response of pig intervertebral disc cells subjected to dynamic hydrostatic pressure. *J Orthop Res* 2006;24:1967-73.
5. Iatridis JC, ap Gwynn I. Mechanisms for mechanical damage in the intervertebral disc annulus fibrosus. *J Biomech* 2004;37:1165-75.
6. Adams MA, Freeman BJ, Morrison HP, et al. Mechanical initiation of intervertebral disc degeneration. *Spine* 2000;25:1625-36.
7. Farfan HF, Cossette JW, Robertson GH, et al. The effects of torsion on the lumbar intervertebral joints: the role of torsion in the production of disc degeneration. *J Bone Joint Surg Am* 1970;52:468-97.
8. Costi JJ, Stokes IA, Gardner-Morse M, et al. Direct measurement of intervertebral disc maximum shear strain in six degrees of freedom: Motions that place disc tissue at risk of injury. *J Biomech* 2007;40:2457-66.
9. Pfirrmann CW, Resnick D. Schmorl nodes of the thoracic and lumbar spine: radiographic-pathologic study of prevalence, characterization, and correlation with degenerative changes of 1,650 spinal levels in 100 cadavers. *Radiology* 2001;219:368-74.
10. MacLean JJ, Lee CR, Grad S, et al. Effects of immobilization and dynamic compression on intervertebral disc cell gene expression in vivo. *Spine* 2003;28:973-81.
11. MacLean JJ, Lee CR, Alini M, et al. The effects of short-term load duration on anabolic and catabolic gene expression in the rat tail intervertebral disc. *J Orthop Res* 2005;23:1120-7.



12. Ching CT, Chow DH, Yao FY, et al. The effect of cyclic compression on the mechanical properties of the inter-vertebral disc: an in vivo study in a rat tail model. *Clin Biomech* (Bristol, Avon) 2003;18:182-9.
13. Kasra M, Goel V, Martin J, et al. Effect of dynamic hydrostatic pressure on rabbit intervertebral disc cells. *J Orthop Res* 2003;21:597-603.
14. Wuertz K, Urban JP, Klasen J, et al. Influence of extracellular osmolarity and mechanical stimulation on gene expression of intervertebral disc cells. *J Orthop Res* 2007.
15. Wilke HJ, Neef P, Caimi M, et al. New in vivo measurements of pressures in the intervertebral disc in daily life. *Spine* 1999;24:755-62.
16. Ishihara H, McNally DS, Urban JP, et al. Effects of hydrostatic pressure on matrix synthesis in different regions of the intervertebral disk. *J Appl Physiol* 1996;80:839-46.
17. Ochia RS, Tencer AF, Ching RP. Effect of loading rate on endplate and vertebral body strength in human lumbar vertebrae. *J Biomech* 2003;36:1875-81.
18. Lee CR, Iatridis JC, Poveda L, et al. In vitro organ culture of the bovine intervertebral disc: effects of vertebral endplate and potential for mechanobiology studies. *Spine* 2006;31:515-22.
19. Korecki CL, MacLean JJ, Iatridis JC. Characterization of an in vitro intervertebral disc organ culture system. *Eur Spine J* 2007;16:1029-37.
20. Johannessen W, Vresilovic EJ, Wright AC, et al. Intervertebral disc mechanics are restored following cyclic loading and unloaded recovery. *Ann Biomed Eng* 2004;32:70-6.
21. MacLean JJ, Owen JP, Iatridis JC. Role of endplates in contributing to compression behaviors of motion segments and intervertebral discs. *J Biomech* 2007;40:55-63.
22. Handa T, Ishihara H, Ohshima H, et al. Effects of hydrostatic pressure on matrix synthesis and matrix metalloproteinase production in the human lumbar intervertebral disc. *Spine* 1997;22:1085-91.
23. Haschtmann D, Stoyanov JV, Ferguson SJ. Influence of diurnal hyperosmotic loading on the metabolism and matrix gene expression of a whole-organ intervertebral disc model. *J Orthop Res* 2006;24:1957-66.

## 4.10 Tables and Figures

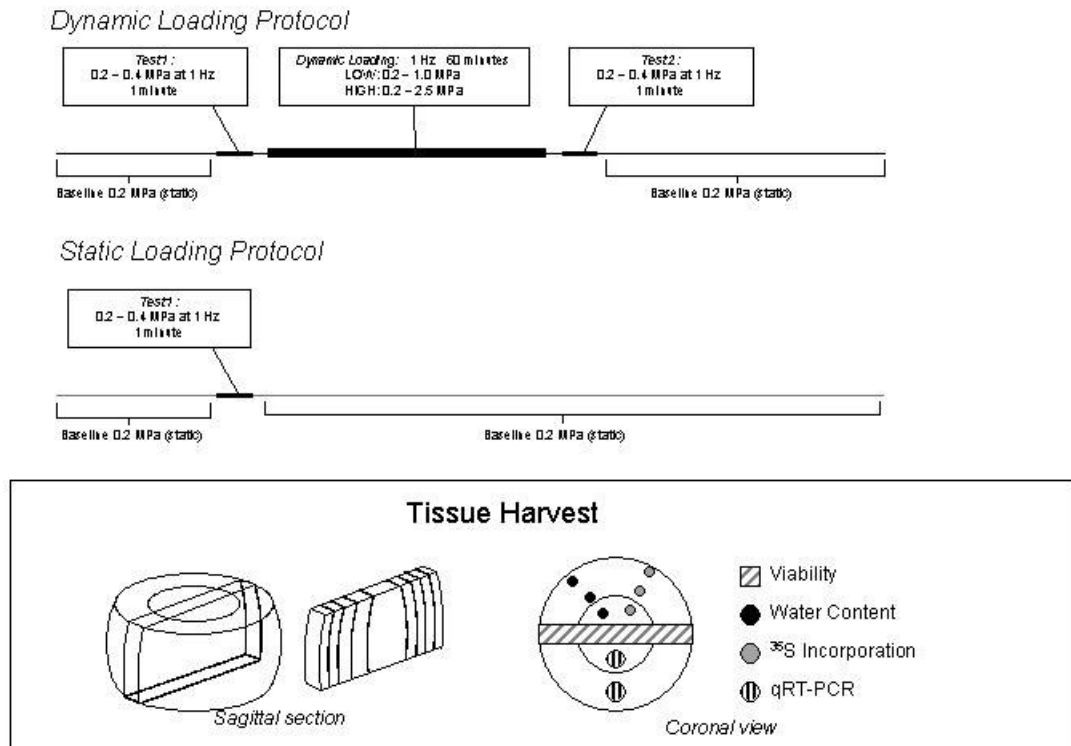


**Figure 4-1: Test protocol schematic detailing loading protocol (Top). Illustration showing tissue harvest protocol (Bottom). Note:schematic diagram not to scale**

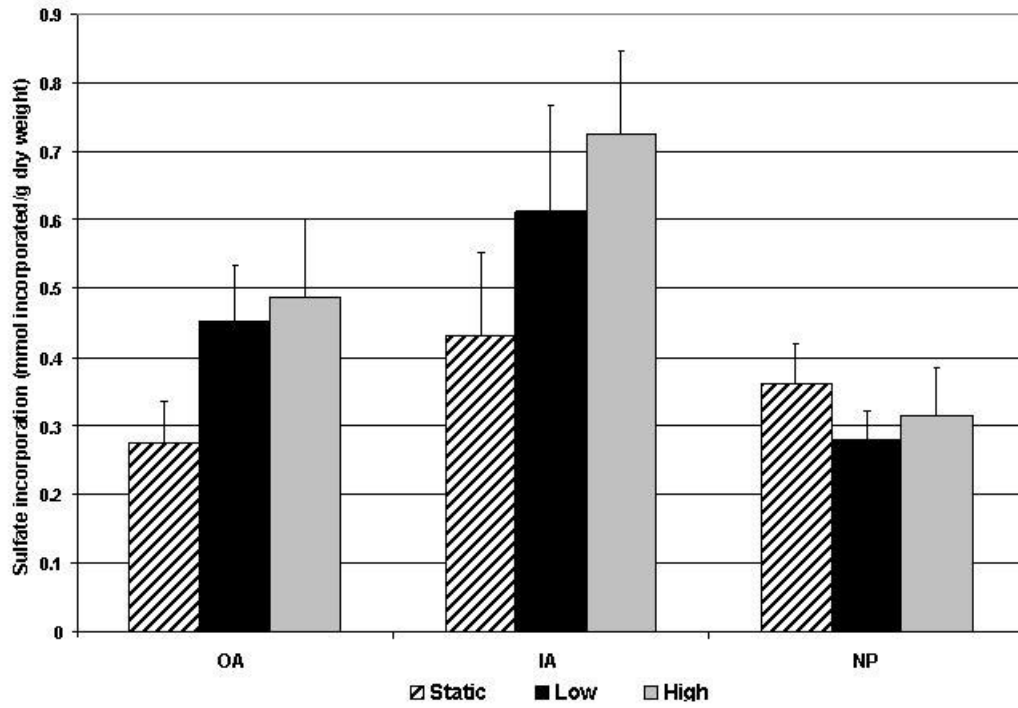
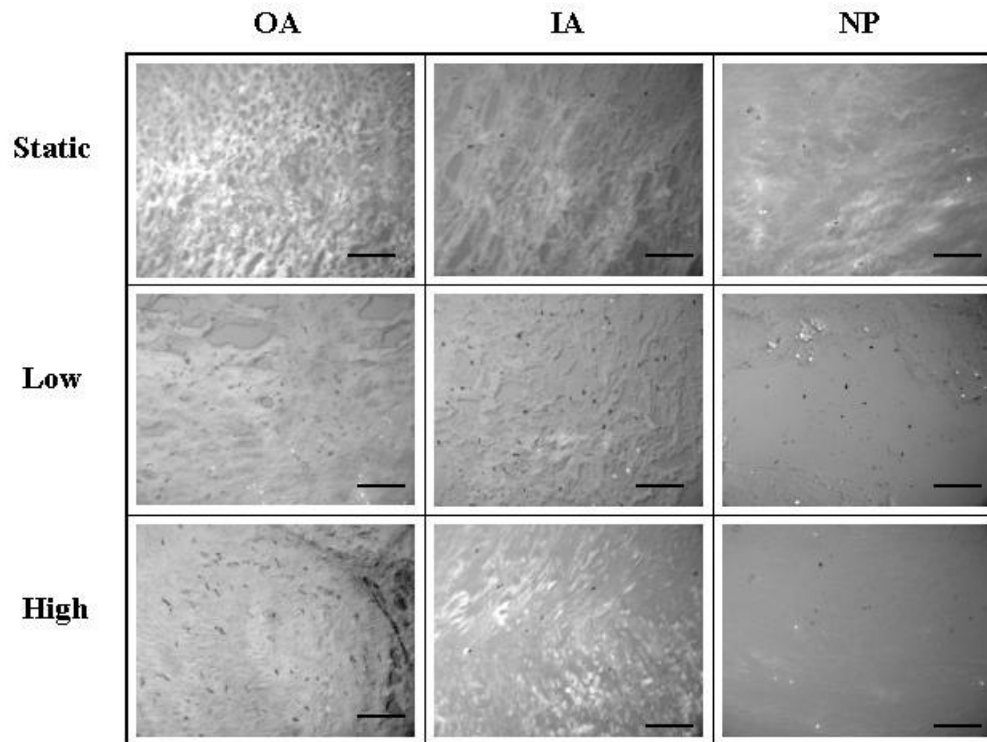


**Figure 4-2: Average  $\pm$  SEM sulfate incorporation rates for all testing groups (OA – outer annulus, IA – inner annulus, NP – nucleus pulposus). A trend of increasing sulfate incorporation was seen in the annulus regions, but not in the nucleus.**



Representative viability images at 20x magnification. black = live, white = dead. Scale bar in black = 400 um

**Figure 4-3: Representative viability images at 20x magnification. black = live, white = dead. Scale bar in black = 400 um. Columns represent tissue regions (OA – outer annulus, IA – inner annulus, NP – nucleus pulposus) and rows represent test groups. No changes in cell viability were observed.**

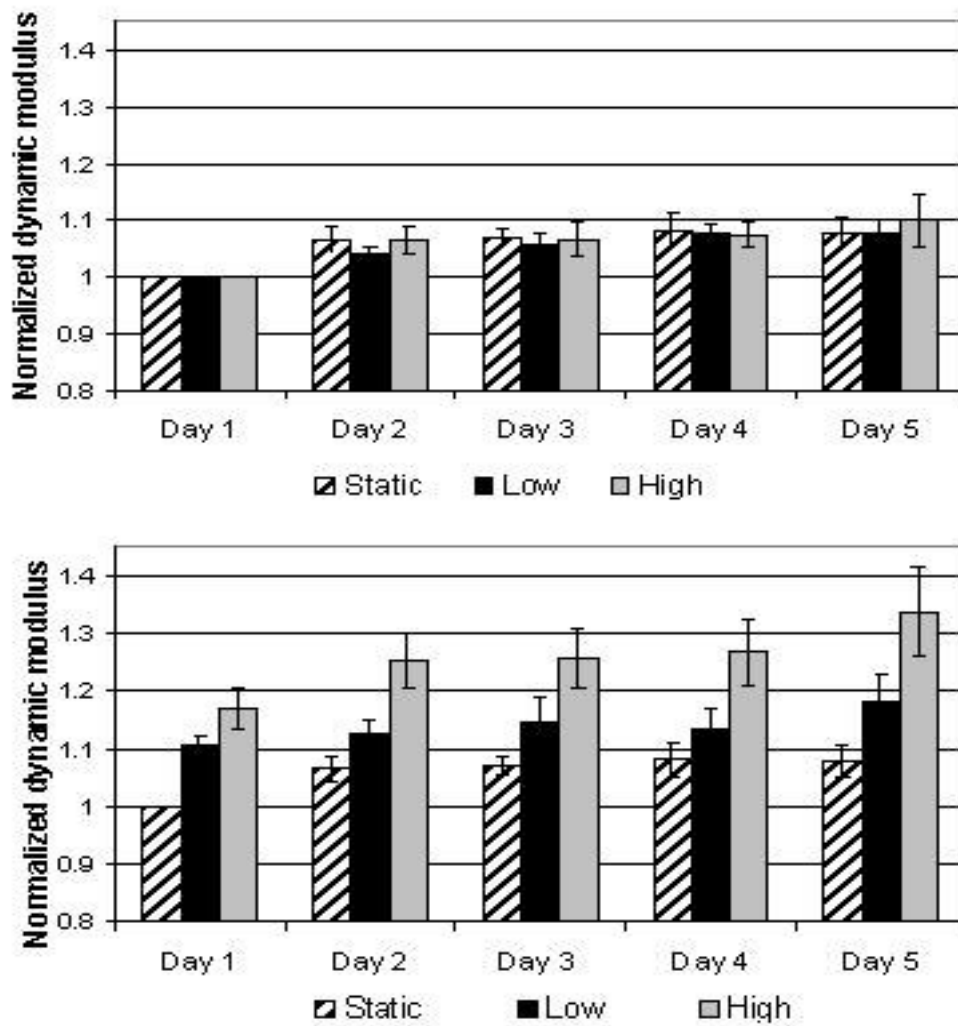
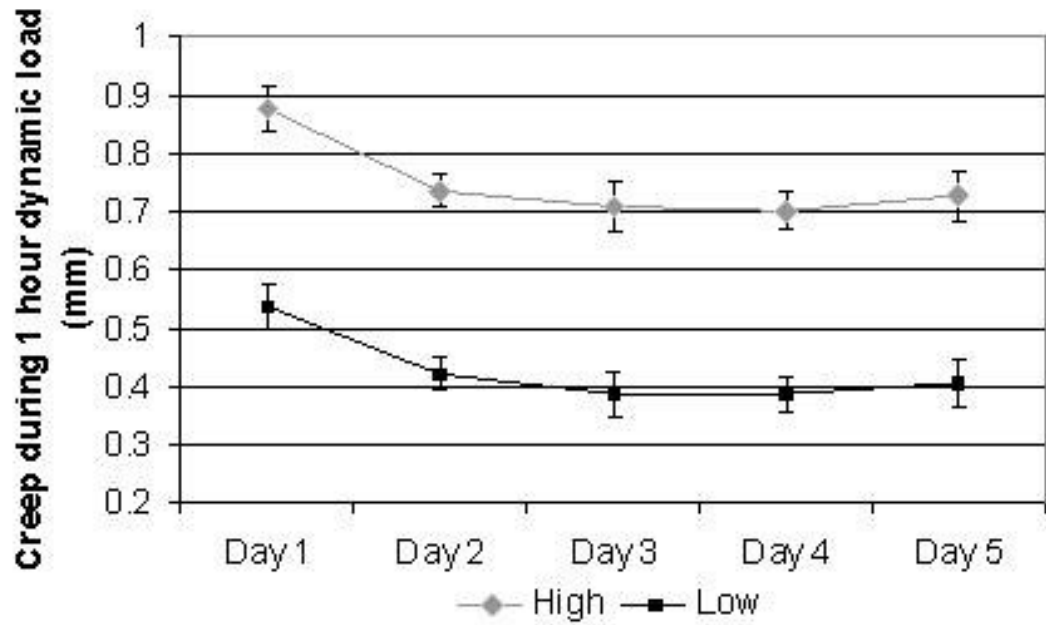


Figure 4-4: Average  $\pm$  SEM nominal dynamic loading modulus for pre-load (top) and post-load (bottom) tests.



**Figure 4-5: Average  $\pm$  SEM height loss for the one hour dynamic loading protocol. Significantly more height was lost at all time points in the high force dynamic loading groups than in the low force group.**

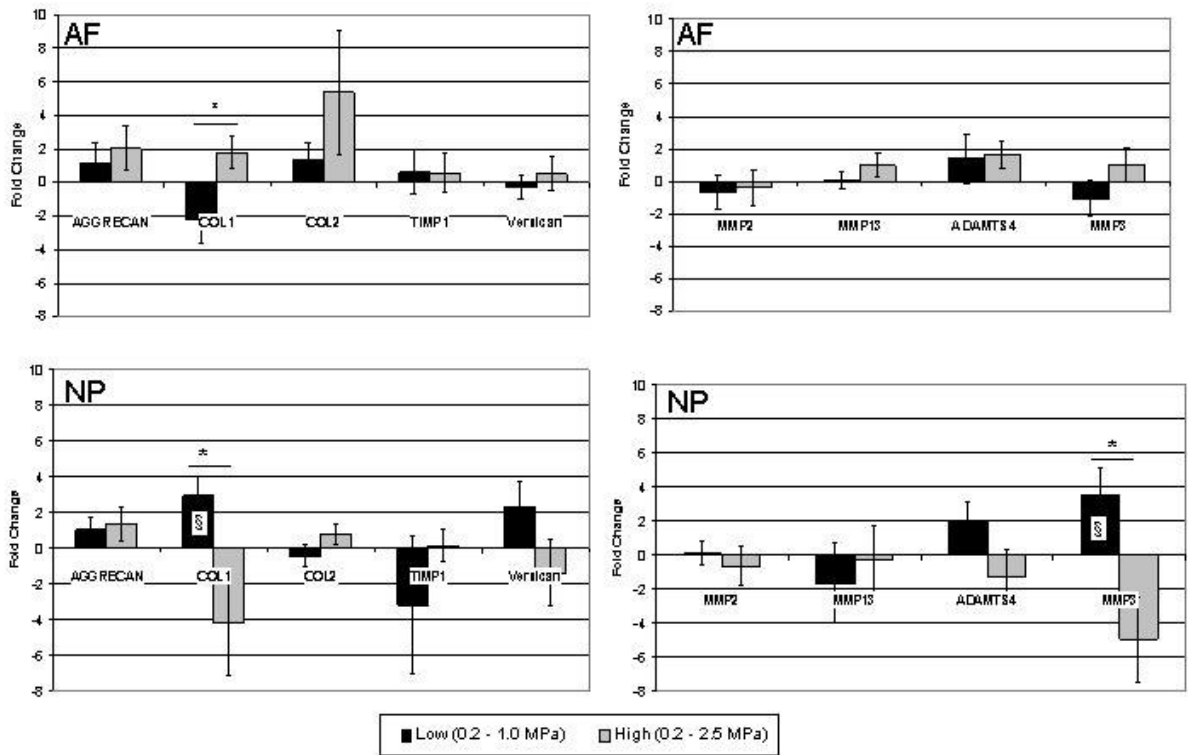
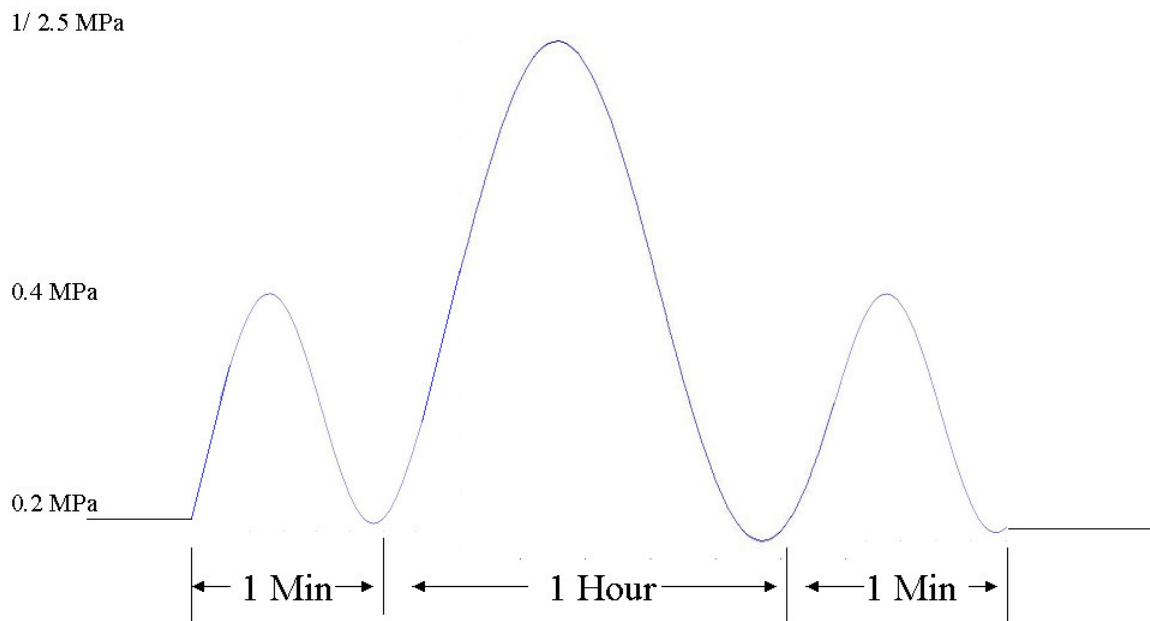


Figure 4-6: Gene expression fold change results as average  $\pm$  SEM for anabolic (aggrecan, collagen types I and II, versican), anti-catabolic (TIMP-1) (left column) and catabolic (MMP -2, -3, 13 and ADAMTS4) (right column) genes for tissue from annulus fibrosus (top row) and nucleus pulposus (bottom row) regions. Significant differences ( $p < 0.05$ ) between groups are marked with a \* while significant differences from static controls (using a t-test with hypothesized mean of zero) are marked with a § symbol (found in low groups in the NP for collagen type I and MMP3). Note that low and high groups are normalized to tail matched static controls.

## 4.11 Study Clarifications

This section is added as an addendum to the previous published chapter to address specific comments that arose during the dissertation defense.

Discs were initially confined for 12 hours with an applied stress of 0.2 MPa to prevent disc swelling (Figure 4-7)



**Figure 4-7:**Schematic of mechanical testing protocol. Discs were initially confined with 0.2 MPa. A one-minute test from 0.2 - 0.4 MPa was performed at 1 Hz. Then discs were loaded from 0.2 - 1 (LOW) or 2.5 MPa (HIGH) at 1 Hz for 1 hour. The 0.2 MPa static load was then returned to the disc to prevent swelling. NOTE NOT TO SCALE

Gene expression changes are defined as changes from the baseline controls (only loaded with 0.2 MPa static load).



The radioactive tracer  $^{35}\text{S-SO}_4$  was used, and is mistakenly referred to as just  $^{35}\text{S}$  in this document.

**CHAPTER 5 Intervertebral Disc Cell Response to Dynamic  
Compression is Age and Frequency Dependent**

Casey L. Korecki<sup>1,2</sup>, Catherine K. Kuo<sup>2</sup>, Rocky S. Tuan<sup>2</sup>, James C. Iatridis<sup>1</sup>

<sup>1</sup>Spine Bioengineering Lab, College of Engineering and Mathematical Sciences,  
University of Vermont, Burlington Vermont 05405, USA

<sup>2</sup>Cartilage Biology and Orthopaedics Branch, National Institute of Arthritis, and  
Musculoskeletal and Skin Diseases, National Institutes of Health, Department of Health  
and Human Services, Bethesda, Maryland 20892, USA

**Running Title (31 characters w/ spaces):** Age & load effects on IVD cells

Acknowledgements: NIH Grant (R01AR051146) and the Intramural Research Program  
of the NIH, National Institute of Arthritis and Musculoskeletal and Skin Diseases.

## 5.1 Abstract

The creation and maintenance of the intervertebral disc extracellular matrix is regulated by mechanical loading, nutrition, and the accumulation of matrix proteins, cytokines and degradation products that are affected by aging and degeneration. Evidence suggests that cellular aging may lead to alterations in the quantity and quality of extracellular matrix produced, and the aims of this study were to examine the role of loading, aging, and the interaction between these two factors in intervertebral disc cell gene expression and biosynthesis in a controlled three-dimensional culture environment. Cells were isolated from young (4-6 months) and mature (18-24 months) bovine caudal discs and separated into annulus fibrosus and nucleus pulposus tissue. Isolated cells were seeded into alginate gels and dynamically compressed for seven days at one of three frequencies (0.1, 1, or 3 Hz) or maintained as a static (free-swelling) control. After seven days, DNA and sulfated glycosaminoglycan contents were analyzed along with real time, quantitative reverse transcription-polymerase chain reaction analysis for collagen types I and II, aggrecan, and matrix metalloproteinase-3 gene expression. Results suggest aging plays an important role in intervertebral disc homeostasis and also influences the cell response to externally applied stimulation by mechanical loading. While isolated intervertebral disc cells responded to mechanical compression in three-dimensional culture, the effect of the frequency was minimal. Altered cellular phenotype and biosynthesis rates appear to be an attribute of the normal cell aging process, independent of changes in cellular microenvironment associated with lost nutrition and disc degeneration. Mature cells may also have a decreased capacity to create or retain

extracellular matrix components in response to mechanical loading compared to young cells.

## 5.2 Introduction

Mechanical stimulation has been demonstrated to affect cell metabolism and gene expression in the intervertebral disc (IVD) *in vivo* (14-16), *in situ* (7), and *in vitro* (10, 11, 24). However, differences in culture systems, methods of load application, and cellular phenotypes between species, have complicated comparison of results between studies. Cellular aging also has demonstrated effects in articular cartilage (17), intervertebral disc (20) and bone (18), among other tissues (5, 21). Investigation of the interaction between mechanical stimulation and cellular aging has potential implications for the understanding of the mechanism of IVD degeneration, and for future repair strategies, such as tissue engineering and cell therapy.

The response of the IVD to dynamic compression has been reported *in vivo*; however, limited literature exists on the effects of dynamic compression *in vitro*. The isolation of IVD cells from their surrounding matrix is advantageous for mechanotransduction studies as it allows for a consistent load to be applied to every cell. Tissue matrix mechanical properties can vary, and evidence of increased pericellular matrix stiffness with aging and disease in chondrocytes (1) points to changes in the ability of an applied load to be transduced to the cell level. The primary method used to apply mechanical stimulation to IVD cells *in vitro* thus far has been hydrostatic pressure, although static compression has also been studied (3). Further investigation is needed, as hydrostatic pressure may fail to simulate *in vivo* cell mechanical stimulation pathways by

neglecting cell strain, and static and dynamic compression have been shown to have dramatically different effects (22).

It is difficult to differentiate the cellular response to aging from that of exposure to a degenerative environment since the two are often coupled. Decreased cellular function and altered synthesis of extracellular matrix components have been demonstrated in articular chondrocytes with normal aging (17), reducing both the quantity and quality of repaired matrix after damage. A recent study on IVD cells demonstrated increasing incidence of cellular senescence correlated with increased disc degeneration, potentially indicating that fewer cells populate the matrix following necrosis and/or apoptosis (6), again leading to diminished capacity for repair. A shift in cell phenotype in the nucleus pulposus also occurs in some species, with some (pig, rat, rabbit) retaining notochordal cells into maturity, whereas others (human, cow, sheep) lack this cell type (9).

This study was composed of three aims. Aim 1 addressed whether tissue donor age affects IVD cell synthesis and gene expression in three-dimensional alginate culture. Bovine IVD tissues, from young (4-6 months) and mature (18-24 months) caudal discs, previously shown to compare well with IVD tissue from humans aged <15 years and 15-40 years, respectively (4), were used to ensure relative homogeneity in genetic, nutritional, and other environmental factors. Cells isolated from tissue of a greater age were hypothesized to have a reduced capacity for recreating extracellular matrix, with reduced DNA and sulfated glycosaminoglycan (sGAG) contents, and lower expression of anabolic genes, such as collagen types I and II and aggrecan. Aim 2 sought to determine

whether dynamic compression loading would affect IVD cell synthesis and gene expression in a frequency dependent manner. Increasing compression frequency was hypothesized to increase the accumulation of extracellular matrix and DNA synthesis, and to increase anabolic gene expression. Aim 3 was to determine the interaction between age and dynamic loading frequency. We hypothesized that decreases in cell metabolism associated with age could be counteracted by an increased cell metabolism brought about by mechanical stimulation, with similar GAG and DNA contents achieved at higher frequencies between young and mature tissue-derived cells, and similar patterns of gene expression.

### **5.3 Materials and Methods**

Intervertebral discs (IVD) were removed from five young (4-6 months) and five mature (18-24 months) bovine tails. Nucleus pulposus (NP) and annulus fibrosus (AF) tissue were separated by careful dissection and placed in washing medium (high glucose DMEM, 10% fetal bovine serum, 200 U/ml penicillin and streptomycin, 0.50 µg/ml amphotericin-B, 10% fetal bovine serum (FBS), 50 µg/ml ascorbic acid and 0.5% v/v 5M NaCl and 0.4M KCl to adjust medium osmolarity) for 4-6 days followed by cell isolation through enzymatic digestion consisting of 1 hour of pronase (0.2%) and 8-10 hours of collagenase type IV (0.2% for AF, 0.125% for NP) at 37C with constant agitation. The resulting cell suspensions were passed through a 70 µm mesh sieve and washed twice with phosphate buffered saline (PBS). A one-time expansion at a high cell density ( $8 \times 10^6$  cells/mm<sup>2</sup>) was performed when necessary to achieve adequate starting

numbers of cells. The duration of monolayer expansion was less than nine days, with medium changes every three to four days.

Alginate gel constructs were created in 96 well plates using a slow set technique (13), with cells seeded at a density of  $4 \times 10^6$  cells/ml. After curing, gels were placed into mechanical stimulation test dishes with culture medium (high glucose DMEM, 100 U/ml penicillin and streptomycin, 0.25  $\mu$ g/ml amphotericin-B, 10% FBS, 50  $\mu$ g/ml ascorbic acid and 0.5% v/v 5M NaCl and 0.4M KCl to adjust medium osmolarity to be similar to that in the IVD in situ) and allowed to equilibrate overnight in a 5% O<sub>2</sub> incubator.

Mechanical stimulation consisted of 2 hours of daily compressive strain from 2-12% for 7 days at one of three frequencies (0.1, 1 or 3 Hz). Additionally, an unstimulated (free-swelling) control was maintained. After 7 days of loading, gels were harvested for analysis. For all groups, gels were maintained at 37C, 5% O<sub>2</sub>. Media was changed every 3-4 days, and was saved at -80C for later analysis.

Nitrite concentrations were measured from aliquots of cell culture medium saved at each medium change using the Griess reaction (Promega, Madison, WI). Standard curves were generated with unused culture medium. For each 50  $\mu$ l sample of culture medium, 50  $\mu$ l of sulfanilamide was added and allowed to incubate for 5-10 minutes away from light. Then 50  $\mu$ l of N-1-naphthylethylenediamine dihydrochloride (NED) solution was added to the wells and again incubated 5-10 minutes protected from light. Sample and standard curve absorbance was analyzed at 550 nm on a microplate reader. Resulting molar concentrations were normalized to the number of gel constructs present in each dish.

Gels were dissociated by the addition of 1 mL of a 55 mM sodium citrate solution. Cell viability was checked using 1 $\mu$ M calcein-AM and 1 $\mu$ M ethidium homodimer-1 (LIVE/DEAD kit, Invitrogen, Carlsbad, CA) in PBS, which was incubated for 15 minutes before visualization. The remaining dissociated gel was centrifuged and the supernatant carefully removed from the separated pellet and stored. Pellets and supernatants were digested (300  $\mu$ g/mL papain, 10 mM L-cystine, 10mM EDTA and 100 mM sodium acetate) at 60°C overnight. Both pellet and supernatant digests were analyzed for DNA content and sGAG content. DNA content was determined using a Picogreen assay kit (Picogreen, Sigma, St. Louis, MO). sGAG content was determined with 1,9-dimethylmethylene blue (DMMB) adjusted to a pH of 1.5 to minimize alginate interference. Chondroitin-6-sulfate was used to generate the standard curve.

Real time, quantitative reverse transcription-polymerase chain reaction (qRT-PCR) was performed on dissociated gels (n = 5 per group). After RNA isolation and cDNA transcription, gene expression of 18S rRNA, aggrecan, collagen types I and II, and matrix metalloproteinase (MMP3) was analyzed using bovine gene-specific primers and SYBR Green. Transcript levels were normalized to that of the 18S rRNA housekeeping gene.

Statistical analyses were performed for each of the hypotheses. First, a one way ANOVA ( $p < 0.05$ ) followed by a Bonferroni post-hoc test was performed for loading effects (LOAD, hypothesis 1) by comparing each loaded group with the age-matched control and again for aging effects (AGE, hypothesis 2) by comparing data between ages at matched condition points. Finally, a two-way ANOVA was performed to address the



interaction between aging and loading effects (AGE\*LOAD) again followed by a Bonferroni post-hoc test.

## 5.4 Results

Viability was maintained throughout the experiment with >93% of cells viable after culturing and loading.

DNA content (Table 1) was greater in mature NP cell constructs ( $286.2 \pm 65.4$  ng) versus young NP cells ( $68.2 \pm 6.4$  ng) ( $p=0.02$ ), and was not significantly affected by loading in the NP. No significant statistical interaction between age and load was found in DNA content in the NP. In the AF, DNA content increased in young AF cells ( $181.7 \pm 21.5$  ng) versus mature AF cells ( $103.3 \pm 10.0$  ng) ( $p<0.0001$ ), and was also affected by loading ( $p<0.0001$ ), with pair-wise increases in the 0.1 Hz ( $156.5 \pm 28.8$  ng) and 3 Hz ( $182.4 \pm 18.6$  ng) loading groups versus controls ( $87.8 \pm 18.6$  ng) and 1 Hz loading ( $93.3 \pm 9.2$  ng). A statistical interaction between age and load was also found ( $p<0.0001$ ).

GAG content (Table 1) in the NP was not significantly different between ages ( $p>0.7$ ), between loading groups ( $p>0.7$ ), and no interaction was seen between the groups ( $p>0.7$ ). In the AF, an effect of age was observed, with higher GAG contents in mature ( $43.5 \pm 1.62$   $\mu$ g) than young AF constructs ( $37.6 \pm 1.84$   $\mu$ g) ( $p = 0.05$ ). No significant effect of loading or relationship between groups was observed ( $p>0.4$ ).

When the sGAG content was normalized to the matched DNA content of each construct (Figure 1), the value was greater in young NP constructs ( $0.656 \pm 0.047$   $\mu$ g/ng) versus mature NP constructs ( $0.228 \pm 0.031$   $\mu$ g/ng) ( $p<0.0001$ ). No effect of loading was found in the NP ( $p=0.2$ ); however, a statistical interaction between age and load was

observed in the NP ( $p < 0.0001$ ). In the AF, a higher sGAG/DNA content was observed in mature AF constructs ( $0.445 \pm 0.028 \mu\text{g}/\text{ng}$ ) compared to young AF constructs ( $0.26 \pm 0.025 \mu\text{g}/\text{ng}$ ) ( $p < 0.001$ ). The 3 Hz load group had lower sGAG/DNA ( $0.25 \pm 0.022 \mu\text{g}/\text{ng}$ ) compared to all other loading groups ( $0.4 \pm 0.031 \mu\text{g}/\text{ng}$ ) ( $p < 0.0001$ ).

Furthermore, a significant interaction between age and load was found ( $p < 0.001$ ).

Nitrite concentrations (Figure 2) in the medium containing both the AF and NP cell constructs remained consistent, without significant differences between young and mature constructs, and between loading groups. No significant interaction between age and load was found for either cell type.

In the NP (Figure 3), expression of collagen types I and II increased significantly in mature cells as compared to young cells ( $p < 0.03$ ). No significant effect of loading was observed ( $p = 0.1$ ). However, a significant relationship between age and loading was observed ( $p < 0.001$ ), with expression of collagen types I and II decreasing in young cells and increasing in mature cells with increasing loading frequency. Aggrecan gene expression in the NP was not significantly affected by age or loading, and no significant interaction was found between the two ( $p > 0.05$ ). MMP3 gene expression was significantly affected by age ( $p < 0.02$ ) but not by loading ( $p = 0.2$ ), with a significant interaction observed between the two ( $p < 0.05$ ). In the AF (Figure 4), collagen type I expression was significantly affected by aging and 3 Hz loading, and a significant interaction was also observed between the two ( $p < 0.001$ ). Expression of collagen type II, aggrecan and MMP3 were all affected by aging and 1 and 3 Hz loading ( $P < 0.001$ ) in the annulus.

## 5.5 Discussion

This study examined the effects of animal age and loading frequency on extracellular matrix production and gene expression of isolated IVD cells in 3D gel culture. Young and mature IVD cells remained viable and mechanically responsive in 3D alginate culture. Generally, anabolic gene expression was increased in mature cells and catabolic gene expression of MMP3 was decreased. However, less sGAG/DNA production was observed in mature cells than in young cells. Therefore, increasing age increased the anabolic, and decreased the catabolic gene expression of IVD cells, but this shift was not reflected in terms of the level of sGAG production. Loading effects were typically frequency independent, indicating that the application of mechanical stimulation had a similar effect regardless of the frequency it was applied. Overall, age was a dominating factor over loading. A significant interaction between age and loading was observed in some cases, particularly in the AF where loading had very distinct anabolic and catabolic responses for mature and young cells.

This study is among the first to examine the response of isolated disc cells to dynamic compression. Increased hydrostatic loading frequencies have been shown to decrease DNA content in the NP (11) and increase DNA content in the AF, leading to a decreased sGAG/DNA content (19). Similarly, this study observed greater DNA contents in the mature NP and the young and mature AF, which further translated into reduced sGAG/DNA contents, suggesting that these cells proliferate at a higher rate than they produce extracellular matrix. In the young NP, however, an increase in the sGAG/DNA value was noted with loading, possibly indicating an age-related change in

the ability for these cells to produce and accumulate sGAG in response to loading. Expression levels of aggrecan and collagen type II have also been shown to be upregulated with dynamic hydrostatic loading (24). In this study, an upregulation of collagen type II was observed in mature NP cells, but not in young NP, or any AF cells. In addition, an upregulation of collagen type I was observed in both mature AF and NP cells, possibly indicating a difference in the cell response to compression versus hydrostatic loading, but not in the young NP or AF, again indicating an age related change in the cellular response to loading.

Alginate has been shown to be a suitable culture system for IVD NP cells (12, 23), but may (2, 3, 12) or may not (8) be appropriate for AF cells. No indication of phenotype shift in the AF cells were seen in this study, with levels of gene expression for collagen type I and aggrecan maintained in control samples after seven days relative to day zero (data not shown). Previous studies of IVD cells cultured in alginate have also indicated a dramatic decrease in cell viability (8), which was not observed in this study, also consistent with previous work (12). It should be noted that in this study the duration of monolayer expansion was also kept to a minimum to ensure phenotype maintenance (23).

This was a displacement-controlled loading experiment with compression frequency being varied and load duration remaining constant. Consequently, both strain rate and duty cycle were varying with the frequency effects. Interestingly, however, very few frequency effects were detected, suggesting that cell strain had larger effects on IVD cells than strain rate or duty cycle in alginate. The three-dimensional alginate matrix is

not expected to generate much pressurization under compression loading, in contrast to the highly viscoelastic IVD tissue matrix, so we further interpret these findings as cell strain effects in three-dimensional culture rather than a true simulation of compression.

Based on these results, we conclude that aging plays an important role in IVD homeostasis and also influences the cell response to externally applied stimulation by mechanical loading. While isolated IVD cells respond to mechanical loading, the effect of the loading frequency was minimal, and mature cells may also have a decreased capacity to create or retain extracellular matrix components in response to mechanical stimulation compared to young cells. These results indicate that altered cell phenotype and biosynthesis rates are an attribute of normal cell aging processes, consistent with previous studies in different tissues (17), and demonstrating that aging effects are independent of changes in cellular microenvironment associated with degeneration and decreases in cell nutrition.

## 5.6 References

1. Alexopoulos LG, Setton LA, Guilak F: The biomechanical role of the chondrocyte pericellular matrix in articular cartilage. *Acta Biomater* 1:317-25, 2005
2. Baer AE, Wang JY, Kraus VB, Setton LA: Collagen gene expression and mechanical properties of intervertebral disc cell-alginate cultures. *J Orthop Res* 19:2-10, 2001
3. Chen J, Yan W, Setton LA: Static compression induces zonal-specific changes in gene expression for extracellular matrix and cytoskeletal proteins in intervertebral disc cells in vitro. *Matrix Biol* 22:573-83, 2004
4. Demers CN, Antoniou J, Mwale F: Value and limitations of using the bovine tail as a model for the human lumbar spine. *Spine* 29:2793-9, 2004
5. Dudhia J, Scott CM, Draper ER, Heinegard D, Pitsillides AA, Smith RK: Aging enhances a mechanically-induced reduction in tendon strength by an active process involving matrix metalloproteinase activity. *Aging Cell* 6:547-56, 2007
6. Gruber HE, Ingram JA, Norton HJ, Hanley EN, Jr.: Senescence in cells of the aging and degenerating intervertebral disc: immunolocalization of senescence-associated beta-galactosidase in human and sand rat discs. *Spine* 32:321-7, 2007
7. Haschtmann D, Stoyanov JV, Ferguson SJ: Influence of diurnal hyperosmotic loading on the metabolism and matrix gene expression of a whole-organ intervertebral disc model. *J Orthop Res* 24:1957-66, 2006
8. Horner HA, Roberts S, Bielby RC, Menage J, Evans H, Urban JP: Cells from different regions of the intervertebral disc: effect of culture system on matrix expression and cell phenotype. *Spine* 27:1018-28, 2002
9. Hunter CJ, Matyas JR, Duncan NA: Cytomorphology of notochordal and chondrocytic cells from the nucleus pulposus: a species comparison. *J Anat* 205:357-62, 2004
10. Kasra M, Goel V, Martin J, Wang ST, Choi W, Buckwalter J: Effect of dynamic hydrostatic pressure on rabbit intervertebral disc cells. *J Orthop Res* 21:597-603, 2003
11. Kasra M, Merryman WD, Loveless KN, Goel VK, Martin JD, Buckwalter JA: Frequency response of pig intervertebral disc cells subjected to dynamic hydrostatic pressure. *J Orthop Res* 24:1967-73, 2006

12. Kluba T, Niemeyer T, Gaissmaier C, Grunder T: Human annulus fibrosus and nucleus pulposus cells of the intervertebral disc: effect of degeneration and culture system on cell phenotype. *Spine* 30:2743-8, 2005
13. Kuo CK, Ma PX: Ionically crosslinked alginate hydrogels as scaffolds for tissue engineering: part 1. Structure, gelation rate and mechanical properties. *Biomaterials* 22:511-21, 2001
14. Maclean JJ, Lee CR, Alini M, Iatridis JC: Anabolic and catabolic mRNA levels of the intervertebral disc vary with the magnitude and frequency of in vivo dynamic compression. *J Orthop Res* 22:1193-200, 2004
15. MacLean JJ, Lee CR, Alini M, Iatridis JC: The effects of short-term load duration on anabolic and catabolic gene expression in the rat tail intervertebral disc. *J Orthop Res* 23:1120-7, 2005
16. MacLean JJ, Lee CR, Grad S, Ito K, Alini M, Iatridis JC: Effects of immobilization and dynamic compression on intervertebral disc cell gene expression in vivo. *Spine* 28:973-81, 2003
17. Martin JA, Buckwalter JA: Aging, articular cartilage chondrocyte senescence and osteoarthritis. *Biogerontology* 3:257-64, 2002
18. Perrien DS, Akel NS, Dupont-Versteegden EE, Skinner RA, Siegel ER, Suva LJ, Gaddy D: Aging alters the skeletal response to disuse in the rat. *Am J Physiol Regul Integr Comp Physiol* 292:R988-96, 2007
19. Reza AT, Nicoll SB: Hydrostatic pressure differentially regulates outer and inner annulus fibrosus cell matrix production in 3D scaffolds. *Ann Biomed Eng* 36:204-13, 2008
20. Taylor TK, Melrose J, Burkhardt D, Ghosh P, Claes LE, Kettler A, Wilke HJ: Spinal biomechanics and aging are major determinants of the proteoglycan metabolism of intervertebral disc cells. *Spine* 25:3014-20, 2000
21. Vannini N, Pfeffer U, Lorusso G, Noonan DM, Albin A: Endothelial cell aging and apoptosis in prevention and disease: E-selectin expression and modulation as a model. *Curr Pharm Des* 14:221-5, 2008
22. Wang DL, Jiang SD, Dai LY: Biologic response of the intervertebral disc to static and dynamic compression in vitro. *Spine* 32:2521-8, 2007

23. Wang JY, Baer AE, Kraus VB, Setton LA: Intervertebral disc cells exhibit differences in gene expression in alginate and monolayer culture. *Spine* 26:1747-51; discussion 1752, 2001
24. Wuertz K, Urban JP, Klasen J, Ignatius A, Wilke HJ, Claes L, Neidlinger-Wilke C: Influence of extracellular osmolarity and mechanical stimulation on gene expression of intervertebral disc cells. *J Orthop Res*, 2007



## 5.7 Tables and Figures

**Table 5-1: Average GAG (ug) and DNA (ng) content plus/minus SEM for constructs. Stars (\*) indicate significantly lower amounts between age groups, (#) indicate significant differences between loading groups**

		<b>Control</b>	<b>0.1 Hz</b>	<b>1 Hz</b>	<b>3 Hz</b>
<b>Young NP</b>	<b>DNA</b>	90 +/- 2.49 (*)	64.9 +/- 5.98 (*)	70.3 +/- 18.29 (*)	47.2 +/- 16.01 (*)
	<b>GAG</b>	42.4 +/- 5.64	44.0 +/- 2.34	45.3 +/- 2.84	39.3 +/- 5.78
<b>Mature NP</b>	<b>DNA</b>	103.5 +/- 53.40	139.8 +/- 108.02	414.9 +/- 158.69	404.4 +/- 133.42
	<b>GAG</b>	38.0 +/- 3.99	42.9 +/- 3.57	42.5 +/- 1.72	43.4 +/- 2.89
<b>Young AF</b>	<b>DNA</b>	129.6 +/- 29.96	272.9 +/- 22.41	81.6 +/- 10.84	221.9 +/- 27.47
	<b>GAG</b>	39.5 +/- 4.62 (*)	37.7 +/- 4.86 (*)	32.2 +/- 1.85 (*)	40.4 +/- 3.93 (*)
<b>Mature AF</b>	<b>DNA</b>	56.5 +/- 1.28 (*)	83.7 +/- 12.84 (*)	101.6 +/- 13.49 (*,#)	154.3 +/- 20.35 (*,#)
	<b>GAG</b>	40.6 +/- 4.18	43.7 +/- 3.37	41.7 +/- 3.17	45.9 +/- 2.73

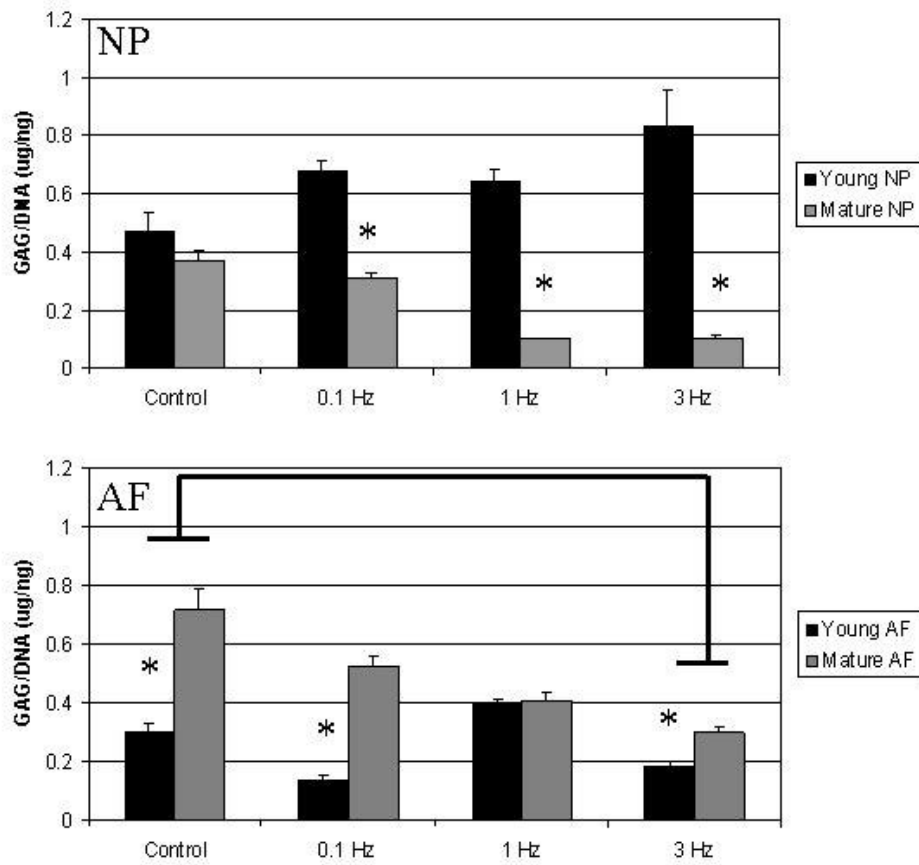


**Figure 5-1: GAG/DNA content (ug/ng) of the nucleus pulposus (top) and anulus fibrosus (bottom) after seven days. Values are shown as averages plus/minus SEM. Results for cells derived from young tissue are shown in black, mature cells in grey. Stars (\*) indicate significantly lower amounts between age groups, bars - indicate significant differences between loading groups.**

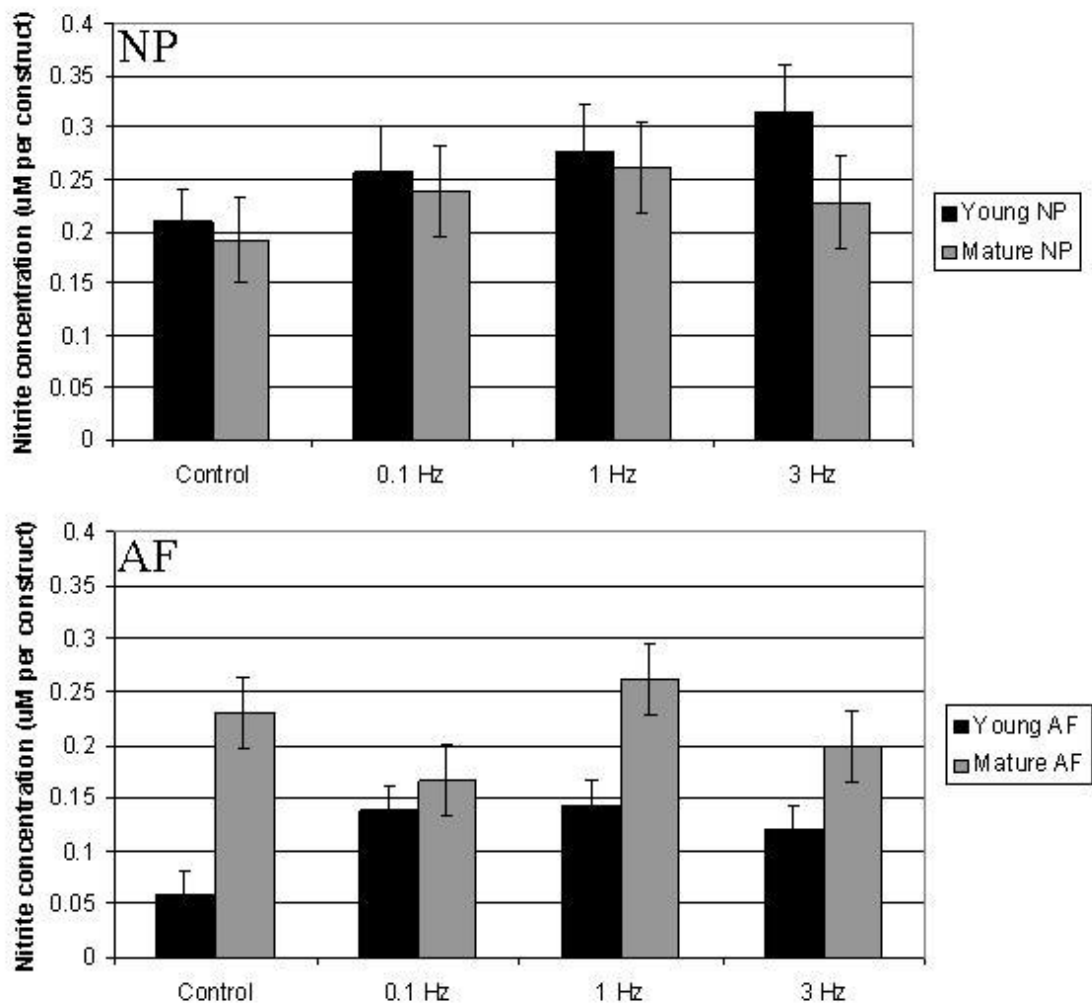


**Figure 5-2: Nitrite concentrations (uM) normalized to the number of constructs in each well of the nucleus pulposus (top) and anulus fibrosus (bottom) after seven days. Values are shown as averages plus/minus SEM. Results for cells derived from young tissue are shown in black, mature cells in grey. No significant differences were found between groups.**

## Nucleus Pulposus

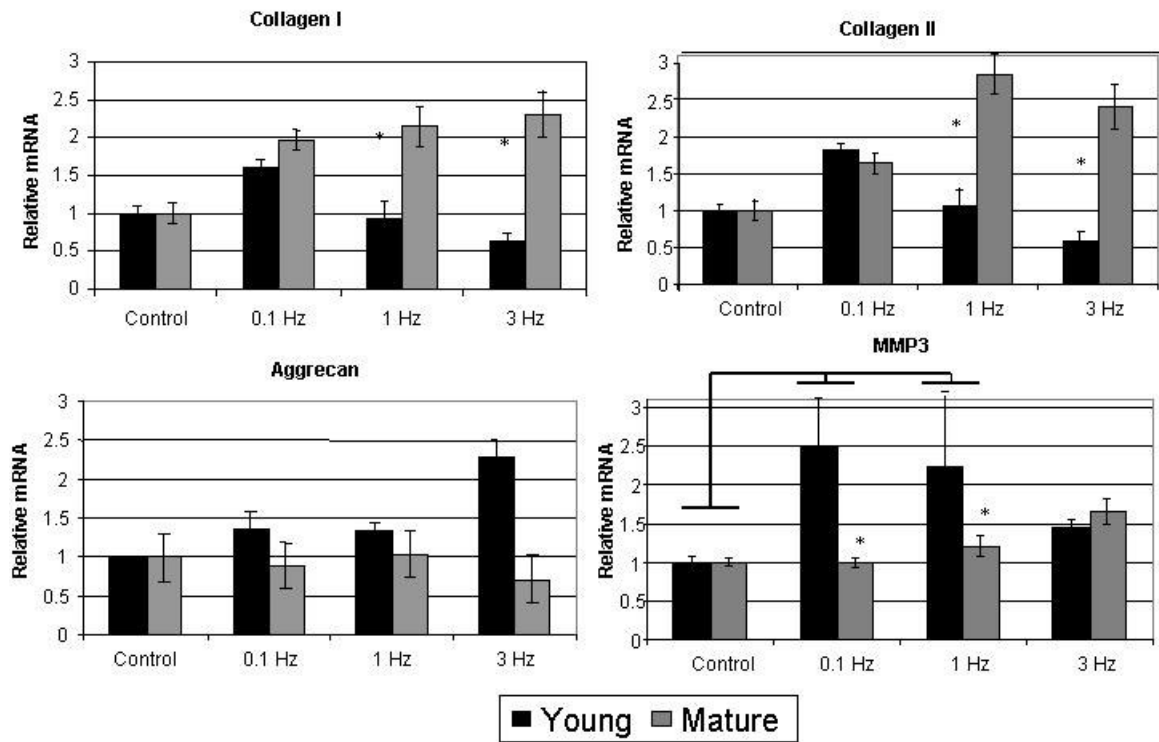


**Figure 5-3: qRT-PCR data for nucleus pulposus cells. Results for cells derived from young tissue are shown in black, mature cells in grey. Values are shown as averages plus/minus SEM. Stars (\*) indicate significantly lower amounts between age groups, bars – indicate significantly lower amounts between age groups, bars – indicate significant differences between loading groups.**

## Anulus Fibrosus

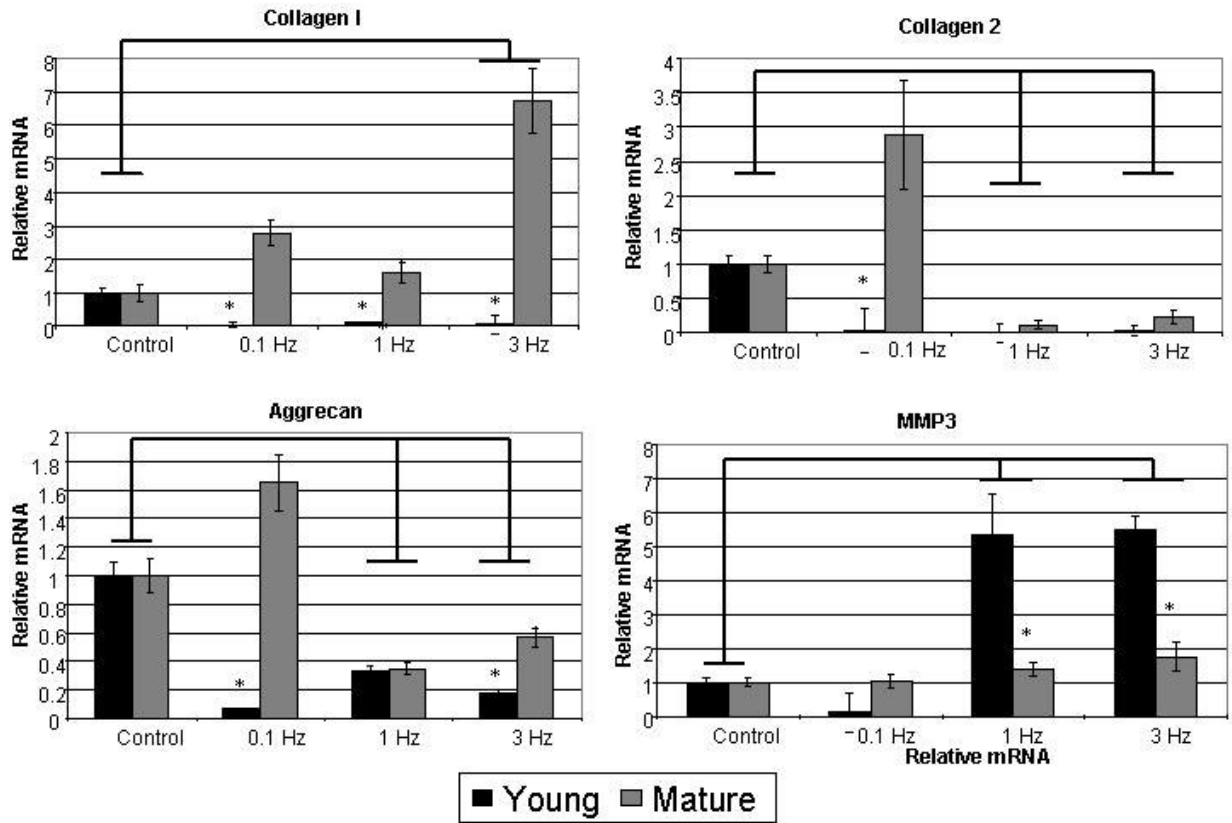


Figure 5-4: qRT-PCR data for anulus fibrosus cells. Results for cells derived from young tissue are shown in black, mature cells in grey. Values are shown as averages plus/minus SEM. Stars (\*) indicate significantly lower amounts between age groups, bars – indicate significant differences between loading groups.

## **5.8 Study Clarifications**

This section is added as an addendum to the previous chapter in review for publication to address specific comments that arose during the dissertation defense.

In this study, the term sGAG – meaning sulfated glycosaminoglycans, is used as the term GAG – meaning glycosaminoglycans was used in previous chapters. For all, the measurement of GAG content was based on the presence of sulfated glycosaminoglycans present. The interchangeable use of these two terms is commonly accepted in this field.

The hypothesis around 'reduced DNA' in mature tissues means the mature cells would proliferate less, and therefore at the end of the culture period the constructs with mature cells would have a lower DNA content.

**CHAPTER 6 Application of Clustering and Biclustering Analyses to**  
**Explore the Role of Mechanics, Aging, Time, and Culture Model on**  
**Gene Expression Patterns**

**6.1 Introduction**

Advances in technology have dramatically increased the amount of data available from biological experiments. For example, microarray experiments can result in the output of 30,000+ genes from a single sample, which must then be compared to one or more other samples also containing 30,000+ genes to identify meaningful trends and the genes associated with such trends. Fortunately, advances in computing power have increased the reasonable number of comparisons in a given experiment, and expanded the potential to contribute to significant findings. While there is no substitute for careful experimental planning to concisely address proposed hypotheses, the advent of such powerful tools as microarray or proteomic assays motivates the development of robust and powerful computing tools capable of handling such large volumes of data. Therefore, as technology continues to advance, and the questions researchers ask continue to become more complex, data analysis methods will become a key consideration.

One method that can be used to begin to identify meaningful trends is clustering analysis. Clustering is a means by which data is assembled into groups that are associated, typically by either a distance or correlation metric. A variety of metrics exist. Two of the most commonly used are Euclidian distance and Pearson correlation

coefficient (D'Haeseleer, 2005). Both have been used successfully in orthopaedic applications, for example clustering gene expression data from orthopaedic tissues (Fitzgerald et al., 2006, Fitzgerald et al., 2004) and to evaluating size ranges of intervertebral disc replacements (Lei et al., 2006).

Once a distance metric is chosen, the choice of clustering type is made. Two of the most common classes of clustering algorithms are called hierarchical and partitioned clustering. Hierarchical clustering is where each cluster is subdivided into smaller and smaller clusters to include the data (D'Haeseleer, 2005). The result can often be represented as a dendrogram or tree. The level at which to stop linking the data together can be chosen (referred to as cutting the tree or dendrogram at a point). Examples of hierarchical clustering include single linkage and complete linkage methods. In partitioned clustering, the data is divided into a predetermined number of subsets, divided by the data point's proximity to the nearest cluster. Examples of partitioning algorithms are k-means and fuzzy c-means clustering (D'Haeseleer, 2005). The differences between these methods can be visually seen below (Figure 6-1, concept from D'Haeseleer, 2005).



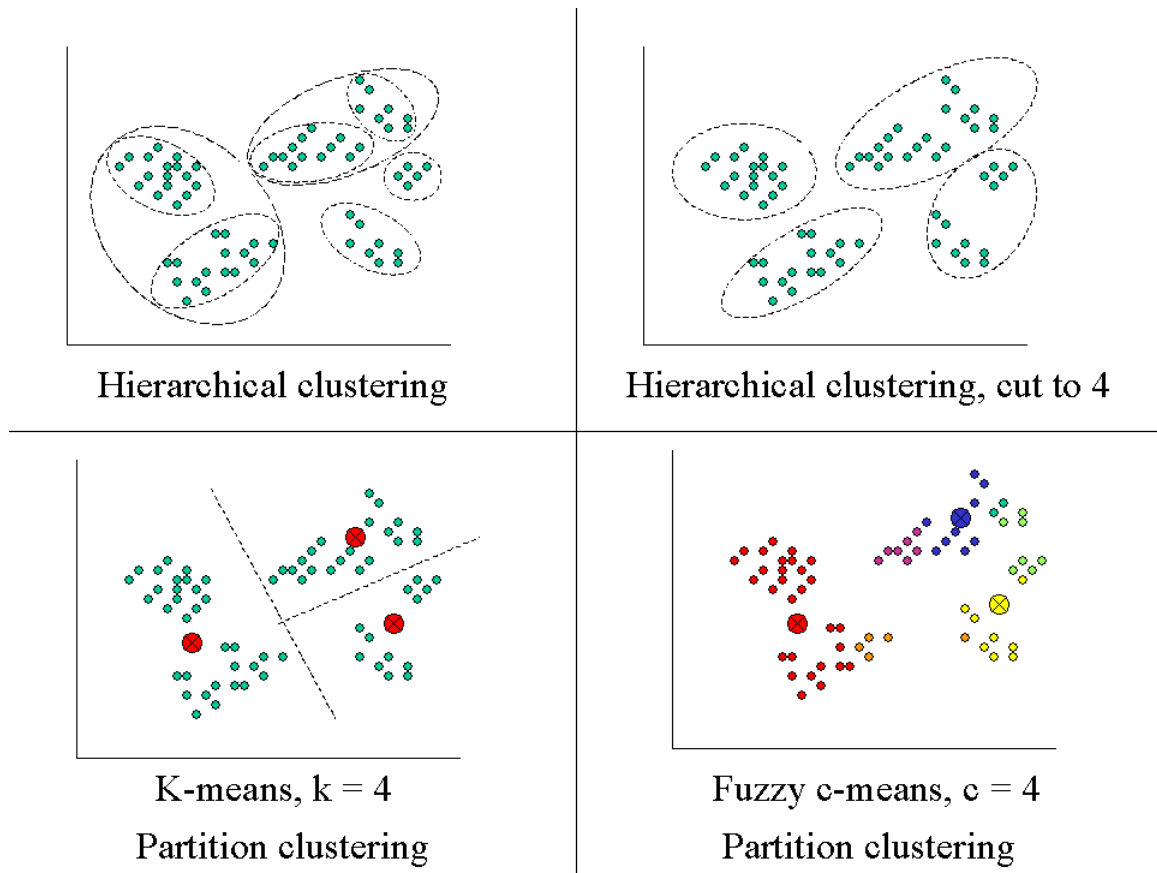


**Figure 6-1: Visual representation of clustering methods.** The top two represent hierarchical methods, where data points are grouped into larger and larger clusters. Meaningful clusters can be isolated by cutting the clustering tree at a certain cluster number (4 for the top right image). The bottom two panels represent partitioning methods. In k-means, (bottom left) three optimal cluster centers are found (red circle with x) and each data point is chosen to belong exclusively to one or another group. In fuzzy c-means (bottom right) optimal cluster centers are found (red, blue, yellow circles with X) and each data point can belong to a combination of the cluster centers (green data belongs to red and yellow centroids)

Ideally, similar groups are found between clustering methodologies (regardless of grouping metric), the groups are stable when the data is subjected to small perturbations, and the results of the clustering are biologically meaningful. The challenge to be able to visualize the data, and the resulting clusters, still exists after clustering is completed. This is because the clusters will exist in the same N number of dimensions as the data (for

example in 27 genes or in 24 experimental groups). The next challenge therefore, is to reduce the dimensionality of the variable space to aid in visualization in 2D or 3D.

Principal component analysis (PCA) is a method of multivariate analysis first introduced in 1901 by Pearson. The underlying theory is to reduce the dimensions of a data set by identifying and combining related variables into new variables, which represent the majority of the variation of the data. In this way, data that is composed of many variables can be reduced and visualized in a smaller coordinate system to aid visualization of complex data.

Non-negative matrix factorization (NMF) can also be used to change the variable space of the analysis. NMF, developed in 1999 (Lee and Seung, 1999), works by decomposing the dataset into two matrices with non-negative entries which allows for the visualization in a 'k' space where k is the number of groups present (Ulloa-Montoya et al., 2007). The original dataset is reproduced by the addition of the data present in each matrix rather than a cancellation of positive and negative elements as in PCA. This makes the relevance and interpretation of these decomposed matrices more intuitive. NMF was applied to yeast data and was estimated to be up to two times more accurate than traditional approaches (Kim and Tidor, 2003). Unlike PCA, which has been used in one previous study of orthopedic tissue mechanobiology (Fitzgerald et al., 2006), the application of NMF to biological problems and data is relatively new and has never been applied to the study of orthopaedic tissues.

It is the goal of this study to apply computational tools developed to handle complex data to visualize the gene expression data from a variety of experimental

conditions including mechanical loading (control and 0.1,1,and 3 Hz), cellular aging (cells from mature or young intervertebral disc tissue), and time (time points at 7, 14 and 21 days). The clustering aspect of this study is defined by two goals. First, the goal was to find experimental groups that are linked by similar gene expression profiles, indicating the response to those experimental conditions are similar. Second, the goal was to find genes that are commonly linked by experimental protocols, indicating the genes have a similar response to the experimental conditions. (Figure 6-2) The first goal can be thought of as seeking to determine what independent variables (in this case aging, loading and time) are similar, and the second goal as exploring which genes have similar expression patterns in response to aging, loading, and time. For example, by grouping the experimental conditions together, one may find all the young cell experiments group together, meaning the effects of age dominate all other experimental conditions. Likewise, by grouping the genes together, similar expression patterns may be found in three selected genes, meaning those genes are most likely regulated along a common pathway or by a common upstream factor.

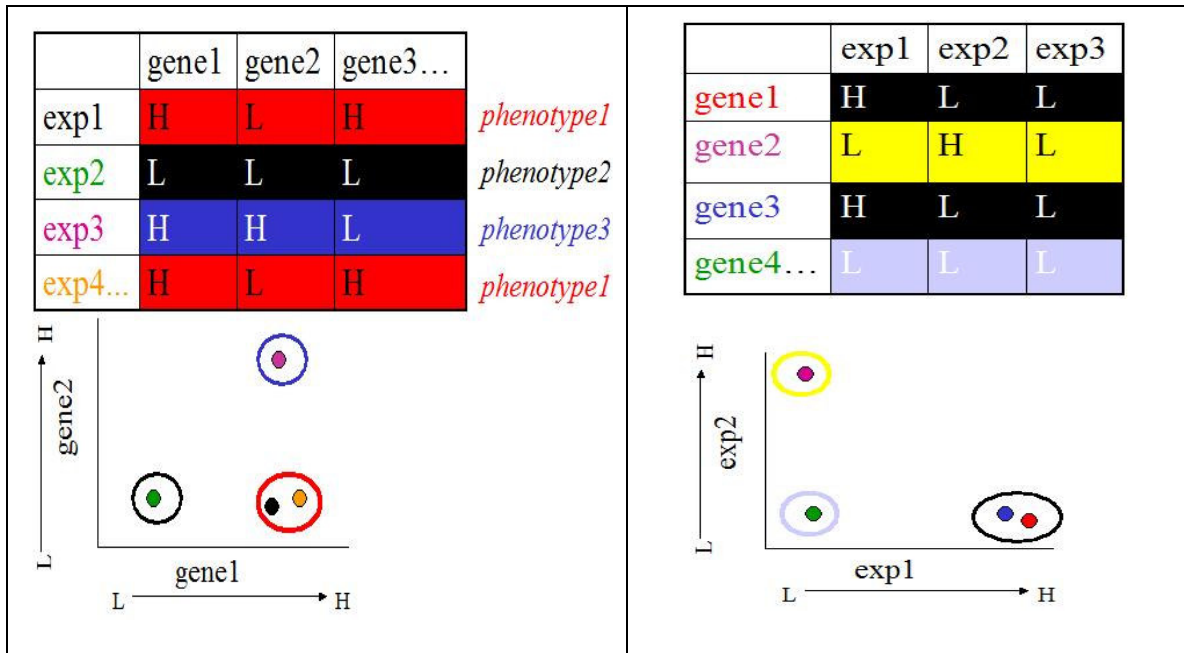


**Figure 6-2: Two clustering approaches were used; first experiments were clustered using their gene expression as a phenotype (L), and clustering genes that exhibit similar expression patterns between experimental conditions (R). In both simplified examples shown here, H and L indicate a ‘high’ or ‘low’ gene expression respectively. The data from the first two columns is represented as the x and y axis of the associated graph. In both cases, two groups were similar (row is highlighted with the same color) and the data points are shown graphically along with a circle representing they are ‘clustered’**

Next, in an attempt to further characterize the data set, the experimental groups found to cluster together (similar phenotype, red rows in Figure 6-2, Left) were identified and the data matrices were isolated. The isolated data matrices were then transposed and subject to clustering of their gene expression (Figure 6-2, Right), in a process known as biclustering. The utility of this approach was to determine what genes were responsible for the different experimental ‘phenotypes’ observed from the first aim.

The further application of this model was two-fold. First, the predictive value in experimental group “phenotype” was established by attempting to use the patterns developed to predict groupings for the data presented in study #2. The intention of this approach was to determine if any phenotype patterns were conserved between studies,

which would further support their role in intervertebral disc mechanotransduction. Second, the predictive ability of the clusters for gene expression response was explored. To this end, four gene sets, whose behavior in the intervertebral disc is better known from literature, were held back from the initial analysis and used as a test set. These genes are known to associate with other genes used in the initial analysis to establish the clusters and their centroids, so their membership should be predictable based on the presence of their known associates. The ability to predict those gene cluster memberships would further validate the ability for clustering analysis to highlight important functional groupings between related genes. The overall goal of these two applications was to determine whether the discovered experimental and gene expression pattern clusters possessed any predictive value.

## **6.2 Methods**

### **6.2.1 Experimental framework**

The proposed experimental groups are similar to those described in Study #3 with the addition of a time component to the response (Table 6-1). Briefly, IVD cells were isolated from the AF and NP of bovine caudal discs and seeded into alginate gel matrices. The three effects under investigation include mechanical loading, age and time of culture. To investigate mechanical loading effects, a dynamic compression regime was applied to the alginate-IVD cell matrices at three frequencies (0.1, 1 3 Hz) while maintaining an unloaded control. To explore age effects, two ages of bovine samples were used: 4-6 months, simulating approximately a <15yr old human disc and 18-24 months, simulating

a 15-40 yr old (Demers et al., 2004). Samples were collected at 7, 14 and 21 days to examine the time course of the response.

**Table 6-1: Experimental groups. 4 loading conditions (Control, 0.1, 1, and 3 Hz) will be explored at 4 time points (Days 0, 7, 14, 21) and in young and mature cells for a total of 32 experimental groups per tissue (AF or NP).**

	<b>Day 0</b>	<b>Day 7</b>	<b>Day 14</b>	<b>Day 21</b>
<b>Control</b>	Mature/Young	Mature/Young	Mature/Young	Mature/Young
<b>0.1 Hz</b>	Mature/Young	Mature/Young	Mature/Young	Mature/Young
<b>1 Hz</b>	Mature/Young	Mature/Young	Mature/Young	Mature/Young
<b>3 Hz</b>	Mature/Young	Mature/Young	Mature/Young	Mature/Young

Quantitative RT-PCR was performed as described in chapter 5. To control for comparisons made across PCR runs (requiring different batches of SYBR green which are typically variant due to manufacturing processes), a control sample of reference bovine IVD cDNA was run on each plate and the threshold value for this control sample was maintained across plates. The genes that were analyzed (Table 6-2) were chosen for their implied or explicit role in the maintenance or pathology of IVD tissue representing the most likely candidates for illustrating functional differences between groups.

Similar to previous strategies in clustering analysis (Fitzgerald et al., 2006, Fitzgerald et al., 2004) genes were also chosen to represent a spectrum of the biological processes, including matrix proteins and proteases, anti-catabolic protease inhibitors, transcription factors, and signaling molecules. These functional classifications are used very loosely in this study.

**Table 6-2: 31 genes were analyzed using real-time RT-PCR for all 32 experimental groups in each tissue (AF or NP).**

Matrix Proteins	Collagen I Collagen II Collagen III CollagenVI Aggrecan Versican Decorin Biglycan Link Vimentin Fibronectin
Matrix Proteases	MMP1 MMP2 MMP3 MMP13 ADAMTS4 ADAMTS5
Anti-Catabolic	TIMP1 TIMP2 TIMP3
Transcription factors	c-fos c-jun MAPK STAT3 ilk
Signaling molecules	TGFβ CTGF IGF IL-6
Housekeeping	GAPDH 18S

## **Matrix proteins**

### *Collagen*

Type I collagen is a main component of the anulus fibrosus, but does not contribute much to the nucleus pulposus. Previous studies, (including study #2) have shown a change in the regulation of collagen I with mechanical loading in the intervertebral disc (Wuertz et al., 2007). Type I is also typically associated with a tissue that has a predominant mechanical function of resisting tensile forces, and is correspondingly present in tendons and ligaments as well. Type II is the opposite case, where it contributes heavily to the nucleus pulposus, but less to the annulus fibrosus. Type II Is typically associated with a tissue that mainly resists compressive forces and is present in articular cartilage. Type III collagen has been reported to increase pericellularly with increased age in the intervertebral disc (Gruber et al., 2007) and also increases with disc degeneration (Roberts et al., 2006), however it is also one of the first

collagen types present in the intervertebral disc during development (Hayes et al., 2001). Collagen VI is a major structural element of microfibrils, reported to be present in the intervertebral disc (Yu et al., 2007) and is located pericellularly (Eyre et al., 2002). The pericellular collagen matrix has been shown to be a mechanism for mechanical signal transduction in articular cartilage (Alexopoulos et al., 2005), a role it likely assumes in the intervertebral disc as well.

### *Proteoglycans*

Proteoglycans typically fall into two classes, the large aggregating proteins (aggrecan and versican) and the small leucine rich repeat proteins (SLRPs) including decorin and biglycan among others. Aggrecan and versican are highly present in the intervertebral disc, both in the annulus and nucleus (Benjamin and Ralphs, 2004, Melrose et al., 2001). Decorin and biglycan have also been reported in the intervertebral disc (Melrose et al., 2001) and have been shown to be affected at early time points by experimentally induced disc degeneration, potentially through mechanical changes induced by the needle puncture (Melrose et al., 2007). Both molecules have been shown to upregulate in response to static compression in the AF (Chen et al., 2004). Link protein serves to anchor the glycosaminoglycan (GAG) chains to the central hyaluronan core to create proteoglycans. It has been shown to have functional differences with aging in chondrocytes (Plaas et al., 1988) and is present in the intervertebral disc (Roberts et al., 1994). Extensive changes in the proteoglycans of cartilage have been noted with increasing animal age (Buckwalter et al., 1994, Buckwalter et al., 1985), including a decrease in the aggregating capacity of these molecules. This has also been shown in the



intervertebral disc (Buckwalter et al., 1994) and is likely associated with a decrease in proteoglycan retention in cultures of mature intervertebral disc cells.

#### *Other structural components*

Vimentin, along with actin and microtubules, make up the cells internal cytoskeleton, and play a role in cell adhesion and migration in some cell types (Ivaska et al., 2007). Previous studies in the intervertebral disc have shown AF cells, but not NP cells, respond to static compression through and upregulation in of vimentin gene expression (Chen et al., 2004). Fibronectin is a glycoprotein associated with wound healing responses which and also have been shown to increase with degeneration in the IVD (Oegema et al., 2000). Fibronectin gene expression has also been reported to be upregulated in the IVD in response to increased compression (Guehring et al., 2005) and may functionally decrease aggrecan and collagen II gene expression in the nucleus pulposus (Anderson et al., 2005).

#### **Matrix Proteases**

Matrix metalloproteinases or MMPs, are of interest to intervertebral disc maintenance and turnover as they degrade many extracellular matrix proteins. MMP1 is also known as interstitial collagenase, and will break down collagen types I, II and III (Entrez gene file). MMP2, also known as gelatinase-A, is known to degrade collagen type IV (Entrez gene file), and is released by the NP cells in response to TNF $\alpha$  in IVD degeneration (Seguin et al., 2006). MMP3, known as stromelysin 1, degrades the proteoglycans described above, fibronectin and collagen III as well as other collagen

types and glycoproteins. MMP13, or collagenase 3, degrades collagen types I and III, and is particularly effective at degrading type II.

ADAMTs molecules (a disintegrin and metalloproteinase with thrombospondin motifs) proteins are involved in the breakdown of aggrecan in the intervertebral disc (Le Maitre et al., 2004). ADAMTs 4 and 5 were analyzed as their role in degrading cartilage proteoglycans have been previously illustrated

### **Anti-catabolic factors**

TIMP (tissue inhibitor of metalloproteinases) proteins generally inhibit MMP activity. In addition, TIMP3 will inhibit ADAMTS proteins, and has been shown to change with age in the NP (Tsuji et al., 2007).

### **Transcription factors**

Six factors in signal transduction were chosen for analysis in this study. The first three, c-fos, c-jun and MAPK were chosen to compare with the work of Fitzgerald et al. (Fitzgerald et al., 2006), and are all known to be affected by mechanical loading in other orthopaedic tissues such as bone and cartilage. MAPK also has other functions in signal transduction, therefore its classification as a transcription factor is very liberal. STAT3 and integrin linked kinase (ILK) are a transcription factors and a kinase along the integrin-mediated mechanical signaling pathway, also both known to be regulated by mechanical conditions. Again the classification of ILK as a 'transcription factor' is very loose, and it should be thought of as a means of signal transduction.

### **Signaling molecules**

Four cytokines were chosen for investigation. The first, transforming growth factor  $\beta$  (TGF $\beta$ ) is a growth factor known to stimulate mesenchymal stem cell differentiation down a chondrogenic lineage, upregulating aggrecan and collagen type II. TGF $\beta$  expression has also been shown to change with age in the IVD (Murakami et al., 2006). Insulin-like growth factor (IGF) has been shown to stimulate IVD cell proliferation in vitro (Pratsinis and Kletsas, 2007) and confer anti-apoptotic effects (Gruber et al., 2000). Connective tissue growth factor (CTGF) has been shown to upregulate biosynthesis by intervertebral disc NP cells (Erwin et al., 2006). Interleukin-6 (IL-6) polymorphisms have been shown to be associated with scoliosis (Aulisa et al., 2007), and IL6 has been shown to be upregulated in an IVD model of persistent inflammation (Ulrich et al., 2007).

### **Housekeeping genes**

GAPDH and 18s are two commonly used housekeeping genes for qRT-PCR. Both housekeeping genes were used as GAPDH has been shown to be affected by mechanical loading in the intervertebral disc (Lee et al., 2005).

Other molecules were also investigated in the course of this study. IL1 and TNF $\alpha$  were initially examined as they have both been reported to increase with increasing degeneration in the intervertebral disc (Le Maitre et al., 2004). No evidence of either molecule was found in the bovine intervertebral disc. Gene sequences associated with primers for other growth factors, such as EGF, and transcription factors such as ELK, were not available for bovine and were therefore not created.

## 6.2.2 Computational Framework

Computation was performed using the MATLAB software package. A clustering toolbox freely available ([www.fmt.vein.hu/softcomp](http://www.fmt.vein.hu/softcomp)) was used and modified for analysis.

### Normalization of Data

The gene expression data was first normalized by the gene expression levels of the housekeeping genes GAPDH and 18s. The magnitudes of the clusters then had to be standardized. Fundamentally, this step is required to ensure the methods are not ‘overwhelmed’ by large magnitudes of change in gene expression levels, and instead are focused on the overall patterns of expression changes between mechanically stimulated and unstimulated cells.

In previous studies (Fitzgerald et al., 2006, Fitzgerald et al., 2004), re-weighting of the data matrix was accomplished by:

$$Z = \frac{X - F}{S_x} \quad (1)$$

$$S_x^2 = \frac{\|X - F\|^2}{T} \quad (2)$$

Where  $\mathbf{X}$  is a gene expression vector,  $\mathbf{F}$  is the vector of gene expression data from an unstimulated control (all =1),  $S_x$  is the modified standard deviation of gene X (after normalizing to unstimulated control),  $T$  was the number of time points (experimental variables) and  $\mathbf{Z}$  is the resulting standardized expression vector. One disadvantage of this method is the loss of the control sample, which may provide important information when comparing between old and young at matched time points, or between time points. To

retain the control time point while still standardizing the data, a normalization method to re-scale all expression values for a given gene between 0 and 1 will be used. All clustering analyses will be performed on this re-scaled data.

### **Clustering metric**

The first metric used was the Euclidian distance. Euclidian distance is defined by:

$$D = \sqrt{\sum_i (x_i - v_i)^2} \quad (3)$$

Where D is the distance metric,  $x_i$  is the value of a clustering group (ie: gene) at a condition i (ie: experiment), and  $v_i$  is the centroid value also at condition i.

To confirm meaningful clusters found by Euclidian distance, another distance metric, manhattan distance, was also used. This metric is given by:

$$D = \sum_i |(x_i - v_i)| \quad (4)$$

Again where D is the distance metric,  $x_i$  is the value of a clustering group (ie: gene) at a condition i (ie: experiment), and  $v_i$  is the centroid value also at condition i.

### **Clustering**

The general form of the data matrix  $\mathbf{X}$  to be clustered is (n x m) where the n rows are the groups to be clustered and the m columns are the characteristics used to define the groups for clustering (attributes groups are clustered on).

#### *K-means clustering*

The k-means clustering algorithm goes as follows:

1. Randomly assign k cluster centroids
2. Calculate membership list and distances using a distance metric.  
Points are assigned to their closest centroid
3. Recalculate centroids to be at the center of the membership list
4. Re-calculate membership list and distances and reassign points to closest centroid
5. Repeat until the centroids move less than a certain given tolerance.

*Fuzzy c-means clustering*

The fuzzy c-means clustering algorithm goes as follows:

1. Compute initial clusters by:

$$v_i^{(l)} = \frac{\sum_{k=1}^N (m_{ik}^{(l-1)})^g x_k}{\sum_{k=1}^N (m_{i,k}^{(l-1)})^g} \quad (5)$$

2. Compute the distance between data points and the cluster centroids, update membership partition list
3. Repeat until centroids move less than a given tolerance.

The variable  $g$  given above is a weighting factor that determines the degree of fuzziness in the clusters. It is constrained to be  $\infty > g > 1$ . As  $g$  approaches 1, the clustering algorithm becomes a hard partitioning algorithm like k-means. In contrast, as  $g$  approaches infinity, the clusters become maximally fuzzy. A value of  $g = 2$  was used for this entire analysis.

### *Validity Indices*

One concern with the implementation of clustering methods such as K-means and Fuzzy C means clustering is the *a priori* specification of cluster number. The exploration of cluster numbers used is important. The approach is to find the minimum number of clusters capable of describing the data, or where the value added by the addition of each sequential cluster starts to decrease. Too many clusters will over-represent the data and may separate groups, which have a meaningful interaction while too few clusters may artificially combine two groups, which should be considered separate. Two methods exist for exploring the efficiency of the number of clusters chosen. The first method is to pick a large cluster number (highly segregate the data) and combine clusters based on predetermined criteria, for instance combining until the combination of two clusters will lead to very large, not well separated clusters. The second method is to evaluate the clustering results from increasing cluster numbers using sets of validity indices. Each validity index represents a different feature of the determined clusters; so more than one index is typically consulted to determine whether the cluster number best describes the data.

In this study, two measurements were used in evaluating the results from k-means clustering, and six for the results from fuzzy c-means clustering. The hard partitions resulting from the k-means only lend to evaluation with two of the validity indices that are reasonable to implement, however the two measurements chosen have been shown to be effective in determining the best cluster number in other studies of gene expression data (Dave, 1996). K-means clustering is also sensitive to the initial positioning of the

cluster centers, so it was considered a priority to run the algorithm many times to establish a globally optimal solution. The nature of the partitions from fuzzy c-means, where data points can belong to many groups, makes this method less sensitive to initial cluster position (however some sensitivity still exists, particularly where cluster center numbers increases relative to the size of the data set.

### **Modified Partition Coefficient (MPC)**

The commonly used partition coefficient (PC) evaluates the amount of overlapping between clusters (Bezdek et al., 1981). However, PC increases with increasing cluster number (c) making its utility suspect. This study used a modified version of the partition coefficient, which eliminates the scaling with c (Dave, 1996). The MPC for a given cluster number c is given by:

$$MPC(c) = 1 - \frac{c}{c-1}(1 - PC(c)) \quad (6)$$

Where

$$PC(c) = \frac{1}{N} \sum_{i=1}^c \sum_{j=1}^N (m_{ij})^2 \quad (7)$$

Where  $m_{ij}$  is the membership of data point j in cluster i and N is the number of data points.

### **Partition Index (SC)**

Partition Index is a sum of individual cluster validity indices divided by the fuzzy cardinality of each cluster (Bensaid et al., 1996). SC is given by:



$$SC(c) = \sum_{i=1}^c \frac{\sum_{j=1}^N (m_{ij})^2 \|x_j - v_i\|^2}{N_i \sum_{k=1}^c \|v_k - v_i\|^2} \quad (8)$$

Where  $m_{ij}$  is the membership of data point  $j$  in cluster  $i$ ,  $x_j$  is the value of  $x$  at condition  $j$ ,  $v_i$  is the centroid value in centroid  $i$ ,  $N$  is the number of conditions,  $v_k$  is the value of the centroid in centroid  $k$ . Partition index is a ratio of the sum of compactness and separation of clusters.

### **Separation Index (S)**

The separation index examines the ration between the compactness of the clusters and the separation between clusters at their minimum distance (Bensaid et al., 1996). Separation index,  $S$ , is given by:

$$S(c) = \frac{\sum_{i=1}^c \sum_{j=1}^N (m_{ij})^2 \|x_j - v_i\|^2}{N \min_{i,k} \|x_j - v_i\|^2} \quad (9)$$

### **Xie and Beni's Index (XB)**

Xie and Beni's index quantifies the ratio of total variation within the clusters and the separation of the clusters (Xie and Beni, 1991). XB was used for both k-means and fuzzy c-means cluster evaluation, although it is intended for fuzzy c-means. It was in this way used to see how a non-optimal validity index would perform for a given method. XB is given by:

$$XB(c) = \frac{\sum_{i=1}^c \sum_{j=1}^N (m_{ij})^m \|x_j - v_i\|^2}{N \min_{i,j} \|x_j - v_i\|^2} \quad (10)$$

Where  $m = 2$ . The optimal cluster solution should minimize this index, as ideally the clusters have less variation than they are separated.

### **Dunn Index (DI)**

The goal of the Dunn Index is to identify well-separated and compact clusters. The application of this index to fuzzy clustering requires hard partitioning of the data, and can be computationally expensive (Ray et al., 1999). The Dunn index was used for both k-means and fuzzy-c-means cluster evaluation.

$$DI(c) = \min_{i \in c} \left\{ \min_{j \in c, i \neq j} \left\{ \frac{\min_{x \in C_i, y \in C_j} d(x, y)}{\max_{k \in c} \left\{ \max_{x, y \in C} d(x, y) \right\}} \right\} \right\} \quad (11)$$

### **Perturbation of Data**

To verify the robustness of the clustering analysis, gaussian noise was added to the data and re-analyzed for reproducibility. The noise added was scaled to a magnitude of +/- the standard error of the mean of the data. This is expected to be a very robust amount of noise, as the within sample variation is typically significantly less than between samples.

To quantify the amount of agreement between two output clusters (for example, between perturbed data set #1 and the original data) a measure called the Rand index will be used. Given two matrices, one representing the membership matrix of the perturbed data (PB) and one representing the original data (OD), the Rand index (RI) is given by:

$$RI = \frac{a + b}{a + b + c + d} \quad (12)$$

Where **a** is the number of points (data points, meaning experimental groups or genes) that are in the same cluster in PB and OD, **b** is the number of points in different clusters between PB and OD, **c** is the number of points in the same cluster in PB and different in OD, and **d** is the number of points in different clusters in PB, but the same cluster in OD. In this index, **a** and **b** are measures of similarity between the two generated cluster membership lists, and **c** and **d** are measures of dissimilarity.

### 6.2.3 Visualization of the results through factorization

Again, the general form of the matrix **X** is (n x m). Factorization can then be accomplished by the general form:

$$X_{iu} \approx (WH)_{iu} = \sum_{a=1}^r W_{ia} H_{au} \quad (13)$$

Where **W** and **H** are matrix factors, of dimension n x r and r x m respectively. The columns of **W** define the new groups, which are a combination of the original groups such that they represent the original data set within the new reduced dimensions. The columns of **H** are then the data corresponding to the new combined groups. The rank, r, is chosen such that

$$(n + m)r < nm \quad (14)$$

The form of the matrices W and H vary between the factorization method chosen and are described in detail below.

Principal component analysis

In PCA, W and H are constrained such that the columns of W are orthonormal and the rows of H are orthogonal to each other. The overall row data is then represented by a linear combination of each distributed representation of the column data. Each individual representation is uniquely defined as an eigenvalue representation.

To find the PCA coordinates, singular value decomposition (SVD) was applied to the gene expression data covariant matrix. To accomplish this, the n x m data covariant matrix X is decomposed as:

$$X = U\Sigma V^T \tag{15}$$

Where the columns and rows of U (size n x n) are orthonormal and the rows and columns of V<sup>T</sup> (size m x m) are orthonormal. Σ is an (n x m) diagonal matrix, such that the diagonal elements are  $\sigma_1 \geq \dots \geq \sigma_r \geq 0$ , and  $\sigma_{r+1} = \dots = \sigma_{\min(n,m)} = 0$ . Finally r = rank(A) = the number of rows and columns in X.

The k most significant components were determined, where k<4 for 3D plotting. The utility of this assumption was also examined by noting each eigenvalue, and ensuring the top 3 were sufficient to account for the majority of the data. These components were then used to do ‘k-dimensional’ PC analysis.

$$X_k \equiv U_k^t X \tag{16}$$

where the m columns of X were projected onto the linear space spanned by the first k columns of U (U<sub>k</sub> are columns 1 through k of U). The eigenvectors of

$$AA^T \langle A^T A \rangle \quad (17)$$

Is the principal components basis for the columns of  $A \langle A^T \rangle$ . Then the data in principal component axes is

$$Y = U^T X \quad (18)$$

and the covariance matrix

$$YY^T / (n - 1) \quad (19)$$

is then  $\text{diag}(V_i)_{n \times n}$ , the rows of  $Y$  are uncorrelated.

### Non-negative Matrix Factorization

In NMF, one requirement is that the sparsity of the matrices be low. Another requirement is that each entry in the matrix  $W$  and  $H$  must be positive. Since only additive combinations are allowed, this leads each component to be more representative of the whole, and their combination to truly represent the concept of the sum of the parts is the whole. This can be quite useful as well, as each component now has a more intuitive meaning. No longer is the message only in the summation of the parts, but rather now each part has a meaning as well, revealing meaningful patterns inside the complex data (Pascual-Montano et al., 2006, Lee and Seung, 1999).

Initial random guesses were created for the matrices  $W$  and  $H$ . Under the constraint that the updated values must be positive, the matrices will update to approximate (Kim and Tidor, 2003)

$$H_{au} \leftarrow H_{au} * \frac{(W^T V)_{au}}{(W^T W H)_{au}} \quad (20)$$

And

$$W_{ia} \leftarrow \frac{(V H^T)_{ia}}{(W H H^T)_{ia}} \quad (21)$$

The optimization criterion used by both Lee and Seung, and Kim and Tidor, 2003 was to minimize the RMS error between the data and reduced dimension data such that

$$E = \|V - WH\| \quad (22)$$

#### 6.2.4 Implementation of the algorithms

As stated in the introduction, this analysis consisted of two aims. The first goal was to find experimental groups that linked by similar gene expression profiles and the second goal was to find genes that are commonly linked by experimental protocols.

##### Similarities in experimental groups

In general terms, the investigation of similar experimental groups was implemented by clustering the gene expression data as shown in Figure 6-2a, particularly the form of the clustering matrix  $\mathbf{X}$  ( $n \times m$ ) was created with the  $n$  experimental conditions by the  $m$  gene expression data. The flow of the implementation is shown in (Figure 6-3).

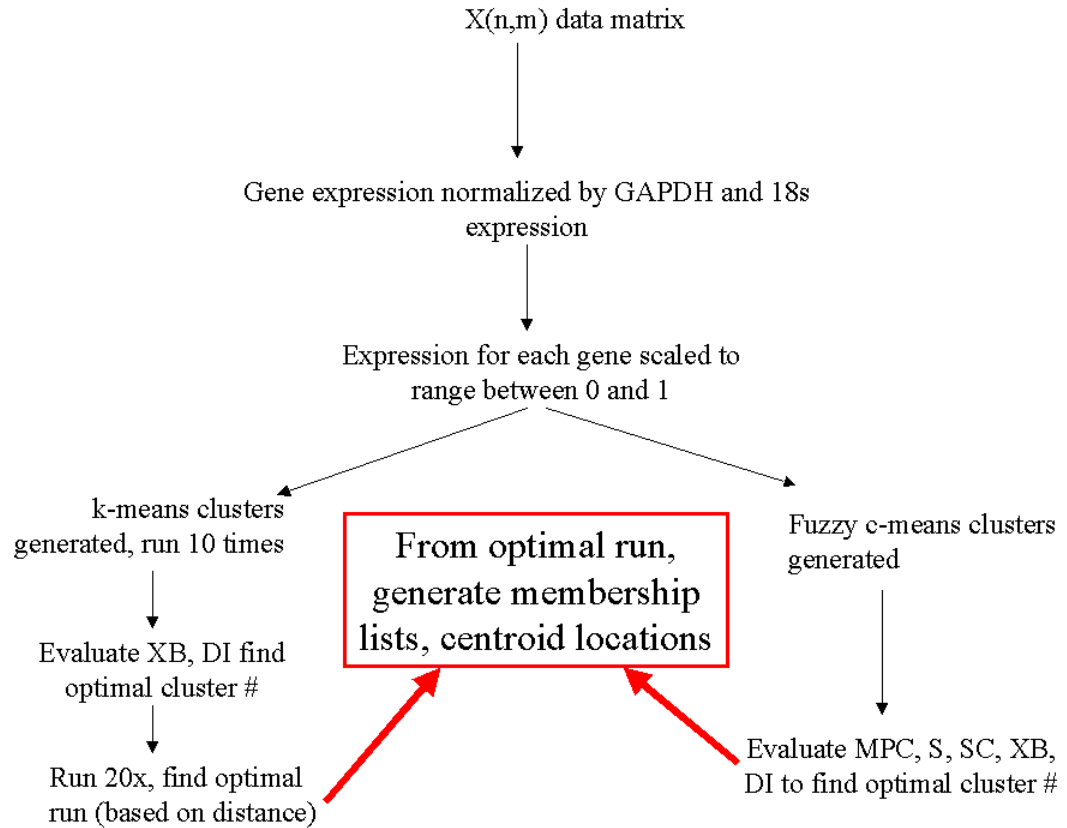


**Figure 6-3: Experimental flow chart**

After data matrix normalization and scaling, k-means clustering was applied to the data, with cluster number ( $k = 2-10$ ) and run 10 times. From there, the XB and DI validity measures were compared to determine ideal cluster number. The k-means cluster algorithm was then run 20 times with the determined ideal cluster number to determine an optimal solution where the distance between centroids and data points was minimized. The membership list and centroid locations were saved.

Fuzzy c-means clustering was likewise applied, with the exception that the algorithm is more insensitive to initial centroids positioning, reducing the need to run the

algorithm repeatedly to obtain a globally optimal answer. Also, more validity indices were examined, as the ability for shared membership can also lead to more options with respect to cluster number. Therefore, fuzzy c-means clustering was performed on normalized data by running the algorithm 10 times with clusters ( $c = 2-10$ ) and evaluating the validity indices MPC, S, SC, XB and DI for optimal cluster number. The fuzzy c-means clustering algorithm was then run with the optimal cluster number to obtain membership lists and centroids for the run with the minimal distance between centroids and data points.

To evaluate the sensitivity of the found membership lists, the process was repeated for 3 sets of Gaussian perturbed data. To corroborate the results, the process was also repeated using a correlation coefficient metric.

## **2. Similarities in gene expression profiles**

The same protocol was followed for grouping genes exhibiting similar profiles, except the  $\mathbf{X}$  ( $n \times m$ ) matrix was created with the  $n$  gene expression data by the  $m$  experimental conditions. The data were normalized and scaled along the gene dimension to reduce the effect of large gene expression magnitude differences between genes. Therefore, in addition to clustering of the full data sets (all AF or all NP), the matrix was also partitioned into young and mature subsets. The subset clustering was performed to examine whether one age (mature or young) was dominating the overall clustering, which was possible since the scaling and normalization did not occur in the matrix dimension containing the experimental dimension ( $m$ ).



Three genes, MMP13, TIMP2, and ADAMTS5 were ‘held back’ from the data set for later comparison and were therefore not used to determine cluster sets.

**3. Gene patterns implicated in experimental grouping**

The experimental groups belonging to each cluster determined from the k-means clustering of experimental phenotype (as in part 1) were isolated. The data matrices were transposed, and the data was examined for similarities in gene expression profiles (as in part 2). Again, k-means and fuzzy clustering algorithms were implemented as shown in Figure 6-3.

**4. Predictive value of clustering results**

To examine whether the clustering results could be applied universally to the study of intervertebral disc mechanobiology, data from reported in study #2 was compared to the clustered groups found in this work (Table 6-3).

**Table 6-3: Comparison between groups from study #2 (chapter 4) and clustered data experimental groups as well as analyzed genes**

Group from Study #2	Group from Study #3	Genes used in both studies (used for comparison)
Control	Mature control (unloaded)	Collagen I and II, Aggrecan, Versican, TIMP1 MMP2, MMP3, ADAMTS4
Low load (1 MPa, 1 Hz)	Mature 1Hz 7 day	
High Load (2.5 MPa, 1 Hz)		

The comparison between the studies is not perfect for several reasons. First, study #2 was an organ culture model whereas the data used for clustering was *in vitro* (isolated) cells seeded into alginate matrices. Organ culture maintains the normal cell-matrix contacts, which may play a crucial role on cell signaling which are missing from the *in vitro* model the clustered gene data was created from. Also, the comparisons between the applied loads is not ideal, as study #2 varied magnitude of applied compression while clustered data varied in frequency of load (and was at a consistent magnitude). Therefore, a group of high or low load grouping with the 1 Hz loading condition from the current gene expression set would be considered interesting. The comparison is quite close as far as age of the cells (both from mature IVDs) and that both experiments consisted of 7 days of loading followed by a time point.

Finally, the ability for the clustered genes to predict the presence of other genes not included in the creation of the original clustering set was examined. Here, three sets of genes that were not used to create the original cluster centers were plotted and the distances between their locations in ‘expression space’ and established centroids were compared to determine which cluster center each would be assigned to with each clustering algorithm. Evidence from intervertebral disc literature suggests they should all be grouped with particular genes used to create the original clusters, meaning that the new data points should show memberships similar to their known associates. For k-means this means being closest to the desired centroid according to Euclidian distance metric. The assumption is that these genes would likely be hard partitioned into the

cluster if the distance (between the gene and centroid) is similar to the distances between the other members of the cluster and the centroid.

## **6.3 Results**

### **6.3.1 Experiment clustering**

#### **6.3.1.1 K-means**

In the AF, K-means clustering resulted in an optimal cluster number of 4.

Validity indices XB and DI for cluster numbers ranging from 2 – 10 are shown in Figure 6-4. After running the algorithm 20 times using  $k = 4$ , the optimal cluster membership list was generated (Figure 6-6). Cluster 1 contained mature 7 day control and 1 Hz, Mature 14 day 1 Hz and 3 Hz, Young 14 day control, 0.1 Hz and 3 Hz, and mature 21 day control and 1 Hz. Cluster 2 contained mature 21 day 0.1 Hz. Cluster 3 contained mature 7 day 0.1 Hz and young 21 day control, 0.1 and 1 Hz. Cluster 4 contained mature 7 day 3 Hz, all young 7 day groups, mature 14 day control and 0.1 Hz, Young 14 day 1 Hz, mature 21 day 3 Hz and young 21 day 3 Hz.

In the NP, K-means clustering resulted in an optimal cluster number of 6.

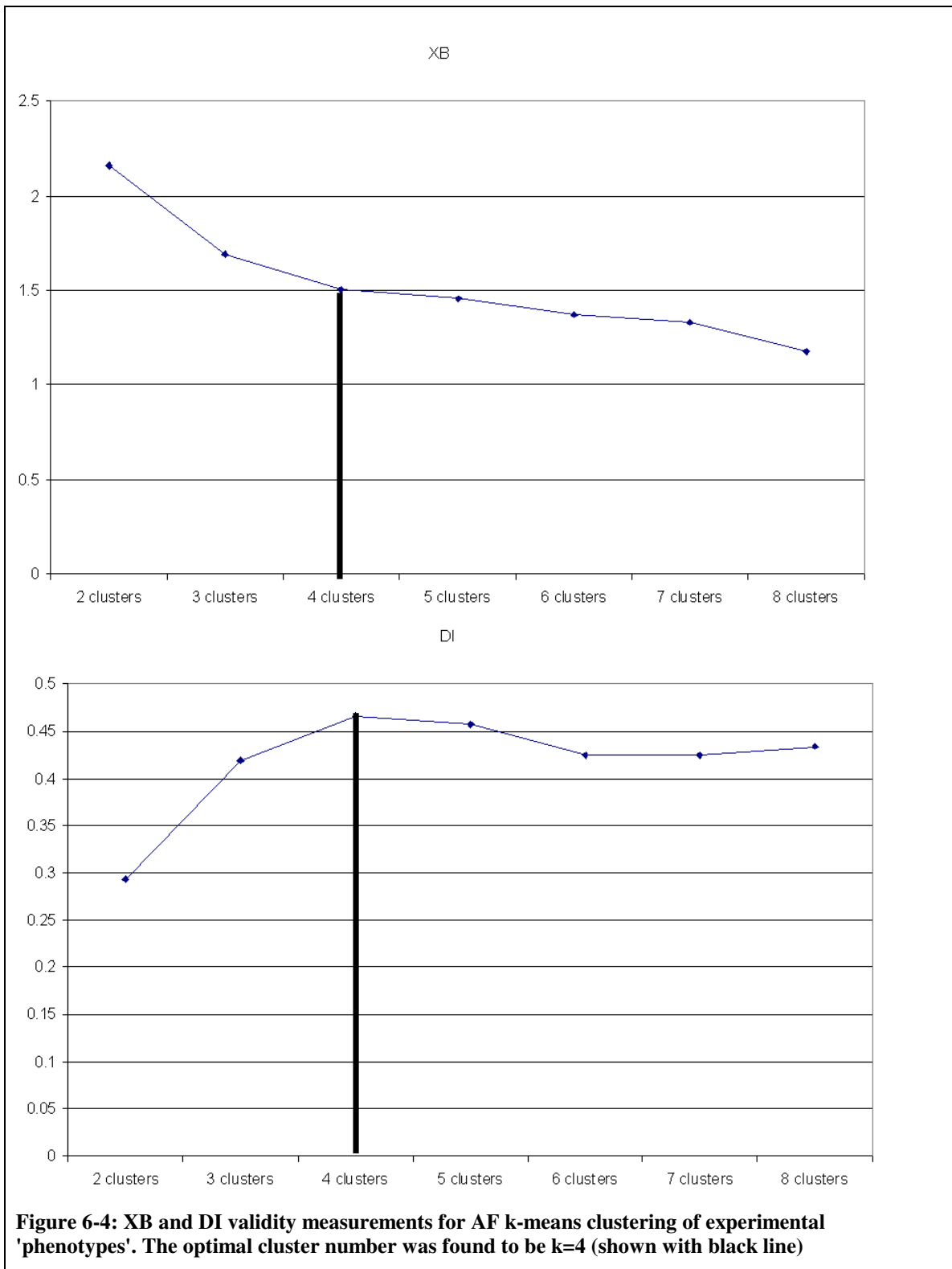
Validity indices XB and DI for cluster numbers ranging from 2 – 10 are shown in Figure 6-5. The optimal cluster membership list was again generated after running the algorithm 20 times with  $k=6$  Figure 6-7. Cluster 1 contained mature 7-day control, 0.1 Hz and 3 Hz. Cluster 2 contained mature 7 day 1 Hz, Mature 14 day 0.1 Hz and mature 21 day 1 Hz. Cluster 3 contained young 7-day control and 1 Hz, mature 14-day control, and mature 0.1 Hz at 21 days. Cluster 4 contained young 7-day 0.1 Hz and 3 Hz, and mature 21-day

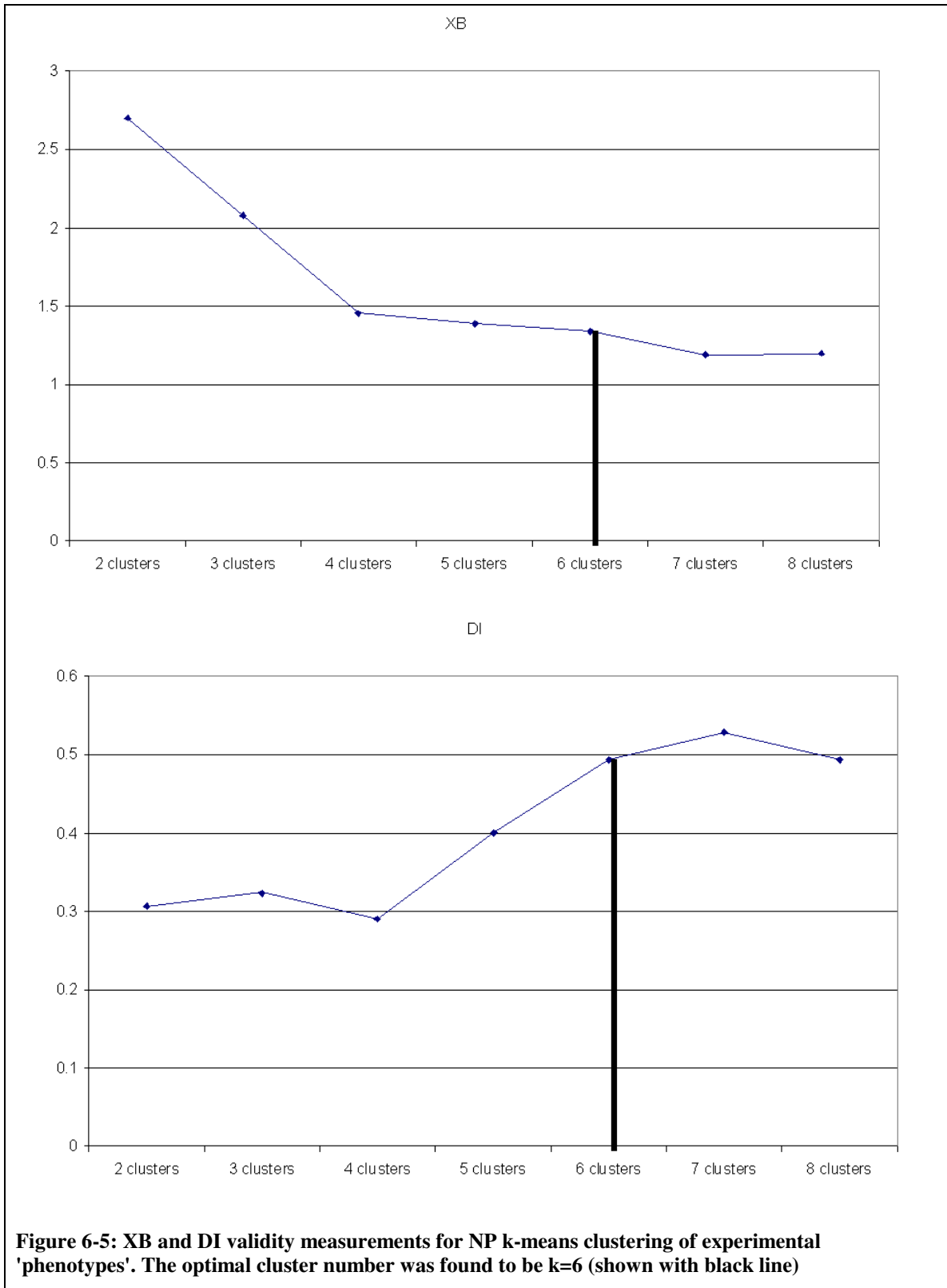
control and 3 Hz. Cluster 5 contained mature 14-day 1 Hz and 3 Hz, and cluster 6 contained all young 14-day and 21-day samples.

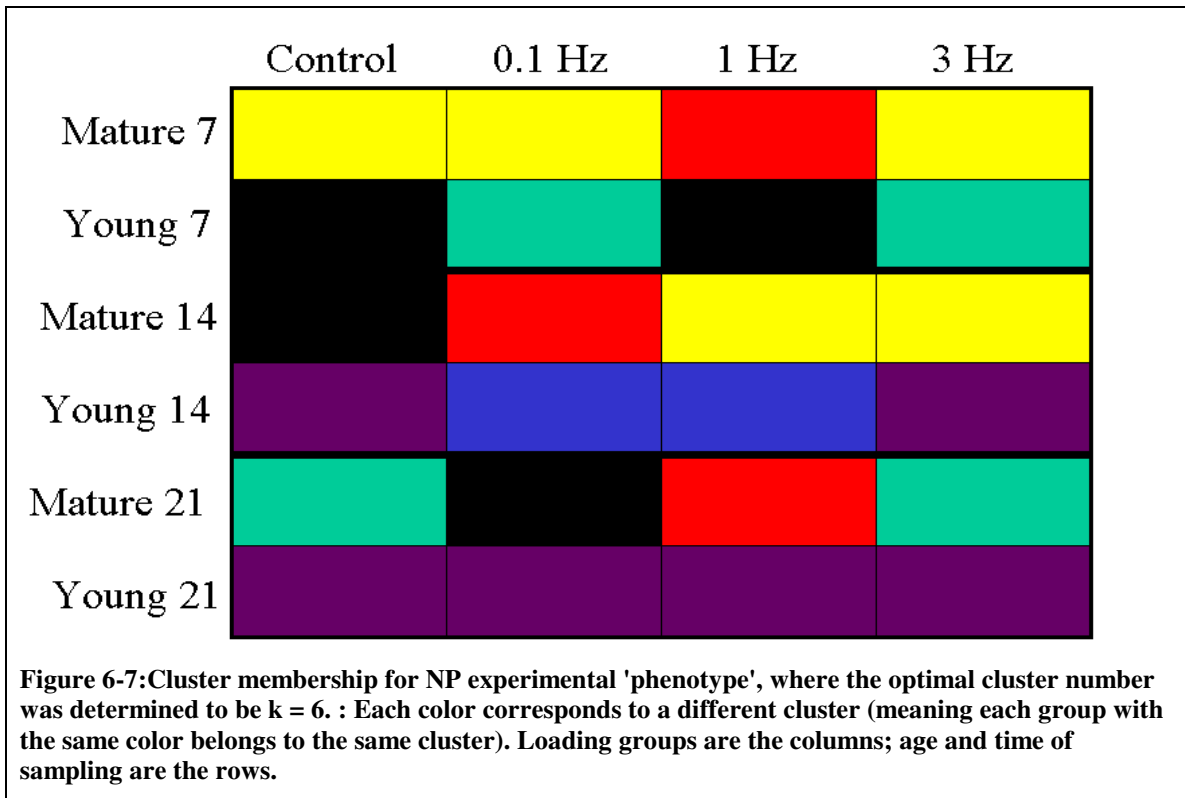
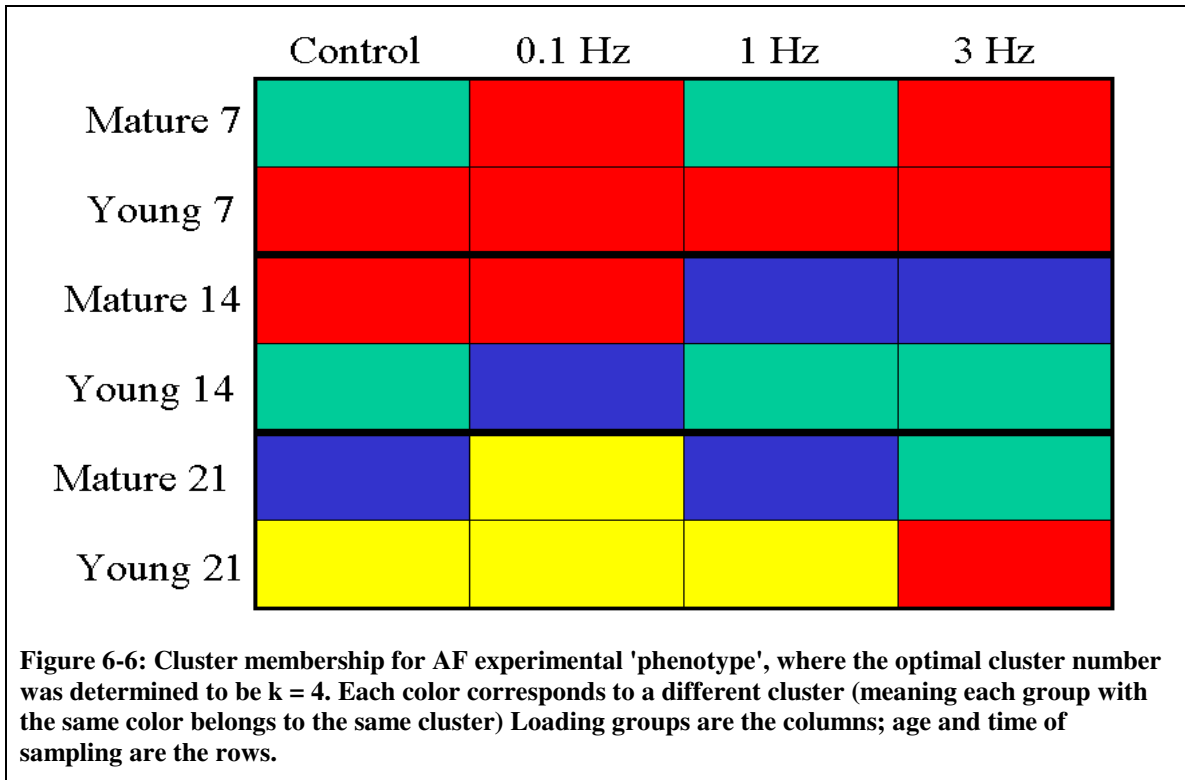
The AF group, containing only 4 clusters for an ideal solution, can possibly be thought of as less complex than the NP, which required 6 clusters for a full description. This could mean that the response to loading and aging in the AF is fairly uniform. In both tissues, the young cells tend to come to a greater cluster membership agreement at 21 days (mostly yellow for AF, all purple for NP), supporting the idea that they are able to respond *in vitro* to mechanical loading, or to re-establish a state of homeostasis, on a more rapid time frame.

The AF response also increased in the number of clusters with time. The seven day samples only had a  $k = 2$  (red and green), the 14 day samples had a  $k=3$  (red, green and blue), and the 21 day samples had all four clusters (red, green, blue and yellow), possibly indicating the different cell age and response to load needs time to fully develop, or is significantly affected by the time those cells spend in culture.

In the NP, a different trend over time is seen, with  $k=4$  for the seven day samples, all six clusters needed for the 14 day time point, and again  $k=4$  for the 21 day time point. This could indicate the response of the NP is on a more rapid time-scale than that of the AF.







### 6.3.1.2 Perturbation of data

The gene expression data was perturbed by the addition of a noise term centered at zero, with a gaussian distribution of +/- the standard error of the mean average for the expression values. After the addition of the noise, the procedure outlined in Figure 6-3 was repeated.

In the AF, the optimal cluster number was again determined to be  $k = 4$  by validity measurements XB and DI (Figure 6-8). The membership list of the optimal run was consistent between the perturbed and original data for 2/3 of the perturbed data sets, with all inconsistencies occurring in the third perturbed data set. Eleven groups were affected by the addition of data noise in the third perturbation: All the 3 Hz load groups except young 21 day, mature and young 14 day 1 Hz and mature 21 day 1 Hz, both mature and young 14 day 0.1 Hz, and mature 21 day controls.

In the NP, the three sets of perturbed data again yielded an optimal number of clusters of  $k = 6$  based on XB and DI validity measurements (Figure 6-9). The NP groups were more affected by noise, with 2/3 of the perturbed data sets causing different clustering results. As with the AF, 11 groups were unaffected by noise: all Mature 7 day groups, the Mature 14 day 0.1 Hz, Young 14 day control, Mature 21 day 1 Hz and all the Young 21 day groups (Figure 6-10 bottom).

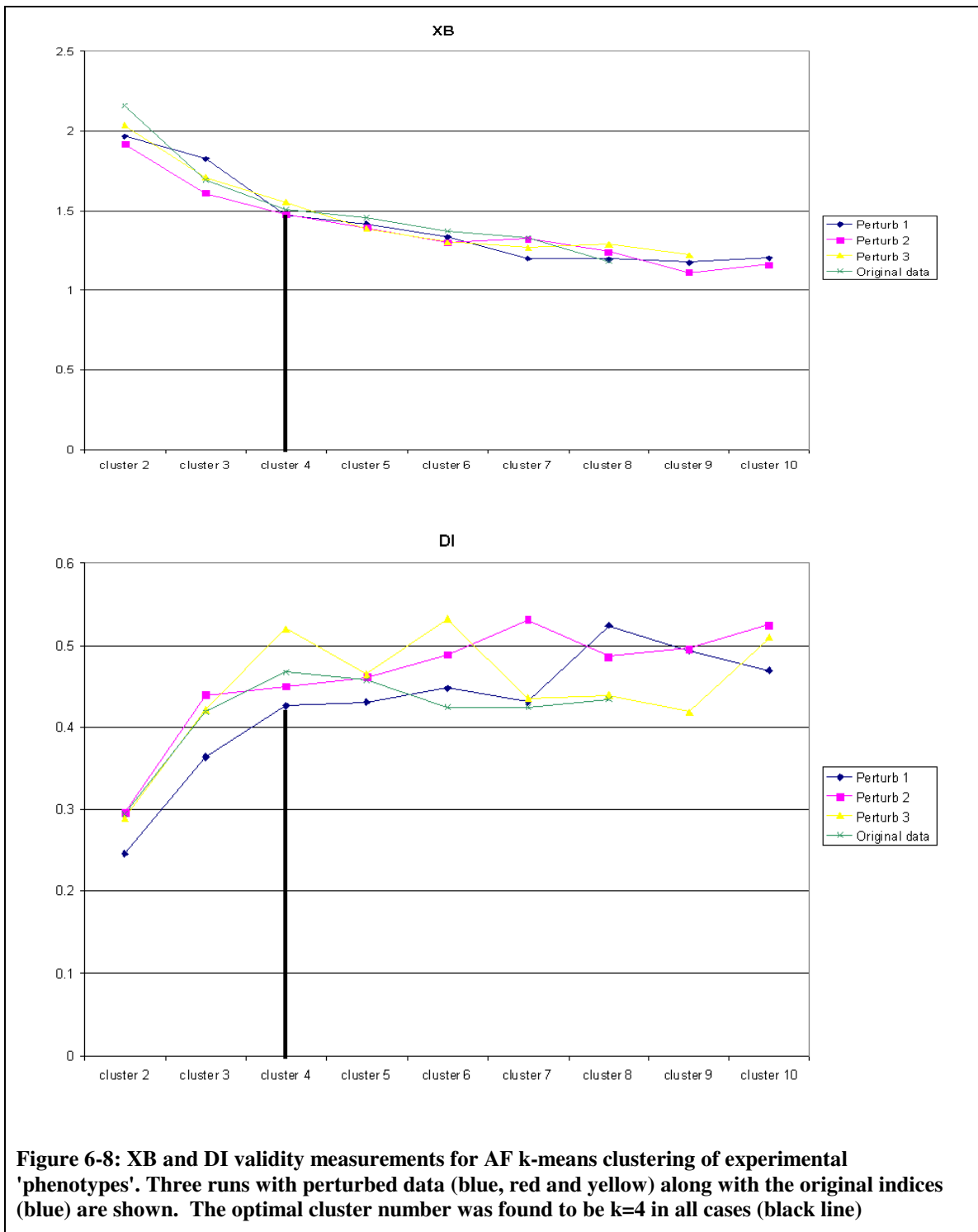
The perturbation of the groups suggests the AF groups are more stable, and closer to the cluster membership centroids than in the NP. It is also interesting to note that the amount of variability with perturbation is dependent on mechanical loading, with most of the 3 Hz groups exhibiting a cluster change with perturbation, and only one of the

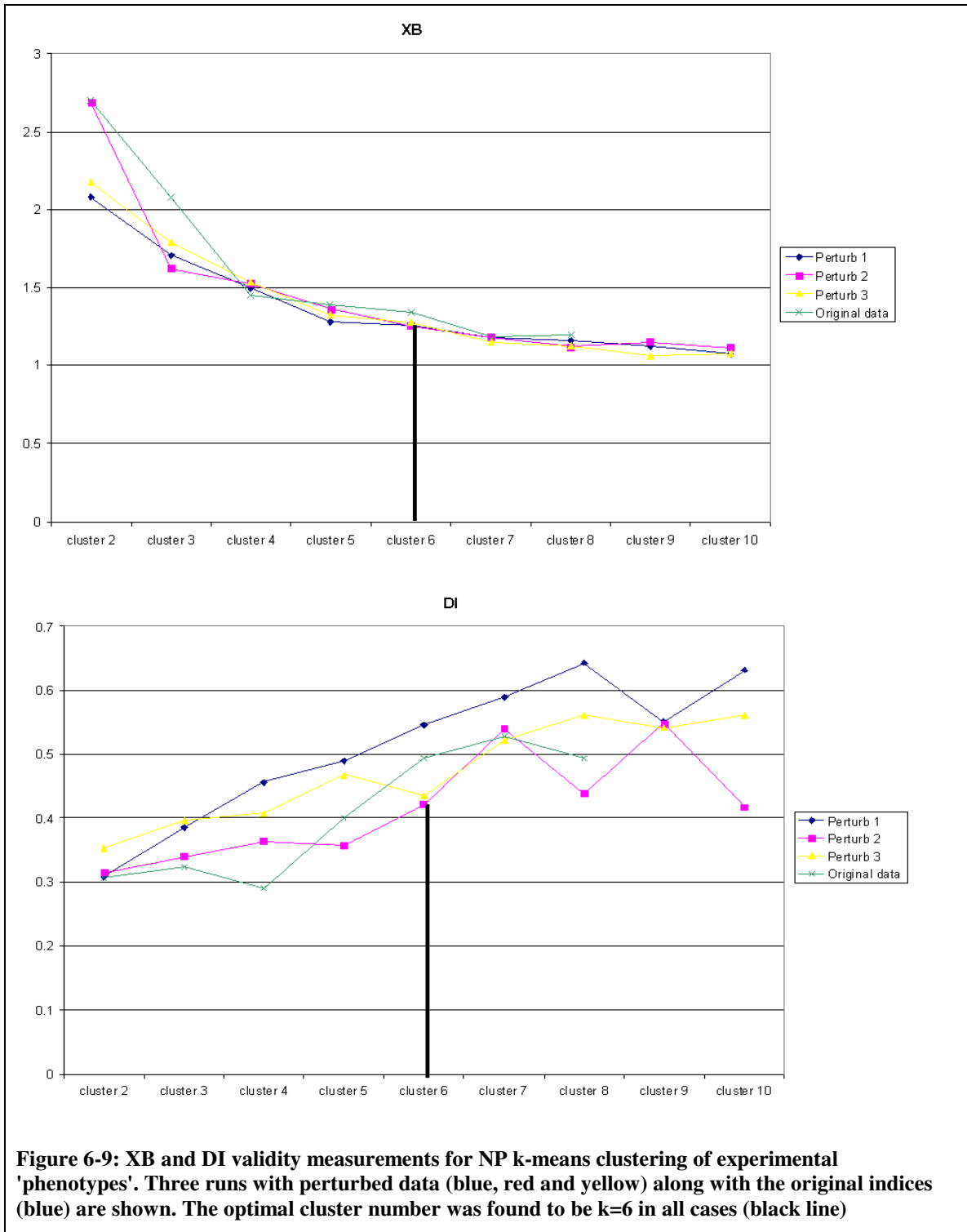


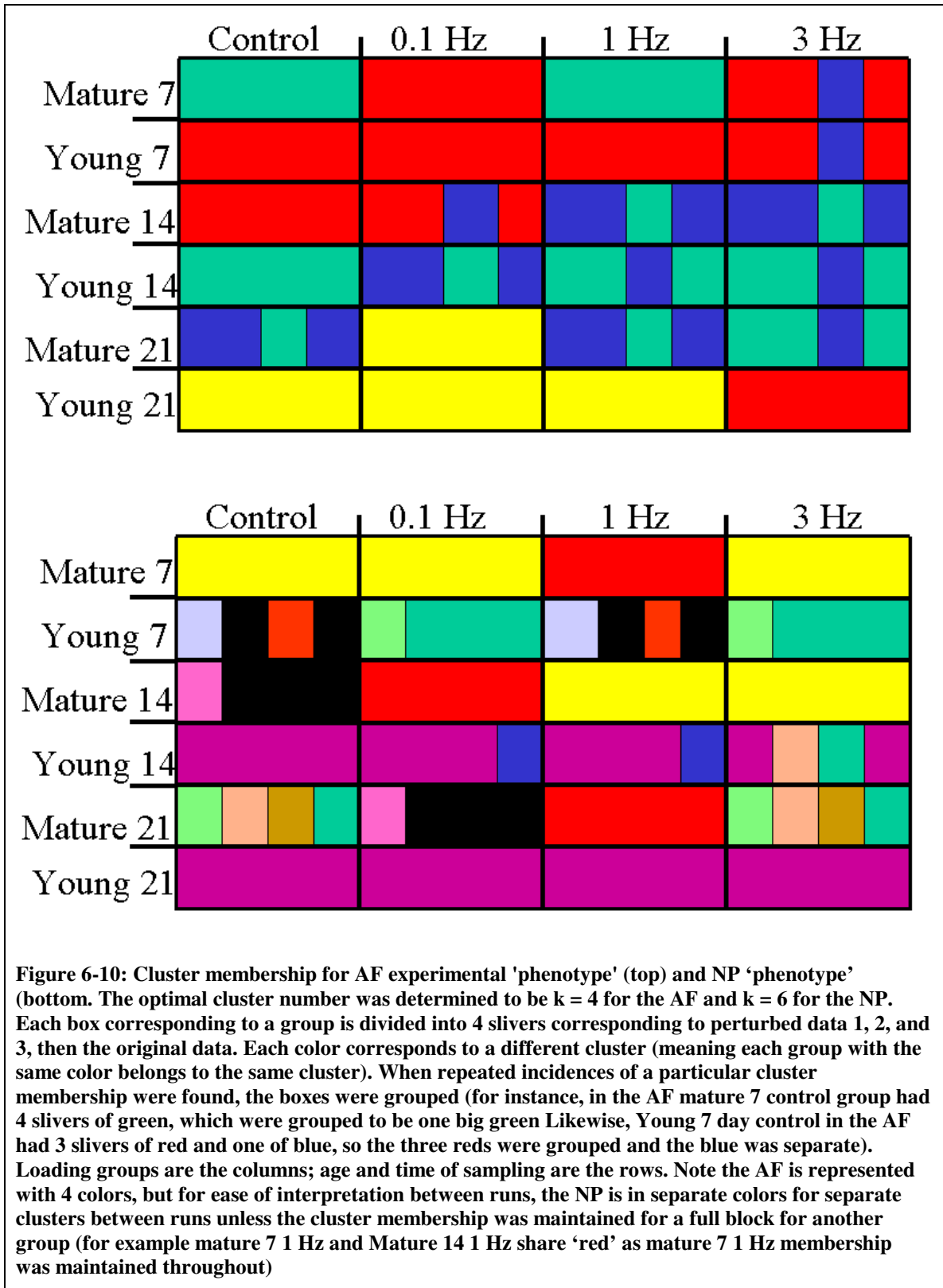
controls exhibiting some change with perturbation. The NP, however, did not follow such a trend with mechanical loading.

**Table 6-4: Rand Indexes for clusters generated from data with the addition of gaussian noise. A Rand Index of 1 means complete agreement between matrices, and approaching zero means no association between matrices**

	<i>Perturbation 1</i>	<i>Perturbation 2</i>	<i>Perturbation 3</i>
AF	1	1	0.815217
NP	0.942029	0.923913	0.887681







### 6.3.1.3 Manhattan city block metric

The resulting clusters were insensitive to the choice of distance metric used to evaluate membership. Each was run 20 at the cluster number found to be optimal for the Euclidian distance metric ( $k = 4$  for AF,  $k = 6$  for NP). For both the AF and NP, the results from the optimal run were identical whether using the Euclidian distance or Manhattan city block metric.

### 6.3.1.4 Fuzzy c-means

As with k-means clustering, fuzzy c-means clustering in the AF resulted in an optimal cluster number of 4. Validity indices MPC, SC, S, XB and DI are all shown in Figure 6-11. The optimal cluster membership is shown in Figure 6-12. A table with each group's membership percentage is also provided (Table 6-5).

Cluster memberships with the fuzzy c-means clustering, corresponded to those with the k-means clustering. As expected, the groups found to be sensitive to perturbation were also found to be contributing to clusters other than their primary memberships in higher percentages than other clusters, indicating their status as groups which may be transitioning between clusters.

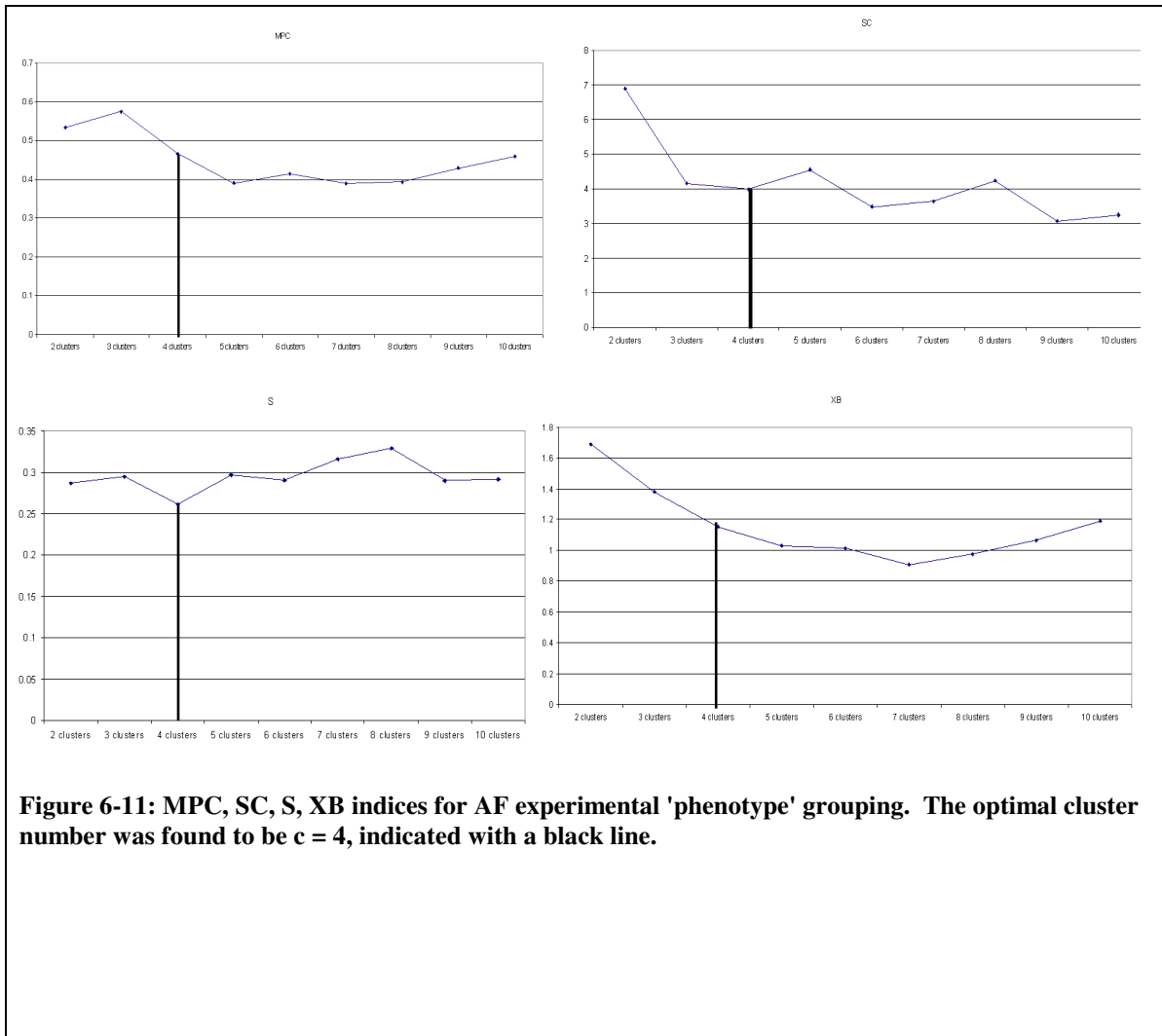


**Figure 6-11: MPC, SC, S, XB indices for AF experimental 'phenotype' grouping. The optimal cluster number was found to be  $c = 4$ , indicated with a black line.**

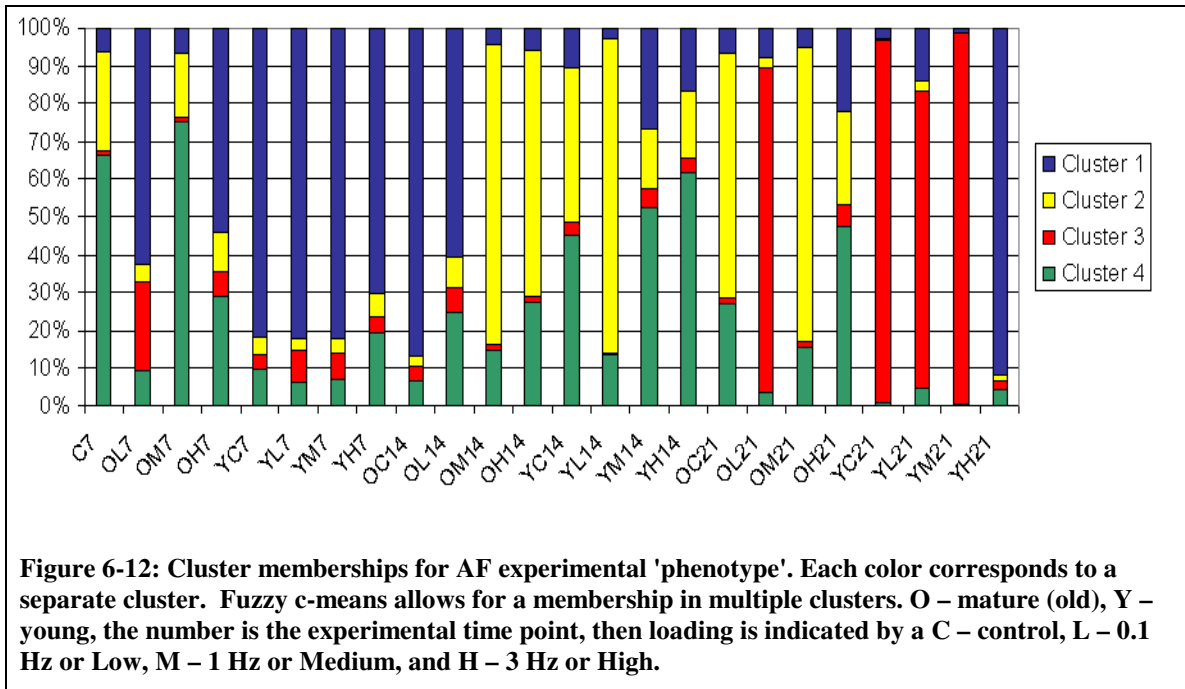


**Table 6-5: Cluster membership as a table for AF experimental 'phenotype'. Color of cells corresponds to their value of membership where >0.75 is red, 0.5 - 0.74 is yellow, 0.25 - 0.49 is green, 0.1 - 0.24 is blue, and white is <0.1. . For naming convention, M – mature, Y – young, the number is the experimental time point, then loading is indicated by a C – control, L – 0.1 Hz or Low, M – 1 Hz or Medium, and H – 3 Hz or High.**

Exp. Group (AF)	Cluster 1	Cluster 2	Cluster 3	Cluster 4
M 7 C	0.014	0.060	0.262	0.664
M 7 0.1Hz	0.237	0.625	0.047	0.091
M 7 1 Hz	0.014	0.065	0.168	0.754
M 7 3 Hz	0.064	0.539	0.106	0.290
Y 7 C	0.041	0.818	0.042	0.098
Y 7 0.1 Hz	0.084	0.825	0.028	0.062
Y 7 1 Hz	0.072	0.824	0.034	0.070
Y 7 3 Hz	0.040	0.704	0.062	0.193
M 14 C	0.038	0.868	0.028	0.066
M 14 0.1 Hz	0.063	0.605	0.082	0.249
M 14 1 Hz	0.015	0.043	0.794	0.148
M 14 3 Hz	0.015	0.057	0.652	0.276
Y 14 C	0.034	0.107	0.406	0.453
Y 14 0.1 Hz	0.007	0.025	0.831	0.136
Y 14 1 Hz	0.049	0.264	0.160	0.527
Y 14 3 Hz	0.035	0.166	0.180	0.619
M 21 C	0.019	0.065	0.647	0.269
M 21 0.1 Hz	0.859	0.082	0.024	0.035
M 21 1 Hz	0.019	0.051	0.775	0.156
M 21 3 Hz	0.057	0.223	0.245	0.475
Y 21 C	0.960	0.026	0.005	0.008
Y 21 0.1 Hz	0.783	0.140	0.029	0.047
Y 21 1 Hz	0.981	0.012	0.003	0.004
Y 21 3 Hz	0.026	0.915	0.017	0.042

>0.75

0.5-0.749

0.25 – 0.49

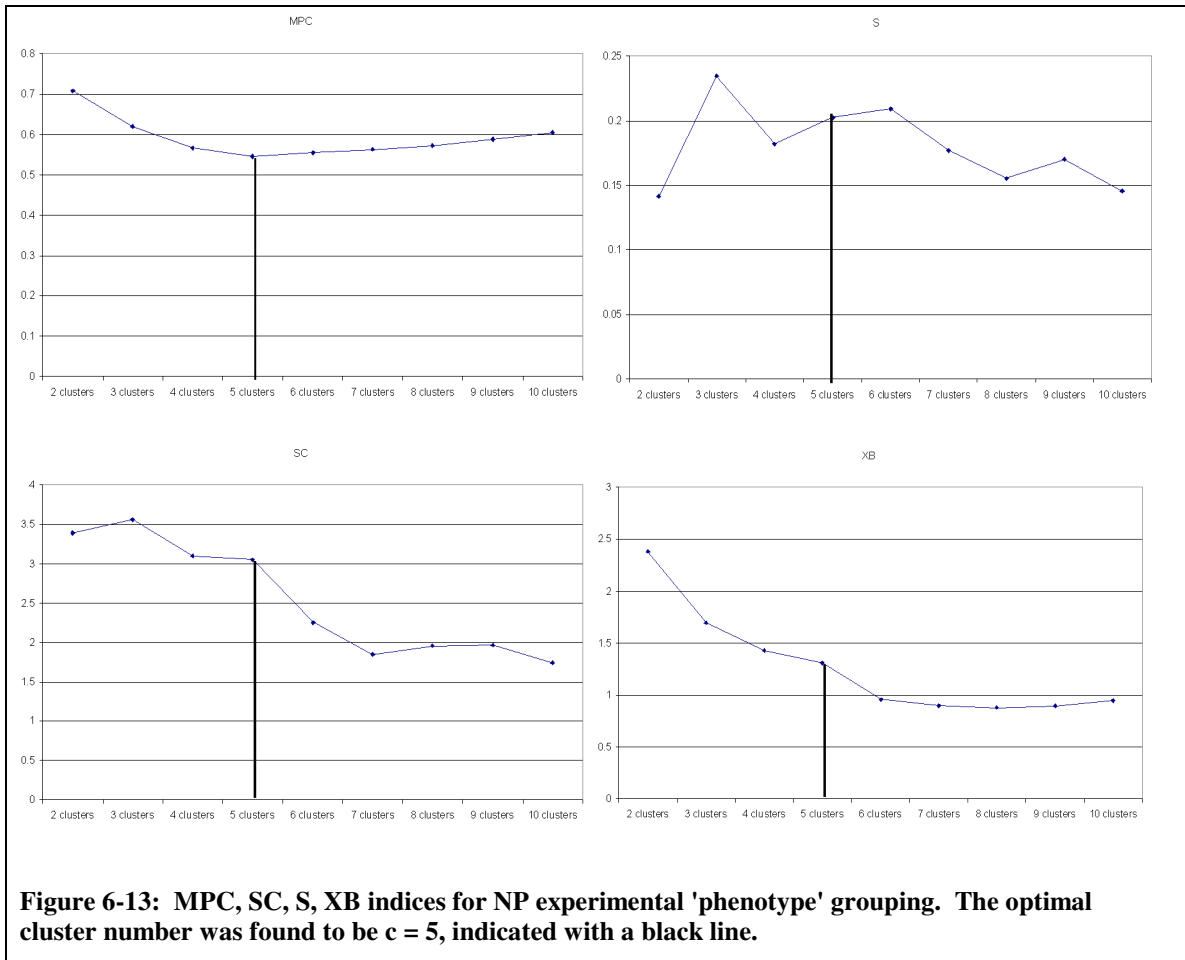
0.1 – 0.249

0-0.99



Fuzzy c-means clustering in the NP resulted in an optimal cluster number of 5. Validity indices MPC, SC, S, XB and DI are all shown in Figure 6-13. The optimal cluster membership is shown in Figure 6-14. A table with each group's membership percentage is also provided (Table 6-6).

The representation of the NP group by only  $c = 5$  (instead of  $k=6$  in k-means clustering) is both an example of the utility of fuzzy clustering and an indication of the transitory nature of the NP cell response. The concept can be understood as imagining that there was one cluster from the k-means clustering which was made up of samples, which were situated between two other clusters, but sufficiently different to warrant their own group. With the application of fuzzy c-means clustering, one can see that this set of samples could be more accurately described as a combination of these two groups rather than as their own group. The presence of these samples, which exist between clusters, indicates the response of the NP is more variable than that of the AF.



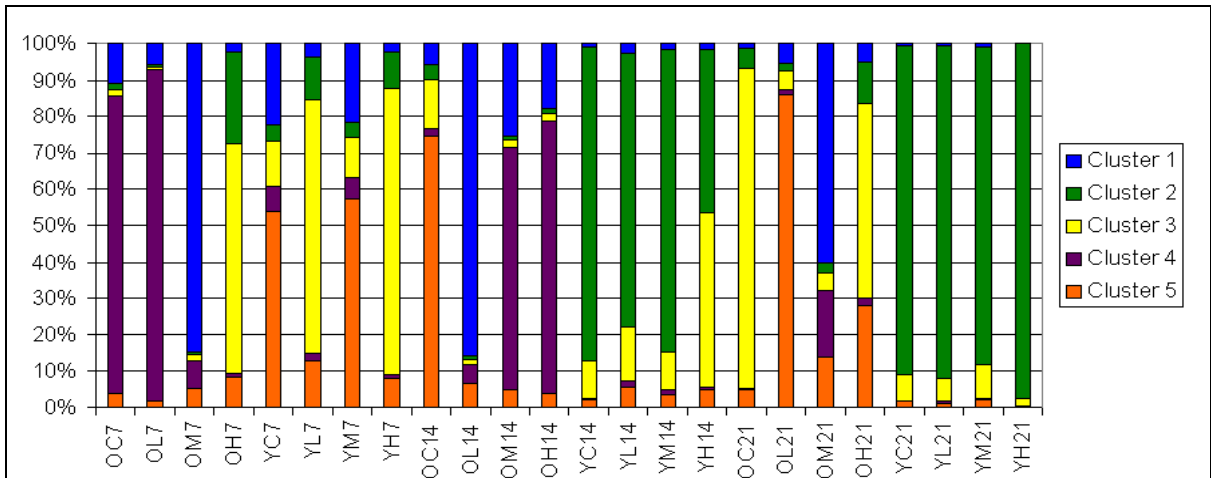


**Figure 6-14: Cluster memberships for NP experimental 'phenotype'. Each color corresponds to a separate cluster. Fuzzy c-means allows for a membership in multiple clusters. O – mature (old), Y – young, the number is the experimental time point, then loading is indicated by a C – control, L – 0.1 Hz or Low, M – 1 Hz or Medium, and H – 3 Hz or High.**

**Table 6-6: Cluster membership as a table for NP experimental 'phenotype'. Color of cells corresponds to their value of membership where >0.75 is red, 0.5 - 0.74 is yellow, 0.25 - 0.49 is green, 0.1 - 0.24 is blue, and white is <0.1. For naming convention, M – mature, Y – young, the number is the experimental time point, then loading is indicated by a C – control, L – 0.1 Hz or Low, M – 1 Hz or Medium, and H – 3 Hz or High**

Exp. Group (AF)	Cluster 1	Cluster 2	Cluster 3	Cluster 4	Cluster 5
M 7 C	0.039486	0.013534	0.021096	0.110616	0.815268
M 7 0.1Hz	0.015314	0.004525	0.007397	0.058652	0.914112
M 7 1 Hz	0.052134	0.008596	0.016775	0.847135	0.07536
M 7 3 Hz	0.082588	0.248986	0.630144	0.025358	0.012924
Y 7 C	0.537579	0.046699	0.122036	0.223758	0.069929
Y 7 0.1 Hz	0.129525	0.117053	0.699021	0.036755	0.017646
Y 7 1 Hz	0.574527	0.043173	0.10951	0.214847	0.057943
Y 7 3 Hz	0.07786	0.097111	0.791435	0.022571	0.011024
M 14 C	0.745861	0.039955	0.137472	0.056869	0.019843
M 14 0.1 Hz	0.065448	0.007978	0.016181	0.860268	0.050124
M 14 1 Hz	0.046381	0.011167	0.019251	0.253766	0.669435
M 14 3 Hz	0.040843	0.01118	0.0184	0.180848	0.748729
Y 14 C	0.020351	0.862165	0.105673	0.007634	0.004178
Y 14 0.1 Hz	0.055947	0.750667	0.148532	0.027654	0.017199
Y 14 1 Hz	0.03553	0.831279	0.106498	0.016637	0.010056
Y 14 3 Hz	0.047366	0.448549	0.479756	0.015957	0.008372
M 21 C	0.04599	0.056702	0.881289	0.010959	0.00506
M 21 0.1 Hz	0.858931	0.018618	0.051078	0.055841	0.015532
M 21 1 Hz	0.135117	0.028299	0.049014	0.602063	0.185506
M 21 3 Hz	0.279499	0.111216	0.536156	0.051418	0.021711
Y 21 C	0.0138	0.904098	0.073856	0.005309	0.002937
Y 21 0.1 Hz	0.012125	0.915805	0.064812	0.004667	0.00259
Y 21 1 Hz	0.018341	0.87627	0.094767	0.00686	0.003762
Y 21 3 Hz	0.00393	0.975099	0.018531	0.001561	0.000879

>0.75

0.5-0.749

0.25 - 0.49

0.1 - 0.249

0-0.99

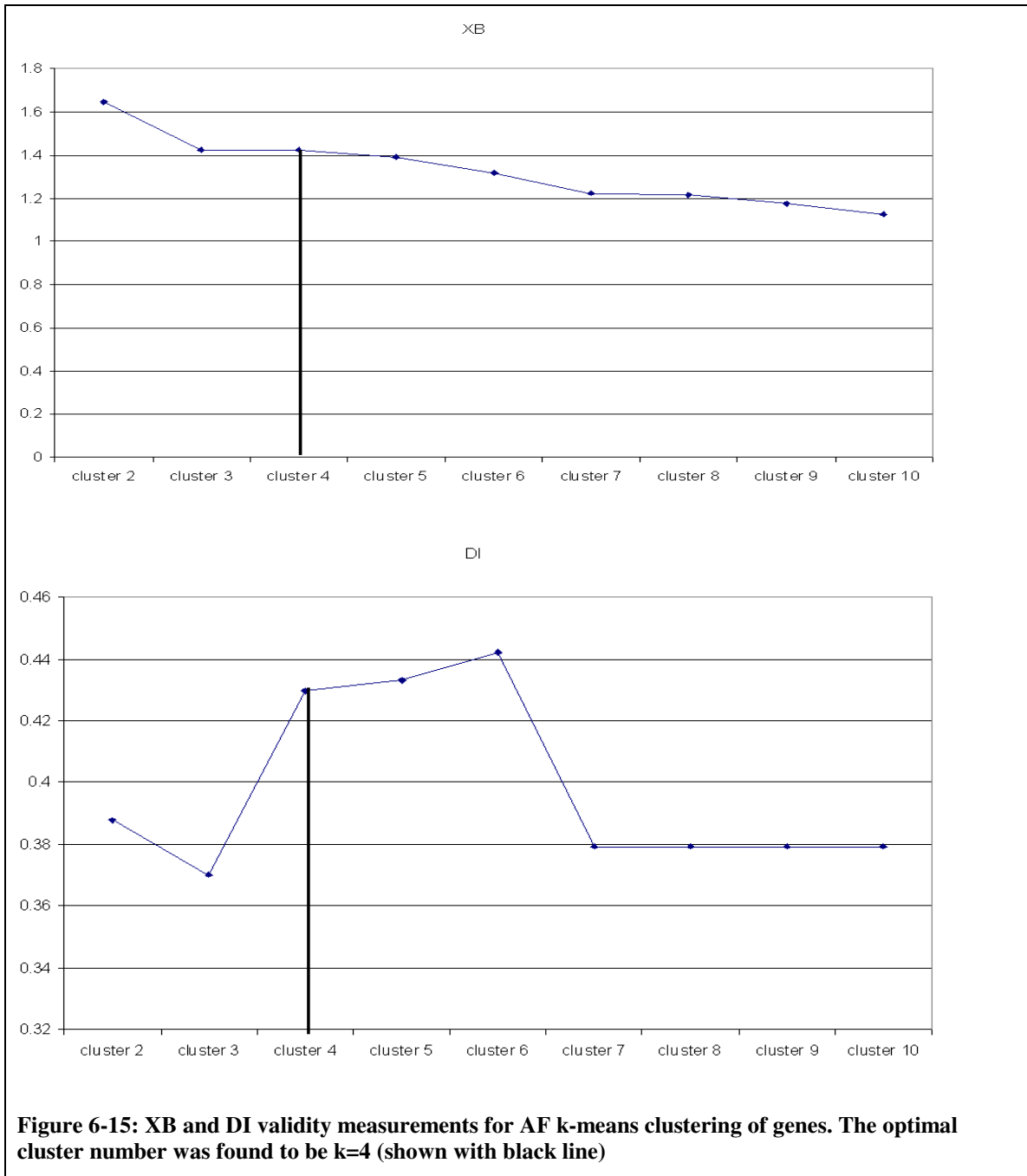
## 6.3.2 Gene Expression Clustering

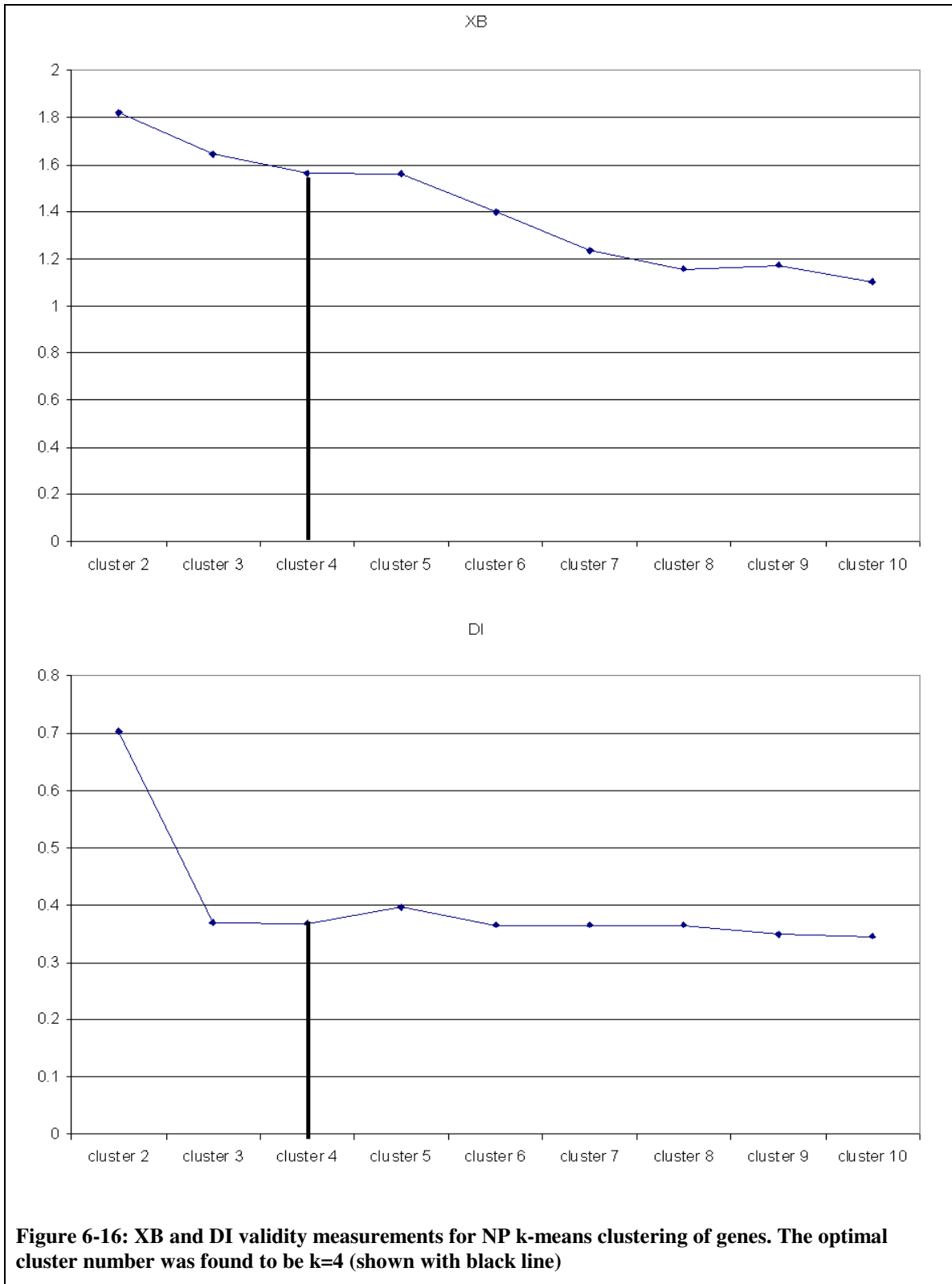
### 6.3.2.1 Full data sets, Kmeans clustering

K-means clustering of the AF gene expression values resulted in an optimal cluster number of  $k = 4$  (Figure 6-15). Cluster 1 contained collagen types I and II, aggrecan, and its catabolic counterpoint adamts4. Cluster 2 contained decorin and vimentin. Cluster 3 contained IGF, IL6, versican, link, fibronectin MMP3 and TIMP1. Cluster 4 had the highest membership, containing the transcription factors cfos, cjun,

mapk, stat3 and ilk, the growth factors TGFB and CTGF, the small proteoglycan biglycan, collagen type III and VI, the catabolic factors MMP1 and MMP2, and the anti-catabolic factor TIMP3 (Table 6-7).

K-means clustering of the NP gene expression values resulted in an optimal cluster number of k=4 (Figure 6-16). Cluster 1 contained collagen type I and ADAMTS4. Cluster 2 contained collagen type II, and aggrecan, versican, mmp3 and TIMP1 and 3, link and decorin, fibronectin, and vimentin. Cluster 3 was composed of the transcription factors cjun, cfos, stat3, mapk and ilk, the catabolic factors MMP1 and MMP2, collagen type III and type VI, biglycan, and the growth factors CTGF and TGFB. Cluster 4 was composed of IL6 and IGF (Table 6-7).





The genes composing each cluster for both the AF and NP are shown in Table 6-5. ‘Linked’ genes, which appear together in each cluster, share a common color in the list.

**Table 6-7: Membership of each cluster for the AF and NP with k-means clustering.**

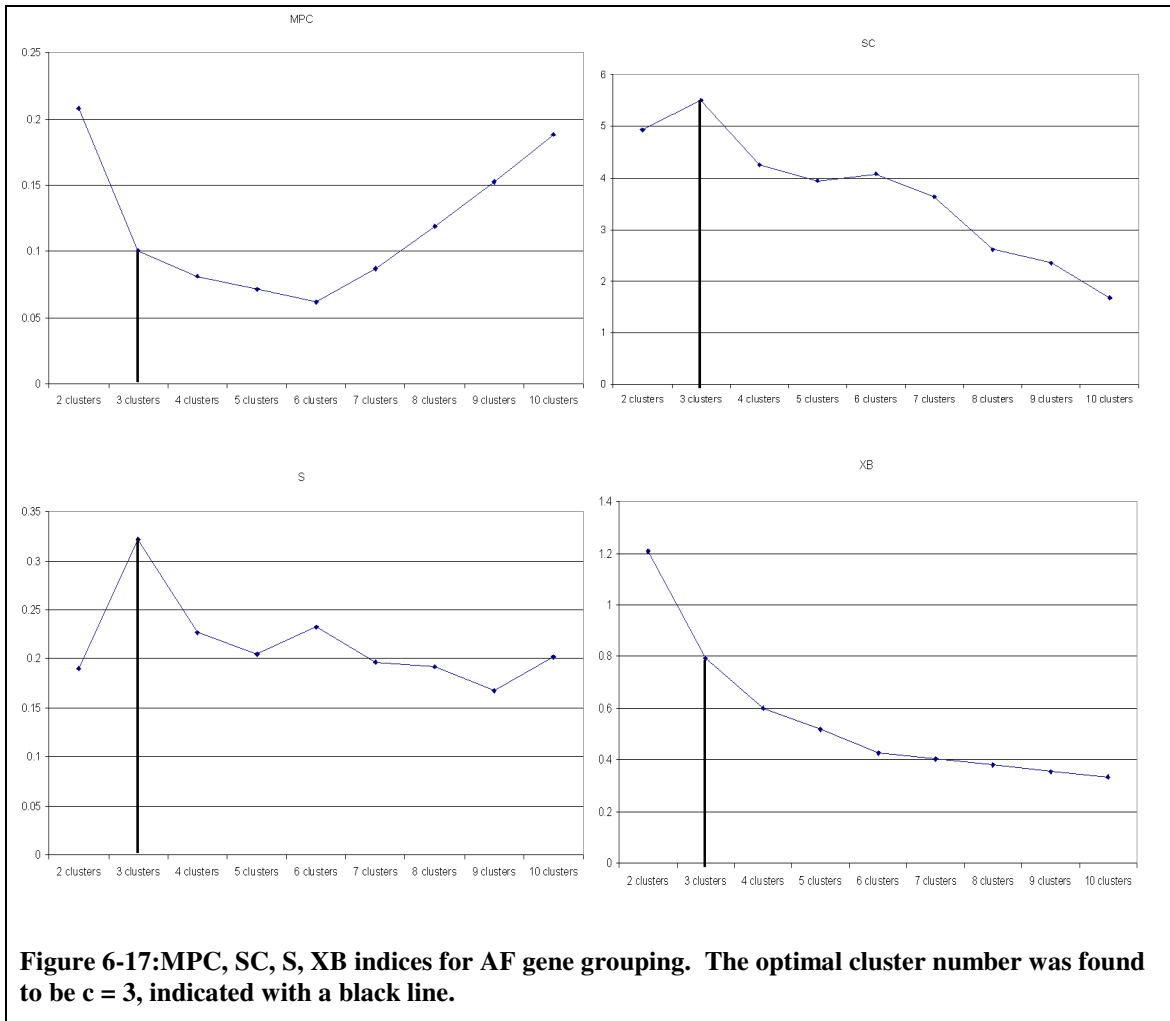
Cluster Number	AF
1	<b>col1</b> <b>adamts4</b> <b>col2</b> <b>agg</b> <b>versican</b> <b>mmp3</b> <b>timp1</b> <b>igf</b>
2	<b>link</b> <b>il6</b> <b>decorin</b>
3	<b>cjun</b> <b>ctgf</b> <b>mmp1</b> <b>tgfB</b> <b>timp3</b> <b>mapk</b> <b>col3</b>
4	<b>biglycan</b> <b>col6</b> <b>cfos</b> <b>stat3</b> <b>mmp2</b> <b>ilk</b> <b>fibronectin</b> <b>vimentin</b>

Cluster Number	NP
1	<b>col1</b> <b>col2</b> <b>agg</b> <b>versican</b> <b>ilk</b>
2	<b>biglycan</b> <b>col6</b> <b>cfos</b> <b>stat3</b> <b>mmp2</b> <b>ctgf</b> <b>tgfB</b> <b>mmp1</b> <b>mapk</b> <b>col3</b>
3	<b>link</b> <b>il6</b> <b>decorin</b> <b>vimentin</b> <b>fibronectin</b> <b>igf</b> <b>mmp3</b> <b>timp1</b> <b>timp3</b>
4	<b>adamts4</b> <b>cjun</b>

### 6.3.2.2 Full data sets, fuzzy c-means

Fuzzy c-means clustering in the AF resulted in an optimal cluster number of  $c = 3$ . Validity indices MPC, SC, S, XB and DI are all shown in Figure 6-17. The optimal cluster membership is shown in Figure 6-18 with a table with each group’s membership percentage also provided (Table 6-8).





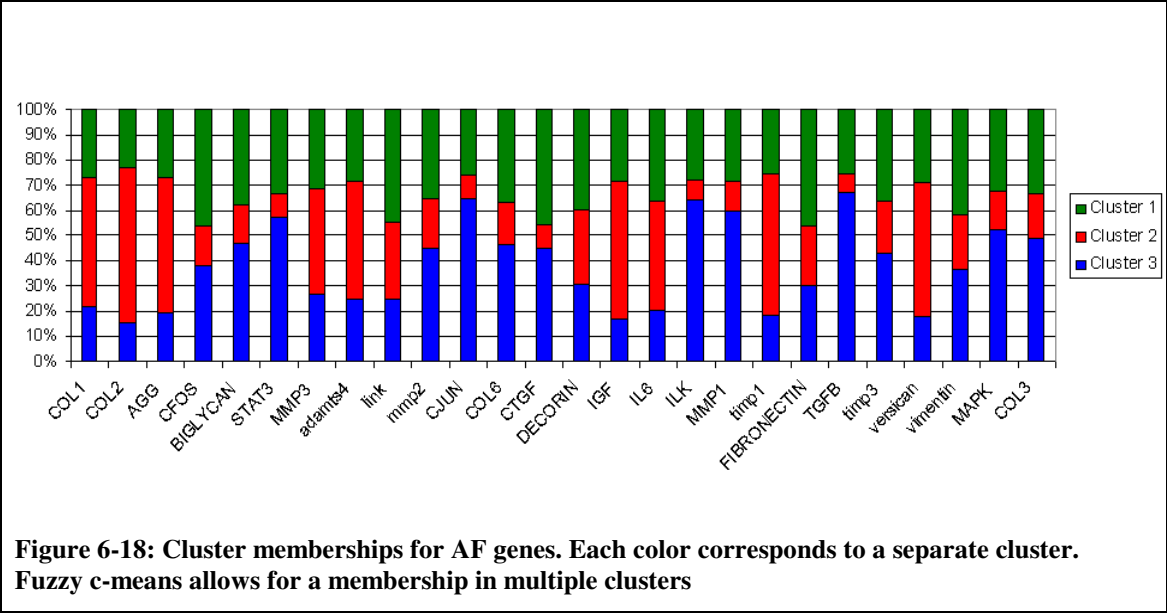


**Table 6-8: Cluster membership as a table for AF genes. Color of cells corresponds to their value of membership where >0.75 is red, 0.5 - 0.74 is yellow, 0.25 - 0.49 is green, 0.1 - 0.24 is blue, and white is <0.1**

Gene Name	Cluster 1	Cluster 2	Cluster 3
COL1	0.215717	0.512749	0.271534
COL2	0.155325	0.609423	0.235252
AGG	0.19361	0.538374	0.268016
CFOS	0.380705	0.157985	0.46131
BIGLYCAN	0.469982	0.156823	0.373195
STAT3	0.572317	0.096639	0.331044
MMP3	0.272384	0.413442	0.314174
adamts4	0.250514	0.465603	0.283883
link	0.251128	0.303063	0.445809
mmp2	0.452154	0.194953	0.352893
CJUN	0.647242	0.092332	0.260426
COL6	0.463786	0.168401	0.367813
CTGF	0.447155	0.099266	0.453579
DECORIN	0.304763	0.297076	0.398161
IGF	0.16837	0.544958	0.286672
IL6	0.207872	0.425249	0.36688
ILK	0.63977	0.079307	0.280923
MMP1	0.598707	0.116971	0.284321
timp1	0.185891	0.562318	0.251792
FIBRONECTIN	0.299278	0.242512	0.45821
TGFB	0.671979	0.074444	0.253577
timp3	0.427978	0.204617	0.367405
versican	0.178764	0.528332	0.292904
vimentin	0.363431	0.218474	0.418095
MAPK	0.521973	0.154202	0.323825
COL3	0.486342	0.180199	0.333459

>0.75

0.5-0.749

0.25 – 0.49

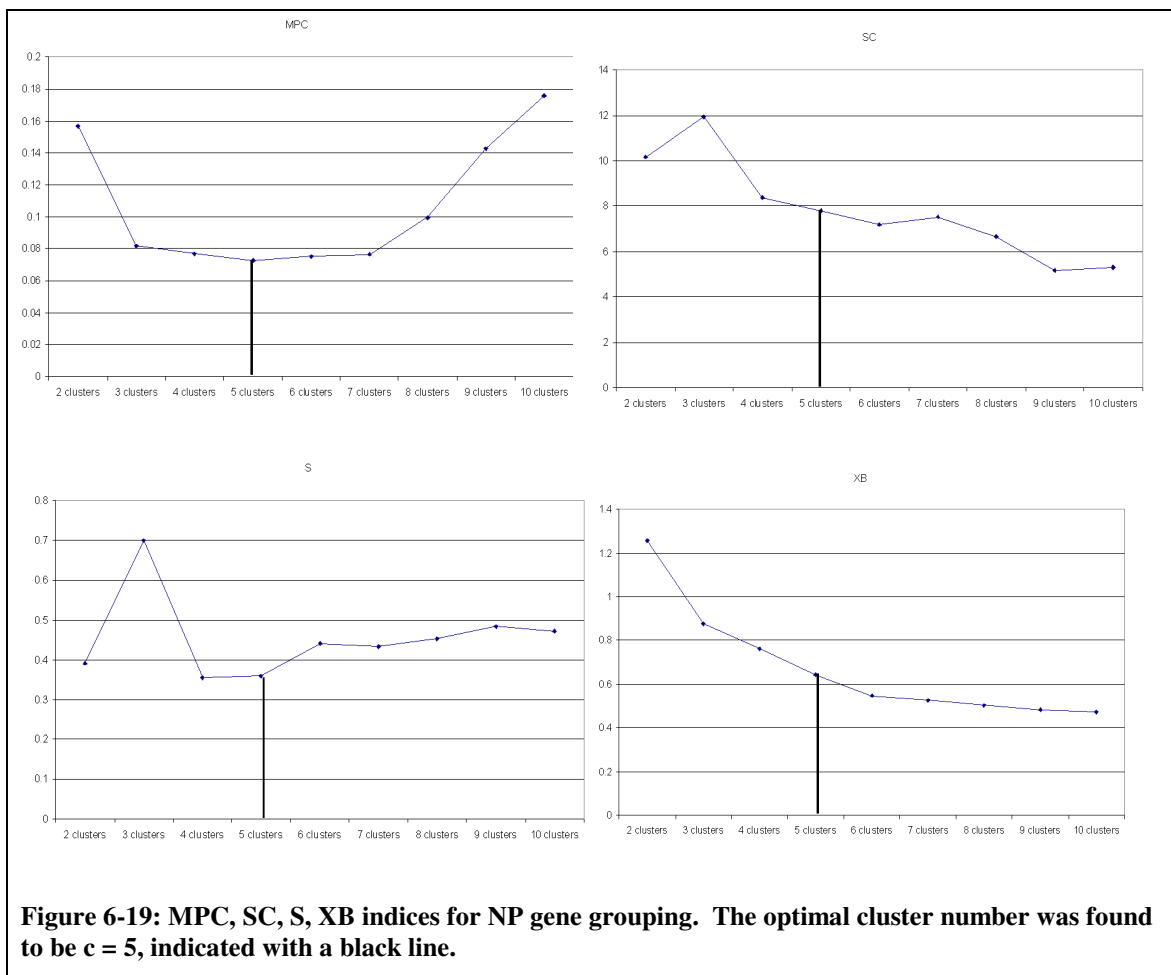
0.1 – 0.249

0-0.99

In the NP, fuzzy c-means clustering resulted in an optimal cluster number of 5. Validity indices MPC, SC, S, XB and DI are shown in Figure 6-4, While a solution may seem apparent at  $c = 3$  as in the AF, note the scale on the scale on SC, which should be minimized. While the solution of  $c=3$  does result in a small jump in SC in the AF, it is only of 0.5, whereas in the NP it results in a jump of 2. The optimal cluster membership

is shown in Figure 6-20, again with a table of group memberships also provided (Table 6-9).

In both the AF and NP, genes displayed a greater amount of membership in multiple clusters than in the experiment grouping approach. This could be due to either the participation of these genes in multipole pathways, or alternatively be an effect of the combination of old and young data sets, possibly adding a source of noise to the data. To address this, the old and young data sets were also analyzed separately.



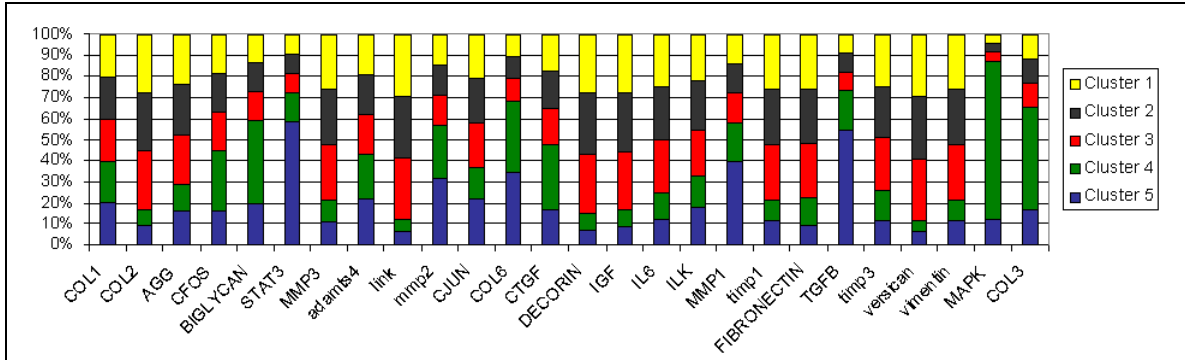
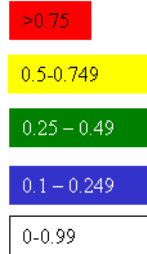


**Figure 6-20: Cluster memberships for AF genes. Each color corresponds to a separate cluster. Fuzzy c-means allows for a membership in multiple clusters**

**Table 6-9: Cluster membership as a table for NP genes. Color of cells corresponds to their value of membership where >0.75 is red, 0.5 - 0.74 is yellow, 0.25 - 0.49 is green, 0.1 - 0.24 is blue, and white is <0.1**

Gene Name	Cluster 1	Cluster 2	Cluster 3	Cluster 4	Cluster 5
COL1	0.206661	0.201752	0.188906	0.201265	0.201417
COL2	0.092932	0.277944	0.07273	0.27824	0.278153
AGG	0.158939	0.238179	0.126379	0.238264	0.238239
CFOS	0.161411	0.184291	0.286837	0.183629	0.183833
BIGLYCAN	0.195123	0.136611	0.395855	0.136132	0.13628
STAT3	0.583391	0.093748	0.136775	0.092914	0.093172
MMP3	0.106244	0.262032	0.105117	0.263538	0.26307
adamts4	0.215593	0.190108	0.215029	0.189548	0.189722
link	0.062383	0.290618	0.069096	0.294569	0.293333
mmp2	0.319909	0.14434	0.247961	0.143813	0.143976
CJUN	0.219446	0.211953	0.148945	0.209439	0.210216
COL6	0.343349	0.105768	0.340248	0.105234	0.1054
CTGF	0.164198	0.174528	0.313303	0.173886	0.174084
DECORIN	0.072916	0.28154	0.079261	0.283436	0.282848
IGF	0.08664	0.278977	0.076693	0.278817	0.278873
IL6	0.118648	0.251681	0.127424	0.25102	0.251227
ILK	0.179262	0.225454	0.147468	0.223625	0.224192
MMP1	0.3978	0.139904	0.183426	0.139349	0.139521
timp1	0.115319	0.262323	0.096231	0.263198	0.262929
FIBRONECTIN	0.098668	0.257246	0.126896	0.258844	0.258345
TGFB	0.550144	0.089186	0.183197	0.088654	0.088819
timp3	0.117791	0.245592	0.144383	0.246214	0.24602
versican	0.063442	0.296539	0.048772	0.295448	0.295799
vimentin	0.113863	0.261574	0.098424	0.263344	0.262794
MAPK	0.118345	0.04221	0.755495	0.041932	0.042018
COL3	0.164167	0.11589	0.489091	0.115341	0.115511



### 6.3.2.3 Sub-matrix analysis – Kmeans

The AF and NP matrices were partitioned into old and young AF and NP (four total sub-matrices) to remove and identify any influence each age had on the overall gene expression patterns found when grouping the genes from the intact data sets. The AF and NP gene membership lists varied between the young and old, and both also varied from the intact data sets. The Rand indices for these groups were computed to further quantify the similarities (and differences) between the sub-matrices and the full data set, and between the mature and young sub-matrices.(Table 6-10)

**Table 6-10: Rand indices indicating similarities in memberships between sub-matrices (with each other and with the full data set). Indices were based on membership lists from an optimal run.**

	<i>Rand Index</i> <i>(Mature and Young)</i>	<i>Rand Index</i> <i>(Young and Full Set)</i>	<i>Rand Index</i> <i>(Mature and Full Set)</i>
AF	0.695	0.874	0.698
NP	0.625	0.788	0.720

**Table 6-11: Membership lists for Mature and Young AF and NP generated by clustering the sub-matrices**

	Members Old AF
Cluster1	coll col2 agg versican mmp3 timp1 link il6
Cluster 2	ctgf decorin
Cluster3	biglycan col6 adams4 mmp2 mmp1
Cluster 4	cfos stat3 cjun ilk igf fibronectin tgfB timp3 vimentin mapk col3

	Members Young AF
Cluster1	coll adams4 col2 agg versican mmp3 timp1 igf il6
Cluster 2	Link fibronectin col3
Cluster3	cjun ctgf tgfB decorin mmp1 timp3 mapk
Cluster 4	cfos stat3 mmp2 biglycan col6 ilk vimentin

	Members Old NP
Cluster1	coll adams4 agg versican stat3 mmp2 cjun col6 ilk mmp1tgfB
Cluster 2	col2 mmp3 timp1 link decorin vimentin igf il6 fibronectin
Cluster3	biglycan mapk col3
Cluster 4	cfos ctgf timp3

	Members Young NP
Cluster1	coll col2 agg versican mmp3 timp1 link fibronectin timp3 vimentin
Cluster 2	biglycan col6 cfos adams4 mmp2 ctgf tgfB mmp1 mapk col3
Cluster3	decorin igf il6 ilk
Cluster 4	stat3 jun

### 6.3.3 Gene patterns in experimental grouping

The experimental groups found to be clustered in part 1 were now separated from the overall gene expression matrix (n = 4 for AF, n = 6 for NP). Those sub-matrices were then transposed, and the genes clustered. This can be conceptually understood by thinking of the experimental groups representing separate phenotypes, and the goal is to



now cluster the genes representing each phenotype to determine the patterns of regulation occurring within each. K-means clustering was used for all the clustering described.

AF

Optimal cluster numbers were determined for each group from XB and DI validity indices. The optimal cluster number was determined to be  $k=4$  for groups 1 and 2, and  $k = 3$  for groups 3 and 4. Tables of each group's cluster membership are shown below. Group 1 contained mature 7-day control and 1 Hz, Young 14 day control, 1 Hz and 3 Hz, and Mature 21 day 3 Hz. Group 2 contained Mature 7 day 0.1 Hz and 3 Hz, all Young 7 day, and Mature 14 day control and 0.1 Hz. Group 3 contained Mature 14 day 1 Hz and 3 Hz, Young 14 day 0.1 Hz, Mature 21 day control and 1 Hz groups

NP

Optimal cluster numbers were  $k = 3$  for all groups except groups 1 and 2 which had an optimal cluster number of  $k = 4$ . Each cluster member is shown below (Table 6-13). Group 1 contained mature 7-day control, 0.1 Hz and 3 Hz. Group 2 contained Young 14 day 0.1 Hz and 1 Hz. Group 3 contained young 7-day control and 1 Hz, mature 14-day control, and mature 0.1 Hz at 21 days. Group 4 contained young 14 control and 3 Hz, and all Young 21 day samples. Group 5 contained mature 14-day 1 Hz and 3 Hz, and Group 6 contained Mature 7 day control, 0.1 Hz, 3 Hz and Mature 14 day 1 Hz and 3 Hz samples.

**Table 6-12: Gene memberships for each experimental outcome cluster in the AF.**

	Members group 1
Cluster1	coll adamts4
Cluster 2	decorin vimentin il6 fibronectin link
Cluster 3	cfos biglycan col6 stat3 mmp2 cjun ctgf tgfb ilk mmp1 timp3 mapk col3
Cluster4	col2 agg mmp3 timp1 igf versican
	Members group 2
Cluster1	coll adamts4
Cluster 2	col2 agg mmp3 timp1 cjun ctgf tgfb decorin versican igf il6 mapk
Cluster3	biglycan col6 stat3 mmp2 ilk mmp1 fibronectin timp3 col3
Cluster 4	cfos link vimentin
	Members group 3
Cluster1	coll adamts4 biglycan col6 decorin
Cluster 2	col2 agg cfos link cjun stat3 mapk ilk mmp1 mmp2 col3 ctgf tgfb il6 fibronectin versican vimentin
Cluster 3	mmp3 timp1 igf timp3
	Members group 4
Cluster1	coll adamts4 col2 agg cfos mmp3 igf ilk versican
Cluster 2	mmp2
Cluster 3	biglycan col6 stat3 link cjun ctgf tgfb decorin vimentin ilk mmp1 timp1 timp3 fibronectin mapk col3

**Table 6-13: Gene memberships for each experimental outcome cluster in the NP.**

Members group 1		Members group 2	
Cluster 1	col2 agg versican link ilk	Cluster 1	coll adams4 stat3 link mmp2 col6 il6 ilk mmp1 fibronectin tgfB timp3 mapk
Cluster 2	cfos biglycan adams4 mmp2 cjun ctgf timp3 mapk col3	Cluster 2	col2 agg cfos mmp3 cjun decorin
Cluster 3	mmp3 timp1 decorin vimentin igf il6 fibronectin	Cluster 3	biglycan ctgf igf versican col3
Cluster 4	coll stat3 col6 mmp1 tgfB	Cluster 4	timp1 vimentin

Members group 3		Members group 4	
Cluster 1	col2 agg coll biglycan stat3 cjun igf il6 versican link ilk timp1 vimentin	Cluster 1	coll decorin
Cluster 2	adams4 mmp2 col6 mmp1 tgfB mapk col3	Cluster 2	col2 agg mmp2 link mmp3 timp1 fibronectin vimentin
Cluster 3	cfos mmp3 ctgf decorin fibronectin timp3	Cluster 3	cfos cjun stat3 mapk ilk mmp1 biglycan col6 adams4 ctgf igf il6 tgfB timp3 versican col3

Members group 5		Members group 6	
Cluster 1	col2 agg mmp3 timp1 adams4 link igf timp3 versican vimentin	Cluster 1	coll adams4
Cluster 2	coll cfos biglycan col6 stat3 mmp2 cjun ctgf ilk mmp1 tgfB mapk col3	Cluster 2	col2 agg cjun stat3 mmp3 timp1 link mmp2 decorin vimentin igf il6 ilk tgfB versican mmp1
Cluster 3	decorin fibronectin	Cluster 3	cfos biglycan col6 ctgf fibronectin timp3 mapk col3

### 6.3.4 Predictive model

The next step was to determine whether the groups that clustered have any predictive value. The two-fold approach to this question sought to first address the ability for the model to predict future experimental groups, and second to predict gene relationships from the data.

#### 6.3.4.1 Predicting other genes

To assess the ability for the developed clusters to describe future gene expression values, three genes were ‘held back’ from the analysis assigning clusters. After clusters were defined, the gene expression values for MMP13, TIMP2, and ADAMTS5 were normalized and the Euclidian distance from the optimal run cluster centers were determined. The gene was then assigned to the closest centroid. As illustrated in section

6.3.2.3, the combination of mature and young gene expression values could influence the membership of the genes of interest. Therefore, the genes were paired with centroids in the mature and young sub-matrices in addition to the combined (full) data set.

In the full data set of the AF (Table 6-14), MMP13 was found associated with collagen types I,II ADAMTS4, versican, MMP3, TIMP1 and IGF. In the sub-matrices, the membership only differed with the addition of link and IL6 and the removal of ADAMTS4 in the mature cells, and the addition of IL6 in the young AF. ADAMTS5 was always associated with ADAMTS4 in all clusters. TIMP2 was in a group with another TIMP at all analyses, however was associated with TIMP1 in the mature cells, but TIMP3 in the full data set and in the young sub-matrix analysis.

In the NP (Table 6-15), MMP13 was associated with ADAMTS4 for all clusters. ADAMTS5 associated with ADAMTS4 again for all groups, except in the young NP where it instead with decorin IGF, IL6, and ILK. TIMP2 always associated with decorin IGF and IL6.

The range of distances found between the 'held back' genes and their closest cluster were similar to the distances between the other genes and the centroids as well, indicating that MMP13, TIMP2 and ADAMTS5 were members of their respective centroids and not significantly outside of the area enclosed by the cluster.

**Table 6-14: Gene distance from centroids found for the full, mature and young full AF data set except the three genes 'held back'. The gene is expected to belong to the group it is closest in space to (smallest distance between the gene expression value and cluster centroid). The smallest value is in bold. Groups correspond to those shown in Table 6-7**

<b><u>Full Set</u></b>	<i>Group 1</i>	<i>Group 2</i>	<i>Group 3</i>	<i>Group 4</i>
MMP13	<b>0.691</b>	0.901	1.212	1.271
ADAMTS5	<b>0.690</b>	0.853	0.942	1.107
TIMP2	0.643	0.678	<b>0.632</b>	0.765

<b><u>Mature</u></b>	<i>Group 1</i>	<i>Group 2</i>	<i>Group 3</i>	<i>Group 4</i>
MMP13	<b>0.540</b>	0.748	0.825	0.804
ADAMTS5	0.519	0.680	<b>0.493</b>	0.564
TIMP2	<b>0.343</b>	0.529	0.619	0.339

<b><u>Young</u></b>	<i>Group 1</i>	<i>Group 2</i>	<i>Group 3</i>	<i>Group 4</i>
MMP13	<b>0.459</b>	0.827	0.864	0.926
ADAMTS5	<b>0.415</b>	0.809	0.767	0.986
TIMP2	0.544	0.480	<b>0.479</b>	0.625

**Table 6-15: Gene distance from centroids found for the full, mature and young NP data except the three genes 'held back'. The gene is expected to belong to the group it is closest in space to (smallest distance between the gene expression value and cluster centroid). Groups correspond to those shown in Table 6-7 (NOTE: members are not the same between AF and NP)**

<b><u>Full</u></b>	<i>Group 1</i>	<i>Group 2</i>	<i>Group 3</i>	<i>Group 4</i>
MMP13	0.5517	0.645	0.726	<b>0.384</b>
ADAMTS5	0.457	0.491	0.522	<b>0.439</b>
TIMP2	0.364	0.507	<b>0.334</b>	0.499

<b><u>Mature</u></b>	<i>Group 1</i>	<i>Group 2</i>	<i>Group 3</i>	<i>Group 4</i>
MMP13	<b>0.444</b>	0.612	0.666	0.756
ADAMTS5	<b>0.280</b>	0.407	0.442	0.461
TIMP2	0.392	<b>0.265</b>	0.534	0.468

<b><u>Young</u></b>	<i>Group 1</i>	<i>Group 2</i>	<i>Group 3</i>	<i>Group 4</i>
MMP13	0.339	<b>0.231</b>	0.299	0.236
ADAMTS5	0.349	0.323	<b>0.261</b>	0.276
TIMP2	0.207	0.197	<b>0.120</b>	0.136

#### 6.3.4.2 Predicting groups of experiments based on ‘phenotype’

To ascertain whether the experimental ‘phenotype’ clusters could be associated with groups from another type of experiment, the data from the study described in chapter 3 was used as a test set of data for the experimental phenotype clustering described in section 6.3.1. Here, the goal was to determine which experimental groups, meaning the data used throughout this clustering analysis, were most related to the three test groups from chapter 3, namely control (static load at 0.2 MPa), Low load (0.2 – 1 MPa at 1 Hz) and High load (0.2 – 2.5 MPa at 1 Hz). While similarities exist between the studies (bovine IVD, mature discs for both), the experimental groups differed from the test groups in mechanism of load application (displacement control for experimental, load control for test), culture method (in alginate for experimental, *in situ* for test) and also in duration (21 days total for experimental, 7 days for test).

The test data was only composed of 8 genes in addition to the two housekeeping genes: collagen types I and II, aggrecan, versican, TIMP1, mmp2 and mmp3 and ADAMTS4. To maintain the structure of the other known data, the full set of experimental data was used to find optimal cluster centroids, and then the centroid dimensions corresponding to these 8 genes were separated and used to calculate the distances reported.

For the AF, membership was found between the test groups and two of the four clusters. The average distance between the test groups and the experimental centroids was 0.457 (Table 6-16). In the NP, each test group was a member of a different cluster,

with an average distance of 0.142 between test groups and experimental cluster centroids (Table 6-17).

**Table 6-16: Distances between test groups and cluster centroids found from experimental 'phenotypes' in the AF. The lowest value, and therefore cluster membership, is noted in bold. Groups correspond to those in Figure 6-6**

	<i>Group 1 (Green)</i>	<i>Group 2 (Red)</i>	<i>Group 3 (Blue)</i>	<i>Group 4 (Yellow)</i>
Control (0.2 MPa, Static)	0.776	0.597	0.930	<b>0.440</b>
Low (0.2-1MPa, 1 Hz)	0.563	0.596	1.026	<b>0.406</b>
High (0.2-2.5MPa, 1 Hz)	<b>0.526</b>	0.534	0.934	0.579

**Table 6-17: Distances between test groups and cluster centroids found from experimental 'phenotypes' in the NP. The lowest value, and therefore cluster membership, is noted in bold. Groups correspond to those in Figure 6-7**

	<i>Group 1 (Yellow)</i>	<i>Group 2 (Red)</i>	<i>Group 3 (Black)</i>	<i>Group 4 (Green)</i>	<i>Group 5 (Purple)</i>	<i>Group 6 (Blue)</i>
Control (0.2 MPa, Static)	0.772	0.372	0.305	0.285	<b>0.148</b>	0.491
Low (0.2-1MPa, 1 Hz)	1.374	0.890	0.417	0.182	0.152	<b>0.079</b>
High (0.2-2.5MPa, 1 Hz)	0.464	0.454	0.247	<b>0.201</b>	0.391	0.831



## 6.4 Discussion

Clustering analysis was used to explore gene expression patterns present in experimental data. The use of a more robust analysis than simply plotting each variable separately was warranted, as the number of independent (24) and dependent (26) variables was large. Four approaches to exploring the data set were proposed. The first approach, clustering of the independent variables (experimental groups) based on their gene expression phenotype, sought to find patterns in the way the experimental groups responded to the independent variables. The second approach, clustering the dependent variables (gene expression values), first explored the universal gene expression patterns in the intervertebral disc (all AF or NP groups), and then utilized known associations in the data (old versus young) to examine more tightly associated gene expression patterns. The third approach, taking the experimental groups from part 1 and clustering their gene expression values in a process known as biclustering, sought to determine what aspects of the gene expression profiles contributed to the separate experimental phenotypes. Finally, the ability for the patterns revealed by clustering to predict classifications on the gene and experimental phenotype level was analyzed.

Clustering on the experimental level revealed less complexity in the AF than in the NP (determined by the overall cluster number, four for the AF, 6 for the NP). In both tissues, the young cells at day 21 had mostly come to a consistent clustering, which can possibly be interpreted as a stable, or more 'normal' phenotype. This would be expected, as the cells are recreating the extracellular matrix within the alginate, and over time they would have accumulated a volume that would place them back in a more 'normal' level

of interaction with the surrounding environment. In the young NP, the cells had largely reached this 'normal' point by day 14, whereas it appears that the mature NP never achieved a stable clustering, either with the NP (all with the same stable point) or on its own (all mature cells having a stable point, separate from that of the young). It is likely that the inability of the mature NP cells to recreate a robust, functioning extracellular matrix, as reported earlier, would be detrimental to the re-establishment of this 'normal' point.

In the AF, however, it appears that the mature cells at day 21 after 0.1 Hz loading were able to achieve a common 'phenotype' with the young AF cells at the same time. It is possible that the application of this low frequency load was enough to stimulate the cells, but not high enough to effect transport of the matrix molecules through the alginate and away from the cells. This also suggests that the AF cells may be less sensitive to the negative effect aging had on the NP cells. Additionally, the earliest time point (day 7) immediately followed the application of the seventh day of loading, and can possibly be thought of as the phenotypic response of each cell to early mechanical stimulation. In the AF, a common phenotype was shared by young and old, with the exception of the mature controls and 1 Hz at day 7, again supporting the concept that the AF cells are less sensitive overall to the effects of aging.

Turning to the clustering of gene expression data, some trends are readily apparent. In the AF and NP, certain genes tend to stay together, for instance collagen type II, aggrecan, and versican which are all structural members of the IVD which would be expected to be upregulated in response to compression. MMP3 and TIMP1 also

grouped together, which may indicate the catabolic nature of MMP3 may be regulated and counteracted by its inhibitor TIMP1. Biglycan and collagen type VI are also similarly regulated, indicating the importance of this small proteoglycan together with this major component of the pericellular matrix of the intervertebral disc cells. The association of MAPK, a signalling factor known to be affected by dynamic compression and collagen type III also indicates the response of the IVD to dynamic compression through a remodeling pathway similar to development, as collagen type III is the earliest collagen type present throughout the fetal IVD. Further segmenting the data based on age reveals patterns that were obscured by the different magnitudes of gene expression levels between age groups. Interestingly, using an index to compare between the membership lists generated by mature and young genes, the similarity between the young and full sets is higher than that between mature and young, or between mature and the full set. This implies the full set is being more highly influenced by the behavior of the young gene expression, and therefore the young gene expression values tend to have a greater magnitude (be more highly expressed).

The biclustering analysis of the experimental phenotypes provides insight into the gene patterns responsible for the differentiation between phenotypes. In the AF, it is notable that the 'normal' day 21 phenotype is the only one where collagen types I and II and aggrecan are all members of the same cluster (as was seen with the overall gene cluster analysis of the AF). While collagen type I is more present in the AF of the intervertebral disc, the genes may have a more similar expression in this case where compression is being applied to the cell, rather than tensile loads as normally experienced

*in vivo*. MMP2 also exists alone in a cluster in this phenotype, in contrast to the other phenotypes where it is usually associated with other genes, notably the anti-catabolic genes TIMP1 and TIMP3. In the NP, the stable phenotype is notably characterized by a disconnect between collagen type I and the block of collagen type II and aggrecan.

The universal nature of the patterns found through the aspects of clustering analysis was examined on the experimental phenotype and the gene level. First, by clustering the experimental phenotypes to determine cluster number and centroids of clusters, and then comparing the locations of particular ‘test’ experimental phenotypes to these clusters, further insight into the similarity of the ‘test’ groups to the experimental groups can be determined. In the AF, the test groups ‘Control’ and ‘Low’ both corresponded to the same cluster, which was also the cluster described above as a ‘normal’ phenotype. This result is highly encouraging, as the *in vivo* discs would not have to recreate their extracellular matrix, and would therefore be expected to be at this ‘normal’ phenotype. The ‘High’ load group corresponded to a cluster including the mature AF cells at control and 1 Hz loading at 7 days. The common factor in these groups is potentially an attempt at early remodeling. In the NP, all three ‘test’ groups fell into a different experimental phenotype cluster. ‘Control’ NP was closest to the ‘normal’ NP phenotype described above. Again, this would be fully expected, as these cells are *in vivo* and would therefore not need to recreate the extracellular matrix. The ‘Low’ load group corresponded to a cluster with two members, Young 14 day 0.1 Hz and 1 Hz. This could be interpreted as phenotype close to ‘normal’, particularly as the perturbation of the experimental phenotypes through gaussian noise often results in those groups also in a

cluster with the 'normal' phenotype. The 'High' load group corresponded to a cluster containing four members, two of the young 7 day (0.1 and 3 Hz) and two mature 21 Hz (control and 3 Hz). While the interpretation of this cluster is not immediately obvious, by taking a lesson from the correspondence of the 'High' AF to a cluster exhibiting an early attempt at remodeling, one can speculate that the 'High' NP is also corresponding to that type of cluster. This would imply the young NP cells are more quickly able to affect an early remodeling response than the mature NP cells (7 days in young versus 21 days for mature).

The second method to examine the applicability of the clusters to unknown data was to examine the cluster memberships of 'test' genes. Three genes were used for this analysis, MMP13, TIMP2 and ADAMTS5. In all cases, genes were found to be associated with clusters at distances well within the range of distances found for other cluster members, indicating they were fully associated with their membership clusters. MMP13 and ADAMTS5 were both associated most commonly with ADAMTS4 in both the NP and AF tissue. In the AF, TIMP2 was in a group with another TIMP at all analyses, however was associated in the NP with with decorin IGF and IL6.

Finally, the visualization of the clusters was facilitated through the use of two variable-space transformation and reduction techniques. Both methods resulted in images that were reduced in dimension, thus enabling visualization of the results in two- or three-dimensions.

## **6.5 Conclusions**

The application of clustering techniques to illuminate patterns in intervertebral disc mechanobiology is a very promising direction for future research. Patterns in both experimental phenotypes and in gene level responses can be found in data, which is composed of many groups in both independent and dependent variables. Biclustering further identifies those genes, which are candidates for further exploration. Most interestingly, the clustering patterns found seem to be applicable to other intervertebral disc study models, and to genes unseen by the clustering algorithm, thus reinforcing the exciting role gene clustering can have in describing the intervertebral disc cell response to applied conditions.

## **CHAPTER 7 Summary**

The mechanical and biological response of the intervertebral disc to compression loading, aging, and time was examined through the use of organ culture and cell culture models. Annulus fibrosus disruption through needle puncture quickly decreased the compressive modulus of the intervertebral disc. However, the disc was resistant to damage and alteration in mechanical properties through the application of compression alone, highlighting the importance of annulus integrity to the overall mechanical behavior of the IVD. Some evidence of biological remodeling was observed histologically in the nucleus pulposus of the needle-punctured discs. No large effects of dynamic compression on the gene expression of matrix molecules typical of the intervertebral disc, nor on the biosynthesis of sulfated glycosaminoglycans was noted. Mechanical compression applied to isolated cells from young and mature animals demonstrated significant effects of aging on the ability for the intervertebral disc cells to recreate extracellular matrix over seven days in culture. Aging also interacted with the frequency of applied load to affect gene expression profiles, however the effect of aging on the cells was much more influential than the effect of applied compression loading.

A dynamic compression-loading regime is not damaging to the mechanical properties of the intervertebral disc. Even at high magnitudes of loading, the intervertebral disc did not display any alterations in structural or mechanical parameters, supporting the concept that the disc is highly adapted for resisting compression loading. The main structural and mechanical weak point in the disc structure is therefore likely the vertebral endplate.

Disc mechanics were significantly affected by annulus fibrosus disruption. In the case of needle puncture, a decrease in compressive modulus was almost instantaneous. Such a defect would be induced by nucleus pulposus herniation, which would be particularly detrimental to the mechanical behavior of the intervertebral disc as the loss of nucleus pulposus tissue would also result in a decrease in the ability for the disc to pressurize, thus resulting in increased compressive, rather than normal tensile forces, on the annulus fibrosus.

Alterations in disc mechanics may precede significant changes in disc extracellular matrix composition and synthesis. However, some genes may be regulated by mechanical loading, for example collagen type I and MMP3 both found to be upregulated in organ culture model of dynamic compression. Aging is of critical importance to the cells of the intervertebral disc, and particularly the nucleus pulposus. Normal aging processes result in nucleus pulposus cells, which are less able to create robust, functional, extracellular matrix. Additionally, while young nucleus pulposus cells can achieve a stable response to mechanical loading over time, mature nucleus pulposus cells do not. In the annulus fibrosus, some level of mechanical stimulation can facilitate a stable 'normal' gene expression profile in both young and mature animals. Interestingly, the expression of matrix components present early in development are also present in the isolated intervertebral disc cell populated alginate gel, indicating the cells may follow a common template to recreate the extracellular matrix after injury or other insult. This provides a mechanism for the age-related increase in collagen type III pericellular, where a cell would respond through a thickening of the pericellular matrix rather than an



effective, tissue-level repair response. The association of collagen type III with MAPK, a transcription factor stimulated by mechanical loading, further supports this theory. The association of major structural molecules (collagen types I and II, aggrecan and versican) with each other also indicates the more effective repair response is slower, and is not as readily achieved in old cells versus young cells.

Future studies should address the role of more complex loading conditions, such as combined bending and compression, in affecting disc cell mechanobiology. More complex loading conditions are more likely to lead to mechanical disruption of the disc, which may have large biological implications. The mechanism behind annular disruption-induced loss of mechanical function should also be explored in more depth, as that has potential implications for the recovery of a disc following discography, discectomy, or following any potential regenerative techniques for the nucleus pulposus where access through the AF would be necessary. The role of aging on intervertebral disc health is a topic that has implications for the ability of a disc to respond and repair over the course of an animal/human's lifetime. Studies on the role of aging on the response to loading and pharmacological interventions would therefore be warranted. Finally, the use of clustering analysis is a promising means to describe the effects of many input variables on the biological response of the disc and may eventually be used to define "normal" phenotypes, and also define "abnormal" and "damaged" phenotypes from their quantitative distances from normal phenotypes. Future work can lead to a descriptive map of intervertebral disc cell responses, and hopefully provide a means by which

biological processes leading to intervertebral disc degeneration can be reduced, counteracted, or treated.

## References

- Abe, Y., Akeda, K., An, H. S., Aoki, Y., Pichika, R., Muehleman, C., Kimura, T. & Masuda, K. (2007) Proinflammatory cytokines stimulate the expression of nerve growth factor by human intervertebral disc cells. *Spine*, 32, 635-42.
- Adams, M., Bogduk, N., Burton, K., Dolan, P. (2002) *The Biomechanics of Back Pain*, London, Churchill Livingstone.
- Adams, M. A. (2004) Biomechanics of back pain. *Acupunct Med*, 22, 178-88.
- Adams, M. A., Freeman, B. J., Morrison, H. P., Nelson, I. W. & Dolan, P. (2000) Mechanical initiation of intervertebral disc degeneration. *Spine*, 25, 1625-36.
- Aebli, N., Goss, B. G., Thorpe, P., Williams, R. & Krebs, J. (2006) In vivo temperature profile of intervertebral discs and vertebral endplates during vertebroplasty: an experimental study in sheep. *Spine*, 31, 1674-8; discussion 1679.
- Akmal, M., Kesani, A., Anand, B., Singh, A., Wiseman, M. & Goodship, A. (2004) Effect of nicotine on spinal disc cells: a cellular mechanism for disc degeneration. *Spine*, 29, 568-75.
- Alexopoulos, L. G., Setton, L. A. & Guilak, F. (2005) The biomechanical role of the chondrocyte pericellular matrix in articular cartilage. *Acta Biomater*, 1, 317-25.
- Alini, M., Eisenstein, S. M., Ito, K., Little, C., Kettler, A. A., Masuda, K., Melrose, J., Ralphs, J., Stokes, I. & Wilke, H. J. (2007) Are animal models useful for studying human disc disorders/degeneration? *Eur Spine J*.
- Allen, M. J., Schoonmaker, J. E., Bauer, T. W., Williams, P. F., Higham, P. A. & Yuan, H. A. (2004) Preclinical evaluation of a poly (vinyl alcohol) hydrogel implant as a replacement for the nucleus pulposus. *Spine*, 29, 515-23.
- An, H. S., Takegami, K., Kamada, H., Nguyen, C. M., Thonar, E. J., Singh, K., Andersson, G. B. & Masuda, K. (2005) Intradiscal administration of osteogenic protein-1 increases intervertebral disc height and proteoglycan content in the nucleus pulposus in normal adolescent rabbits. *Spine*, 30, 25-31; discussion 31-2.
- Anderson, D. G., Li, X. & Balian, G. (2005) A fibronectin fragment alters the metabolism by rabbit intervertebral disc cells in vitro. *Spine*, 30, 1242-6.
- Andersson, G. B. (1998) What are the age-related changes in the spine? *Baillieres Clin Rheumatol*, 12, 161-73.

- Aoki, Y., Akeda, K., An, H., Muehleman, C., Takahashi, K., Moriya, H. & Masuda, K. (2006) Nerve fiber ingrowth into scar tissue formed following nucleus pulposus extrusion in the rabbit anular-puncture disc degeneration model: effects of depth of puncture. *Spine*, 31, E774-80.
- Aota, Y., An, H. S., Imai, Y., Thonar, E. J., Muehleman, C. & Masuda, K. (2006) Comparison of cellular response in bovine intervertebral disc cells and articular chondrocytes: effects of lipopolysaccharide on proteoglycan metabolism. *Cell Tissue Res*, 326, 787-93.
- Ariga, K., Yonenobu, K., Nakase, T., Hosono, N., Okuda, S., Meng, W., Tamura, Y. & Yoshikawa, H. (2003) Mechanical stress-induced apoptosis of endplate chondrocytes in organ-cultured mouse intervertebral discs: an ex vivo study. *Spine*, 28, 1528-33.
- Ashton, I. K. & Eisenstein, S. M. (1996) The effect of substance P on proliferation and proteoglycan deposition of cells derived from rabbit intervertebral disc. *Spine*, 21, 421-6.
- Aszodi, A., Chan, D., Hunziker, E., Bateman, J. F. & Fassler, R. (1998) Collagen II is essential for the removal of the notochord and the formation of intervertebral discs. *J Cell Biol*, 143, 1399-412.
- Aulisa, L., Papaleo, P., Pola, E., Angelini, F., Aulisa, A. G., Tamburrelli, F. C., Pola, P. & Logroscino, C. A. (2007) Association between IL-6 and MMP-3 gene polymorphisms and adolescent idiopathic scoliosis: a case-control study. *Spine*, 32, 2700-2.
- Ayotte, D. C., Ito, K. & Tepic, S. (2001) Direction-dependent resistance to flow in the endplate of the intervertebral disc: an ex vivo study. *J Orthop Res*, 19, 1073-7.
- Baer, A. E., Laursen, T. A., Guilak, F. & Setton, L. A. (2003) The micromechanical environment of intervertebral disc cells determined by a finite deformation, anisotropic, and biphasic finite element model. *J Biomech Eng*, 125, 1-11.
- Baer, A. E., Wang, J. Y., Kraus, V. B. & Setton, L. A. (2001) Collagen gene expression and mechanical properties of intervertebral disc cell-alginate cultures. *J Orthop Res*, 19, 2-10.
- Barrero, L. H., Hsu, Y. H., Terwedow, H., Perry, M. J., Dennerlein, J. T., Brain, J. D. & Xu, X. (2006) Prevalence and physical determinants of low back pain in a rural Chinese population. *Spine*, 31, 2728-34.

- Bass, E. C., Nau, W. H., Diederich, C. J., Liebenberg, E., Shu, R., Pellegrino, R., Sutton, J., Attawia, M., Hu, S. S., Ferrier, W. T. & Lotz, J. C. (2006) Intradiscal thermal therapy does not stimulate biologic remodeling in an in vivo sheep model. *Spine*, 31, 139-45.
- Battie, M. C. & Videman, T. (2006) Lumbar disc degeneration: epidemiology and genetics. *J Bone Joint Surg Am*, 88 Suppl 2, 3-9.
- Battie, M. C., Videman, T., Gibbons, L. E., Fisher, L. D., Manninen, H. & Gill, K. (1995) 1995 Volvo Award in clinical sciences. Determinants of lumbar disc degeneration. A study relating lifetime exposures and magnetic resonance imaging findings in identical twins. *Spine*, 20, 2601-12.
- Bayliss, M. T., Johnstone, B. & O'Brien, J. P. (1988) 1988 Volvo award in basic science. Proteoglycan synthesis in the human intervertebral disc. Variation with age, region and pathology. *Spine*, 13, 972-81.
- Benjamin, M. & Ralphs, J. R. (2004) Biology of fibrocartilage cells. *Int Rev Cytol*, 233, 1-45.
- Bensaid, A.M., Hall, L.O., Bezdek, J.C., Clarke, L.P., Silbiger, M.L., Arrington, J.A., Murtaugh, R.F. (1996) Validity-guided (Re)Clustering with applications to image segmentation. *IEEE Transactions on Fuzzy Systems*, 4:112-123
- Bezdek, J.C. (1981) *Pattern Recognition with Fuzzy Objective Function Algorithms*. Plenum Press
- Bibby, S. R., Fairbank, J. C., Urban, M. R. & Urban, J. P. (2002) Cell viability in scoliotic discs in relation to disc deformity and nutrient levels. *Spine*, 27, 2220-8; discussion 2227-8.
- Bibby, S. R. & Urban, J. P. (2004) Effect of nutrient deprivation on the viability of intervertebral disc cells. *Eur Spine J*.
- Bio, F., Sadhra, S., Jackson, C. & Burge, P. (2007) Low back pain in underground gold miners in Ghana. *Ghana Med J*, 41, 21-5.
- Bradford, D. S., Oegema, T. R., Jr., Cooper, K. M., Wakano, K. & Chao, E. Y. (1984) Chymopapain, chemonucleolysis, and nucleus pulposus regeneration. A biochemical and biomechanical study. *Spine*, 9, 135-47.
- Buckwalter, J. A., Kuettner, K. E. & Thonar, E. J. (1985) Age-related changes in articular cartilage proteoglycans: electron microscopic studies. *J Orthop Res*, 3, 251-7.

- Buckwalter, J. A., Roughley, P. J. & Rosenberg, L. C. (1994) Age-related changes in cartilage proteoglycans: quantitative electron microscopic studies. *Microsc Res Tech*, 28, 398-408.
- Cappello, R., Bird, J. L., Pfeiffer, D., Bayliss, M. T. & Dudhia, J. (2006) Notochordal cell produce and assemble extracellular matrix in a distinct manner, which may be responsible for the maintenance of healthy nucleus pulposus. *Spine*, 31, 873-82; discussion 883.
- Cassidy, J. D. (1998) Saskatchewan health and back pain survey. *Spine*, 23, 1923.
- Cassidy, J. J., Hiltner, A. & Baer, E. (1989) Hierarchical structure of the intervertebral disc. *Connect Tissue Res*, 23, 75-88.
- Chen, J., Yan, W. & Setton, L. A. (2004) Static compression induces zonal-specific changes in gene expression for extracellular matrix and cytoskeletal proteins in intervertebral disc cells in vitro. *Matrix Biol*, 22, 573-83.
- Chiba, K., Andersson, G. B., Masuda, K., Momohara, S., Williams, J. M. & Thonar, E. J. (1998) A new culture system to study the metabolism of the intervertebral disc in vitro. *Spine*, 23, 1821-7; discussion 1828.
- Chiba, K., Masuda, K., Andersson, G. B., Momohara, S. & Thonar, E. J. (2006) Matrix replenishment by intervertebral disc cells after chemonucleolysis in vitro with chondroitinase ABC and chymopapain. *Spine J*.
- Ching, C. T., Chow, D. H., Yao, F. Y. & Holmes, A. D. (2003) The effect of cyclic compression on the mechanical properties of the inter-vertebral disc: an in vivo study in a rat tail model. *Clin Biomech (Bristol, Avon)*, 18, 182-9.
- Ching, C. T., Chow, D. H., Yao, F. Y. & Holmes, A. D. (2004) Changes in nuclear composition following cyclic compression of the intervertebral disc in an in vivo rat-tail model. *Med Eng Phys*, 26, 587-94.
- Chujo, T., An, H. S., Akeda, K., Miyamoto, K., Muehleman, C., Attawia, M., Andersson, G. & Masuda, K. (2006) Effects of growth differentiation factor-5 on the intervertebral disc--in vitro bovine study and in vivo rabbit disc degeneration model study. *Spine*, 31, 2909-17.
- Cinotti, G., Della Rocca, C., Romeo, S., Vittur, F., Toffanin, R. & Trasimeni, G. (2005) Degenerative changes of porcine intervertebral disc induced by vertebral endplate injuries. *Spine*, 30, 174-80.

- Costi, J. J., Stokes, I. A., Gardner-Morse, M., Laible, J. P., Scoffone, H. M. & Iatridis, J. C. (2007) Direct measurement of intervertebral disc maximum shear strain in six degrees of freedom: Motions that place disc tissue at risk of injury. *J Biomech*, 40, 2457-66.
- Cote, P., Cassidy, J. D. & Carroll, L. (1998) The Saskatchewan Health and Back Pain Survey. The prevalence of neck pain and related disability in Saskatchewan adults. *Spine*, 23, 1689-98.
- Court, C., Colliou, O. K., Chin, J. R., Liebenberg, E., Bradford, D. S. & Lotz, J. C. (2001) The effect of static in vivo bending on the murine intervertebral disc. *Spine J*, 1, 239-45.
- Cunningham, B. W., Lowery, G. L., Serhan, H. A., Dmitriev, A. E., Orbegoso, C. M., McAfee, P. C., Fraser, R. D., Ross, R. E. & Kulkarni, S. S. (2002) Total disc replacement arthroplasty using the AcroFlex lumbar disc: a non-human primate model. *Eur Spine J*, 11 Suppl 2, S115-23.
- D'haeseleer, P. (2005) How does gene expression clustering work? *Nat Biotechnol*, 23, 1499-501.
- Dave, R. (1996) Validating fuzzy partitions obtained through c-shells clustering. *PATTERN RECOGNITION LETTERS*, 17, 613-623.
- Demers, C. N., Antoniou, J. & Mwale, F. (2004) Value and limitations of using the bovine tail as a model for the human lumbar spine. *Spine*, 29, 2793-9.
- Dipaola, C. P., Farmer, J. C., Manova, K. & Niswander, L. A. (2005) Molecular signaling in intervertebral disk development. *J Orthop Res*, 23, 1112-9.
- Drerup, B., Granitzka, M., Assheuer, J. & Zerlett, G. (1999) Assessment of disc injury in subjects exposed to long-term whole-body vibration. *Eur Spine J*, 8, 458-67.
- Duda, G. N., Eilers, M., Loh, L., Hoffman, J. E., Kaab, M. & Schaser, K. (2001) Chondrocyte death precedes structural damage in blunt impact trauma. *Clin Orthop*, 302-9.
- Dudhia, J., Scott, C. M., Draper, E. R., Heinegard, D., Pitsillides, A. A. & Smith, R. K. (2007) Aging enhances a mechanically-induced reduction in tendon strength by an active process involving matrix metalloproteinase activity. *Aging Cell*, 6, 547-56.
- Dupuis, H. (1994) Medical and occupational preconditions for vibration-induced spinal disorders: occupational disease no. 2110 in Germany. *Int Arch Occup Environ Health*, 66, 303-8.

- Ejeskar, A. & Holm, S. (1979) Oxygen tension measurements in the intervertebral disc. A methodological and experimental study. *Ups J Med Sci*, 84, 83-93.
- Ekstrom, L., Holm, S., Holm, A. K. & Hansson, T. (2004) In vivo porcine intradiscal pressure as a function of external loading. *J Spinal Disord Tech*, 17, 312-6.
- Ekstrom, L., Kaigle, A., Hult, E., Holm, S., Rostedt, M. & Hansson, T. (1996) Intervertebral disc response to cyclic loading--an animal model. *Proc Inst Mech Eng [H]*, 210, 249-58.
- Erwin, W. M., Ashman, K., O'donnell, P. & Inman, R. D. (2006) Nucleus pulposus notochord cells secrete connective tissue growth factor and up-regulate proteoglycan expression by intervertebral disc chondrocytes. *Arthritis Rheum*, 54, 3859-67.
- Erwin, W. M. & Inman, R. D. (2006) Notochord cells regulate intervertebral disc chondrocyte proteoglycan production and cell proliferation. *Spine*, 31, 1094-9.
- Evans, W., Jobe, W. & Seibert, C. (1989) A cross-sectional prevalence study of lumbar disc degeneration in a working population. *Spine*, 14, 60-4.
- Eyre, D. R., Matsui, Y. & Wu, J. J. (2002) Collagen polymorphisms of the intervertebral disc. *Biochem Soc Trans*, 30, 844-8.
- Farfan, H. F., Cossette, J. W., Robertson, G. H., Wells, R. V. & Kraus, H. (1970) The effects of torsion on the lumbar intervertebral joints: the role of torsion in the production of disc degeneration. *J Bone Joint Surg Am*, 52, 468-97.
- Fitzgerald, J. B., Jin, M., Dean, D., Wood, D. J., Zheng, M. H. & Grodzinsky, A. J. (2004) Mechanical compression of cartilage explants induces multiple time-dependent gene expression patterns and involves intracellular calcium and cyclic AMP. *J Biol Chem*, 279, 19502-11.
- Fitzgerald, J. B., Jin, M. & Grodzinsky, A. J. (2006) Shear and compression differentially regulate clusters of functionally related temporal transcription patterns in cartilage tissue. *J Biol Chem*, 281, 24095-103.
- Forslund, C., Persson, J., Stromqvist, B., Lidgren, L. & McCarthy, I. D. (2006) Effects of high-intensity focused ultrasound on the intervertebral disc: a potential therapy for disc herniations. *J Clin Ultrasound*, 34, 330-8.



- Friedrich, M., Cermak, T. & Heiller, I. (2000) Spinal troubles in sewage workers: epidemiological data and work disability due to low back pain. *Int Arch Occup Environ Health*, 73, 245-54.
- Frymoyer, J. W., Pope, M. H., Clements, J. H., Wilder, D. G., Macpherson, B. & Ashikaga, T. (1983) Risk factors in low-back pain. An epidemiological survey. *J Bone Joint Surg Am*, 65, 213-8.
- Gan, J. C., Ducheyne, P., Vresilovic, E. & Shapiro, I. M. (2000) Bioactive glass serves as a substrate for maintenance of phenotype of nucleus pulposus cells of the intervertebral disc. *J Biomed Mater Res*, 51, 596-604.
- Gan, J. C., Ducheyne, P., Vresilovic, E. J. & Shapiro, I. M. (2003) Intervertebral disc tissue engineering II: cultures of nucleus pulposus cells. *Clin Orthop Relat Res*, 315-24.
- Gan, J. C., Ducheyne, P., Vresilovic, E. J., Swaim, W. & Shapiro, I. M. (2003) Intervertebral disc tissue engineering I: characterization of the nucleus pulposus. *Clin Orthop Relat Res*, 305-14.
- Gantenbein, B., Grunhagen, T., Lee, C. R., Van Donkelaar, C. C., Alini, M. & Ito, K. (2006) An in vitro organ culturing system for intervertebral disc explants with vertebral endplates: a feasibility study with ovine caudal discs. *Spine*, 31, 2665-73.
- Ghaffari, M., Alipour, A., Jensen, I., Farshad, A. A. & Vingard, E. (2006) Low back pain among Iranian industrial workers. *Occup Med (Lond)*, 56, 455-60.
- Gibbons, L. E., Battie, M. C. & Videman, T. (1995) Changes in occupational physical loading during the lifetimes of Finnish men. *Scand J Work Environ Health*, 21, 208-14.
- Gorensek, M., Jaksimovic, C., Kregar-Velikonja, N., Gorensek, M., Knezevic, M., Jeras, M., Pavlovic, V. & Cor, A. (2004) Nucleus pulposus repair with cultured autologous elastic cartilage derived chondrocytes. *Cell Mol Biol Lett*, 9, 363-73.
- Gourmelen, J., Chastang, J. F., Ozguler, A., Lanoe, J. L., Ravaud, J. F. & Leclerc, A. (2007) Frequency of low back pain among men and women aged 30 to 64 years in France. Results of two national surveys. *Ann Readapt Med Phys*.
- Grogan, S. P., Aklin, B., Frenz, M., Brunner, T., Schaffner, T. & Mainil-Varlet, P. (2002) In vitro model for the study of necrosis and apoptosis in native cartilage. *J Pathol*, 198, 5-13.

- Gruber, H. E. & Hanley, E. N., Jr. (2003) Biologic strategies for the therapy of intervertebral disc degeneration. *Expert Opin Biol Ther*, 3, 1209-14.
- Gruber, H. E., Ingram, J. A. & Hanley, E. N., Jr. (2007) Morphologic complexity of the pericellular matrix in the annulus of the human intervertebral disc. *Biotech Histochem*, 82, 217-25.
- Gruber, H. E., Ingram, J. A., Norton, H. J. & Hanley, E. N., Jr. (2007) Senescence in cells of the aging and degenerating intervertebral disc: immunolocalization of senescence-associated beta-galactosidase in human and sand rat discs. *Spine*, 32, 321-7.
- Gruber, H. E., Leslie, K., Ingram, J., Hoelscher, G., Norton, H. J. & Hanley, E. N., Jr. (2004) Colony formation and matrix production by human anulus cells: modulation in three-dimensional culture. *Spine*, 29, E267-74.
- Gruber, H. E., Norton, H. J. & Hanley, E. N., Jr. (2000) Anti-apoptotic effects of IGF-1 and PDGF on human intervertebral disc cells in vitro. *Spine*, 25, 2153-7.
- Gruber, H. E., Stasky, A. A. & Hanley, E. N., Jr. (1997) Characterization and phenotypic stability of human disc cells in vitro. *Matrix Biol*, 16, 285-8.
- Guehring, T., Omlor, G. W., Lorenz, H., Bertram, H., Steck, E., Richter, W., Carstens, C. & Kroeber, M. (2005) Stimulation of gene expression and loss of anular architecture caused by experimental disc degeneration--an in vivo animal study. *Spine*, 30, 2510-5.
- Hadjipavlou, A. G., Simmons, J. W., Yang, J. P., Bi, L. X., Ansari, G. A., Kaphalia, B. S., Simmons, D. J., Nicodemus, C. L., Necessary, J. T., Lane, R. & Esch, O. (1998) Torsional injury resulting in disc degeneration: I. An in vivo rabbit model. *J Spinal Disord*, 11, 312-7.
- Hadjipavlou, A. G., Simmons, J. W., Yang, J. P., Bi, L. X., Simmons, D. J. & Necessary, J. T. (1998) Torsional injury resulting in disc degeneration in the rabbit: II. Associative changes in dorsal root ganglion and spinal cord neurotransmitter production. *J Spinal Disord*, 11, 318-21.
- Hamilton, D. J., Seguin, C. A., Wang, J., Pilliar, R. M. & Kandel, R. A. (2006) Formation of a nucleus pulposus-cartilage endplate construct in vitro. *Biomaterials*, 27, 397-405.
- Han, S. M., Lee, S. Y., Cho, M. H. & Lee, J. K. (2001) Disc hydration measured by magnetic resonance imaging in relation to its compressive stiffness in rat models. *Proc Inst Mech Eng [H]*, 215, 497-501.

- Handa, T., Ishihara, H., Ohshima, H., Osada, R., Tsuji, H. & Obata, K. (1997) Effects of hydrostatic pressure on matrix synthesis and matrix metalloproteinase production in the human lumbar intervertebral disc. *Spine*, 22, 1085-91.
- Haro, H., Kato, T., Komori, H., Osada, M. & Shinomiya, K. (2002) Vascular endothelial growth factor (VEGF)-induced angiogenesis in herniated disc resorption. *J Orthop Res*, 20, 409-15.
- Haro, H., Komori, H., Kato, T., Hara, Y., Tagawa, M., Shinomiya, K. & Spengler, D. M. (2005) Experimental studies on the effects of recombinant human matrix metalloproteinases on herniated disc tissues--how to facilitate the natural resorption process of herniated discs. *J Orthop Res*, 23, 412-9.
- Haschtmann, D., Stoyanov, J. V., Ettinger, L., Nolte, L. P. & Ferguson, S. J. (2006) Establishment of a novel intervertebral disc/endplate culture model: analysis of an ex vivo in vitro whole-organ rabbit culture system. *Spine*, 31, 2918-25.
- Haschtmann, D., Stoyanov, J. V. & Ferguson, S. J. (2006) Influence of diurnal hyperosmotic loading on the metabolism and matrix gene expression of a whole-organ intervertebral disc model. *J Orthop Res*, 24, 1957-66.
- Hashizume, H., Kawakami, M., Yoshida, M., Okada, M., Enyo, Y. & Inomata, Y. (2007) Sarpogrelate hydrochloride, a 5-HT<sub>2A</sub> receptor antagonist, attenuates neurogenic pain induced by nucleus pulposus in rats. *Spine*, 32, 315-20.
- Hayes, A. J., Benjamin, M. & Ralphs, J. R. (2001) Extracellular matrix in development of the intervertebral disc. *Matrix Biol*, 20, 107-21.
- Horner, H. A., Roberts, S., Bielby, R. C., Menage, J., Evans, H. & Urban, J. P. (2002) Cells from different regions of the intervertebral disc: effect of culture system on matrix expression and cell phenotype. *Spine*, 27, 1018-28.
- Hsieh, A. H. & Lotz, J. C. (2003) Prolonged spinal loading induces matrix metalloproteinase-2 activation in intervertebral discs. *Spine*, 28, 1781-8.
- Hu, N., Cunningham, B. W., McAfee, P. C., Kim, S. W., Seftor, J. C., Cappuccino, A. & Pimenta, L. (2006) Porous coated motion cervical disc replacement: a biomechanical, histomorphometric, and biologic wear analysis in a caprine model. *Spine*, 31, 1666-73.
- Huang, K. Y., Yan, J. J., Hsieh, C. C., Chang, M. S. & Lin, R. M. (2007) The in vivo biological effects of intradiscal recombinant human bone morphogenetic protein-2 on the injured intervertebral disc: an animal experiment. *Spine*, 32, 1174-80.

- Hunter, C. J., Matyas, J. R. & Duncan, N. A. (2003) The three-dimensional architecture of the notochordal nucleus pulposus: novel observations on cell structures in the canine intervertebral disc. *J Anat*, 202, 279-91.
- Hunter, C. J., Matyas, J. R. & Duncan, N. A. (2004) Cytomorphology of notochordal and chondrocytic cells from the nucleus pulposus: a species comparison. *J Anat*, 205, 357-62.
- Hutton, W. C., Ganey, T. M., Elmer, W. A., Kozlowska, E., Ugbo, J. L., Doh, E. S. & Whitesides, T. E., Jr. (2000) Does long-term compressive loading on the intervertebral disc cause degeneration? *Spine*, 25, 2993-3004.
- Hutton, W. C., Toribatake, Y., Elmer, W. A., Ganey, T. M., Tomita, K. & Whitesides, T. E. (1998) The effect of compressive force applied to the intervertebral disc in vivo. A study of proteoglycans and collagen. *Spine*, 23, 2524-37.
- Hutton, W. C., Yoon, S. T., Elmer, W. A., Li, J., Murakami, H., Minamide, A. & Akamaru, T. (2002) Effect of tail suspension (or simulated weightlessness) on the lumbar intervertebral disc: study of proteoglycans and collagen. *Spine*, 27, 1286-90.
- Iatridis, J. C. & Ap Gwynn, I. (2004) Mechanisms for mechanical damage in the intervertebral disc annulus fibrosus. *J Biomech*, 37, 1165-75.
- Iatridis, J. C., Mente, P. L., Stokes, I. A., Aronsson, D. D. & Alini, M. (1999) Compression-induced changes in intervertebral disc properties in a rat tail model. *Spine*, 24, 996-1002.
- Ichimura, K., Tsuji, H., Matsui, H. & Makiyama, N. (1991) Cell culture of the intervertebral disc of rats: factors influencing culture, proteoglycan, collagen, and deoxyribonucleic acid synthesis. *J Spinal Disord*, 4, 428-36.
- Igarashi, T., Kikuchi, S., Shubayev, V. & Myers, R. R. (2000) 2000 Volvo Award winner in basic science studies: Exogenous tumor necrosis factor-alpha mimics nucleus pulposus-induced neuropathology. Molecular, histologic, and behavioral comparisons in rats. *Spine*, 25, 2975-80.
- Imai, Y., Miyamoto, K., An, H. S., Thonar, E. J., Andersson, G. B. & Masuda, K. (2007) Recombinant human osteogenic protein-1 upregulates proteoglycan metabolism of human annulus fibrosus and nucleus pulposus cells. *Spine*, 32, 1303-9; discussion 1310.

- Imai, Y., Okuma, M., An, H. S., Nakagawa, K., Yamada, M., Muehleman, C., Thonar, E. & Masuda, K. (2007) Restoration of disc height loss by recombinant human osteogenic protein-1 injection into intervertebral discs undergoing degeneration induced by an intradiscal injection of chondroitinase ABC. *Spine*, 32, 1197-205.
- Ishihara, H., McNally, D. S., Urban, J. P. & Hall, A. C. (1996) Effects of hydrostatic pressure on matrix synthesis in different regions of the intervertebral disk. *J Appl Physiol*, 80, 839-46.
- Ishihara, H., Warensjo, K., Roberts, S. & Urban, J. P. (1997) Proteoglycan synthesis in the intervertebral disk nucleus: the role of extracellular osmolality. *Am J Physiol*, 272, C1499-506.
- Ivaska, J., Pallari, H. M., Nevo, J. & Eriksson, J. E. (2007) Novel functions of vimentin in cell adhesion, migration, and signaling. *Exp Cell Res*, 313, 2050-62.
- Iwashina, T., Mochida, J., Miyazaki, T., Watanabe, T., Iwabuchi, S., Ando, K., Hotta, T. & Sakai, D. (2006) Low-intensity pulsed ultrasound stimulates cell proliferation and proteoglycan production in rabbit intervertebral disc cells cultured in alginate. *Biomaterials*, 27, 354-61.
- Iwatsuki, K., Yoshimine, T., Sasaki, M., Yasuda, K., Akiyama, C. & Nakahira, R. (2005) The effect of laser irradiation for nucleus pulposus: an experimental study. *Neurol Res*, 27, 319-23.
- Jacoby, A. S., Melrose, J., Robinson, B. G., Hyland, V. J. & Ghosh, P. (1993) Secretory leucocyte proteinase inhibitor is produced by human articular cartilage chondrocytes and intervertebral disc fibrochondrocytes. *Eur J Biochem*, 218, 951-7.
- Jeffrey, J. E., Gregory, D. W. & Aspden, R. M. (1995) Matrix damage and chondrocyte viability following a single impact load on articular cartilage. *Arch Biochem Biophys*, 322, 87-96.
- Jimbo, K., Park, J. S., Yokosuka, K., Sato, K. & Nagata, K. (2005) Positive feedback loop of interleukin-1beta upregulating production of inflammatory mediators in human intervertebral disc cells in vitro. *J Neurosurg Spine*, 2, 589-95.
- Johannessen, W., Vresilovic, E. J., Wright, A. C. & Elliott, D. M. (2004) Intervertebral disc mechanics are restored following cyclic loading and unloaded recovery. *Ann Biomed Eng*, 32, 70-6.
- Johnson, W. E., Wootton, A., El Haj, A., Eisenstein, S. M., Curtis, A. S. & Roberts, S. (2006) Topographical guidance of intervertebral disc cell growth in vitro: towards

the development of tissue repair strategies for the annulus fibrosus. *Eur Spine J*, 15 Suppl 3, S389-96.

- Kadoya, K., Kotani, Y., Abumi, K., Takada, T., Shimamoto, N., Shikinami, Y., Kadosawa, T. & Kaneda, K. (2001) Biomechanical and morphologic evaluation of a three-dimensional fabric sheep artificial intervertebral disc: in vitro and in vivo analysis. *Spine*, 26, 1562-9.
- Kaigle, A., Ekstrom, L., Holm, S., Rostedt, M. & Hansson, T. (1998) In vivo dynamic stiffness of the porcine lumbar spine exposed to cyclic loading: influence of load and degeneration. *J Spinal Disord*, 11, 65-70.
- Kaigle, A. M., Holm, S. H. & Hansson, T. H. (1995) Experimental instability in the lumbar spine. *Spine*, 20, 421-30.
- Kaigle, A. M., Holm, S. H. & Hansson, T. H. (1997) 1997 Volvo Award winner in biomechanical studies. Kinematic behavior of the porcine lumbar spine: a chronic lesion model. *Spine*, 22, 2796-806.
- Kairemo, K. J., Lappalainen, A. K., Kaapa, E., Laitinen, O. M., Hyytinen, T., Karonen, S. L. & Gronblad, M. (2001) In vivo detection of intervertebral disk injury using a radiolabeled monoclonal antibody against keratan sulfate. *J Nucl Med*, 42, 476-82.
- Kang, J. D., Georgescu, H. I., McIntyre-Larkin, L., Stefanovic-Racic, M., Donaldson, W. F., 3rd & Evans, C. H. (1996) Herniated lumbar intervertebral discs spontaneously produce matrix metalloproteinases, nitric oxide, interleukin-6, and prostaglandin E2. *Spine*, 21, 271-7.
- Karppinen, J., Inkinen, R. I., Kaapa, E., Lammi, M. J., Tammi, M. I., Holm, S. & Vanharanta, H. (1995) Effects of tiaprofenic acid and indomethacin on proteoglycans in the degenerating porcine intervertebral disc. *Spine*, 20, 1170-7.
- Kasra, M., Goel, V., Martin, J., Wang, S. T., Choi, W. & Buckwalter, J. (2003) Effect of dynamic hydrostatic pressure on rabbit intervertebral disc cells. *J Orthop Res*, 21, 597-603.
- Kasra, M., Merryman, W. D., Loveless, K. N., Goel, V. K., Martin, J. D. & Buckwalter, J. A. (2006) Frequency response of pig intervertebral disc cells subjected to dynamic hydrostatic pressure. *J Orthop Res*, 24, 1967-73.
- Kato, T., Haro, H., Komori, H. & Shinomiya, K. (2004) Sequential dynamics of inflammatory cytokine, angiogenesis inducing factor and matrix degrading

- enzymes during spontaneous resorption of the herniated disc. *J Orthop Res*, 22, 895-900.
- Keller, T. S., Hansson, T. H., Holm, S. H., Pope, M. M. & Spengler, D. M. (1988) In vivo creep behavior of the normal and degenerated porcine intervertebral disk: a preliminary report. *J Spinal Disord*, 1, 267-78.
- Kim, K. S., Yoon, S. T., Park, J. S., Li, J., Park, M. S. & Hutton, W. C. (2003) Inhibition of proteoglycan and type II collagen synthesis of disc nucleus cells by nicotine. *J Neurosurg*, 99, 291-7.
- Kim, K. W., Ha, K. Y., Park, J. B., Woo, Y. K., Chung, H. N. & An, H. S. (2005) Expressions of membrane-type I matrix metalloproteinase, Ki-67 protein, and type II collagen by chondrocytes migrating from cartilage endplate into nucleus pulposus in rat intervertebral discs: a cartilage endplate-fracture model using an intervertebral disc organ culture. *Spine*, 30, 1373-8.
- Kim, P. M. & Tidor, B. (2003) Subsystem identification through dimensionality reduction of large-scale gene expression data. *Genome Res*, 13, 1706-18.
- Kluba, T., Niemeyer, T., Gaissmaier, C. & Grunder, T. (2005) Human annulus fibrosis and nucleus pulposus cells of the intervertebral disc: effect of degeneration and culture system on cell phenotype. *Spine*, 30, 2743-8.
- Korecki, C. L., Maclean, J. J. & Iatridis, J. C. (2007) Characterization of an in vitro intervertebral disc organ culture system. *Eur Spine J*, 16, 1029-37.
- Krijnen, M. R., Valstar, E. R., Smit, T. H. & Wuisman, P. I. (2006) Does bioresorbable cage material influence segment stability in spinal interbody fusion? *Clin Orthop Relat Res*, 448, 33-8.
- Kroeber, M., Unglaub, F., Guehring, T., Nerlich, A., Hadi, T., Lotz, J. & Carstens, C. (2005) Effects of controlled dynamic disc distraction on degenerated intervertebral discs: an in vivo study on the rabbit lumbar spine model. *Spine*, 30, 181-7.
- Kroeber, M. W., Unglaub, F., Wang, H., Schmid, C., Thomsen, M., Nerlich, A. & Richter, W. (2002) New in vivo animal model to create intervertebral disc degeneration and to investigate the effects of therapeutic strategies to stimulate disc regeneration. *Spine*, 27, 2684-90.
- Kroemer, G., Dallaporta, B. & Resche-Rigon, M. (1998) The mitochondrial death/life regulator in apoptosis and necrosis. *Annu Rev Physiol*, 60, 619-42.

- Kuo, C. K. & Ma, P. X. (2001) Ionically crosslinked alginate hydrogels as scaffolds for tissue engineering: part 1. Structure, gelation rate and mechanical properties. *Biomaterials*, 22, 511-21.
- Kurz, B., Jin, M., Patwari, P., Cheng, D. M., Lark, M. W. & Grodzinsky, A. J. (2001) Biosynthetic response and mechanical properties of articular cartilage after injurious compression. *J Orthop Res*, 19, 1140-6.
- Lauerman, W. C., Platenberg, R. C., Cain, J. E. & Deeney, V. F. (1992) Age-related disk degeneration: preliminary report of a naturally occurring baboon model. *J Spinal Disord*, 5, 170-4.
- Le Maitre, C. L., Freemont, A. J. & Hoyland, J. A. (2004) Localization of degradative enzymes and their inhibitors in the degenerate human intervertebral disc. *J Pathol*, 204, 47-54.
- Le Maitre, C. L., Hoyland, J. A. & Freemont, A. J. (2004) Studies of human intervertebral disc cell function in a constrained in vitro tissue culture system. *Spine*, 29, 1187-95.
- Ledet, E. H., Carl, A. L., Dirisio, D. J., Tymeson, M. P., Andersen, L. B., Sheehan, C. E., Kallakury, B., Slivka, M. & Serhan, H. (2002) A pilot study to evaluate the effectiveness of small intestinal submucosa used to repair spinal ligaments in the goat. *Spine J*, 2, 188-96.
- Ledet, E. H., Sachs, B. L., Brunski, J. B., Gatto, C. E. & Donzelli, P. S. (2000) Real-time in vivo loading in the lumbar spine: part 1. Interbody implant: load cell design and preliminary results. *Spine*, 25, 2595-600.
- Lee, C. R., Grad, S., Maclean, J. J., Iatridis, J. C. & Alini, M. (2005) Effect of mechanical loading on mRNA levels of common endogenous controls in articular chondrocytes and intervertebral disk. *Anal Biochem*, 341, 372-5.
- Lee, C. R., Iatridis, J. C., Poveda, L. & Alini, M. (2006) In vitro organ culture of the bovine intervertebral disc: effects of vertebral endplate and potential for mechanobiology studies. *Spine*, 31, 515-22.
- Lee, D. D. & Seung, H. S. (1999) Learning the parts of objects by non-negative matrix factorization. *Nature*, 401, 788-91.
- Lee, J. Y., Hall, R., Pelinkovic, D., Cassinelli, E., Usas, A., Gilbertson, L., Huard, J. & Kang, J. (2001) New use of a three-dimensional pellet culture system for human intervertebral disc cells: initial characterization and potential use for tissue engineering. *Spine*, 26, 2316-22.



- Lei, D., Holder, R. L., Smith, F. W., Wardlaw, D. & Hukins, D. W. (2006) Cluster analysis as a method for determining size ranges for spinal implants: disc lumbar replacement prosthesis dimensions from magnetic resonance images. *Spine*, 31, 2979-83; discussion 2984.
- Leivseth, G., Salvesen, R., Hemminghytt, S., Brinckmann, P. & Frobin, W. (1999) Do human lumbar discs reconstitute after chemonucleolysis? A 7-year follow-up study. *Spine*, 24, 342-7; discussion 348.
- Leo, B. M., Li, X., Balian, G. & Anderson, D. G. (2004) In vivo bioluminescent imaging of virus-mediated gene transfer and transduced cell transplantation in the intervertebral disc. *Spine*, 29, 838-44.
- Lettice, L. A., Purdie, L. A., Carlson, G. J., Kilanowski, F., Dorin, J. & Hill, R. E. (1999) The mouse bagpipe gene controls development of axial skeleton, skull, and spleen. *Proc Natl Acad Sci U S A*, 96, 9695-700.
- Li, H., Laursen, M., Lind, M., Sun, C. & Bunger, C. (2000) The influence of human intervertebral disc tissue on the metabolism of osteoblast-like cells. *Acta Orthop Scand*, 71, 503-7.
- Lim, T. H., Ramakrishnan, P. S., Kurriger, G. L., Martin, J. A., Stevens, J. W., Kim, J. & Mendoza, S. A. (2006) Rat spinal motion segment in organ culture: a cell viability study. *Spine*, 31, 1291-7; discussion 1298.
- Liu, J., Roughley, P. J. & Mort, J. S. (1991) Identification of human intervertebral disc stromelysin and its involvement in matrix degradation. *J Orthop Res*, 9, 568-75.
- Lotz, J. C. & Chin, J. R. (2000) Intervertebral disc cell death is dependent on the magnitude and duration of spinal loading. *Spine*, 25, 1477-83.
- Lotz, J. C., Colliou, O. K., Chin, J. R., Duncan, N. A. & Liebenberg, E. (1998) Compression-induced degeneration of the intervertebral disc: an in vivo mouse model and finite-element study. *Spine*, 23, 2493-506.
- Lowe, T. G., Wilson, L., Chien, J. T., Line, B. G., Klopp, L., Wheeler, D. & Molz, F. (2005) A posterior tether for fusionless modulation of sagittal plane growth in a sheep model. *Spine*, 30, S69-74.
- Lu, D. S., Shono, Y., Oda, I., Abumi, K. & Kaneda, K. (1997) Effects of chondroitinase ABC and chymopapain on spinal motion segment biomechanics. An in vivo biomechanical, radiologic, and histologic canine study. *Spine*, 22, 1828-34; discussion 1834-5.

- Luk, K. D., Ruan, D. K., Lu, D. S. & Fei, Z. Q. (2003) Fresh frozen intervertebral disc allografting in a bipedal animal model. *Spine*, 28, 864-9; discussion 870.
- Luo, X., Pietrobon, R., Sun, S. X., Liu, G. G. & Hey, L. (2004) Estimates and patterns of direct health care expenditures among individuals with back pain in the United States. *Spine*, 29, 79-86.
- Maclean, J. J., Lee, C. R., Alini, M. & Iatridis, J. C. (2004) Anabolic and catabolic mRNA levels of the intervertebral disc vary with the magnitude and frequency of in vivo dynamic compression. *J Orthop Res*, 22, 1193-200.
- Maclean, J. J., Lee, C. R., Alini, M. & Iatridis, J. C. (2005) The effects of short-term load duration on anabolic and catabolic gene expression in the rat tail intervertebral disc. *J Orthop Res*, 23, 1120-7.
- Maclean, J. J., Lee, C. R., Grad, S., Ito, K., Alini, M. & Iatridis, J. C. (2003) Effects of immobilization and dynamic compression on intervertebral disc cell gene expression in vivo. *Spine*, 28, 973-81.
- Maclean, J. J., Owen, J. P. & Iatridis, J. C. (2007) Role of endplates in contributing to compression behaviors of motion segments and intervertebral discs. *J Biomech*, 40, 55-63.
- Madsen, B., Spencer-Dene, B., Poulson, R., Hall, D., Lu, P. J., Scott, K., Shaw, A. T., Burchell, J. M., Freemont, P. & Taylor-Papadimitriou, J. (2002) Characterisation and developmental expression of mouse Plu-1, a homologue of a human nuclear protein (PLU-1) which is specifically up-regulated in breast cancer. *Gene Expr Patterns*, 2, 275-82.
- Maldonado, B. A. & Oegema, T. R., Jr. (1992) Initial characterization of the metabolism of intervertebral disc cells encapsulated in microspheres. *J Orthop Res*, 10, 677-90.
- Maroudas, A., Stockwell, R. A., Nachemson, A. & Urban, J. (1975) Factors involved in the nutrition of the human lumbar intervertebral disc: cellularity and diffusion of glucose in vitro. *J Anat*, 120, 113-30.
- Martin, J. A. & Buckwalter, J. A. (2002) Aging, articular cartilage chondrocyte senescence and osteoarthritis. *Biogerontology*, 3, 257-64.
- Masuda, K. & An, H. S. (2006) Prevention of disc degeneration with growth factors. *Eur Spine J*, 15 Suppl 3, S422-32.

- Masuda, K., Aota, Y., Muehleman, C., Imai, Y., Okuma, M., Thonar, E. J., Andersson, G. B. & An, H. S. (2005) A novel rabbit model of mild, reproducible disc degeneration by an annulus needle puncture: correlation between the degree of disc injury and radiological and histological appearances of disc degeneration. *Spine*, 30, 5-14.
- Masuda, K., Miyabayashi, T., Meachum, S. H. & Eurell, T. E. (2002) Proliferation of canine intervertebral disk chondrocytes in three-dimensional alginate microsphere culture. *J Vet Med Sci*, 64, 79-82.
- Maynard, J. A. (1998) Effects of 2 weeks hypergravity on the composition of the intervertebral disc. *Aviat Space Environ Med*, 69, A23-7.
- Melrose, J., Ghosh, P. & Taylor, T. K. (1994) Proteoglycan heterogeneity in the normal adult ovine intervertebral disc. *Matrix Biol*, 14, 61-75.
- Melrose, J., Ghosh, P. & Taylor, T. K. (2001) A comparative analysis of the differential spatial and temporal distributions of the large (aggrecan, versican) and small (decorin, biglycan, fibromodulin) proteoglycans of the intervertebral disc. *J Anat*, 198, 3-15.
- Melrose, J., Smith, S. & Ghosh, P. (2000) Differential expression of proteoglycan epitopes by ovine intervertebral disc cells. *J Anat*, 197 (Pt 2), 189-98.
- Melrose, J., Smith, S. & Ghosh, P. (2003) Assessment of the cellular heterogeneity of the ovine intervertebral disc: comparison with synovial fibroblasts and articular chondrocytes. *Eur Spine J*, 12, 57-65.
- Melrose, J., Smith, S., Ghosh, P. & Taylor, T. K. (2001) Differential expression of proteoglycan epitopes and growth characteristics of intervertebral disc cells grown in alginate bead culture. *Cells Tissues Organs*, 168, 137-46.
- Melrose, J., Smith, S. M., Fuller, E. S., Young, A. A., Roughley, P. J., Dart, A. & Little, C. B. (2007) Biglycan and fibromodulin fragmentation correlates with temporal and spatial annular remodelling in experimentally injured ovine intervertebral discs. *Eur Spine J*, 16, 2193-205.
- Milentijevic, D., Helfet, D. L. & Torzilli, P. A. (2003) Influence of stress magnitude on water loss and chondrocyte viability in impacted articular cartilage. *J Biomech Eng*, 125, 594-601.

- Minamide, A., Hashizume, H., Yoshida, M., Kawakami, M., Hayashi, N. & Tamaki, T. (1999) Effects of basic fibroblast growth factor on spontaneous resorption of herniated intervertebral discs. An experimental study in the rabbit. *Spine*, 24, 940-5.
- Miyamoto, K., An, H. S., Sah, R. L., Akeda, K., Okuma, M., Otten, L., Thonar, E. J. & Masuda, K. (2005) Exposure to pulsed low intensity ultrasound stimulates extracellular matrix metabolism of bovine intervertebral disc cells cultured in alginate beads. *Spine*, 30, 2398-405.
- Miyamoto, K., Masuda, K., Kim, J. G., Inoue, N., Akeda, K., Andersson, G. B. & An, H. S. (2006) Intradiscal injections of osteogenic protein-1 restore the viscoelastic properties of degenerated intervertebral discs. *Spine J*, 6, 692-703.
- Morel, V. & Quinn, T. M. (2004) Cartilage injury by ramp compression near the gel diffusion rate. *J Orthop Res*, 22, 145-51.
- Moskowitz, R. W., Ziv, I., Denko, C. W., Boja, B., Jones, P. K. & Adler, J. H. (1990) Spondylosis in sand rats: a model of intervertebral disc degeneration and hyperostosis. *J Orthop Res*, 8, 401-11.
- Murakami, H., Yoon, S. T., Attallah-Wasif, E. S., Tsai, K. J., Fei, Q. & Hutton, W. C. (2006) The expression of anabolic cytokines in intervertebral discs in age-related degeneration. *Spine*, 31, 1770-4.
- Nagae, M., Ikeda, T., Mikami, Y., Hase, H., Ozawa, H., Matsuda, K., Sakamoto, H., Tabata, Y., Kawata, M. & Kubo, T. (2007) Intervertebral disc regeneration using platelet-rich plasma and biodegradable gelatin hydrogel microspheres. *Tissue Eng*, 13, 147-58.
- Nau, W. H., Diederich, C. J., Shu, R., Kinsey, A., Bass, E., Lotz, J., Hu, S., Simko, J., Ferrier, W., Sutton, J., Attawia, M. & Pellegrino, R. (2007) Intradiscal thermal therapy using interstitial ultrasound: an in vivo investigation in ovine cervical spine. *Spine*, 32, 503-11.
- Neidlinger-Wilke, C., Wurtz, K., Urban, J. P., Borm, W., Arand, M., Ignatius, A., Wilke, H. J. & Claes, L. E. (2006) Regulation of gene expression in intervertebral disc cells by low and high hydrostatic pressure. *Eur Spine J*, 15 Suppl 3, S372-8.

- Nemoto, O., Yamagishi, M., Yamada, H., Kikuchi, T. & Takaishi, H. (1997) Matrix metalloproteinase-3 production by human degenerated intervertebral disc. *J Spinal Disord*, 10, 493-8.
- Neufeld, J. H. (1992) Induced narrowing and back adaptation of lumbar intervertebral discs in biomechanically stressed rats. *Spine*, 17, 811-6.
- Nishida, K., Doita, M., Takada, T., Kakutani, K., Miyamoto, H., Shimomura, T., Maeno, K. & Kurosaka, M. (2006) Sustained transgene expression in intervertebral disc cells in vivo mediated by microbubble-enhanced ultrasound gene therapy. *Spine*, 31, 1415-9.
- Nishida, K., Kang, J. D., Gilbertson, L. G., Moon, S. H., Suh, J. K., Vogt, M. T., Robbins, P. D. & Evans, C. H. (1999) Modulation of the biologic activity of the rabbit intervertebral disc by gene therapy: an in vivo study of adenovirus-mediated transfer of the human transforming growth factor beta 1 encoding gene. *Spine*, 24, 2419-25.
- Nishida, K., Kang, J. D., Suh, J. K., Robbins, P. D., Evans, C. H. & Gilbertson, L. G. (1998) Adenovirus-mediated gene transfer to nucleus pulposus cells. Implications for the treatment of intervertebral disc degeneration. *Spine*, 23, 2437-42; discussion 2443.
- Nitobe, T., Harata, S., Okamoto, Y., Nakamura, T. & Endo, M. (1988) Degradation and biosynthesis of proteoglycans in the nucleus pulposus of canine intervertebral disc after chymopapain treatment. *Spine*, 13, 1332-9.
- Norcross, J. P., Lester, G. E., Weinhold, P. & Dahners, L. E. (2003) An in vivo model of degenerative disc disease. *J Orthop Res*, 21, 183-8.
- O'connell, G. D., Vresilovic, E. J. & Elliott, D. M. (2007) Comparison of animals used in disc research to human lumbar disc geometry. *Spine*, 32, 328-33.
- Ochia, R. S., Tencer, A. F. & Ching, R. P. (2003) Effect of loading rate on endplate and vertebral body strength in human lumbar vertebrae. *J Biomech*, 36, 1875-81.
- Oda, I., Cunningham, B. W., Buckley, R. A., Goebel, M. J., Haggerty, C. J., Orbegoso, C. M. & McAfee, P. C. (1999) Does spinal kyphotic deformity influence the biomechanical characteristics of the adjacent motion segments? An in vivo animal model. *Spine*, 24, 2139-46.
- Oegema, T. R., Jr., Bradford, D. S. & Cooper, K. M. (1979) Aggregated proteoglycan synthesis in organ cultures of human nucleus pulposus. *J Biol Chem*, 254, 10579-81.

- Oegema, T. R., Jr., Johnson, S. L., Aguiar, D. J. & Ogilvie, J. W. (2000) Fibronectin and its fragments increase with degeneration in the human intervertebral disc. *Spine*, 25, 2742-7.
- Ohshima, H. & Urban, J. P. (1992) The effect of lactate and pH on proteoglycan and protein synthesis rates in the intervertebral disc. *Spine*, 17, 1079-82.
- Ohshima, H., Urban, J. P. & Bergel, D. H. (1995) Effect of static load on matrix synthesis rates in the intervertebral disc measured in vitro by a new perfusion technique. *J Orthop Res*, 13, 22-9.
- Okuma, M., Mochida, J., Nishimura, K., Sakabe, K. & Seiki, K. (2000) Reinsertion of stimulated nucleus pulposus cells retards intervertebral disc degeneration: an in vitro and in vivo experimental study. *J Orthop Res*, 18, 988-97.
- Omlor, G. W., Lorenz, H., Engelleiter, K., Richter, W., Carstens, C., Kroeber, M. W. & Guehring, T. (2006) Changes in gene expression and protein distribution at different stages of mechanically induced disc degeneration--an in vivo study on the New Zealand white rabbit. *J Orthop Res*, 24, 385-92.
- Osada, R., Ohshima, H., Ishihara, H., Yudoh, K., Sakai, K., Matsui, H. & Tsuji, H. (1996) Autocrine/paracrine mechanism of insulin-like growth factor-1 secretion, and the effect of insulin-like growth factor-1 on proteoglycan synthesis in bovine intervertebral discs. *J Orthop Res*, 14, 690-9.
- Oshima, H., Ishihara, H., Urban, J. P. & Tsuji, H. (1993) The use of coccygeal discs to study intervertebral disc metabolism. *J Orthop Res*, 11, 332-8.
- Osti, O. L., Vernon-Roberts, B. & Fraser, R. D. (1990) 1990 Volvo Award in experimental studies. Anulus tears and intervertebral disc degeneration. An experimental study using an animal model. *Spine*, 15, 762-7.
- Pascual-Montano, A., Carmona-Saez, P., Chagoyen, M., Tirado, F., Carazo, J. M. & Pascual-Marqui, R. D. (2006) bioNMF: a versatile tool for non-negative matrix factorization in biology. *BMC Bioinformatics*, 7, 366.
- Pattison, S. T., Melrose, J., Ghosh, P. & Taylor, T. K. (2001) Regulation of gelatinase-A (MMP-2) production by ovine intervertebral disc nucleus pulposus cells grown in alginate bead culture by Transforming Growth Factor-beta(1) and insulin like growth factor-I. *Cell Biol Int*, 25, 679-89.
- Pazzaglia, S. (2006) Ptc1 heterozygous knockout mice as a model of multi-organ tumorigenesis. *Cancer Lett*, 234, 124-34.

- Pazzaglia, U. E., Salisbury, J. R. & Byers, P. D. (1989) Development and involution of the notochord in the human spine. *J R Soc Med*, 82, 413-5.
- Perrien, D. S., Akel, N. S., Dupont-Versteegden, E. E., Skinner, R. A., Siegel, E. R., Suva, L. J. & Gaddy, D. (2007) Aging alters the skeletal response to disuse in the rat. *Am J Physiol Regul Integr Comp Physiol*, 292, R988-96.
- Pfarrmann, C. W. & Resnick, D. (2001) Schmorl nodes of the thoracic and lumbar spine: radiographic-pathologic study of prevalence, characterization, and correlation with degenerative changes of 1,650 spinal levels in 100 cadavers. *Radiology*, 219, 368-74.
- Plaas, A. H., Sandy, J. D. & Kimura, J. H. (1988) Biosynthesis of cartilage proteoglycan and link protein by articular chondrocytes from immature and mature rabbits. *J Biol Chem*, 263, 7560-6.
- Poiraudeau, S., Monteiro, I., Anract, P., Blanchard, O., Revel, M. & Corvol, M. T. (1999) Phenotypic characteristics of rabbit intervertebral disc cells. Comparison with cartilage cells from the same animals. *Spine*, 24, 837-44.
- Pratsinis, H. & Kletsas, D. (2007) PDGF, bFGF and IGF-I stimulate the proliferation of intervertebral disc cells in vitro via the activation of the ERK and Akt signaling pathways. *Eur Spine J*, 16, 1858-66.
- Quinn, T. M., Grodzinsky, A. J., Hunziker, E. B. & Sandy, J. D. (1998) Effects of injurious compression on matrix turnover around individual cells in calf articular cartilage explants. *J Orthop Res*, 16, 490-9.
- Rand, N., Reichert, F., Floman, Y. & Rotshenker, S. (1997) Murine nucleus pulposus-derived cells secrete interleukins-1-beta, -6, and -10 and granulocyte-macrophage colony-stimulating factor in cell culture. *Spine*, 22, 2598-601; discussion 2602.
- Rand, N. S., Dawson, J. M., Juliao, S. F., Spengler, D. M. & Floman, Y. (2001) In vivo macrophage recruitment by murine intervertebral disc cells. *J Spinal Disord*, 14, 339-42.
- S. Ray, R.H. Turi, (1999) Determination of number of clusters in K-means clustering and application in colour image segmentation, in: *Proceedings of the 4th International Conference on Advances in Pattern Recognition and Digital Techniques (ICAPRDT'99)*, Calcutta, India, 27-29
- Revell, P. A., Damien, E., Di Silvio, L., Gurav, N., Longinotti, C. & Ambrosio, L. (2007) Tissue engineered intervertebral disc repair in the pig using injectable polymers. *J Mater Sci Mater Med*, 18, 303-8.

- Reza, A. T. & Nicoll, S. B. (2008) Hydrostatic pressure differentially regulates outer and inner annulus fibrosus cell matrix production in 3D scaffolds. *Ann Biomed Eng*, 36, 204-13.
- Riew, K. D., Lou, J., Wright, N. M., Cheng, S. L., Bae, K. T. & Avioli, L. V. (2003) Thoracoscopic intradiscal spine fusion using a minimally invasive gene-therapy technique. *J Bone Joint Surg Am*, 85-A, 866-71.
- Risbud, M. V., Di Martino, A., Guttapalli, A., Seghatoleslami, R., Denaro, V., Vaccaro, A. R., Albert, T. J. & Shapiro, I. M. (2006) Toward an optimum system for intervertebral disc organ culture: TGF-beta 3 enhances nucleus pulposus and annulus fibrosus survival and function through modulation of TGF-beta-R expression and ERK signaling. *Spine*, 31, 884-90.
- Risbud, M. V., Izzo, M. W., Adams, C. S., Arnold, W. W., Hillibrand, A. S., Vresilovic, E. J., Vaccaro, A. R., Albert, T. J. & Shapiro, I. M. (2003) An organ culture system for the study of the nucleus pulposus: description of the system and evaluation of the cells. *Spine*, 28, 2652-8; discussion 2658-9.
- Roberts, S., Caterson, B., Evans, H. & Eisenstein, S. M. (1994) Proteoglycan components of the intervertebral disc and cartilage endplate: an immunolocalization study of animal and human tissues. *Histochem J*, 26, 402-11.
- Roberts, S., Evans, H., Trivedi, J. & Menage, J. (2006) Histology and pathology of the human intervertebral disc. *J Bone Joint Surg Am*, 88 Suppl 2, 10-4.
- Roberts, S., Menage, J., Sivan, S. & Urban, J. P. (2008) Bovine explant model of degeneration of the intervertebral disc. *BMC Musculoskelet Disord*, 9, 24.
- Roughley, P., Hoemann, C., Desrosiers, E., Mwale, F., Antoniou, J. & Alini, M. (2006) The potential of chitosan-based gels containing intervertebral disc cells for nucleus pulposus supplementation. *Biomaterials*, 27, 388-96.
- Roughley, P. J., Alini, M. & Antoniou, J. (2002) The role of proteoglycans in aging, degeneration and repair of the intervertebral disc. *Biochem Soc Trans*, 30, 869-74.
- Rufai, A., Benjamin, M. & Ralphs, J. R. (1995) The development of fibrocartilage in the rat intervertebral disc. *Anat Embryol (Berl)*, 192, 53-62.



- Sahlman, J., Inkinen, R., Hirvonen, T., Lammi, M. J., Lammi, P. E., Nieminen, J., Lapveteläinen, T., Prockop, D. J., Arita, M., Li, S. W., Hyttinen, M. M., Helminen, H. J. & Puustjarvi, K. (2001) Premature vertebral endplate ossification and mild disc degeneration in mice after inactivation of one allele belonging to the Col2a1 gene for Type II collagen. *Spine*, 26, 2558-65.
- Sakai, D., Mochida, J., Iwashina, T., Watanabe, T., Nakai, T., Ando, K. & Hotta, T. (2005) Differentiation of mesenchymal stem cells transplanted to a rabbit degenerative disc model: potential and limitations for stem cell therapy in disc regeneration. *Spine*, 30, 2379-87.
- Sakai, D., Mochida, J., Iwashina, T., Watanabe, T., Suyama, K., Ando, K. & Hotta, T. (2006) Atelocollagen for culture of human nucleus pulposus cells forming nucleus pulposus-like tissue in vitro: influence on the proliferation and proteoglycan production of HNPSV-1 cells. *Biomaterials*, 27, 346-53.
- Sasaki, M., Takahashi, T., Miyahara, K. & Hirose a, T. (2001) Effects of chondroitinase ABC on intradiscal pressure in sheep: an in vivo study. *Spine*, 26, 463-8.
- Seguin, C. A., Bojarski, M., Pilliar, R. M., Roughley, P. J. & Kandel, R. A. (2006) Differential regulation of matrix degrading enzymes in a TNFalpha-induced model of nucleus pulposus tissue degeneration. *Matrix Biol*, 25, 409-18.
- Shinmei, M., Kikuchi, T., Yamagishi, M. & Shimomura, Y. (1988) The role of interleukin-1 on proteoglycan metabolism of rabbit annulus fibrosus cells cultured in vitro. *Spine*, 13, 1284-90.
- So, K., Takemoto, M., Fujibayashi, S., Neo, M., Kyomoto, M., Hayami, T., Hyon, S. H. & Nakamura, T. (2007) Antidegenerative effects of partial disc replacement in an animal surgery model. *Spine*, 32, 1586-91.
- Sobajima, S., Kim, J. S., Gilbertson, L. G. & Kang, J. D. (2004) Gene therapy for degenerative disc disease. *Gene Ther*, 11, 390-401.
- Stern, S., Lindenhayn, K. & Perka, C. (2004) Human intervertebral disc cell culture for disc disorders. *Clin Orthop Relat Res*, 238-44.
- Stokes, I. A. & Iatridis, J. C. (2004) Mechanical conditions that accelerate intervertebral disc degeneration: overload versus immobilization. *Spine*, 29, 2724-32.
- Sun, Y., Hurtig, M., Pilliar, R. M., Grynblas, M. & Kandel, R. A. (2001) Characterization of nucleus pulposus-like tissue formed in vitro. *J Orthop Res*, 19, 1078-84.

- Takada, T., Nishida, K., Doita, M., Miyamoto, H. & Kurosaka, M. (2004) Interleukin-6 production is upregulated by interaction between disc tissue and macrophages. *Spine*, 29, 1089-92; discussion 1093.
- Takahata, M., Kotani, Y., Abumi, K., Shikinami, Y., Kadosawa, T., Kaneda, K. & Minami, A. (2003) Bone ingrowth fixation of artificial intervertebral disc consisting of bioceramic-coated three-dimensional fabric. *Spine*, 28, 637-44; discussion 644.
- Takegami, K., Thonar, E. J., An, H. S., Kamada, H. & Masuda, K. (2002) Osteogenic protein-1 enhances matrix replenishment by intervertebral disc cells previously exposed to interleukin-1. *Spine*, 27, 1318-25.
- Taylor, T. K., Melrose, J., Burkhardt, D., Ghosh, P., Claes, L. E., Kettler, A. & Wilke, H. J. (2000) Spinal biomechanics and aging are major determinants of the proteoglycan metabolism of intervertebral disc cells. *Spine*, 25, 3014-20.
- Thompson, J. P., Oegema, T. R., Jr. & Bradford, D. S. (1991) Stimulation of mature canine intervertebral disc by growth factors. *Spine*, 16, 253-60.
- Tsuji, T., Chiba, K., Imabayashi, H., Fujita, Y., Hosogane, N., Okada, Y. & Toyama, Y. (2007) Age-related changes in expression of tissue inhibitor of metalloproteinases-3 associated with transition from the notochordal nucleus pulposus to the fibrocartilaginous nucleus pulposus in rabbit intervertebral disc. *Spine*, 32, 849-56.
- Ulloa-Montoya, F., Kidder, B. L., Pauwelyn, K. A., Chase, L. G., Luttun, A., Crabbe, A., Geraerts, M., Sharov, A. A., Piao, Y., Ko, M. S., Hu, W. S. & Verfaillie, C. M. (2007) Comparative transcriptome analysis of embryonic and adult stem cells with extended and limited differentiation capacity. *Genome Biol*, 8, R163.
- Ulrich, J. A., Liebenberg, E. C., Thuillier, D. U. & Lotz, J. C. (2007) ISSLS prize winner: repeated disc injury causes persistent inflammation. *Spine*, 32, 2812-9.
- Urban, J. P., Holm, S. & Maroudas, A. (1978) Diffusion of small solutes into the intervertebral disc: as in vivo study. *Biorheology*, 15, 203-21.
- Urban, J. P., Holm, S., Maroudas, A. & Nachemson, A. (1977) Nutrition of the intervertebral disk. An in vivo study of solute transport. *Clin Orthop Relat Res*, 101-14.
- Urban, M. R., Fairbank, J. C., Etherington, P. J., Loh, F. L., Winlove, C. P. & Urban, J. P. (2001) Electrochemical measurement of transport into scoliotic intervertebral discs in vivo using nitrous oxide as a tracer. *Spine*, 26, 984-90.

- Van Dieen, J. H., Weinans, H. & Toussaint, H. M. (1999) Fractures of the lumbar vertebral endplate in the etiology of low back pain: a hypothesis on the causative role of spinal compression in aspecific low back pain. *Med Hypotheses*, 53, 246-52.
- Vannini, N., Pfeffer, U., Lorusso, G., Noonan, D. M. & Albini, A. (2008) Endothelial cell aging and apoptosis in prevention and disease: E-selectin expression and modulation as a model. *Curr Pharm Des*, 14, 221-5.
- Venn, G. & Mason, R. M. (1983) Biosynthesis and metabolism in vivo of intervertebral-disc proteoglycans in the mouse. *Biochem J*, 215, 217-25.
- Vernon-Roberts, B., Moore, R. J. & Fraser, R. D. (2007) The natural history of age-related disc degeneration: the pathology and sequelae of tears. *Spine*, 32, 2797-804.
- Vernon-Roberts, B. & Pirie, C. J. (1977) Degenerative changes in the intervertebral discs of the lumbar spine and their sequelae. *Rheumatol Rehabil*, 16, 13-21.
- Videman, T. & Battie, M. C. (1999) The influence of occupation on lumbar degeneration. *Spine*, 24, 1164-8.
- Videman, T., Nurminen, M. & Troup, J. D. (1990) 1990 Volvo Award in clinical sciences. Lumbar spinal pathology in cadaveric material in relation to history of back pain, occupation, and physical loading. *Spine*, 15, 728-40.
- Vuono-Hawkins, M., Zimmerman, M. C., Lee, C. K., Carter, F. M., Parsons, J. R. & Langrana, N. A. (1994) Mechanical evaluation of a canine intervertebral disc spacer: in situ and in vivo studies. *J Orthop Res*, 12, 119-27.
- Wakano, K., Kasman, R., Chao, E. Y., Bradford, D. S. & Oegema, T. R. (1983) Biomechanical analysis of canine intervertebral discs after chymopapain injection. A preliminary report. *Spine*, 8, 59-68.
- Wallach, C. J., Sobajima, S., Watanabe, Y., Kim, J. S., Georgescu, H. I., Robbins, P., Gilbertson, L. G. & Kang, J. D. (2003) Gene transfer of the catabolic inhibitor TIMP-1 increases measured proteoglycans in cells from degenerated human intervertebral discs. *Spine*, 28, 2331-7.
- Walsh, A. J., Bradford, D. S. & Lotz, J. C. (2004) In vivo growth factor treatment of degenerated intervertebral discs. *Spine*, 29, 156-63.

- Walsh, A. J. & Lotz, J. C. (2004) Biological response of the intervertebral disc to dynamic loading. *J Biomech*, 37, 329-37.
- Walters, R., Rahmat, R., Fraser, R. & Moore, R. (2006) Preventing and treating discitis: cephazolin penetration in ovine lumbar intervertebral disc. *Eur Spine J*, 15, 1397-403.
- Walters, R. M., Smith, S. H., Hutchinson, M. J., Dolan, A. M., Fraser, R. D. & Moore, R. J. (2005) Effects of intervertebral disc infection on the developing ovine spine. *Spine*, 30, 1252-7.
- Wang, D. L., Jiang, S. D. & Dai, L. Y. (2007) Biologic response of the intervertebral disc to static and dynamic compression in vitro. *Spine*, 32, 2521-8.
- Wang, H., Kroeber, M., Hanke, M., Ries, R., Schmid, C., Poller, W. & Richter, W. (2004) Release of active and depot GDF-5 after adenovirus-mediated overexpression stimulates rabbit and human intervertebral disc cells. *J Mol Med*, 82, 126-34.
- Wang, J. Y., Baer, A. E., Kraus, V. B. & Setton, L. A. (2001) Intervertebral disc cells exhibit differences in gene expression in alginate and monolayer culture. *Spine*, 26, 1747-51; discussion 1752.
- Wilke, H. J., Neef, P., Caimi, M., Hoogland, T. & Claes, L. E. (1999) New in vivo measurements of pressures in the intervertebral disc in daily life. *Spine*, 24, 755-62.
- Wiseman, M. A., Birch, H. L., Akmal, M. & Goodship, A. E. (2005) Segmental variation in the in vitro cell metabolism of nucleus pulposus cells isolated from a series of bovine caudal intervertebral discs. *Spine*, 30, 505-11.
- Wuertz, K., Urban, J. P., Klasen, J., Ignatius, A., Wilke, H. J., Claes, L. & Neidlinger-Wilke, C. (2007) Influence of extracellular osmolarity and mechanical stimulation on gene expression of intervertebral disc cells. *J Orthop Res*.
- Xie, X.L., and Beni, G. A. (1991) Validity measurement for fuzzy clustering. *IEE trans. PAMI*, 3(8):841-846
- Yang, S. H., Chen, P. Q., Chen, Y. F. & Lin, F. H. (2005) An in-vitro study on regeneration of human nucleus pulposus by using gelatin/chondroitin-6-sulfate/hyaluronan tri-copolymer scaffold. *Artif Organs*, 29, 806-14.

- Yoganandan, N., Larson, S. J., Pintar, F. A., Gallagher, M., Reinartz, J. & Droese, K. (1994) Intravertebral pressure changes caused by spinal microtrauma. *Neurosurgery*, 35, 415-21; discussion 421.
- Yoo, J. U., Papay, R. S. & Malemud, C. J. (1992) Suppression of proteoglycan synthesis in chondrocyte cultures derived from canine intervertebral disc. *Spine*, 17, 221-4.
- Yoon, S. T. (2004) The potential of gene therapy for the treatment of disc degeneration. *Orthop Clin North Am*, 35, 95-100.
- Yoon, S. T., Park, J. S., Kim, K. S., Li, J., Attallah-Wasif, E. S., Hutton, W. C. & Boden, S. D. (2004) ISSLS prize winner: LMP-1 upregulates intervertebral disc cell production of proteoglycans and BMPs in vitro and in vivo. *Spine*, 29, 2603-11.
- Yu, J., Tirlapur, U., Fairbank, J., Handford, P., Roberts, S., Winlove, C. P., Cui, Z. & Urban, J. (2007) Microfibrils, elastin fibres and collagen fibres in the human intervertebral disc and bovine tail disc. *J Anat*, 210, 460-71.
- Yu, J., Winlove, P. C., Roberts, S. & Urban, J. P. (2002) Elastic fibre organization in the intervertebral discs of the bovine tail. *J Anat*, 201, 465-75.
- Zhan, Z., Shao, Z., Xiong, X., Yang, S., Du, J., Zheng, Q., Wang, H., Guo, X. & Liu, Y. (2004) Ad/CMV- hTGF-beta1 treats rabbit intervertebral discs degeneration in vivo. *J Huazhong Univ Sci Technolog Med Sci*, 24, 599-601, 624.
- Zhang, Y., An, H. S., Song, S., Toofanfard, M., Masuda, K., Andersson, G. B. & Thonar, E. J. (2004) Growth factor osteogenic protein-1: differing effects on cells from three distinct zones in the bovine intervertebral disc. *Am J Phys Med Rehabil*, 83, 515-21.
- Zhou, H., Hou, S., Shang, W., Wu, W., Cheng, Y., Mei, F. & Peng, B. (2007) A new in vivo animal model to create intervertebral disc degeneration characterized by MRI, radiography, CT/discogram, biochemistry, and histology. *Spine*, 32, 864-72.

## **Appendix 1: Immunohistochemistry methods**

Immunohistochemistry methods for images in Chapter 2.

### **Purpose:**

Visualization of collagen extracellular matrix molecules in 18-24 mo. old bovine intervertebral disc (IVD) tissue.

### **Procedure:**

Tissue samples were removed from the bovine IVD (see diagram). Tissue was then placed in 10% neutral buffered formalin for 4 hours at 4C. After removal from the formalin, the samples were rinsed briefly in PBS and placed in a solution of 30% sucrose at 4C overnight. Tissue samples were then placed in cryomolds, coated in OCT and frozen using liquid nitrogen cooled isopentane, and stored at -80C until sectioning. Tissue blocks were sectioned into 10 µm thick slides, transferred to superfrost plus slides, and stored at -80C.

Slides were removed from the -80C freezer and allowed to dry for 20 minutes at room temperature. Sections were then fixed in acetone for 5 min at room temperature in a fume hood). After removal from the acetone, slides were allowed to dry for 5 mins and rehydrated in PBS. Slides were then transferred to Thermo Shandon Sequenza Slide racks and washed again with PBS (200µl 3x). Slides were then washed with 0.1% Triton-X at room temperature for 15 minutes, followed by another wash with PBS (3x).

Due to the bovine's age and the formalin fixation, a pretreatment step was necessary. The enzymes of interest were decided to be Hyluronidase (1,000 units in PBS, pH = 5.0), Pronase (in PBS, pH = 7.4), Proteinase-K (1mg/ml in ammonium acetate pH =

6.5), Collagenase (1mg/ml in 0.1M Tris and 1mMol calcium chloride dihydride, pH = 7.5), and Trypsin (0.5% in PBS). The following protocols were attempted:

Protocol 1)

Pronase – 15 min at 37C

Hyaluronidase – 1 hr at 37C

Protocol 2)

Proteinase K – 15 min at 37C

Hyaluronidase – 1 hour at 37C

Protocol 3)

Collagenase – 1 hour at 40C

PBS – 1 hour at 37C

Protocol 4)

Collagenase – 1 hour at 40C

Hyaluronidase – 1 hr at 37C

Protocol 5)

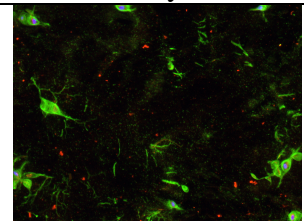
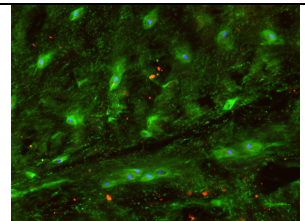
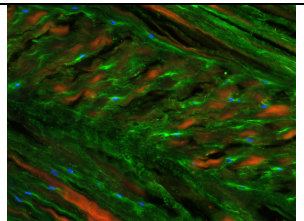
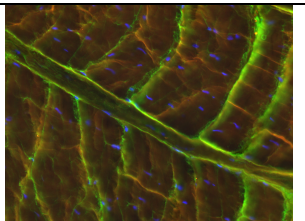
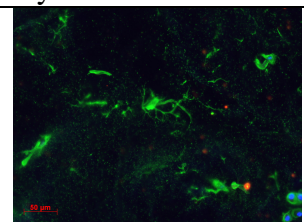
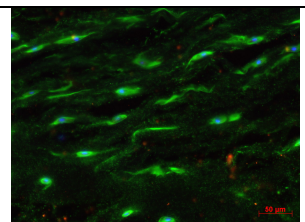
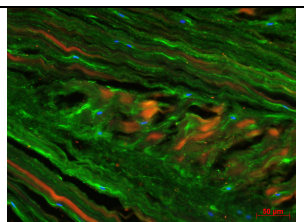
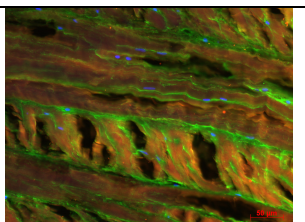
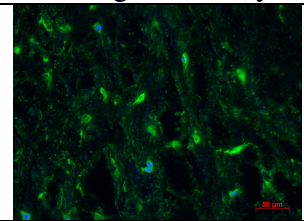
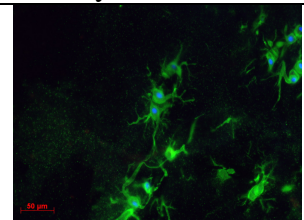
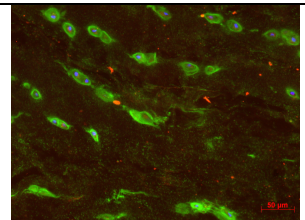
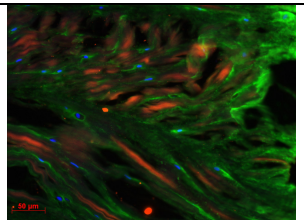
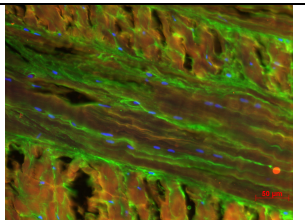
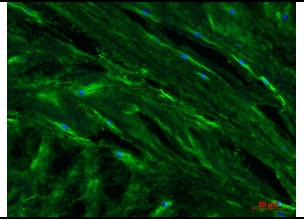
Trypsin – 15 min at 37C

PBS – 1 hour at 37C

Blocking of non-specific interactions was accomplished by incubating the slides with 1% BSA, 0.1% Gelatin, 0.05% Tween-20, and 2% normal goat serum overnight at 4C (also can be done for 1 hour at RT). Slides were washed with PBS (3x) followed by incubation for 1.5 hours at room temp in primary antibodies for collagen I (mouse) and VI (rabbit) both at 1:100 dilution, 1.0% BSA and 0.1% gelatin. Again slides were washed in PBS (1x) and fluorescently conjugated antibodies (1:100) in PBS were added. Slides were incubated for 1.5 hour at room temp, followed by a PBS wash (3x). DAPI at 0.25 mg/ml in PBS was then added for 5 minutes at room temp. Coverslips were mounted on the slides using aqueous gel mounting medium, they were allowed to dry overnight and clear nail polish was used to seal the edges.

**Summary of observations: Protocol 4 found to be ideal.**

Blue = DNA Green = Type VI Collagen Red = Type I Collagen  
 Pronase + Hyluronidase

			
NP	NP/Inner AF	Inner AF	Outer AF
Proteinase-K + Hyaluronidase			
			
NP	NP/Inner AF	Inner AF	Outer AF
Collagenase Only			
			
NP	NP/Inner AF	Inner AF	Outer AF
Collagenase + Hyaluronidase			
			
NP	NP/Inner AF	Inner AF	Outer AF
Trypsin			
			
NP	NP/Inner AF	Inner AF	Outer AF



## **Appendix 2: Data for clustering analysis**

Overall number of biological replicates used

Sample ID	AF	NP
OC7	4	4
OL7	3	3
OM7	3	3
OH7	3	3
YC7	3	3
YL7	3	2
YM7	3	2
YH7	3	2
OC14	3	3
OL14	2	2
OM14	2	3
OH14	2	3
YC14	3	2
YL14	3	2
YM14	3	2
YH14	3	2
OC21	2	2
OL21	2	2
OM21	2	2
OH21	1	2
YC21	1	2
YL21	1	2
YM21	1	2
YH21	1	2

### NP Tissue samples

Sample ID	18s AVE	18s SD	GAPDH AVE	GAPDH SD	COL1 AVG	COL1 SD	COL2 AVG	COL2 SD
OC7	15.1	0.09	20.0	0.16	22.7	0.07	23.2	0.30
OL7	16.3	0.07	20.3	0.12	23.0	2.22	22.6	1.42
OM7	18.5	0.23	21.5	0.09	22.2	0.29	29.9	1.72
OH7	20.6	0.02	18.3	0.11	23.2	0.05	23.3	0.08
YC7	20.6	0.19	21.0	0.37	21.9	0.17	22.0	0.11
YL7	21.7	1.37	24.9	0.24	26.1	0.42	25.6	0.01
YM7	21.4	0.12	20.7	0.16	23.4	0.10	23.5	0.28
YH7	23.3	1.05	26.3	0.39	24.1	0.13	29.4	0.18
OC14	24.8	0.37	22.5	1.11	22.9	0.19	23.4	0.30
OL14	20.2	0.16	20.1	0.74	22.7	0.20	23.2	0.16
OM14	18.0	0.07	18.6	0.40	21.8	0.16	22.4	0.12
OH14	17.8	0.03	19.0	0.72	23.4	0.24	23.8	0.05
YC14	26.0	1.49	33.9	0.11	29.9	0.03	25.5	0.10
YL14	30.6	0.40	41.2	2.90	30.9	0.00	28.3	0.12
YM14	30.0	0.49	37.6	2.20	31.7	3.30	30.5	0.01
YH14	28.1	1.32	29.8	0.67	32.2	0.57	32.1	0.05
OC21	25.8	0.99	27.0	0.37	28.0	0.22	28.5	0.56
OL21	26.8	0.18	20.2	0.19	23.8	0.27	24.2	0.13
OM21	21.8	0.00	18.3	0.93	22.6	0.32	23.0	0.21
OH21	27.8	0.06	23.5	0.44	30.9	0.91	32.2	1.60
YC21	27.4	1.00	34.5	2.22	33.9	1.58	35.4	3.95
YL21	27.6	2.39	33.0	0.00	30.1	0.00	28.8	0.31
YM21	25.8	4.44	34.9	0.09	29.1	0.20	28.5	0.45
YH21	26.0	1.55	35.7	0.22	30.1	0.18	28.9	1.50

Sample ID	AGG AVG	AGG SD	CFOS AVE	CFOS SD	BGY AVE	BGY SD	STAT3 AVE	STAT3 SD
OC7	21.8	0.07	29.6	0.18	25.3	0.17	30.5	0.38
OL7	20.7	0.13	28.5	0.08	25.9	0.07	30.6	0.18
OM7	22.3	0.09	30.3	0.67	29.0	0.16	30.3	0.40
OH7	24.6	0.21	35.4	0.00	36.5	0.00	33.7	0.00
YC7	25.6	0.20	27.3	0.05	27.5	0.12	27.8	0.07
YL7	26.8	0.00	24.7	0.01	20.9	0.14	26.2	0.01
YM7	29.0	0.60	25.7	0.02	23.9	0.14	27.9	0.11
YH7	21.7	0.06	30.8	0.16	29.2	0.15	30.1	0.31
OC14	30.4	0.54	34.3	0.16	37.4	0.62	36.0	0.00
OL14	30.2	0.52	29.4	0.14	29.3	0.37	31.8	0.12
OM14	28.7	0.22	26.8	0.12	24.7	0.17	29.9	0.09
OH14	31.4	0.79	27.2	0.13	25.7	0.33	29.6	0.28
YC14	26.1	0.02	36.2	0.00	35.7	0.00	35.1	0.00
YL14	27.5	0.00	37.0	0.00	37.0	0.00	35.4	2.86
YM14	27.4	0.00	38.6	0.00	35.1	0.00	35.3	0.00
YH14	28.7	0.02	36.9	0.00	38.1	1.29	35.4	0.00
OC21	29.6	0.07	34.7	0.00	36.1	0.00	37.4	0.00
OL21	35.5	0.23	32.9	0.45	37.0	0.04	35.1	0.00
OM21	27.1	0.00	27.3	0.08	32.9	0.39	32.7	0.62
OH21	37.0	0.00	35.5	1.15	36.0	1.11	39.4	0.00
YC21	36.6	0.08	37.6	1.38	37.2	0.00	37.1	0.00
YL21	27.6	0.00	39.7	0.00	34.5	0.00	36.3	0.00
YM21	40.0	0.00	35.1	0.68	35.2	1.00	36.1	0.00
YH21	32.6	0.01	37.0	0.00	35.3	1.00	35.8	0.40

Sample ID	MMP3 AVG	MMP3 SD	AD4 AVE	AD4 SD	LINK AVE	LINK SD	MMP2 AVE	MMP2 SD
OC7	30.1	0.21	32.2	0.78	26.0	0.04	26.4	0.26
OL7	30.8	0.25	37.2	5.61	26.1	0.16	27.3	0.39
OM7	31.5	0.10	40.2	4.21	26.2	0.23	30.7	0.69
OH7	31.7	0.08	29.4	1.12	30.1	0.00	31.3	0.11
YC7	33.4	0.10	32.7	0.22	26.3	0.20	24.3	0.30
YL7	34.6	0.31	30.6	0.21	28.1	0.00	21.3	0.60
YM7	33.4	0.31	44.0	0.24	25.7	0.04	23.1	0.22
YH7	43.2	0.04	33.2	0.41	26.8	0.00	33.5	0.35
OC14	32.0	0.04	35.5	0.53	25.0	0.02	36.0	0.00
OL14	29.5	0.13	37.2	0.21	25.0	0.09	29.0	0.19
OM14	28.1	0.22	34.1	0.00	24.2	0.08	25.4	0.03
OH14	28.5	0.14	42.0	7.04	25.8	0.15	25.5	0.15
YC14	35.0	0.05	40.2	0.00	27.9	0.00	36.8	0.56
YL14	37.4	0.00	40.8	0.00	30.1	0.20	37.0	0.30
YM14	38.9	0.00	42.5	0.00	30.4	0.10	36.9	0.44
YH14	45.0	7.57	40.2	0.00	33.4	0.00	36.0	0.34
OC21	37.4	1.90	40.4	0.00	30.8	0.33	36.0	0.37
OL21	29.6	0.16	46.0	0.00	26.0	0.01	38.0	2.21
OM21	24.2	0.10	54.4	4.82	24.4	0.01	29.2	0.07
OH21	28.0	0.18	40.3	0.00	29.2	0.11	36.0	0.93
YC21	42.0	6.25	45.7	0.00	34.8	0.00	36.2	0.75
YL21	39.0	0.00	39.8	0.00	32.4	0.00	38.5	0.83
YM21	38.9	3.88	44.8	0.00	31.8	0.00	36.0	0.75
YH21	35.4	0.36	38.9	0.00	33.6	0.00	36.7	0.00

Sample ID	CJUN AVE	CJUN SD	COL6 AVE	COL6 SD	CTGF AVE	CTGF SD	DEC AVE	DEC SD
OC7	29.2	0.23	25.2	0.10	30.7	0.38	22.4	0.21
OL7	29.6	0.50	27.1	0.42	30.6	0.44	22.1	0.43
OM7	28.9	0.00	29.4	0.21	31.4	0.26	22.7	0.27
OH7	28.9	0.20	33.9	0.36	38.2	0.21	22.7	0.02
YC7	27.7	0.30	23.4	0.29	27.6	0.12	22.4	0.12
YL7	25.0	0.35	23.5	0.94	24.6	0.30	24.2	0.07
YM7	26.9	0.75	28.3	0.42	30.0	0.11	21.6	0.33
YH7	29.9	0.88	21.7	0.13	30.5	0.01	25.6	0.32
OC14	33.5	0.47	35.0	0.21	35.9	0.87	21.6	0.22
OL14	29.9	0.25	30.3	0.31	31.0	0.41	21.9	0.20
OM14	26.8	0.13	27.2	0.31	27.8	0.22	22.4	0.22
OH14	29.3	0.14	28.5	0.12	29.2	0.13	21.9	0.16
YC14	35.5	0.88	36.6	0.21	35.8	1.27	30.9	0.93
YL14	36.0	0.84	36.1	0.21	38.8	0.21	32.5	0.23
YM14	38.1	0.51	36.2	0.21	36.0	0.23	33.4	0.18
YH14	34.3	0.82	36.8	0.21	34.5	0.31	28.9	0.16
OC21	32.0	0.12	36.1	0.41	35.1	2.60	27.6	0.26
OL21	32.0	0.21	34.0	0.02	35.4	0.04	22.2	0.08
OM21	30.0	0.15	34.6	0.71	28.0	0.02	20.1	0.06
OH21	35.3	1.40	35.8	0.41	38.7	1.36	24.5	0.04
YC21	35.7	0.74	34.1	0.43	35.2	0.13	32.3	0.31
YL21	34.0	0.00	34.5	0.00	36.7	0.13	32.2	0.12
YM21	33.6	0.00	34.6	0.00	36.5	0.91	30.6	0.00
YH21	35.5	0.00	34.2	0.00	35.7	0.00	32.3	0.00

Sample ID	IGF AVE	IGF SD	IL6 AVE	IL6 SD	ILK AVE	ILK SD	MMP1 AVE	MMP1 SD
OC7	33.5	0.42	25.8	0.71	29.2	0.43	28.8	0.08
OL7	34.4	1.34	32.6	0.52	29.2	0.35	30.5	0.52
OM7	32.4	0.69	29.7	0.68	30.9	0.28	32.7	0.48
OH7	34.1	1.09	29.7	0.71	30.0	0.23	32.7	0.89
YC7	35.1	0.14	28.2	0.91	27.4	0.32	26.8	0.21
YL7	32.0	1.00	31.4	0.95	30.4	0.32	26.0	0.53
YM7	32.5	1.84	25.8	0.94	25.4	0.12	30.6	0.92
YH7	33.4	1.94	31.2	0.49	31.2	0.67	24.5	0.12
OC14	33.6	0.45	30.2	0.59	34.7	1.24	37.2	0.12
OL14	33.1	0.95	29.8	0.44	30.0	0.55	32.8	0.50
OM14	31.7	1.58	29.0	0.47	28.0	0.33	30.9	0.28
OH14	34.0	0.92	30.1	0.27	27.2	0.09	30.2	0.60
YC14	34.0	1.30	34.3	0.22	37.5	0.14	37.4	0.43
YL14	35.5	0.37	38.3	1.38	36.0	0.08	37.3	0.46
YM14	32.6	0.67	37.4	0.67	36.0	0.08	37.1	0.62
YH14	33.3	1.53	38.4	0.71	37.0	0.04	36.5	0.69
OC21	33.4	3.15	34.0	0.35	30.0	0.02	36.0	0.96
OL21	32.9	3.10	31.3	0.33	34.5	0.18	36.4	0.94
OM21	32.4	0.92	29.4	0.37	28.1	0.06	35.5	0.90
OH21	32.2	0.94	31.3	0.69	37.8	0.71	36.0	0.92
YC21	34.0	0.85	36.0	0.86	37.1	0.00	36.4	0.33
YL21	35.9	0.06	36.0	0.69	33.7	0.00	36.2	0.42
YM21	32.3	1.33	36.4	0.00	34.0	0.00	34.7	0.00
YH21	33.9	1.67	36.0	0.00	31.2	0.00	34.7	0.00

Sample ID	TMP1 AVE	TMP1 SD	FBIN AVE	FBIN SD	TGFB AVE	TGFB SD	TMP3 AVE	TMP3 SD
OC7	21.1	0.22	24.7	0.17	29.1	0.18	29.1	0.15
OL7	21.1	0.15	24.4	0.05	29.5	0.39	29.3	0.30
OM7	22.1	0.14	24.6	0.14	31.1	0.90	26.8	0.13
OH7	22.5	0.22	29.7	0.21	32.0	0.90	35.1	0.50
YC7	22.1	0.24	24.5	0.33	27.5	0.81	34.3	0.42
YL7	24.6	0.35	27.1	0.66	24.4	0.35	26.6	0.65
YM7	21.7	0.11	24.1	0.12	26.1	0.73	29.4	0.86
YH7	25.8	0.22	28.9	0.35	25.3	0.90	29.4	0.63
OC14	24.5	0.14	21.4	0.05	35.4	0.75	32.6	0.66
OL14	23.6	0.13	21.8	0.07	30.6	0.44	28.8	0.36
OM14	22.8	0.11	21.8	0.04	26.7	0.02	28.3	0.32
OH14	23.6	0.12	22.2	0.11	29.8	0.53	25.6	0.11
YC14	30.1	0.81	24.6	0.12	36.2	0.79	35.5	0.21
YL14	34.2	1.24	30.0	0.35	36.4	0.79	36.1	0.31
YM14	30.0	0.49	30.0	0.62	36.4	0.21	36.6	0.00
YH14	30.1	0.50	31.9	0.64	35.3	0.12	36.0	0.00
OC21	28.2	0.16	27.7	0.20	37.0	0.32	31.6	0.00
OL21	23.6	0.08	21.4	0.15	36.7	0.23	31.0	0.04
OM21	20.4	0.06	20.7	0.11	35.6	0.59	24.8	0.64
OH21	22.9	0.13	24.8	0.05	37.0	0.21	29.3	0.00
YC21	32.0	0.17	34.1	0.01	35.3	0.23	36.3	0.00
YL21	35.6	0.12	30.0	0.21	36.0	0.21	36.4	0.00
YM21	28.8	0.30	28.5	0.40	36.2	0.00	34.6	0.00
YH21	29.6	0.23	31.7	0.78	35.5	0.00	36.0	0.00

Sample ID	VCAN AVE	VCAN SD	VIM AVE	VIM SD	MAPK AVE	MAPK SD	COL3 AVE	COL3 SD
OC7	30.2	0.08	21.4	0.28	29.3	0.03	28.0	0.71
OL7	28.9	0.34	21.5	0.18	30.2	0.13	31.8	0.10
OM7	29.7	0.66	21.7	0.24	32.9	0.95	31.9	0.62
OH7	31.6	0.23	24.7	0.20	38.1	0.73	38.0	0.63
YC7	30.4	0.45	24.7	0.64	28.0	0.18	25.5	0.33
YL7	30.3	0.64	23.0	0.15	25.1	0.16	26.0	0.75
YM7	29.6	0.24	23.1	0.13	27.7	0.92	27.8	0.71
YH7	32.0	0.30	23.8	0.06	31.4	0.85	30.8	0.59
OC14	31.2	0.08	21.6	0.35	36.5	0.31	30.8	0.08
OL14	29.6	0.21	21.8	0.28	32.1	0.48	29.7	0.92
OM14	28.6	0.45	21.2	0.13	29.8	0.74	28.2	0.27
OH14	29.0	0.10	22.5	0.37	30.0	0.82	30.1	0.57
YC14	34.8	0.00	29.2	0.18	38.7	0.53	38.8	0.43
YL14	31.3	0.01	30.8	2.02	36.5	0.88	37.2	0.05
YM14	28.3	0.89	25.1	0.25	36.5	0.25	35.3	0.73
YH14	36.8	0.00	28.6	0.05	36.5	0.18	35.3	0.43
OC21	33.5	0.03	27.4	0.04	34.2	0.58	35.4	0.02
OL21	32.3	0.15	22.3	0.08	37.8	0.27	35.3	0.65
OM21	29.7	0.47	21.9	0.14	35.8	0.74	35.3	0.58
OH21	34.4	0.20	21.9	0.26	35.7	0.00	35.3	0.12
YC21	34.0	0.70	32.0	0.31	38.2	0.00	35.3	0.40
YL21	32.5	0.56	32.3	1.16	37.6	0.00	35.2	0.88
YM21	34.3	0.88	29.5	0.30	36.5	0.00	35.9	0.86
YH21	34.1	0.68	30.7	0.31	37.3	0.45	36.1	0.95

Sample ID	MMP13 AVE	MMP13 SD	AD5 AVE	AD5 SD	TMP2 AVE	TMP2 SD
OC7	25.6	0.31	34.8	0.31	22.2	0.17
OL7	27.5	1.86	31.0	0.86	22.6	0.27
OM7	30.1	0.14	33.6	0.60	23.6	0.11
OH7	20.5	0.02	30.7	0.30	23.7	0.09
YC7	23.2	0.42	31.0	0.30	23.0	0.28
YL7	21.1	0.43	31.1	0.36	25.0	0.10
YM7	26.4	0.35	28.6	0.52	23.0	0.46
YH7	28.7	0.17	46.8	6.88	27.5	0.97
OC14	29.0	0.32	42.1	2.42	25.5	0.37
OL14	28.9	0.20	36.2	0.13	25.5	0.08
OM14	26.9	0.20	33.8	0.24	25.6	0.07
OH14	30.9	0.11	32.7	0.96	25.4	0.10
YC14	24.4	0.30	41.0	0.85	32.6	0.91
YL14	31.0	0.24	40.0	0.45	37.2	0.36
YM14	34.4	0.43	40.0	0.62	36.2	0.26
YH14	33.8	0.06	40.3	1.28	30.5	0.48
OC21	24.5	0.30	38.1	3.86	29.7	0.26
OL21	30.2	0.45	40.3	0.46	24.7	0.08
OM21	34.5	0.70	37.3	0.98	23.1	2.15
OH21	35.4	0.94	36.9	0.13	27.9	0.06
YC21	36.0	0.41	37.6	0.64	34.5	0.00
YL21	33.0	0.30	39.8	0.00	36.9	1.12
YM21	34.8	0.18	35.6	0.49	33.1	1.08
YH21	23.7	0.29	36.7	0.85	33.5	0.12

### AF Tissue Samples

Sample ID	18s AVE	18s SD	GAPDH AVE	GAPDH SD	COL1 AVG	COL1 SD	COL2 AVG	COL2 SD
OC7	19.6	0.34	21.0	0.42	26.9	0.82	27.4	0.57
OL7	25.6	0.41	26.1	0.04	32.9	0.64	37.1	0.60
OM7	19.9	0.49	20.9	0.10	28.1	0.20	28.2	0.17
OH7	23.7	0.97	21.7	0.22	21.9	0.66	33.1	0.65
YC7	19.4	0.68	26.2	0.47	29.9	0.43	30.2	0.49
YL7	24.9	0.75	25.1	0.65	29.1	0.46	29.6	0.79
YM7	22.7	0.88	26.2	0.73	30.4	0.99	42.6	0.08
YH7	21.7	0.50	24.4	0.99	31.0	0.59	32.0	0.74
OC14	21.3	0.91	23.5	0.11	24.1	0.88	25.1	0.85
OL14	25.5	0.85	20.3	0.94	26.6	0.30	27.9	0.75
OM14	15.6	0.86	21.9	0.46	30.2	0.30	30.9	0.37
OH14	16.3	0.50	21.3	0.31	26.2	0.04	27.0	0.74
YC14	22.1	0.75	16.9	0.56	22.2	0.64	23.3	0.13
YL14	17.0	0.94	21.1	0.53	26.8	0.37	27.9	0.07
YM14	19.9	0.51	23.5	0.93	22.3	0.91	22.7	0.10
YH14	24.6	0.52	18.1	0.91	26.0	0.21	26.8	0.72
OC21	18.4	0.07	19.8	0.43	23.0	0.12	23.4	0.25
OL21	28.2	0.99	37.2	0.84	31.6	0.60	33.0	0.10
OM21	16.6	0.92	19.2	0.74	25.9	0.73	26.3	0.04
OH21	23.6	0.00	19.0	0.00	26.4	0.00	27.0	0.00
YC21	28.6	0.00	30.6	0.00	30.6	0.00	27.8	0.00
YL21	25.7	0.00	30.9	0.00	31.5	0.00	28.2	0.00
YM21	29.6	0.00	31.1	0.00	31.6	0.00	28.8	0.00
YH21	21.4	0.00	27.4	0.00	32.3	0.00	30.6	0.00
Sample ID	AGG AVG	AGG SD	CFOS AVE	CFOS SD	BGY AVE	BGY SD	STAT3 AVE	STAT3 SD
OC7	26.1	0.15	31.4	0.18	30.1	0.25	34.7	0.22
OL7	31.3	0.45	36.6	0.96	35.2	0.01	37.1	0.05
OM7	26.2	0.76	33.1	0.22	32.4	0.16	34.3	0.29
OH7	34.0	0.75	28.0	0.56	35.3	0.26	34.8	0.66
YC7	34.5	0.73	28.9	0.89	29.2	0.46	31.1	0.33
YL7	29.0	0.32	34.4	0.75	34.9	0.77	36.2	0.61
YM7	35.8	0.69	32.5	0.39	28.9	0.89	33.8	0.97
YH7	29.3	0.60	33.2	0.53	33.0	0.37	35.9	0.14
OC14	22.3	0.06	29.1	0.57	25.2	0.21	31.0	0.59
OL14	23.5	0.75	37.4	0.13	35.4	0.74	37.4	0.99
OM14	25.9	0.10	31.2	0.80	26.9	0.13	31.4	0.69
OH14	24.9	0.16	25.9	0.81	23.8	0.98	27.8	0.28
YC14	19.7	0.14	32.0	0.88	35.6	0.51	35.5	0.22
YL14	24.6	0.14	30.7	0.38	27.3	0.26	31.9	0.69
YM14	28.3	0.71	32.4	0.25	27.3	0.34	31.9	0.16
YH14	22.6	0.56	37.4	0.33	35.4	0.68	37.4	0.96
OC21	34.2	0.94	29.6	0.22	24.8	0.05	29.3	0.95
OL21	35.9	0.74	36.6	0.84	25.7	0.94	29.1	0.68
OM21	33.7	0.59	27.7	0.37	25.7	0.01	29.1	0.52
OH21	27.3	0.00	28.6	0.00	34.6	0.00	29.1	0.00
YC21	34.3	0.00	39.2	0.00	33.7	0.00	36.7	0.00
YL21	35.8	0.00	35.7	0.00	33.7	0.00	35.7	0.00
YM21	35.8	0.00	35.7	0.00	35.6	0.00	36.0	0.00
YH21	31.5	0.00	33.7	0.00	32.9	0.00	36.7	0.00

Sample ID	MMP3 AVG	MMP3 SD	AD4 AVE	AD4 SD	LINK AVE	LINK SD	MMP2 AVE	MMP2 SD
OC7	27.2	0.25	42.7	0.74	26.4	0.74	29.9	0.91
OL7	32.3	0.37	30.4	0.01	31.5	0.36	35.6	0.27
OM7	24.6	0.89	30.4	0.66	28.5	0.69	27.0	0.03
OH7	26.2	0.13	50.3	0.57	23.7	0.99	31.7	0.67
YC7	35.3	0.01	37.6	0.81	26.5	0.93	29.1	0.05
YL7	34.3	0.73	41.6	0.36	28.7	0.44	34.7	0.57
YM7	35.2	0.21	36.3	0.07	30.2	0.84	31.0	0.53
YH7	33.5	0.01	33.5	0.91	33.7	0.05	32.2	0.57
OC14	30.8	0.65	35.1	0.67	25.9	0.36	26.0	0.63
OL14	25.4	0.75	32.0	0.67	35.1	0.96	37.2	0.03
OM14	25.4	0.86	32.9	0.14	29.9	0.72	26.2	0.69
OH14	26.9	0.83	34.0	0.48	26.1	0.82	21.8	0.41
YC14	24.3	0.04	29.9	0.13	26.0	0.60	33.7	0.63
YL14	27.6	0.22	33.2	0.04	25.7	0.38	26.9	0.07
YM14	29.6	1.00	33.7	0.64	25.8	0.94	30.7	0.11
YH14	24.1	0.30	30.4	0.57	35.1	0.95	37.2	0.27
OC21	27.5	0.05	39.0	0.55	26.6	0.39	24.9	0.15
OL21	40.2	0.66	50.1	0.67	31.3	0.41	25.7	0.26
OM21	24.6	0.47	34.2	0.05	25.9	0.41	23.5	0.67
OH21	25.5	0.00	58.0	0.00	24.7	0.00	31.0	0.00
YC21	37.0	0.00	37.2	0.00	35.0	0.00	36.3	0.00
YL21	35.3	0.00	37.2	0.00	32.8	0.00	0.0	0.00
YM21	38.1	0.00	37.2	0.00	35.2	0.00	34.9	0.00
YH21	28.6	0.00	37.0	0.00	33.0	0.00	32.4	0.00
Sample ID	CJUN AVE	CJUN SD	COL6 AVE	COL6 SD	CTGF AVE	CTGF SD	DEC AVE	DEC SD
OC7	33.4	0.55	30.7	0.85	33.1	0.26	23.2	0.98
OL7	36.3	0.62	34.5	0.26	36.5	0.49	27.2	0.70
OM7	31.9	0.50	27.9	0.76	35.8	0.80	29.5	0.16
OH7	33.6	0.70	34.2	0.10	33.8	0.50	25.1	0.70
YC7	29.4	0.69	26.4	0.92	30.0	0.37	26.3	0.18
YL7	35.1	0.55	36.3	0.34	36.5	0.93	26.7	0.90
YM7	33.0	0.38	28.9	0.68	35.2	0.51	29.8	0.90
YH7	32.9	0.97	32.8	0.03	37.4	0.79	28.4	0.47
OC14	33.8	0.59	27.5	0.18	31.4	0.24	23.4	0.63
OL14	30.8	0.66	35.0	0.12	33.5	0.09	27.6	0.78
OM14	31.4	0.62	26.6	0.92	34.3	0.71	24.2	0.27
OH14	28.2	0.41	23.7	0.89	27.0	0.11	20.9	0.67
YC14	35.2	0.62	35.0	0.57	33.5	0.45	21.0	0.13
YL14	31.1	0.52	27.1	0.91	31.8	0.86	24.2	0.75
YM14	35.7	0.81	27.3	0.21	37.0	0.33	38.6	0.37
YH14	30.8	0.52	35.0	0.81	33.5	0.48	27.6	0.63
OC21	29.9	0.63	23.9	0.46	30.4	0.11	22.2	0.35
OL21	30.7	0.76	25.7	0.68	30.7	0.74	25.8	0.23
OM21	28.6	0.46	24.6	0.83	26.2	0.69	21.4	0.86
OH21	34.3	0.00	34.6	0.00	30.1	0.00	19.9	0.00
YC21	35.3	0.00	30.7	0.00	37.0	0.00	33.8	0.00
YL21	35.2	0.00	30.7	0.00	37.7	0.00	34.9	0.00
YM21	36.3	0.00	30.7	0.00	37.8	0.00	37.9	0.00
YH21	35.1	0.00	33.0	0.00	35.8	0.00	31.3	0.00

Sample ID	IGF AVE	IGF SD	IL6 AVE	IL6 SD	ILK AVE	ILK SD	MMP1 AVE	MMP1 SD
OC7	33.3	0.10	28.1	0.36	31.3	0.74	33.4	0.92
OL7	33.5	0.97	34.1	0.55	36.9	0.93	36.9	0.66
OM7	34.4	0.67	31.4	0.89	31.3	0.85	32.1	0.34
OH7	34.3	0.65	28.7	0.16	32.9	0.59	35.9	0.04
YC7	31.9	0.28	30.9	0.97	29.6	0.48	35.3	0.13
YL7	35.6	0.59	31.8	0.64	35.8	0.57	37.3	0.08
YM7	32.5	0.26	35.7	0.56	30.8	0.78	35.6	0.90
YH7	33.4	0.66	30.0	0.85	33.9	0.71	36.7	0.83
OC14	32.8	0.93	31.8	0.31	29.1	0.60	28.8	0.40
OL14	33.3	0.88	34.6	0.10	34.5	0.85	30.9	0.16
OM14	35.8	0.98	27.8	0.46	30.4	0.17	29.3	0.71
OH14	33.7	0.16	27.7	0.03	27.1	0.21	25.2	0.45
YC14	31.1	0.22	28.5	0.75	33.8	0.09	35.3	0.00
YL14	32.3	0.07	28.6	0.75	30.6	0.74	29.9	0.52
YM14	35.2	0.22	31.0	0.25	33.4	0.58	37.2	0.75
YH14	33.3	0.94	34.6	0.62	34.5	0.73	30.9	0.79
OC21	36.6	0.06	28.3	0.54	28.9	0.80	27.7	0.52
OL21	32.0	0.99	34.6	0.15	27.7	0.28	27.7	0.13
OM21	34.8	0.03	30.0	0.66	26.7	0.22	27.0	0.04
OH21	34.5	0.00	26.0	0.00	30.2	0.00	36.1	0.00
YC21	34.8	0.00	30.6	0.00	37.0	0.00	32.1	0.00
YL21	31.0	0.00	30.7	0.00	37.5	0.00	32.4	0.00
YM21	34.5	0.00	30.4	0.00	35.1	0.00	33.5	0.00
YH21	35.0	0.00	32.4	0.00	34.3	0.00	32.5	0.00

Sample ID	TMP1 AVE	TMP1 SD	FBIN AVE	FBIN SD	TGFβ AVE	TGFβ SD	TMP3 AVE	TMP3 SD
OC7	23.3	0.70	24.3	0.20	33.8	0.45	30.6	0.10
OL7	25.6	0.39	29.1	0.22	35.6	0.79	24.0	0.52
OM7	21.5	0.30	25.7	0.40	33.1	0.74	28.6	0.74
OH7	23.5	0.75	28.5	0.90	29.9	0.72	31.7	0.10
YC7	26.4	0.19	28.6	0.73	30.4	0.02	26.8	0.35
YL7	26.0	0.97	26.6	0.65	35.5	0.53	30.0	0.25
YM7	27.4	0.16	28.5	0.86	34.4	0.19	31.9	0.24
YH7	25.5	0.03	31.7	0.15	32.5	0.54	35.0	0.91
OC14	26.9	0.18	23.9	0.05	29.4	1.00	26.3	0.99
OL14	21.0	0.70	29.6	0.15	32.5	0.28	26.3	0.74
OM14	22.7	0.10	26.8	0.22	30.6	0.41	27.0	0.65
OH14	24.3	0.33	23.3	0.70	27.5	0.82	26.2	0.23
YC14	18.0	0.51	23.6	0.51	35.6	0.08	25.7	0.89
YL14	22.2	0.24	28.0	0.48	31.5	0.81	22.7	0.23
YM14	23.3	0.71	22.6	0.83	35.8	0.11	32.5	0.64
YH14	19.3	0.53	29.6	0.55	32.5	0.22	26.3	0.30
OC21	23.3	0.86	24.3	0.66	29.2	0.14	29.8	0.38
OL21	29.0	0.82	27.6	0.85	30.7	0.95	25.7	0.85
OM21	21.9	0.39	23.0	0.67	26.9	0.70	23.7	0.52
OH21	22.6	0.00	21.3	0.00	35.1	0.00	28.8	0.00
YC21	30.8	0.00	31.9	0.00	35.1	0.00	34.1	0.00
YL21	30.2	0.00	33.2	0.00	36.8	0.00	36.3	0.00
YM21	30.3	0.00	32.1	0.00	35.1	0.00	36.7	0.00
YH21	27.5	0.00	32.6	0.00	35.3	0.00	29.6	0.00



Sample ID	VCAN AVE	VCAN SD	VIM AVE	VIM SD	MAPK AVE	MAPK SD	COL3 AVE	COL3 SD
OC7	31.1	0.03	22.3	0.86	34.1	0.90	31.8	0.23
OL7	34.5	0.38	26.6	0.58	37.7	0.35	31.0	0.65
OM7	29.6	0.44	29.4	0.37	31.4	0.96	34.1	0.51
OH7	31.4	0.30	24.9	0.99	35.1	0.25	34.6	0.59
YC7	31.2	0.63	22.5	0.61	29.9	0.47	30.2	0.75
YL7	32.9	0.35	25.9	0.43	33.6	0.61	36.0	0.65
YM7	30.1	0.88	27.7	0.12	32.3	0.65	33.5	0.95
YH7	33.7	0.66	28.7	0.41	33.3	0.47	31.0	0.26
OC14	30.7	0.73	24.1	0.48	30.6	0.94	30.7	0.94
OL14	30.7	0.35	32.4	0.72	29.2	0.47	31.0	0.55
OM14	30.0	0.34	23.6	0.74	31.1	0.10	31.0	0.81
OH14	27.8	0.37	23.0	0.32	28.2	0.65	26.1	0.67
YC14	29.7	0.86	19.9	0.50	37.0	0.72	31.0	0.26
YL14	30.7	0.79	23.3	0.32	31.4	0.61	31.5	0.39
YM14	30.7	0.38	33.4	0.78	37.6	0.10	29.2	0.79
YH14	30.7	0.44	32.4	0.76	29.2	0.46	29.2	0.98
OC21	29.0	0.49	21.2	0.89	29.4	0.07	28.7	0.44
OL21	35.9	0.34	27.4	0.51	31.0	0.25	31.0	0.97
OM21	30.2	0.65	22.4	0.22	28.2	0.14	29.0	0.25
OH21	31.9	0.00	22.2	0.00	35.6	0.00	38.8	0.00
YC21	33.3	0.00	31.6	0.00	35.8	0.00	36.0	0.00
YL21	32.4	0.00	31.4	0.00	35.8	0.00	34.4	0.00
YM21	35.9	0.00	32.4	0.00	35.8	0.00	35.8	0.00
YH21	31.4	0.00	29.4	0.00	35.8	0.00	39.4	0.00

Sample ID	MMP13 AVE	MMP13 SD	AD5 AVE	AD5 SD	TMP2 AVE	TMP2 SD
OC7	24.7	0.54	33.8	0.94	23.4	0.38
OL7	30.4	0.29	33.7	0.97	27.1	0.90
OM7	24.3	0.73	31.7	0.53	23.7	0.64
OH7	25.4	0.57	33.8	0.99	24.9	0.46
YC7	30.4	0.46	32.9	0.40	27.7	0.51
YL7	29.1	0.29	31.9	0.38	27.2	0.33
YM7	23.6	0.50	33.8	0.15	28.9	0.97
YH7	23.4	0.58	27.6	0.07	28.2	0.33
OC14	35.8	0.95	34.6	0.69	26.7	0.61
OL14	25.1	0.12	28.0	0.95	22.1	0.57
OM14	24.7	0.13	29.4	0.74	24.0	0.75
OH14	35.2	0.06	31.2	0.57	24.1	0.07
YC14	21.6	0.76	25.0	0.99	19.1	0.85
YL14	25.1	0.85	29.2	0.44	23.2	0.25
YM14	28.6	0.17	39.0	0.23	25.6	0.11
YH14	23.8	0.66	25.7	0.84	20.6	0.45
OC21	24.1	0.78	29.5	0.37	23.3	0.17
OL21	37.5	0.01	54.8	0.33	28.3	0.80
OM21	30.1	0.80	33.4	0.97	22.6	0.49
OH21	27.4	0.00	42.4	0.00	22.8	0.00
YC21	23.7	0.00	31.4	0.00	34.6	0.00
YL21	35.8	0.00	27.6	0.00	34.3	0.00
YM21	34.5	0.00	33.7	0.00	35.5	0.00
YH21	25.2	0.00	31.5	0.00	30.3	0.00